Characterisation of Clonal Dental Pulp Progenitors and the Effects of *In Vitro* Expansion and Hydrogen Peroxide

A thesis submitted in fulfilment of the requirements of the degree of
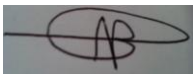
Doctor of Philosophy

Cardiff University

September 2013

Amr Alraies BDS, MSc

Tissue Engineering and Reparative Dentistry,

School of Dentistry,
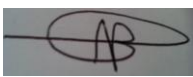
Cardiff University

DECLARATION

This work has not been submitted in substance for any other degree or award at this or any other university or place of learning, nor is being submitted concurrently in candidature for any degree or other award.

Signed   Date 09/12/2013

STATEMENT 1

This thesis is being submitted in partial fulfilment of the requirements for the degree of PhD.
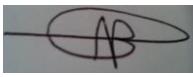
Signed   Date 09/12/2013

STATEMENT 2

This thesis is the result of my own independent work/investigation, except where otherwise stated.
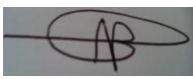
Other sources are acknowledged by explicit references. The views expressed are my own.

Signed   Date 09/12/2013

STATEMENT 3

I hereby give consent for my thesis, if accepted, to be available for photocopying and for inter-library loan, and for the title and summary to be made available to outside organisations.

Signed   Date 09/12/2013

Acknowledgements

AWARDS AND PRIZES

The work on chapter 2 and chapter 3 has been presented in local and international conferences and was awarded the following prizes:

2012   International Association for Dental Research (IADR) Conference in Helsinki, Unilever Best Poster Prize.

2011   Cardiff Stem Cell Research Day, Best Poster Presentation.

Summary

Dental pulp progenitor cells (DPPCs) are among many stem cell sources potentially beneficial for tissue engineering. DPPCs offer advantages over other mesenchymal stem cell sources, due to their accessibility and multi-lineage differentiation. However, distinct DPPC clones exist within dental pulp, with contrasting proliferative/regenerative capabilities. This is a key consideration for the exploitation of DPPCs, in terms of the abilities of isolated clones to undergo sufficient *in vitro* proliferative expansion, while maintaining their regenerative potential.

This Thesis supports the heterogeneous nature of DPPCs, demonstrating significant variations in population doublings (PDs) and senescence, with highly proliferative clones exhibiting greater proliferation (>80PDs) under normal and oxidative stress (H_2O_2 treatment) conditions, compared to low proliferative clones (<40PDs) demonstrating altered morphology, increased SA-β-galactosidase staining and senescence marker (p53/p16) expression. Although negative for human telomerase expression, highly proliferative clones possessed longer telomeres (>18kb); maintained stem cell marker expression (CD73, CD90, CD105) and osteogenic/chondrogenic differentiation in culture. In contrast, low proliferative clones exhibited shorter telomeres (<6kb), reduced marker expression and increased adipogenesis.

DPPC heterogeneity was further evident upon Raman Spectroscopy analysis, which distinguished between undifferentiated high and low proliferative clones and undifferentiated DPPCs and clones following chondrogenic differentiation. High and low proliferative clonal behaviour was also assessed in type I collagen gels, demonstrating increased contraction and reduced cell proliferation in detached versus attached gels, irrespective of clonal type. Increased contraction was due to increased MMP-2 expression by both clonal types, while highly proliferative clones also expressed MMP-9, especially at late PDs.

These findings indicate significant variations in DPPC clonal proliferative/differentiation capabilities, partly explained by telomere length/cellular ageing differences. Identification of clonal populations with contrasting tissue regeneration capacities supports the development of screening strategies (e.g. Raman Spectroscopy) for the selective isolation of highly proliferative clones from dental pulp for therapeutic use, or assessing DPPC differentiation in 3D culture.

Abbreviations

3D	Three Dimensional
α-MEM	Alpha-Modification Minimal Essential Medium
ACT-1	Automatic Camera Tamer
ALP	Alkaline Phosphatase
ANOVA	Analysis of Variance
BDNF	Brain-Derived Nurotrophic Factor
β-gal	β-Galactosidase Enzyme
BMP	Bone Morphogenic Protein
BMSC	Bone Marrow Stromal/Stem Cell
bFGF	Basic Fibroblast Growth Factor
bp	Base Pairs
BSA	Bovine Serum Albumin
BSP	Bone Sialoprotein
Ca^{2+}	Calcium
CD	Cluster of Differentiation
cDNA	Complimentary Deoxyribonucleic Acid
CO_2	Carbon Dioxide
dd.H_2O	Double Distilled Water
DIG	Digoxigenin
DMP1	Dentin Matrix Protein1
DMSO	Dimethyl Sulfoxide
DNA	Deoxyribonucleic Acid
DPPC	Dental Pulp Progenitor Cell
DPSC	Dental Pulp Stem Cell
DPSS	Diode Pumped Solid-State
DSP	Dentine Sialoprotein
DSPP	Dentine Sialophosphoprotein
ECM	Extracellular Matrix
EDTA	Ethylenediaminetetraacetate
EGF	Epidermal Growth Factor

EnSC	Endothelial Stem Cell
Eph	Ephrin (Signalling Pathway)
ERK	Extracellular-Signal-Regulated Kinase
ESC	Embryonic Stem Cell
FACS	Fluorescence Activated Cell Sorting
FCS	Fetal Calf Serum
Fe^{2+}	Ferrous
Fe^{3+}	Ferric
FGF	Fibroblast Growth Factor
FITC	Fluorescein Isothiocyanate
$Flk1^{+}$	Fetal Liver Kinase^{+}
FNA	Fibronectin Adherent
GAG	Glycosaminoglycans
H_2O	Water
H_2O_2	Hydrogen peroxide
HCl	Hydrochloric Acid
HOCl	Hypochlorous Acid
HSC	Hematopoietic Stem Cell
IGF-1	Insulin-Like Growth Factor I
IL	Interleukin
IMS	Industrial Methylated Solution
IR	Infrared
LANGFR/CD271	Low Affinity Nerve Growth Factor Receptor
Li	Corresponding Length
LIF	Leukaemia Inhibitory Factor
LPL	Lipoprotein Lipase
MACS	Magnetic Activated Cell Sorting
MAP	Mitogen-Activated Protein
MEPE	Matrix Extracllular Phosphoglycoprotein
mg^{2+}	Magnesium
M-MLV	Moloney-Murine Leukaemia Virus
MMP	Matrix Metalloproteinase
MSC	Mesenchymal Stem Cell

MT1-MMP	Membrane-Tethered Metalloenzyme
MW	Molecular Weight
NA	Numerical Aperture
NCP	Non-Collagenous Protein
NeuN	Neuronal Nuclear Protein
NRES	National Research Ethics Service
NSE	Neuronal Marker Neuron-Specific Enolase
O_2^-	Superoxide Radical
OCN	Osteocalcin
Oct4	Octamer-Binding Transcription Factor 4
ODi	Mean Density
$\cdot$OH	Hydroxyl
ON	Osteonectin
OPN	Osteopontin
PBS	Phosphate Buffered Saline
PC	Principal Component
PCA	Principal Component Analysis
PCR	Polymerase Chain Reaction
PD	Population Doubling
PDL	Population Doubling Level
PFA	Paraformaldehyde
PDGF	Platelet-Derived Growth Factor
PPARγ	Peroxisome Proliferator-Activated Receptor Gamma
RGD	Arg-Gly-Asp
RNA	Ribonucleic Acid
ROS	Reactive Oxygen Species
RT-PCR	Reverse Transcription-Polymerase Chain Reaction
Runx2	Runt-Related Transcription Factor 2
SDS-PAGE	Sodium Dodecyl Sulfate- Polyacrylamide Gel Electrophoresis
SE	Standard Error of Mean
SEM	Scanning Electron Microscopy
SIBLINGs	Small Integrin Binding Ligand, N-Linked Glycoprotein
SOD	Superoxide Dismutase

Sox2/9	SRY (Sex Determining Region-Y)-Box 2/9
SSAO	Semicarbazide-Sensitive Amine Oxidase
SSC	Standard Sodium Citrate
SSEA-4	Stage-Specific Embryonic Antigens
STAT3	Signal Transducer and Activator of Transcription 3
STELA	Single Telomere Length Analysis
SVZ	Subventricular Zone
TA	Transit Amplifying
TAE	Tris Acetate EDTA
TBS	Tris-Buffered Saline
TERT	Telomerase Reverse Transcriptase
TGF-β	Transforming Growth Factor-Beta
TIMP	Tissue Inhibitors of MMP
TNF	Tumor Necrosis Factor
TRF	Terminal Restriction Fragment
Trp	Tryptophan
Tyr	Tyrosine
UK	United Kingdom
USA	United States of America
VEGF	Vascular Endothelial Growth Factor

Units of Measurement

%	Percentage
°C	Degrees Celsius
×g	Gravitational Acceleration
bp	Base Pair
cm	Centimetre
mm	Millimetre
μm	Micrometre
nm	Nanometre
g	Gram
kb	Kilo Base Pair

M	Molar
mM	Millimolar
μM	Micromolar
mg	Milligram
μg	Microgram
ng	Nanogram
L	Litre
mL	Millilitre
μL	Microlitre
h	Hours
min	Minutes
s	Seconds
rpm	Revolutions Per Minute
V	Volts
mW	Milliwatt

Contents

Chapter 1 - Introduction

Chapter 2 - Effects of *in vitro* Expansion and Oxidative Stress on Dental Pulp Progenitor Cells Proliferative Lifespan

Chapter 3 - Effects of *In Vitro* Expansion and H_2O_2 on Differentiation Ability of Dental Pulp Progenitor Clones

Chapter 4 – Identification of Clonal Dental Pulp Variations Using Raman Spectroscopy

Chapter 5 - Type I Collagen Gel Interaction with DPPCs

Chapter 6 - Discussion

Chapter 1:
Main Introduction

1.1   Overview

Tissue engineering is an emerging field in medicine, especially with ever-increasing ageing populations worldwide (Zippel et al., 2010). Tissue engineering is defined as a strategy based on combining cells with biomaterial scaffolds that aims to repair, replace, or regenerate dysfunctional cells, tissue or organs to restore function that has become dysfunctional (Sittinger et al., 1996; Daar and Greenwood, 2007). Due to ethical concerns with the clinical application of embryonic stem cells, adult mesenchymal stem cells (MSCs) are a vital tool in tissue engineering and regenerative medicine, due to their capacity for self-renewal, clonogenicity and ability to differentiate into various cell lineages (Gafni et al., 2004; Lin et al., 2008). As such, the use of stem cells in combination with appropriate biomaterial scaffolds is expected to offer significant potential in the development of cell-based therapies for the repair and replacement of numerous diseased and damaged tissues.

MSCs were first isolated by Friedenstein and his group (1968) from the bone marrow as fibroblastic stromal cells that were able to form adherent colonies in culture (Friedenstein et al., 1987). Although bone marrow is the most exploited stem cell source, others including dental pulp progenitor cells (DPPCs), are increasingly being recognized as a viable alternative stem cell source for the development of effective cell-based therapies (Gronthos et al., 2000). These cells may be a better candidate for use in clinical applications in comparison with other MSCs isolated from bone marrow, adipose tissue or umbilical cord blood because they have similar gene expression profile to bone marrow stem cells (Huang et al., 2009b), high plasticity, good interaction with scaffold, very low morbidity and due to the ease of accessibility as they are discarded following tooth extraction (Graziano et al., 2008). Indeed MSCs have been demonstrated as a promising tool to support tissue engineering in many fields such bone repair (Quarto et al., 2001), cartilage repair (Centeno et al., 2008; Veronesi et al., 2013) and skin regeneration (Ma et al., 2009).

1

A significant limitation of stem cell therapy is that such cells exist in low abundance (Friedenstein et al., 1982). This means an extensive *in vitro* expansion is necessary to produce sufficient cell numbers for clinical use that influences their biological properties, which is accompanied by increased oxidative stress. Oxidative stress may lead to loss of their stemness and multipotency (Banfi et al., 2000; Siddappa et al., 2007), and eventually cellular senescence (Stenderup et al., 2003; Bonab et al., 2006). Another factor that may affect the use of these cells in tissue engineering, is the diversity of each clone isolated (Gronthos et al., 2002). Heterogeneous cells are expected to produce unwanted biological activity while homogeneous cells are more desirable to use in the clinic. However, this is not always the case, as a heterogeneous population from the dental pulp was found to be key in the success of clinical intervention for treating spinal cord injury (Sakai et al., 2012). This thesis will focus on investigating homogeneous DPPCs clones. In order to investigate individual clones, a quick non-invasive method to characterise dental pulp progenitor cells prior to their use in stem cell based therapies is required, and will be looked at in this study alongside the effect of *in vitro* expansion in normal culture and senescent co-culture, with sub-lethal hydrogen peroxide (H_2O_2) doses.

Furthermore, DPPCs behave differently in their natural niche than on *in vitro* culture plastic. In this study, type 1 collagen gels are used in order to imitate the natural niche environment of these cells. This will give a better understanding of DPPCs native interactions with the ECM, which will be beneficial for tissue engineering before application of DPPCs in clinical medicine.

Overall this study will investigate the effect of *in vitro* culture expansion on DPPCs stemness and to study the variations between clones and develop a screening strategy for the selective isolation of the efficacious DPPC clones for therapeutic use.

1.2 Stem Cells

Stem cells are unspecialized cells that are capable of differentiating into other cells and have the ability to self-regenerate, depending on the signalling pathway, which is believed to be controlled by different growth factors on the stem cell niche (Blau et al., 2001; Lin et al., 2008). Stem cells are present in most connective tissues and

believed to have an important role in replacement of injured and damaged tissue. Stem cells are considered to be a promising therapy to cure many diseases in the future (Denham et al., 2005) and even though stem cells are still in the research stage, some therapies arising from tissue engineering have already entered the clinical stage (reviewed in Atala, 2012). There are two main type of stem cells; embryonic stem cells (ESCs) and adult stem cells.

1.2.1 Embryonic Stem Cells

ESCs are cells that derive from one of the earliest stages of embryonic development. These are derived from the inner cell mass of the 5-6 day old human blastocyte (Bongso and Lee, 2005). The first human ESCs isolated from inner cell mass were performed by Thomson and his colleagues, in 1998. ESCs are pluripotent cells which mean they can differentiate into any of the germ layers that form the body; endoderm, mesoderm and ectoderm (Lin et al., 2008).

Human ESCs show high telomerase activity. Telomerase acts as a shielding structure that protects both ends of the chromosome. These are composed of special DNA repetitive sequences of TTAGGG in association with a variety of telomere-binding proteins including telomerase reverse transcriptase (TERT) that possesses reverse transcriptase activity and is used as marker to evaluate the telomerase activation. At the end of DNA strand there is an extension, due to the 3' strand being a little longer than the 5' strand (Serakinci et al., 2008). This process maintains a normal euploid karyotype in long term culture which make these cells unique and have favourable use in therapeutic applications (Hoffman and Carpenter, 2005). Telomeres protect the chromosomes from degradation or any actions that can lead to cell death. However, when cells replicate they cannot be completely replicated. They are slowly shortened until they reach a point called "replicative senescence" (Hiyama and Hiyama, 2007). Furthermore, the high telomerase activation of ECSs decreases during differentiation. In addition, ROS can accelerate telomere shortening because telomeres are at least partially deficient for oxidative DNA damage (Saretzki et al., 2008; Saretzki, 2009).

ESCs have characteristic markers such as stage-specific embryonic antigens (SSEA-4), TRA-1-60, TRA-1-81(Hoffman and Carpenter, 2005). Octamer-binding transcription factor-4 (Oct4), Sox2 and Nanog are other transcription factors expressed in ESCs, which are essential to maintain the pluripotent phenotypes of these cells (Rodda et al., 2005). Oct4 is a transcription factor of the POU family, which is restricted to cells of early embryos and undifferentiated ESCs. Oct4 is rapidly down-regulated in gastrulation and for this reason a low level of Oct4 is essential for ESCs to differentiate into different cell lines. However, Oct4 remains expressed in embryonic neural crest (Guo et al., 2002) which means it may be expressed in the dental pulp (Huang et al., 2009b). On the other hand, Nanog over-expression also maintains ESCs self-renew ability (Yates and Chambers, 2005). However, Nanog cannot function in the absence of Oct4 (Chambers et al., 2003). There are many signals and growth factors that regulate the ESCs self-renewal ability. Leukaemia Inhibitory Factor (LIF) activates Signal Transducer and Activator of Transcription 3 (STAT3) to support the undifferentiated phase of mouse ESCs. In addition to LIF, Bone morphogenic protein 4 (BMP4) extrinsic factor and Wnt pathway maintain mouse ESCs self-renewal (Ying et al., 2003). In humans, LIF and BMP4 are not enough to maintain ESCs pluripotency. Instead, growth factors such as fibroblast growth factor (FGF) signalling are considered to be essential to the self-renewal of human embryonic stem cells. However, the mechanism of these processes is still unclear (reviewed in Pan and Thomson, 2007). Furthermore, ESCs express some surface antigen that are found in adult stem cells such as Oct4, CD 117, CD 135 and CD 91 (Hoffman and Carpenter, 2005) which indicates that adult stem cells have some similar characteristics to ESCs. As ESCs have the capacity to generate any type of cells in the body, they are a promising target for tissue replacement. However, the use of these cells has ethical challenges, with respect to their source where it may require the destruction of a human embryo. For this reason, using other types of stem cells for tissue replacement has been introduced (Liao, 2005; Lin et al., 2008).

1.2.2 Adult Stem Cells

Adult stem cells, sometimes called somatic stem cells, are undifferentiated cells that are found in tissues throughout the body with renewal capacity after embryonic development (Lin et al., 2008). Stem cells generate intermediate cell type called

progenitor cells, before they achieve their fully differentiate state. Their main function is to replace cells that die because of injury or disease (Verstappen et al., 2009). Adult stem cells are located in different adult tissues, including bone marrow, peripheral blood, the subventricular zone (SVZ) of the brain, dental pulp, blood vessels, skeletal muscle, epithelia of the skin, cornea, retina, liver, and pancreas (Bongso and Lee, 2005). These cells differentiate into specific tissues depending on their site where specific signals are taking within their niche. Adult stem cells have a more limited range of differentiation lineages but less ethical concerns compared with ESCs (Gafni et al., 2004; Lin et al., 2008). In the beginning, no one considered the possibility that stem cells in adult tissues could generate *in vitro* other types of tissue, different than the tissue in which they normally reside. Later, several studies showed that adult stem cells from bone marrow were able to differentiate into different cell linages such as mature cells of the liver (Theise et al., 2000; Alison et al., 2000) and neural cells (Sanchez-Ramos et al., 2000). Telomerase activity in adult stem cells is controversial. Even those adult stem cells tend to give rise to a high number of daughter cells but they do not express high level of telomerase like ESCs. In addition, some adult stem cells such as MSCs they do not express any telomerase which means there are other mechanisms to maintain the telomere other than telomerase (Hiyama and Hiyama, 2007; Saretzki, 2009). There are several types of adult stem cells. These types of cells are mostly classified according to their location in the body.

1.2.2.1 Mesenchymal Stem Cells (MSCs)

Friedenstein et al., (1968) was the first to discover MSCs in the bone marrow and defined them as osteogenic stem cells. However, the first person who called these cells MSCs, was Caplan in 1991. These cells were able to form colonies composed of fibroblastoid cells raised from one cell (Fridenstein et al., 1970). It has been noticed that MSCs are commonly associated with blood vessels, which means MSCs are found in many parts of the body, such as bone marrow, blood and dental pulp. MSCs are mononuclear cells with fibroblastic like morphology (Mareschi et al., 2001). These cells are capable of differentiating into many types of cells, such as osteoblasts (Rickard et al., 1996), chondrocytes (Ashton et al., 1980) adipocytes (Bennet et al., 1991), and myoblasts (Wakitani et al., 1995) *in vitro*. In addition,

MSCs can form bone and cartilage *in vivo*, when seeded upon ceramic carriers (Friedenstein et al., 1987; Goshima et al., 1991). Some studies show that MSCs have the potential to differentiate into non-mesodermal lineages including skin (Sasaki et al., 2008) and neurons (Kopen et al., 1999; Zhao et al., 2002; Suon et al., 2004). Due to their diversity in differentiation, ease of handling and accessibility, such properties make MSCs an attractive target for tissue engineering. So far, MSCs in the tissue engineering facilitate studies in the growth of bone, cartilage, muscle, skin and neural tissue (Rosenbaum et al., 2008).

In order to use these cells in tissue engineering, better understanding of how they behave and differentiate into specific lineages is required. Different signals and growth factors often lead to different MSC differentiation. The Mitogen-Activated Protein (MAP) kinase pathway is identified to control and regulate the proliferation and differentiation of MSCs. There are several growth factors and hormones that activate this pathway (Jaiswal et al., 2000). The differentiation of MSCs into osteoblasts is stimulated by introducing these growth factors such as epidermal growth factor (EGF), dexamethasone, and vitamin C into the culture medium (Maniatopoulos et al., 1988; Kratchmarova et al., 2005). Many *in vitro* studies show the ability of MSCs to differentiate into neural cells. When human or mouse MSCs are cultured with EGF and brain-derived nurotrophic factor (BDNF), the cells started to express neuroepithelial marker (nestin) and the neuronal nuclear protein (NeuN), which can be considered as evidence that MSCs differentiate into neural cells (Sanchez-Ramos et al., 2000). Another study by Woodbury et al (2000) was able to differentiate peripheral MSCs into neurons. In this study, cells were cultured in serum-containing medium supplemented with β-mercaptoethanol. After 24 h, changes in the morphology were observed. The next step was culturing the cells in medium containing basic fibroblast growth factor (bFGF). These results demonstrated that MSCs exhibited the neuronal marker neuron-specific enolase (NSE) (Woodbury et al., 2000). Another study found that MSCs can express keratin 14, a specific cell marker for keratinocytes, when cells were exposed to bone morphogenetic protein-4 (BMP-4) for 6 days *in vitro* while *in vivo* MSCs are recruited to the wound site by specific chemokine (SLC/CCL21) where they contribute in wound healing process and may differentiate into different skin cells

(Sasaki et al., 2008). MSC also have the ability to differentiate into endothelial cells (Reyes et al., 2002). By culturing MSCs *in vitro* with vascular endothelial growth factor (VEGF), CD34$^+$ and fetal liver kinase$^+$ (Flk1$^+$), endothelial expressions were detected. These expressions would be expected for endothelial cells (Reyes et al., 2002). Furthermore, mechanical loading plays an important role in MSCs differentiation. A study showed that MSCs lose their fibroblastic morphology and begin to show expression of chondrocytes, when grown in 3D culture, containing a serum-free nutrient medium, with addition of a member of the transforming growth factor (TGF) super family (Barry et al., 2001). All these studies into MSCs differentiation may help in tissue regeneration and cell therapy.

Nowadays, there is a lot of debate over the identification of MSCs. Until recently, there are many techniques available but no single method is seen as ideal. These techniques include colony forming efficiency, gene expression and cell surface markers (Kuhn and Tuan, 2009; Morikawa et al., 2009). Another recent technique using collagen type II, alkaline phosphatase and Oil Red O staining assays, are applied to identify MSCs isolated from bone marrow. This technique depends on the ability of these cells to form osteoblasts, chondrocytes and adipocytes (Pittenger et al., 1999). With regards to identifying MSCs by using cell surface markers, many studies have shown that MSCs from different sources express several markers such as CD73, CD105, CD90, CD44, CD29, CD166 and CD271 (Bühring et al.,2009; Kuhn and Tuan, 2009; Market et al., 2009). Unfortunately, there are no specific markers for MSCs only (Javazon et al., 2004), but it is generally agreed that MSCs do not express CD34, CD45, CD14 or CD 11 which could help in identifying these cells (Chamberlain et al., 2007; Sasaki et al., 2008). Furthermore, several studies state that MSCs must express CD105, CD90 and CD73 or they cannot be considered to be MSCs (Rosenbaum et al., 2008; Kuhn and Tuan, 2009). CD105 or endoglin is a vital molecule in vascular development and angiogensis (Seon and Kumar, 2001; Takahashi et al., 2001; Wikstrom et al., 2002). Gene mutations in CD105 in humans are responsible for an autosomal dominant disorder, called hereditary haemorrhagic talengiectasia type 1, characterised by recurrent haemorrhage (Shovlin and Letarte, 1999). Endoglin is a receptor for TGFβ1 and TGFβ3 where TGFβ signalling regulates cell proliferation and differentiation (Pepper, 1997). Studies have shown

that CD73 or ecto-5'-nucleotidase have many functions including adhesion of lymphocytes (Airas et al., 1995) and may play role in T-cell proliferation (Massaia et al., 1990). Studies have shown that CD90 or Thy-1 is expressed in human fibroblasts, neurons, blood stem cells and endothelial cells (Rege and Hagood, 2006). CD 90 is involved in many functions including T-cell activation (Barboni et al., 1991) and fibroblast proliferation (Silvera and Phipps, 1995).

There are many methods available to isolate MSCs, including the fibronectin adhesion assay (Jones and Watt, 1993). This method depends on MSCs having a high surface expression of β1 integrins. MSCs express three kinds of β1 integrins; α5β1, the fibronectin receptor, α2β1 which plays a major role in binding to laminin and collagen and α3β1 which is a receptor of laminin. For this reason, fibronectin, an extracellular matrix glycoprotein, is used as it strongly binds to α5β1 which is strongly expressed by MSCs. In the Jones and Watt study, they found that β1 integrin density was directly proportional with colony forming efficiency which meant that β1 integrin density is increased in the cell surface of stem cells due to its proliferative potential. Another way to isolate MSCs is through magnetic activated cell sorting (MACS). This method is based on the isolation of cells by magnetism by adding MACS microbeads, developed by Miltenyi Biotec. These microbeads have a biodegradable matrix and they do not change activity or the structure of the cells. This technology had been used by many research groups, such as Quirici et al., 2002; Huang et al., 2009a; Lu et al., 2009. Another method which could be used to isolate stem cells is fluorescence activated cell sorting (FACS) by flow cytometry. It has the same principles as MACS. In this method monoclonal antibodies are used for the selection of cell markers expressed by MSCs. It has been used in several studies, such as Schwab and Gargett, 2007. Both methods (MACS and FACS) sorted cells based on their cell surface receptors such as CD146, CD271, CD71 and CD34 (Quirici et al., 2002; Schwab and Gargett, 2007; Huang et al., 2009a; Lu et al., 2009).

MSCs are considered to be a promising tool for the future of tissue engineering and regenerative medicine. However, they are some drawbacks such as their rare population (Friedenstein et al., 1982). This means an extensive *in vitro*

expansion necessary to produce sufficient cell numbers for clinical use. This is going to influence their biological properties which will be investigated in this study.

1.2.2.2 Hematopoietic Stem Cells (HSCs)

HSCs are adult stem cells. Their main function is maintaining a functional blood system throughout life, by their differentiation and proliferation into many types of blood and lymphoid cells, such as erythrocytes, granulocytes, monocytes, T-cells and B-cells (Stocum, 2001). HSCs are believed to exist in few numbers of specialized niches within the bone marrow, about one cell in every 10^5 bone marrow cells. They are also found in umbilical cord blood and the liver. HSCs are believed to be multipotent, because of their high plasticity and their ability to differentiate into many types of cells (reviewed in Stocum, 2001; Bongso and Lee, 2005; Forsberg and Smith-Berdan, 2009). HSCs are mainly isolated from bone marrow and are characterised by either FACS or MACS methods based on their surface markers, including CD34, C-KIT and CD90 (Stocum, 2001; Challen et al., 2009).

HSCs are considered as the most successful type of stem cells for therapy. HSCs transplantation is used as standard of care for many patients with congenital or acquired disorders of the hematopoietic system, such as leukaemia and lymphoma from the mid-seventies until now (Hołowiecki, 2008). There are several sources of HSCs for transplantation. The main one is the bone marrow, where side- effects in the donor are rare, about 2 deaths in every 8000 cases (Anderlini et al., 2001). Allogeneic bone marrow transplantation has been used for many years to treat patients with genetic immunodeficiency, metabolic disorders, bone marrow failure syndromes or in patients who have undergone radiation or chemotherapy. However, the majority of patients cannot match with an appropriate donor which leads to many complications. Recently, another source of HSCs have been found, which can reduce these complications is umbilical cord blood (Stocum, 2001). The first use of this transplantation technique was performed in a child with Fanconi's anemia (Gluckman et al., 1989). The following table was taken from Copelan, 2006 (Table 1.1), which shows the most common diseases treated with hematopoietic stem cell transplantation.

Table1.1. The most common diseases with hematopoietic stem cell transplantation (Copelan, 2006).

Autologous Transplantation		Allogeneic Transplantation	
Cancers	**Other Diseases**	**Cancers**	**Other Diseases**
Multiple myeloma	Autoimmune disorders	Acute myeloid leukemia	Aplastic anemia
Hodgkin's disease	Amyloidosis	Acute lymphoblastic leukemia	Fanconi's anemia
Non-Hodgkin's lymphoma		Chronic myeloid leukemia	Blackfan-Diamond anemia
Ovarian cancer		Hodgkin's disease	Thalassemia major
Neuroblastoma		Non-Hodgkin's lymphoma	Sickle cell anemia
Acute myeloid leukemia		Multiple myeloma	Paroxsymal noctrunal hemoglobinuria

1.2.2.3 Other Types of Adult Stem Cells

There are other type of adult stem cells that may contribute in the development of dental pulp based on their ectomesenchymal origins (Sinanan et al., 2004) such as endothelial stem cells (EnSCs), and neural crest stem cells. EnSCs were first isolated by Asahara et al (1997) from the human blood in the bone marrow. They expressed cell markers that were found in mature endothelium and HSCs including the vascular endothelial growth factor receptor-2 (VEGFR-2), CD34 and CD133 (Andreou et al., 2006). The main functions of EnSCs are repairing of endothelial damage, formation of new blood vessels and paracrine signalling (Sen et al., 2011). Alterations in numbers and functions of EnSCs may associate with many diseases such as cardiovascular diseases, diabetes and hypertension (Sen et al., 2011). EnSCs play an important role in tissue engineering of blood vessels (Zeng et al., 2010) and because of their role in signalling they are considered as a good candidate to use in tissue engineering to enhance the function of other adult stem cells (Fedorovich et al., 2010). For example, co-culture of DPPCs and EnSCs led to enhance the differentiation into osteogenic cell type when compared with culturing of DPPCs alone (Dissanayaka et al., 2012).

The neural crest is considered as a good model in stem cell biology because it gives rise to cells that form most of the skeleton and connective tissues of the head, face, neck and teeth. They also give rise for most of the peripheral nervous system (Kalcheim and Burstyn-Cohen, 2005; Chung et al., 2009). During neural crest development, Snail family members including Snail and Slug transcription factors and Notch family members are among the earliest markers that are expressed and used as indication of the neural crest stem cells (Kalcheim and Burstyn-Cohen, 2005). Neural crest stem cells are a heterogeneous population with different potentials of proliferation and differentiation (Lee et al., 2007). These cells can be isolated from many tissues such as skin, hair follicle and dental pulp and because of their differentiation capacity and high proliferative capacity without raising ethical concern they are a good candidate for clinical use (Ibarretxe et al., 2012). These cells have been successfully used to contribute in recovery of spinal cord injury in animal models (Hu et al., 2010).

1.2.3 Asymmetric Stem Cell Division

Adult stem cells have the ability for self-renewal and differentiate into multiple cell lineages, with short life-spans. To achieve self-renewal capabilities and differentiation functions, stem cells divide slowly and symmetrically to produce an identical daughter cell with low proliferative capacity and multipotential differentiation. Some of these adult stem cells go on to divide asymmetrically and give rise to one identical daughter cell and another progenitor cell called a transit amplifying (TA) cell. TA cells have high proliferative potential and low differentiation ability and give rise to more committed progenitors with reduced proliferative potential (Figure 1.1) (Ho, 2005). Despite enormous progress in the stem cell field, there are still many unanswered questions about stem cell division (Inaba and Yamashita, 2012). Asymmetric stem cell division is controlled in the stem cell niche by a combination of intrinsic and extrinsic cellular mechanisms. These mechanisms are becoming elucidated with advancing technology. For example, time-lapse microscopy has been used to demonstrate that neural progenitor cells in the cortex divided asymmetrically, to produce different cell lines (Ho, 2005). One example showing the vitality of asymmetric stem cell division in humans is that asymmetry maintains long term haematopoiesis, by the formation of blood cellular content, derived from HSCs (Ho, 2005) (Figure1.1). It is noteworthy that even if both daughters of a stem cell division express stem cell markers after few times of division, it does not exclude the possibility that one daughter is less proficient as a stem cell than the other over the long period of culturing (Inaba and Yamashita, 2012). This observation is important for tissue engineering field because it will take in consideration that these cells need more investigation to select the appropriate cells to use in stem cell therapy.

Figure.1.1. Asymmetric stem cell division (Ho, 2005).

Stem cells

Transient amplifying pool
(symmetric self-renewing divisions)

Asymmetric division

Stem cell

Asymmetric division

Differentiation
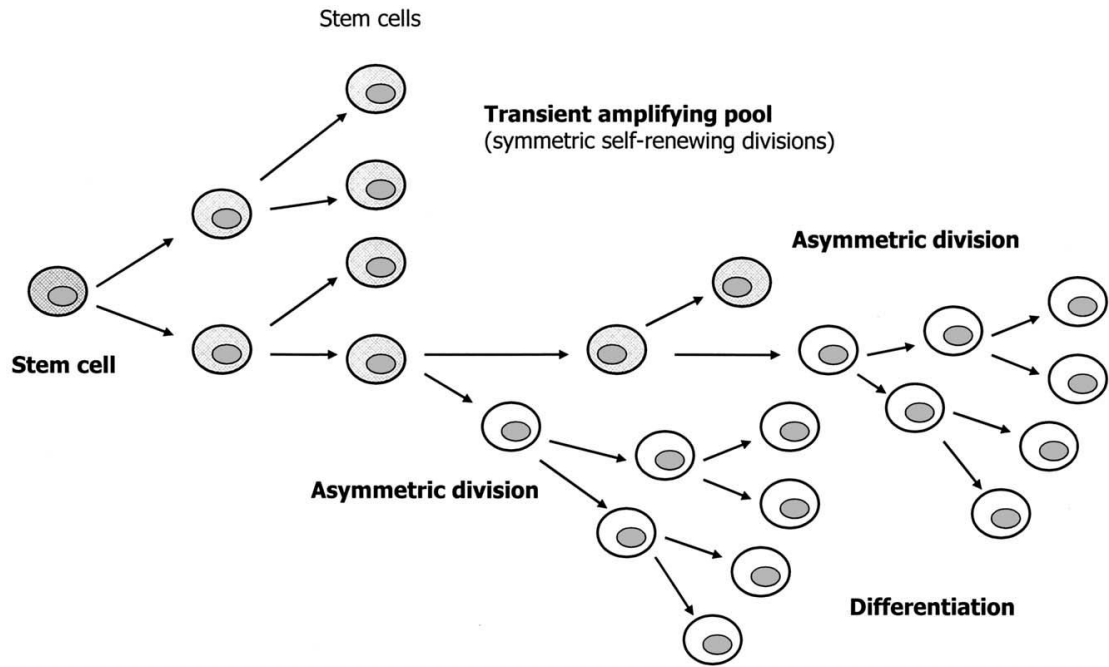
1.2.4 Stem Cell Niches

Generally, the word niche has several meanings according to the context in which it is used. For example, in ecology it refers to a habitat, while in French, it means a dog house (Scadden. 2006). In stem cell biology, the niche is a microenvironment place that contains elements which control stem cell differentiation, stem cell survival and stem cell renewal (Huang et al., 2009b). These elements include growth factors, cell-cell interaction and adhesion between the extracellular matrix and the cells (Discher et al., 2009). Stem cells reside in a quiescent state within their special niche and they start to proliferate and migrate when they respond to injury or physiological changes to their niche by systemic signals such as Notch (Mitsiadis et al., 2007; Drummond-Barbosa, 2008). The stem cell niche concept was first proposed in 1978 by Schofield, as a specialized microenvironment housing stem cells in mammalian haematology. It has been observed that adult stem cells behave slightly differently outside their niche. For example, HSCs, their niche is located in the bone marrow. In this niche, their main function is the maintenance of blood cells and immune systems throughout life. However, HSCs appear to have limited function when they are circulating freely outside their niche. The reasons why HSCs act properly inside the niche are specific signals provided by the niche (Scadden, 2006).

Using stem cells as a successful treatment is still hindered by several challenges. One of these challenges is the complete control of stem cells growth and differentiation (Vazin and Schaffer, 2010). It is believed that a better understanding of the stem cell niche will provide a better control of stem cells behaviour (Voog and Jones, 2010). Studying the stem cell niche *in vivo* provides better control of stem cell survival and their behaviour, in response to injury (Bendall et al., 2008). Most of our knowledge about the stem cell niche comes from studying cells of Drosophila. These studies explain how the direct contact of adjacent non-stem cells to the stem cell niche, play an important role in stem cell behaviour (reviewed by Fuchs et al., 2004). Later, other studies in the Drosophila model showed that extracellular matrix molecules and cadherin molecules have an influence on stem cell niche (Vazin and Schaffer, 2010). In mammals, the study of stem cell niche *in vivo* is more complicated than in lower organisms, because of the diversity of their components. However, the knowledge gained from lower organisms provides an important

principle to understanding mammalian stem cell niche through signalling between cells or cells and the extracellular matrix (Vazin and Schaffer, 2010). A stem cell niche inside the bone marrow is surrounded by osteoblasts. Studies in mice models show that by increasing the quantity and activity of osteoblasts the number of HSC is increased (Calvi et al., 2003; Zhang et al., 2003; Lo Celso et al., 2009). The extracellular matrix (ECM) around the stem cell niche also plays a role in stem cell behaviour, due to its content of signalling mediators and growth factors. For example, osteopontin (OPN), an important gene in bone remodelling, plays a role in HSCs regulation by interacting with CD44, a receptor in HSCs. A study in animals shows that a deficiency in OPN will lead to increases in HSCs. This means that OPN acts as restraint on HSCs number (Scadden, 2006). Another factor which affects the stem cell niche is oxidative stress which is going to be explained in the next chapter. Another important factor inside the niche is signalling. Osteoblasts can maintain HSC self-renewal and prevent differentiation by expressing Notch ligands jagged 1 to stimulate receptors on the HSC surface (Calvi et al., 2003). In addition, BMP/TGFβ superfamily may play role in the maintenance of HSCs in their niche (Zhang et al., 2003).

MSCs niches are found in different locations. Bone marrow is believed to be a major site for MSCs as well as HSCs. Dental pulp is another possible niche for MSCs (Shi and Gronthos, 2003). MSCs in the dental pulp have been localised in the perivascular and perineural sheath regions, by using antibodies against STRO-1, CD146 and pericyte-associated antigen (Huang et al., 2009b). Other studies have localized MSCs in capillaries and nerve networks within the cell free zone (Lizier et al., 2012), and the subodontoblastic cell-rich layer in the dental pulp (Hosoya et al., 2012). An example of the importance of signalling in the maintenance of the dental pulp stem cell niche, are ephrin (Eph) receptors which are components of signalling pathways involved in mammalian development. Eph receptors regulate the migration of DPSCs by several signalling pathway (Matsuo and Otaki, 2012). This finding suggests that Eph/Ephrin interaction may play a role in maintenance of DPSCs inside their niche (Stokowski et al., 2007). Another study by Bundesen et al., 2003 found that following spinal cord injury in rat, EphB/Ephrin-B expression is decreased and

cells subsequently migrate to the injury site. We can conclude from these two results that Eph receptors maintain the stem cell niche in the healthy phase.

1.2.5   Stem Cell Senescence

Ageing is a complex process that occurs due to cell damage which, leads to organ failure and eventually death. Every time the cell divides, it is susceptible to telomere shorting, which leads to cell senescence (Serakinci et al., 2008; Wagner et al., 2008). Cell senescence can be defined as the loss of a cell's ability to divide (Hayflick and Moorhead, 1961), which is different from apoptotic cells, as senescent cells remain alive, despite a change in their function (Itahana et al., 2001). The majority of cells in the human body have a limitation in their replicative potential described as the Hayflick limit (Petersen and Niklason, 2007). At the end of every chromosome there is a region of repetitive DNA known as a telomere that consists of tandem chromatin TTAGGG. Importantly, telomeres protect the end of chromosomes from weakening. After each cell replication the telomere becomes shorter due to incomplete linear chromosomal replication, by DNA polymerase, which can lead to damage to the ends of the chromosomes leading to cell senescence. Additionally, the process of oxidative stress can also shorten telomeres (Flores et al., 2006; Serakinci et al., 2008).

MSCs exist for as long as the organ they reside in (Fehrer and Lepperdinger, 2005). One of the reasons that make them survive this long is the telomeres which are required for both cell duplication and differentiation, which means MSCs should at least express some telomerase, in order to achieve these features (Fehrer and Lepperdinger, 2005). However, some MSCs show no or low level of telomerase activity (Zimmermann et al., 2003), which suggests there are other mechanisms within these cells, which are enable them to keep proliferating or maintaining their multipotent potential (Hiyama and Hiyama, 2007). Altogether, this suggests that MSCs *in vivo* are subjected to little or no telomere erosion. Therefore, if telomere maintenance can be achieved *in vitro*, this would mean huge benefits to tissue engineering (Fehrer and Lepperdinger, 2005).

MSCs exist in very low populations in their niche. In order to study these cells, it is essential to culture them for proliferation. For this reason, it is important to understand the process of aging during their proliferation in culture (Bonab et al., 2006). Population doubling (PD) is considered as a simple method to help estimate cell growth *in vitro* and the most obvious marker for cell senescence. Earlier studies have shown that human MSCs are more likely to lose their proliferative potential during expansion *in vitro* (Mets and Verdonk, 1981; Digirolamo et al., 1999; D'Ippolito et, al 1999). The number of days of culturing or passages of MSCs *in vitro* varies between studies depending on many factors, including the components of the medium are used, the cell source and the age of the donor. Bonab et al., 2006, expanded MSCs from the bone marrow of healthy individuals which showed a mean long-term culture of 118 days, the mean passage number was 9 and the average of PD declined from 7.7 to 1.2 in the 10th passage. Another study suggests that MSCs cannot be expanded beyond 7 passages (Market et al., 2009). Several studies show that donor age affects the rate of *in vitro* senescence in MSC (Stenderup et al., 2003; Mareschi et al., 2006). In the Mareschi study, it showed that PDs are almost doubled from paediatric donors, compared with adult donors. During passaging studies, MSCs were also show to be subject to molecular changes. During ageing, it has been suggested that MSCs decrease osteogenesis and chondrogenesis, while they increase their adipogenesis ability (Murglia et al., 2000; Moerman et al., 2004; Wall et al., 2007). These changes may affect the benefits of MSCs on cell therapy. Another criterion that distinguishes senescent cells is morphology. As cells progress through their proliferative lifespan, morphological changes take place. In early stage, cells tend to be bipolar and spindle shaped. However, cells are larger, wider, flattened and irregular in shape when they senesce (Sethe et al., 2006). They are also become multinucleated with loss of polarity (Matsumara et al., 1980). Furthermore, it is been found that there is correlation between increasing of cell size and increasing of actin microfilaments organisation (Wang and Gundersen, 1984). Another marker for cell senescence is β-galactosidase activity. This enzyme is easy to detect by using histochemical stain in senescent cells, but not in quiescent or immortal cells (Dimri et al., 1995).

1.3   Tissue Engineering and Regenerative Medicine

There is a growing need for tissue engineering because of increasing in life expectancy which is accompanied with elderly diseases such as osteoporosis (Kanis et al., 1994) and Alzheimer's disease (Pouryamout et al., 2012). Moreover, a wide range of diseases cause organ failure which often cannot repair itself. The accepted treatment of these conditions in the past 50 years was to remove the injured part and replace it with different types of structure, either synthetic such as knee replacement, intraocular lens and prosthetic heart valves or natural such as an organ from donor (Williams, 2006). However, there are limitations of these replacements including shortage of donor organs, rejection, the need of life-long immunosuppressants and biocompatibility (Williams, 2006). Therefore, the development of regenerative medicine has been promoted to outcome these shortcomings. Tissue engineering and regenerative medicine are aimed to restore normal structure and function through the production of new tissue that regenerates exactly that which has been lost by using combination of cells, and tissue inducing substances such as growth factors placed within matrices such as collagen (Langer and Vacanti, 1993).

1.3.1   Role of Biomaterials in Tissue Engineering

The purpose of using scaffolds in tissue engineering along with desired seeded cells is to imitate the biologic and mechanical function of ECM that naturally occurs in the human body to help deliver these cells to the desired sites in the body and therefore restore the damaged tissue (Kim and Mooney, 1998). Scaffolds have been used for a long time in the tissue engineering field (Ma et al., 1999; Altman et al., 2002; Li et al., 2006; Tai et al., 2010). Significant efforts have been made to construct scaffolds that are similar to the natural extracellular matrix. These scaffolds are made from different type of material that can be divided into two main types: synthetic and natural. Natural biomaterials used in scaffolds for stem cell cultures are either made from ECM components (collagen or hydroxyapatite) or other natural sources (silk, fibroin or chitosan). Synthetic materials include polyglycolide and polylactide (Dawson et al., 2008; Vazin and Schaffer, 2010; House et al., 2010). The ideal biomaterials to use in tissue engineering field should be biodegradable, bio-resorbable and has good mechanical properties without inducing any unwanted response such as inflammation or swelling (Bergsma et al., 1995; Atala, 2012).

Moreover, a combination of adhesion peptides such as Arg-Gly-Asp (RGD) and fibronectin, which are naturally found in collagens and growth factors, enhanced cell adhesion and migration inside biomaterial scaffold (reviewed in Gurtner et al., 2007). Many extracellular matrix components such as collagen, fibrinogen, hyaluronan acid, glycosaminoglycans (GAGs) have been used as scaffold materials (Dawson et al., 2008). These components provide a physical structure and natural signals which control stem cells behaviour (Vazin and Schaffer, 2010). For example, a collagen/hyaluronan matrix was found to be enhanced neural stem/progenitor cells differentiation (Bränvall et al., 2007).

Collagen is the most common protein found in the human body (Karamichos et al., 2007). Collagen type I is most commonly used in scaffolds because of its abundance, ubiquity and biocompatibility (Glowacki and Mizuno, 2008). Also, collagen contains cell adhesion domain sequences (e.g., RGD) that may contribute in maintaining the phenotype and activity of many types of cells, including fibroblasts (Silver and Pins, 1992). Primary hepatocytes have a low proliferation ability and gradual loss of function by expressing low albumin level when they are grown *in vitro*. However, when they are grown on collagen type I modified scaffolds they show higher albumin levels which exhibit that they are functioning better on collagen scaffold (Tai et al., 2010). It is also highly desirable to use collagen gels for the culture of BMSCs because it maintains cell attachment and proliferation (Hesse et al., 2010). DPSCs have almost same properties with BMSCs (Huang et al., 2009b) and for this reason collagen type I will be used to culture DPSCs in this study. Collagen type I is the most abundant protein in dentine and a major component for primary and reparative dentin formation (Linde, 1989). Collagen type I scaffold with other components including dentin matrix protein-1 and BMP-7 with DPSCs have been used in tissue engineering of the tooth in order to attempt to form hard tissue and it has been shown that these elements enhance DPSCs differentiation (Prescott et al., 2008; Wang et al., 2010). In the present study cultures these cells and imitates compromise tissues in the collagen gel are to be investigated.

1.3.2   Mesenchymal Stem Cells and Tissue Engineering

Tissue engineering is defined as the use of combination of living cells with biodegradable material to regenerate the affected tissue in the patient (Lanza et al., 2007). Recently, many aspects of tissue engineering have been investigated including methods of cell isolation, expansion, differentiation and transplantation (Khademhosseini et al., 2009). Cells can be used for therapy via injection with carriers such as hydrogels or even alone without a carrier (Atala, 2012). Many types of stem cells have been used for tissue engineering purposes such as embryonic stem cells (Hwang et al., 2006), hematopoietic stem cell (Copelan, 2006), Bone marrow progenitor cells (Cho et al., 2006), adipose derived stem cells (Bunnell et al., 2008), neural stem cells (Olson et al., 2009), dental follicle stem cells (Honda et al., 2010) and DPPCs (Arthur et al., 2009).

MSCs are considered as promising tools in the tissue engineering field since they have the ability to give rise to progenitor cells. These cells can be expanded in culture and differentiate into specific cell lineages to replace the damaged cells. Many research groups have isolated MSCs from different tissues and characterised them to find the best conditions to grow them in order to use in numerous medical applications. Culture medium, addition of growth factors, mechanical stimuli and oxygen levels are examples of conditions that influence MSCs stemness, proliferation and differentiation capacity (reviewed in Lavrentieva et al., 2013).

DPPCs have been suggested for use in bone tissue engineering because they have the ability to differentiate into osteocytes *in vitro* and *in vivo.* Osteogeneses has been confirmed by Alkaline Phosphatase, Van Kossa staining and reverse transcription-polymerase chain reaction (RT-PCR) analysis of osteogenesis-specific genes (Li et al., 2011; Khanna-Jain et al., 2012; Akkouch et al., 2013). Furthermore, DPPCs showed better osteogenesis differentiation in compare with BMPCs in terms of expression of bone markers which make them a good candidate to be used in bone tissue engineering applications (Alge et al., 2010).

Conversely, the use of MSCs in tissue engineering is hampered by large donor variability and the loss of stemness during *in vitro* expansion which eventually leads

to cell senescence (Alves et al., 2013). In order to investigate the correlation between the age of donor or *in vitro* expansion with MSCs differentiation capacity, a number of studies have been performed (Bonab et al., 2006; Siddappa et al., 2007; Agata et al., 2010; Kim et al., 2012). A specific study compared the effect of *in-vitro* culture by time with increasing passage number, and found that the former has more effect on MSCs than the latter (Stenderup et al., 2003). It showed that increasing the number of *in-vitro* passages led to a decrease of their ability to differentiate into osteogenic and adipogenic lines while the donor age did not affect the differentiation ability between young and old groups (Stenderup et al., 2003). However, this is not always the case. There are many conflicting results about the age effects which may be due to age of the donor or the ageing within the *in vitro* culture. These conflicting results were showing that this aging either has no effect on differentiation ability of the cells (Justesen et al., 2002; Scharstuhl et al., 2007) or it affects the differentiation into either adipocytes or osteoblasts or even both (Wall et al., 2007; Stolzing et al., 2008; Kretlow et al., 2008). Nonetheless, most of the studies demonstrated changes in cell proliferation and cell senescence during ageing (Stenderup et al., 2003; Mareschi et al., 2006; Kretlow et al., 2008). In this study, the effect of *in vitro* culture in term of cell senescence, differentiation capacity and telomere length will be studied upon different clones of MSCs. Cellular senescence during *in vitro* expansion of MSCs could be the result of intrinsic (telomere length) or extrinsic (oxidative stress, DNA damage) factors (Ben-Porath and Weinberg, 2005). Accumulation of DNA damage during *in vitro* culture, which could be induced by oxidative stress due to the presence of hydrogen peroxide, has been linked to the loss of differentiation potential of human MSCs (Alves et al., 2010).

1.4   Oxidative Stress

Oxidative stress is induced as a consequence of the generation of reactive oxygen species (ROS) which is a collective term including; oxygen-derived free radicals, such as the superoxide radical ($O_2^{.-}$) and hydroxyl ($^.OH$) radical species, and non-radical derivatives of oxygen, such as hydrogen peroxide (H_2O_2) and hypochlorous acid (HOCl) (reviewed in Waddington et al., 2000). ROS are produced naturally through a variety of cellular processes. However, excessive production of ROS contributes to severe damage to cellular components, loss of cell function, and

ultimately apoptosis. The free radical is defined as any species capable of independent existence that contains one or more unpaired electrons in an outer orbit (Halliwell *et al.,* 1992). They are generated as by-products of metabolism in cells and react indiscriminately with organic molecules due to their instability. These molecules include proteins, lipids, carbohydrates and nucleic acids (reviewed in Waddington *et al.,* 2000). Oxidative stress occurs as a result of biochemical disequilibrium, between ROS production and antioxidants, which cause accumulation of oxidative stress leading to oxidative damage (reviewed in Waddington *et al.,* 2000). This has led ROS to be involved in a variety of disease states, including AIDS, cancer, atherosclerosis, chronic inflammatory conditions, diabetes mellitus and in the ageing process (Halliwell *et al.,* 1992; Ames *et al.,* 1993; Beckman and Ames, 1998; Evans *et al.,* 2004; Moussa, 2008). Under normal conditions, cells lose about 90pb each population doubling, while when they subjected to oxidative stress they lose more than 500pb each population doubling (Von Zglinicki et al., 1995). Their influence on stem cells may vary between inhibition of self renewal ability and at the same time, serving as a signal stimulating stem cell differentiation based on their concentration (reviewed in Dayem et al., 2010).

H_2O_2 is a type of ROS that exists in almost all human cells with mitochondria being the main source during metabolism (Halliwell et al., 2000; Giorgio et al., 2007). H_2O_2 is believed to be cytotoxic and cause damage to the DNA (Ballinger et al., 1999). However, studies have revealed that H_2O_2 can also be used as a signalling molecule involved in many different cellular processes (Rhee, 2006; Veal et al., 2007). For example, H_2O_2 appeared to be a key messenger for cell adhesion by activating tyrosine kinases (Giannoni et al., 2005). Both positive and negative effects depend on H_2O_2 concentration and cell type (Rhee, 2006; Veal et al., 2007). Indeed, human tissues are exposed to different concentrations of H_2O_2 which varies from less than 1mM in blood plasma (Frei et al., 1988) to more than 100mM in the oral cavity (Long et al., 1999). It is noteworthy to know that damage to DNA and other cellular components does not come directly from H_2O_2 but from its ready conversion to the indiscriminately reactive hydroxyl radical (OH) which is the result of reduction of

H_2O_2 by ferrous or cuprous ion known as Fenton reaction (Martins and Meneghini, 1994; Halliwell et al., 2000) :-

$$Fe2^+ \quad + \quad H_2O_2 \quad \rightarrow \quad .OH \quad + \quad OH- \quad + \quad Fe3^+$$
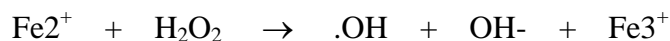
Human cells protect themselves against this danger by a network of endogenous antioxidant defences (reviewed by Waddington et al., 2000).

1.4.1 Antioxidants

Antioxidants are exogenous or endogenous molecules, which have the ability to prevent or slow the oxidation of other molecules. Antioxidants prevent oxidation by scavenging ROS or their precursors. These are very important for human health, for the prevention of oxidative damage to cellular components, such as proteins, lipids and DNA (reviewed by Waddington et al., 2000; Andriantsitohaina et al., 2012). There is a wide diversity of antioxidants in the human body, which may be enzymatic or non-enzymatic in nature (Sies, 1997). There are many compounds of non-enzymatic antioxidants including ascorbic acid, lipoic acid and carotenoids (Andriantsitohaina et al., 2012). Their activity as antioxidant is low and acts mostly due to their metal ion binding capacity (Lee et al., 2008). For enzymatic antioxidants, there are three main enzymes which play a role in protecting cells against oxidative stress. These include Superoxide dismutases (SODs), catalase and glutathione peroxidases. SODs are the most important antioxidants in mammalian tissues, because they defend against oxidation in almost all cells. There are three major SOD types which have been identified in humans to date, SOD1 or CuZn-SOD contains a copper and zinc containing homodimer (Zelko et al., 2002). It is located in the cytoplasm. SOD2 or Mn-SOD exists as a tetramer and is located in the mitochondria (Zelko et al., 2002). SOD3 or EC-SOD is found in the extracellular space and forms a glycosylated homotetramer (Fattman et al., 2003). Catalase is an enzyme found in most living organisms which are exposed to oxygen. Mainly, it is found in the peroxisomes. These enzymatic antioxidants work in collaboration to protect human body against oxidative stress, where SODs catalyze the dismutation of O_2^- into H_2O_2 and O_2 and then H_2O_2 reduced to H_2O by catalase (Andriantsitohaina et al., 2012). Although antioxidant seems important in scavenging ROS, that cause diseases such as atherosclerosis, it has been found to be non-effective to apply it *in vivo* because of the complexity of their reactions (reviewed by Halliwell, 2012).

Stem cells have shown a high ability to resist oxidative stress by increasing their antioxidant capacity (Dernbach et al., 2004; He et al., 2004). This will support using stem cells in tissue engineering and regenerative medicine as it has been shown that using muscle-derived stem cells increased antioxidant-resistant capacity which led to enhance regenerative capacity in skeletal and cardiac muscle (Urish et al., 2009).

1.4.2   Oxidative Stress and Stem Cells

Imbalance between ROS and antioxidants will result in accumulation of oxidative stress inside the cells. This could cause damage to cell components, including proteins, lipids and nucleic acids which may result in adverse biologic effects, such as changes in the signalling pathways or gene expression (Camargo et al., 2009). For example, a study showed that endothelial progenitor cells (EnPCs) lose their function in response to oxidative stress (Case et al., 2008). Moreover, H_2O_2 treatment for endothelial progenitor cells reduced their clonogenic capacity and impaired the ability of them to form blood vessels *in vitro* and *in vivo* (Ingram et al., 2007).   Also, in a rat model of myocardial infarction, increased production of ROS has been linked with reduced EnPC levels (Thum et al., 2006). Although, ROS are toxic, they also function as signalling molecules inside the stem cells niche, controlling apoptosis, proliferation, self-renewal, senescence and differentiation (Case et al., 2008). One ROS that plays a role in activation of several cell surface receptors is H_2O_2. For example, neutrophils are activated to engulf and kill foreign bodies depending on NOX (a subunit of NADPH Oxidase) which release very small amount of H_2O_2 as signals (reviewed in Rhee, 2006). Also, p38 MPAK pathway, which is involved in cell differentiation and apoptosis, is activated when oxidative stress increases in HSCs. This shows that the regulation of oxidative stress is vital to maintain HSCs quiescence (Arai and Suda, 2007). Furthermore, another study found that BMSC niche for HSCs is believed to be a hypoxic environment. This environment maintains the stemness of the cells and protects the stem cell against ROS, as low oxygen results in decreased respiration by mitochondria and prolonged cell lifespan (Eliasson and Jönsson, 2010).

Furthermore, it has been proved that stem cells can resist oxygen overload more than other cells. This has been shown in endothelial progenitor cells which

demonstrated more resistance to oxidative stress than mature umbilical vein endothelial cells by revealing higher production of antioxidative enzymes (Dernbach et al., 2004).

1.4.3   Oxidative Stress and Dental Pulp Progenitor Cells

In the dental pulp, there are many different sources of oxidative stress. These sources could be divided to internal and external. Accumulation of oxidative stress with aging is one of internal sources. This accumulation causes damaging to the DNA, which eventually leads to cell death (Rossi et al., 2008). Another internal source is inflammation. A recent study showed that the development of pulpitis accompanied with a decrease of monoamine oxidase (MAO), which catalyzes the oxidation of monoamines, and increase in the amount of semicarbazide-sensitive amine oxidase (SSAO), which is involved in the inflammation and oxidative stress in other tissues (Vavilova et al., 2009). Finally, diabetes is also could be another internal source of oxidative stress. Several studies have demonstrated that the levels of all ROS increase during diabetes (Alp *et al.,* 2003; Sadi and Guray, 2009). Hyperglycaemia increases the production of O_2^-, H_2O_2 and $^.OH$, by the mitochondrial electron transport chain, which inhibits GAPDH activity (Góth, 2008). Such events can induce mutations in mitochondrial DNA, which cause the major overproduction of ROS (Kowluru and Chan, 2007). A recent study showed that diabetes causes modification in the structure of the dental pulp by inducing the expression of inflammatory mediators which eventually increase the amount of oxidative stress (Leite et al., 2008).

Several types of dental materials and treatment techniques are the main external sources that could cause oxidative stress in the dental pulp. Dentin bonding agents, such as HEMA and TEGDMA, used to improve the contact between filling materials and the prepared cavity of the dental wall. These materials are believed to be cytotoxic and cause the formation of ROS which eventually may lead to cell death (Demirci et al., 2008). Some dental treatment techniques such as magnetostrictive ultrasonic scalers and high speed handpieces could also generate heat to the tooth surface and so raise the temperature of the dental pulp (Nicoll and Peters, 1998; Cavalcanti et al., 2003). Changing the temperature of the dental pulp can induce an

inflammatory reaction. A number of studies in animal models found that applying heat to the dental pulp will increase interleukin (IL-1) and tumor necrosis factor (TNF-α) expression (Chang et al., 2009). TNF-α is known to induce ROS and decrease antioxidant enzymes which leads to elevation of oxidative stress (Dhingra et al., 2007). Dental bleaching is based on H_2O_2 applied to the enamel surface which may traverse dentinal tubules that will affect the pulp cavity (Ubaldini et al., 2013). For this reason and because cells investigated in this study are located in several niches in the dental pulp (Sloan and Waddington, 2009), an introduction about the tooth structure and the development of these cells will help for more understanding of these cells and their markers.

1.5   Tooth Development

The first arch epithelium, which gives rise to the maxilla and mandible, has a main influence on the induction of tooth development (Mina and Kollar, 1987). The dental pulp is created of ectomesenchymal components, resulting from interaction between ectoderm and mesoderm layers, during the six week of embryogenesis (Sinanan et al., 2004). Ectomesenchyme cells participate in tooth development, from the cranial neural crest cells which later form dental papilla. Other studies have demonstrated that the dentine matrix, odontoblasts and most of the pulpal tissue are of cranial neural crest origin (Chai et al., 2000; Sloan and Smith, 2007).

Primary odontoblasts differentiate from dental papilla cells, in response to signals derived from the inner dental epithelium and mediated by the basement membrane. These dental papilla cells come into contact with the basement membrane at the last line of division, resulting in two daughter cells. One of these cells becomes terminally differentiated odontoblast after it responds to the molecular signals mediated through basement membrane. The other one remains in the cell-rich zone where cells are kept in the undifferentiated state (Ruch et al., 1995; Sloan and Smith, 2007). These cells are called undifferentiated mesenchymal cells.

1.6   Dental Pulp

Dental pulp is soft tissue, arising from ectomesenchymal and mesenchymal origin which develops from the dental papilla. It consists of connective tissue, water, blood vessels, nerves, lymphatics, fibroblasts, immune cells and odontoblasts (Trowbridge, 2003). Dental pulp contains a heterogeneous cell population. The majority of these cells are fibroblast-like cells, with inflammatory, immune and DPPCs (Goldberg et al., 2008). Indeed, it is proposed that DPPCs exist in several niches within dental pulp. However, the nature and origins of these DPPC clones with contrasting proliferative capacities have yet to be elucidated. This is because DPPCs have two origins; one is neural crest and the other is mesoderm and it is difficult to distinguish between them (Komada et al., 2012). Mostly they have been reported that they reside in the perivascular/pericyte zone (Alliot-Licht et al., 2001; Shi and Gronthos, 2003; Téclès et al., 2005). Others suggested that DPPCs could be located anywhere in the coronal pulp, such as subodontoblastic layers controlled by Notch signalling molecules (Løvschall et al., 2005) or in the capillaries and nerve networks in cell free zone (Lizier et al., 2012). In mouse incisor teeth, the cervical loop was suggested to be another location where DPPCs reside because this where odontoblast differentiation begins (Feng et al., 2011). During tooth eruption and before the completion of root development, odontoblasts are responsible for the secretion of the primary dentin which comprises most of the tooth mass surrounding the pulp (Smith et al., 1995). After the completion of root development, secondary dentin is secreted at a much slower rate than primary dentin throughout life (Smith et al., 1995). Reactionary dentin is secreted from surviving post mitotic odontoblast cells in response to mild injury. During severe trauma to the tooth, such as excessive caries and fracture, the death of several odontoblasts will occur and then DPPSCs may differentiate into odontoblasts like cells which are responsible for the secretion of tertiary dentin called reparative dentin (Smith et al., 1995; Duque et al., 2006). The isolation of pulp cells, from different species, has been achieved in many studies. However, Gronthos et al., 2000 were the first group to characterize a unique population of postnatal human dental pulp stem cells (DPSCs), these cells demonstrating an ability to self-renew using colony forming efficiency assay and differentiation into odontoblasts-like cells (Sloan and Smith, 2007, Gronthos et al., 2000).

1.7   Dental Repair

Unaffected odontoblasts protect the dental pulp by producing a reactionary dentin, in response to mild caries or pathological abrasion or superficial tooth preparation in the dental clinic (Lesot et al., 1993). On the other hand, severe injury to the dental pulp, such as severe caries or trauma may cause death of odontoblasts by bacterial toxins. In this case, a subpopulation of pulpal cells, DPPCs, which is believed to reside in the cell rich subodontoblast layer of Höehl are recruited to proliferate and differentiate into odontoblast like cells. A recent study suggested that DPPCs niche reside in the perivascular regions of the pulpal cavity, from which they migrate to the site of injury (Tecles et al., 2005). DPPSCs produce an extracellular matrix to act as dentinal reparative bridge. However, this matrix is permeable which makes it unable to protect pulp against bacteria. For this reason, studying these cells may be help to find new therapeutic agents to protect the pulp (Tziafas et al. 2000; Goldberg et al., 2008).

During dental repair, growth factors play a role in recruitment of DPSCs. The main growth factors that are believed to be responsible to control DPSCs proliferation and differentiation are transforming growth factor beta (TGFβ) superfamily including BMPs, platelet-derived growth factor (PDGF) and insulin-like growth factor (IGF) (King et al., 1997; Iohara et al., 2004; Saito et al., 2004). The BMPs family and their receptors are understood to influence DPSCs, by causing them differentiate into odontoblast like cells to secrete dentin (Satio et al., 2004). Several studies have found that BMP-7 TGF-β1 and –β2 stimulate the secretion of extracellular matrix by odontoblasts in a rat tooth slice model and *in vitro* (Sloan and Smith, 1999; Sloan et al., 2000). Following pulpal injury, an inflammatory response develops which could harmfully affect the growth factors such as BMP-7 which is found to be insufficient to induce dentin with inflamed pulp compared with healthy pulp (Rutherford and Gu, 2000).

1.8   Dentine Matrix

Bone and dentin are mineralized tissues that have close organic matrix composition, which are mostly made of type 1 collagen (Qin et al., 2007). The main function of dentin is to protect the pulp and to provide support for overlying enamel and

cementum. The mature dentin consists of 70% mineral, 20% organic matrix and 10% water (Kim and Simmer, 2007). During dentin formation, odontoblasts secrete unmineralized type 1 collagen called predentin, with other molecules such as glycoproteins, sialoproteins and phosphoproteins (Silva et al., 2004). After that, predentin is mineralized by the deposition of hydroxyapatite crystals onto the fibrous matrix. The dentin molecules become trapped in the mineralized phase, bound to matrix components (Silva et al., 2004).

The dentin matrix includes different type of collagens mainly type 1 (86%) and type 3. It also contains different types of non-collagenous proteins (NCPs) with other proteins such as proteoglycans. SIBLINGs (small integrin binding ligand, N-linked glycoprotein) family is one of important class of non-collagenous proteins, consisting of dentin matrix protein1 (DMP1), osteopontin (OPN), bone sialoprotein (BSP), matrix extracellular phosphoglycoprotein (MEPE) and dentin sialophosphoprotein (DSPP). These proteins could be used as markers to confirm the differentiation of DPPCs into odontoblasts. SIBLINGs proteins are secreted by odontoblasts or osteoblasts during formation and the mineralization of both dentin and bone. These proteins are also found to be expressed in soft tissues, such as kidney and salivary gland (MacDougall et al., 2006).

DMP1 was first identified in odontoblasts and later in some soft tissues, including different types of tumours. It is an acidic phosphorylated protein, rich in phosphoserine, glutamic acid and aspartic acid that regulates apatite crystals in mineralising tissues and mediates cell attachment through RGD domain. In DMP1 knockout mice there is defective dentin development which shows the important of this protein in dentin formation (Von Marschall and Fisher, 2008).

Dentin phosphoprotein (DPP) and DSPP are the most abundant dentine specific proteins, related to dentin nucleation and mineralisation. It is found in bone but in much lower concentration than in dentin. Both of these proteins are found to be encoded in one gene. DPP and DSPP functions are still unclear. However, as they are expressed primarily in odontoblasts and predentin, before the beginning of mineralisation it may be further involve in dentin formation. Also, DSP is found to

have a slight effect on the formation of hydroxyapatite which has a role in dentinogenesis. A tooth defect was found in DSPP null mice similar to human dentinogensis imperfecta III with hypomineralization suggesting that DSPP has a role in dentin formation (MacDougall et al., 2006; Maciejewska et al., 2006; Yamakoshi et al., 2005).

In addition to these proteins, the dentin matrix has been identified to have many molecules, including TGF-βs, fibroblast growth factors, insulin like growth factors and BMPs which are considered to play an important role in odontoblast differentiation (Sloan and Smith, 2007).

1.9 Aims

The four main aims in this study of human DPPCs are:

1- To investigate the effect of *in vitro* expansion of DPPC clones isolated from two different patients by investigating proliferation and differentiation. In addition, the effect of age-related changes on telomere length that occurs in DPPCs will be investigated, followed by oxidative stress induced senescence and the effect on telomere length.

2- To identify differences between individual clones in terms of proliferation rate, stem cell marker expression, differentiation capacity, resistance to oxidative stress and telomere lengths.

3- To research the most convenient method for identifying the preferable clones for use in tissue engineering and regenerative medicine. There is still no single easy technique to investigate the clones that are most convenient for use without the need for *in vitro* expansion and other multiple methods. For this reason, Raman spectroscopy will be used as a suitable identification method.

4- To investigate the interaction of DPPCs with collagen matrices, to evaluate whether type 1 collagen could be used to imitate the natural niche of DPPCs, which will give better understanding of these cells for use in tissue engineering.

Chapter 2:

Effects of *In Vitro* Expansion and Oxidative Stress on Dental Pulp Progenitor Cells Proliferative Lifespan

2.1 Introduction

Dental pulp progenitor cells (DPPCs) are an adult stem cell population that express similar markers as other mesenchymal stem cells (MSCs) (Huang et al., 2009b). Gronthos et al (2000) first reported the identification and isolation of DPPCs. DPPCs are described as having a typical fibroblast like morphology with a high clonogenic ability, rapid proliferation rate, and capacity to form mineralized tissue that express alkaline phosphatase, osteocalcin (OCN), and osteopontin (OPN), both *in vitro* and *in vivo*. DPPCs are proposed to be better candidates for use in clinical applications compared with other MSCs isolated from bone marrow, adipose tissue, and umbilical cord blood, because they have minor ethical issues, are easily accessible, and produce very low morbidity as these cells are obtained from extracted teeth (Nakashima et al., 2009). DPPCs are easy to harvest from extracted teeth, mainly third molars since their extraction is a common procedure. Third molars extracted at an early stage of their development make them a rich source for isolation of DPPCs, and they interact with biomaterials making them ideal for tissue reconstruction (reviewed in Graziano et al., 2008; Nakashima et al., 2009; Sloan and Waddington, 2009; Atari et al., 2012). In addition, they have extensive differentiation capabilities, including a high potential for neural differentiation (Sakai et al., 2012).

DPPCs isolated using the single colony method, is demonstrated to isolate highly proliferative clones with the capacity for multiple differentiation (Sloan et al., 2009). However, the pulp tissue is heterogeneous, and many papers suggest that clones are located in different niches within the pulp (Section 1.6). Fitzgerald and colleagues showed that undifferentiated DPPCs reach synthesis phase (S-phase) at different times i.e. proliferation, but differentiation occurs at the same time for all cells. The differentiation synchronisation could be due to the establishment of cell-to-cell communication (Fitzgerald et al., 1990). Therefore, DPPCs exhibit different behaviour in different studies, according to the method of isolation, age of the donor,

the condition of the pulp and other reasons. So far, at least two different stem cell populations have been identified; one arising from the neural crest and the other from mesenchymal origin (Waddington et al., 2009). Stem cells from both origins exhibit similar cell surface marker expression in terms of adult stem cells, such as Stro-1. However, cells of mesenchymal origin strongly express $\beta 1$ integrin which binds to fibronectin of the extracellular matrix in the dental pulp, while neural crest cells strongly express neural crest-associated markers such as low affinity nerve growth factor receptor (LANGFR) (Waddington et al., 2009). In general, both these cell subsets express numerous markers, including CD13, CD29, CD44, CD59, CD73, CD90, CD105, CD146 and STRO-1, but do not express haematopoietic markers such as CD14, CD24, CD34, CD45, CD19 (Lindroos et al., 2008, Huang et al., 2009b, Karaöz et al., 2010). Although there are many studies on DPPCs, the stemness ability of these cells is still unclear which hinder their ability to be applied clinically. Another one of these drawbacks is the cell senescence induced during *in vitro* cell culture.

2.1.1 Factors Influencing Mesenchymal Stem Cells Behaviour Which May Affect Their Quality Implication for Cell Therapy

After many years of research on MSCs, work has now developed towards the assessment of MSC therapies in clinical trials for multiple medical applications. However, their status as being true stem cells and their ability to differentiate to highly specialized cells, such as cardiomyocytes and neurons are still not satisfactory (Brooke et al., 2007). One of the drawbacks of using these cells in medical application is that the number of cells for prospective isolation is very low, estimated at 0.01%- 0.001% of the total number cells within bone marrow (Friedenstein et al., 1982). This means that these cells will require extensive *in vitro* expansion before sufficient cells are obtained for possible clinical use. However, expansion may have an effect on the quality of the cells eventually obtained. It has been shown that MSCs from human bone marrow tend to lose their multipotentiality, proliferation rate and ability to differentiate to bone, during expansion *in vitro* (Banfi et al., 2000). Indeed, cell senescence is a key factor that affects cells in culture, as described below. Also, another factor that may affect the use of these cells in tissue engineering is the diversity in each clone being isolated. Heterogeneous cells are expected to produce

unwanted biological activity while homogenous cells more desirable to use in the clinic (Karystinou et al., 2009). The claim of clonal variation was supported in the dental pulp MSCs clones by several studies. One of these studies found that only three clones out of twenty clones derived from dental pulp have the ability to proliferate over 20PDs (Gronthos et al., 2002). In the bone marrow, only four clones out of fifty grow beyond 50PDs and some clones take 44 days to reach 20PDs while others take 130 days to reach the same milestone (Karystinou et al., 2009). Also, these variations have been shown in many levels such as the site they have been isolated (Huang et al., 2009b) the donor age (Gala et al., 2011) and even variations from the same site of the same donor (Karystinou et al., 2009). Huang et al., 2009b have shown that the PD of DPPCs varies between one site to another. For example, progenitor cells from dental pulp varied from 60-120PDs and from deciduous teeth were over 140PDs while from bone marrow it varied between 30 and 50PDs. It has been shown that Progenitor cells from bone marrow are age dependant (Pittenger et al., 1999)

2.1.2   Telomeres and Telomere-independent Senescence

Telomeres are believed to predict the future life of cells. Telomeres are special regions at the ends of eukaryotic chromosomal DNAs. Human cells contain 92 telomeres but controversy surrounds whether it is the average telomere length or the shortest telomere that decides the cell age (Brandl et al., 2011). Loss of telomeric DNA has been observed *in vitro* for each population doubling in same matter *in vivo* when cells divided which is estimated 50bp after each cell passage (Harley et al., 1990). This process of telomere shortening as consequences of repeated cell division is called replicative senescence (Hayflick and Moorhead, 1961). Telomeres are protected by ribonucleoprotein enzyme telomerase. It has been reported that lack of telomerase cause shortening of telomeres (Yu et al., 1990). It is known that telomerase is required for both cell duplication and differentiation which means MSCs should at least express some telomerase in order to achieve these targets. Altogether, this suggests that MSCs *in vivo* are subjected to little or no telomere erosion. Therefore, if telomere maintenance can be achieved *in vitro*, this would be beneficial from a tissue engineering point of view (Fehrer and Lepperdinger, 2005). However, there are several immortalised *in vitro* cell lines that have long telomeres

without expression of the telomerase (Bryan and Reddel, 1997). Therefore we could hypothesis that the telomere length maintenance is not only protected by telomerase but there are other factors that protect the telomere length to maintain the cell proliferation. When cells senesce due to telomere shortening it is referred to as telomere-dependent senescence. On the other hand, when cells become senescent for reasons other than telomere shortening it is referred to as telomere-independent senescence (reviewed in Reddel, 1998). One of the causes of cell ageing is accumulation of oxidative stress resulting from cellular metabolism (Harman, 1956). All actions that cause cell senescence will activate various signaling pathways. These signals include p53, p21$^{Cip1/Waf1}$ and p16^{Ink4a} (Campisi et al., 2007). DNA damage mediated by tumour suppressor gene p53 protein initiates growth arrest and cell senescence by inducing p21, which subsequently increases p16 (Chen and Ames, 1994; Itahana et al., 2001). Under condition of stress, p16 inhibits formation of active cyclin D-CDK complex, preventing Retinoblastoma protein phosphorylation, to block the cells to transfer from G1 into S phase (Sharpless and DePinho, 1999). In addition, p53 has a role in mediating apoptosis in cells (Huang et al. 2011). Another factor, is expression of certain oncogenes such as Ha-Ras, which causes senescence in active telomerase cells (Wei et al., 1999). In conclusion, the telomere is affected by several factors such as the telomere attrition that is generated during cell proliferation by either the end replication problem or oxidative stress activity (Flores and Blasco, 2010). For this reason, telomere shortening could be considered as a marker that indicates of cell senescence.

There is no one way to determine cell senescence. This study investigated telomere length, expression of β-galactosidase enzyme (β-gal), population doubling level (PDL) and cell morphology. Indeed, the gradual loss of the telomere length has been confirmed to be contributed to cell senescence (Harley et al., 1990). In human diploid cells, the average of the telomeres lengths varys between 0.5kb and more than 20kb (Reviewed in Aubert et al., 2012). Cells in different organs have different telomere length. For example, cells in fetal liver (~13kb) have longer average telomeres length than in cord blood (~12kb) and bone marrow (~8.5kb), respectively (Vaziri et al., 1994). Also during aging, the telomere length in humans shorten by 20-60bp per year depending in the location of the cells. These differences in telomere

attrition may be explained by cellular environment, the mechanisms that maintain the telomere length and the proliferative capacity of cells (Takubo et al., 2002). Also, cells tend to lose their telomere length each population doubling when they cultured *in vitro* (Zglinicki et al., 1995). Telomere lengths are not restricted to tissues only but also between cells from same origin in the same individual (Rufer et al., 2001; Weng et al., 1997). Terminal restriction fragment (TRF) was the first technique used to measure telomere length (Moyzis et al., 1988). It calculates approximately the average of telomere length within a population of cells which found a correlation between telomere length and replicative capacity of different populations of cells (Allsopp et al., 1992). In terms of tissue engineering, cells with longer telomere length show better response to regenerate tissue after injury (Montgomery et al., 2011).

Another criterion that distinguishes senescent cells is morphology. As cells progress through their proliferative lifespan, morphological changes take place. In early stage, cells tend to be bipolar and spindle in shape. However, when they senesce they become larger, wider, flattened and irregular in shape (Bayreuther et al., 1988; reviewed in sethe et al., 2006). Also they become multinucleated with loss of polarity (Matsumara et al., 1980). Furthermore, it has been found that there is correlation between increase in cell size and increase of actin microfilaments organisation (Wang and Gundersen, 1984). Another marker for cell senescence is β-gal enzyme. This enzyme is easy to detect by using histochemical stain in senescent cells but not in quiescent or immortal cells (Dimri et al., 1995).

The most obvious marker for cell senescence is PDL. MSCs *in vitro* show different population doublings according to the site they have been derived from. For instance, the average population doublings from human dental, bone marrow and deciduous teeth MSCs is between 60-120, 30-50 and over 140PDs, respectively (Huang et al., 2009b). However, there are conflicting results in term of the proliferation rate. Gronthos et al., 2000 showed that human DPSC proliferate faster than BMMSC while it was the opposite in another study (Jo et al., 2007). Indeed, before using these cells in therapy, techniques for generation of large numbers of MSCs should be established without affecting their differentiation potential.

However, this study aims to highlight factors that lead to senescence of these cells during expansion *in vitro* such as H_2O_2.

2.1.3   Stem Cells and Hydrogen Peroxide

ROS are considered as a crucial determinant of cellular ageing (reviewed in Giorgio et al., 2007). However the main cause of cell damage by ROS, is when hydroxyl radical ($^-$OH) species react with other components in the cell (Ueda et al., 2006). Stress-induced senescence can happen after a few cell divisions which seem to be independent of telomere status. However in some cases, oxidative stress is believed to be telomeres dependant. Oxidative stresses have been suggested to be a major cause of telomere shortening in cultured cells (Von Zeglinicki et al., 2003). Rubio et al (2004) found that cells with longer telomeres are more sensitive to H_2O_2 than cells without telomeres or are short telomeres. Interestingly, H_2O_2 induced senescence in these cells without affecting telomeric length, which makes one speculate that there are another aspects of telomeres rather than length which could affect the response of these cells to ROS. Indeed ROS are more likely to attack the GGG sequence of telomeres (Henle et al., 1999). Also the amount and the time of exposure of H_2O_2 are other factors that determine the influence on cell senescence. Low dose of H_2O_2 for long period had no effect on cell proliferation or morphology of MSCs from bone marrow while increasing the H_2O_2 amount to over 100μM, accelerated telomere attrition occurred (Brandl et al., 2011). In terms of telomerase, there are conflicting results on whether telomerase protects cells from H_2O_2 or not (Rubio et al., 2004).

Cellular responses towards different H_2O_2 concentrations vary depending on many factors, such as cell type and origin of these cells (Veal, 2007). There is much evidence to show that stem cells can resist oxygen overload more than other cells by regulating their own antioxidant defence systems (Lekli et al., 2009). For example, endothelial progenitor cells show more resistance to death than mature umbilical vein endothelial cells, when subjected to oxidative stress. In addition, cells produce more antioxidant enzymes in comparison with other cell types, at the same site (Dernbach et al., 2004). Under normal conditions cells lose about 90bp each population doubling, while when subjected to oxidative stress, cells lose more than 500bp with each population doubling (Zglinicki et al., 1995).

2.2 Aims

Dental pulp may provide a potential source of progenitor cells for tissue engineering purposes. However, these would require considerable *in vitro* expansion before use, potentially leading to loss of proliferative lifespan and cellular senescence, which may be accompanied by increased oxidative stress, altered cellular responses and differentiation. The aim of this chapter, therefore, was to examine the effect of oxidative stress on DPPCs, in terms of population doubling levels (PDLs) and senescence.

2.3 Materials and Methods

2.3.1 Isolation of Dental Pulp Progenitor Cells

Normal human wisdom teeth were collected from three adult patients at the School of Dentistry, Cardiff University with informed patient consent and ethical approval by the South East Wales Research Ethics Committee of the National Research Ethics Service (NRES), UK. A copy of the patient information sheet and consent form is included at the appendix. Teeth were sterilised by soaking in 70% ethanol and the attached soft tissue removed using a paper towel, prior to dissection. Teeth were grooved in the centre of three areas (mesial, distal and occlusal) with a rotary bone saw. On a dissection board, a chisel and hammer were used to separate each tooth into two halves and the pulp removed with a forceps and placed into universals filled with culture medium to maintain hydration. Pulp tissues were minced on a glass slide and cells were placed into 5ml bijoux tubes containing 1ml of 4μg/μl collagenase/dispase enzymes (Roche, Welwyn Garden City, UK). Pulps were incubated for 1 h, with regular agitation every 20 min, to increase cell dissociation. Pulpal tissues from individual patients were prepared separately. The contents of each bijoux were passed through a 70μm mesh cell strainer into a 50ml Falcon tube (BD Falcon, UK), to obtain a single cell suspension. The cell strainer was washed in 10ml medium. Cells were centrifuged at 1,800rpm (Labofuge400, Thermo Scientific, USA) for 5 min and further resuspended in 1ml medium. Cell numbers were calculated using 0.4% trypan blue vitality stain (Sigma, UK) for monolayer cell culture. A 10μl aliquot of each cell suspension was diluted in a known amount of the

stain and cells counted in a Neubauer Haemocytometer by light microscopy (Nikon eclipse TS100, UK). Cells were subsequently seeded in fibronectin coated 6 well plates (Sarstedt, Leicester, UK) at 4000/cm^2.

2.3.1.1 Fibronectin Adhesion Assay

Following the protocol of Waddington et al., (2008), 10µg/ml fibronectin, derived from human plasma (Sigma) was reconstituted in 0.1M PBS at pH 7.4 containing 1mM Ca^{2+} and 1mM Mg^{2+}. Fibronectin (1ml/well) was pre-coated onto wells of 6-well plates overnight. The fibronectin pre-coated wells were seeded with the cell suspension at 4,000 cells per cm^2 (40,000 cells/ well). Cells were allowed to adhere at 37°C, 5% CO_2 for 20 min. Following adhesion, the culture medium and non-adherent cells were removed and the wells refilled with 2ml fresh culture medium. Cells were fed every 2 days with 2ml of fresh working medium each time.

During the culture, the isolated DPPCs were monitored using an inverted light microscopy (Nikon Eclipse TS100, Tokyo, Japan) at x10 magnification and the number of cells per colony recorded. Jones and Watt (1993) defined a colony as a cluster with a minimum of 32 cells. By day 12, identifiable colonies were isolated by using 1ml sterilised pipette tips with the ends trimmed off leaving a cylindrical tube; with its edges smeared with petroleum jelly; and placed onto the wells to form an isolated water-tight seal around the marked colonies. Pre-warmed accutase (100µl, PAA, Velizy-Villacoublay, France) was added at 37°C, 5% CO_2 and the isolated clones were then expanded until the numbers were sufficient for seeding into T-75 flasks.

2.3.2   Cell Culture

Cell culture was performed under sterile conditions, using sterile tissue culture plates and flasks (Sarstedt, Leicester, UK). All procedures were performed in aseptic class II tissue culture hoods (Astec Microflow, Andover, UK). Cells were maintained in a 5% CO_2 in a humidified chamber at 37°C. Medium and accutase were pre-warmed to 37°C in a water bath, prior to administering to cells. When cells were approximately 80% confluent in T-75 flask, cells were washed with 0.1M phosphate buffered saline (PBS, pH 7.4) before being treating with 2ml of the pre-warmed accutase. Incubation

was performed at 37°C until the cells had become detached from the culture vessel (approximately 5min). The accutase was subsequently inactivated by the addition of serum-containing in the culture medium before centrifugate at 1800rpm. The resulting pellet was resuspended in the culture medium before cell counting and reseeding as described before.

2.3.2.1 General Media

Cells were maintained in α-modified Minimum Essential Medium (αMEM) containing ribonucleosides, deoxyribonucleosides, L-glutamine and phenol red, in addition antibiotics (100 units/ml penicillin G sodium, 0.1μg/ml streptomycin sulphate and 0.25μg/ml amphotericin; Invitrogen, Paisley, UK). Working medium for cell culture consisted of αMEM with 20% foetal calf serum (FCS, Invitrogen, UK), 4mM L-glutamine (Invitrogen, UK) and 100μM L-ascorbate 2-phosphates (Sigma-Aldrich, UK), except where stated.

2.3.2.2 Freezing and Thawing Cells

To cryopreserve cells, cells were centrifuged, counted with trypan blue (Sigma, UK) and resuspended in 1ml freezing mix containing 10% Dimethyl Sulfoxide (DMSO) (Sigma, UK) and 90% FCS. Freezing mix was added to the cryovials placed in freezing pot at -70°C. After 24 h, cryovials were transferred to liquid nitrogen for long term storage. When cells were required, cells were rapidly thawed by transferring to a 37°C water bath. The cells were immediately resuspended in 5ml medium and centrifuged as stated above. Cells then were rewashed with medium and expanded in culture.

2.3.3   Population Doubling

To determine the rates of cell proliferation of each DPPC clone, cumulative PDs were plotted against time. The total numbers of viable cells during the cell counts from each passage were obtained using a haemocytometer and the number of cells reseeded was recorded. The PD of each cell population was calculated using the following formula:

$$PD = \frac{\log_{10}(\text{total cell count obtained}) - \log_{10}(\text{total cell count re-seeded})}{\log_{10}(2)}$$

2.3.4 Extracting mRNA from Isolated Clonal Cultures

An RNeasy Mini Kit (Qiagen, Manchester, UK) was used to extract mRNA following the manufacturer's protocol. Cells were initially cultured in 6-well plates (Sarstedt, Leicester, UK) until 90% confluence. Each well of cells was then lysed with 300 µL of Buffer RLT lysis buffer (Qiagen, UK) supplemented with 10 µL/mL of β-mercaptoethanol (Sigma-Aldrich, UK). The lysate was transferred to a QiaShredder column (Qiagen, UK) 600 µL at a time for centrifugation at 13,500 ×g for 2 min (Spectrafuge 24D, Jencons, UK) to shear cellular components, including DNA, and separating cellular debris. Subsequent, cell lysate was treated with 1:1 volumes of 70% molecular-grade ethanol (Sigma-Aldrich, UK) and mixed thoroughly by pipette action. The sample was then transferred into an RNeasy Mini Kit column (Qiagen, UK) and centrifuged at 10,000 ×g for 15 s. The flow-through was discarded and the column was washed with 350µL of Buffer RW1 (Qiagen, UK) and centrifuged again at 10,000 ×g for 15 s. The flow-though was discarded and the column was treated with a mixture of 10µL of DNase I stock and 70µL Buffer RDD (both Qiagen, UK). This was incubated at room temperature for 15 min for on-column digestion to remove any contaminating genomic DNA. 350µL of Buffer RW1 was added to the column and then washed by centrifugation at 10,000 ×g for 15 s. A further 2× 500µL of Buffer RPE was added and centrifuged for 1 min each time with the flow-through discarded after each spin. The column insert was then transferred into an RNase-free 1.5mL eppendorf (Fisher Scientific, Loughborough,, UK) and 40µL DNase free water (Promega, Southampton, UK) was added for eluting the RNA by centrifuging at 10,000 ×g for 1 min. The eluate was pippetted back into the column and centrifuged again to maximise yield. Total RNA collected in the eppendorf was stored at -80°C.

To quantify the amount of RNA in each sample a NanoVue (GE Healthcare, Amersham, UK) was used. The NanoVue was standardised with 2µL of DNase free water as a blank before using 2µL of RNA sample to quantify. The absorbance ratio at 260:280 nm between 1.7 and 2.2 indicated sufficient RNA purity.

2.3.5 PCR Methods to Characterise Cell Marker Expression

2.3.5.1 Reserve Transcription (RT) PCR

RT-PCR was performed using the Moloney murine leukaemia virus (M-MLV) reagents from Promega. 1 µg of total RNA was treated with 0.5µg of Random Primers (Promega) with the addition of DNase free water to adjust to a final volume of 15 µL. This mixture was then placed in a G-storm™ GS1 thermal cycler (Genetic Research Instrumentation Ltd, Braintree, UK) and incubated at 70°C for 5 min to unravel RNA. The product was immediately cooled and stored on ice before 5µL of 5× M-MLV buffer was added along with 0.625µL of RNasin, 1.25µL of 10mM dNTPs, 1µL of M-MLV reverse transcriptase (all Promega) and the addition of DNase free water brought the final volume to 25µL. The sample was gently mixed with a pipette and placed into a thermal cycler at 37°C for 1h, followed by 95°C for 5 min. The newly generated cDNA was stored at -20°C until the next use of PCR reaction.

2.3.5.2 Polymerase Chain Reaction (PCR)

All PCR reactions were set up by the addition of 1µl of cDNA/control generated by reverse transcription to 5µl 5x Green GoTaq™ Flexi Buffer (Promega), 1µl 25mM MgCl, 0.5µl 10µM PCR Nucleotide Mix, .0.25µl 5U/µl GoTaq™ DNA Polymerase, 1.25µl 0.04µg/µl Forward Primer (Table2.1), and 1.25µl 0.04µg/µl Reverse Primer (Table 3.1). All reaction volumes were made up to 25µl with nuclease free water. Reactions were run on a G-storm™ GS1 thermal cycler (Genetic Research Instrumentation Ltd) with an initial denaturing step of 95ºC for 5 min, followed by 35-40 cycles of a 1 min 95ºC denaturing step, a 1 min 55-62ºC annealing step (as it stated in table) and a 1 min 72ºC extension step. A final extension step at 72ºC for 5 min was run, ending the reaction. All PCR products were loaded in agarose gels to visualise by Gel Doc 2000 (BioRad, Hemel Hempstead, UK).

Positive human controls, human embryonic stem cell (HuES09), was supplied by Dr. Lindsay Davies, (Cardiff University, UK) for embryonic and neural crest markers. Total human RNA purchased from stratagene (Invitrogen, UK) was used as positive control for hemapiotic marker CD45. Positive controls of MSCs markers

were performed on total human RNA (Howard-Jones, Thesis). For negative controls, water and RT-negative controls were used. The PCR was carried out with primers for mesenchymal markers, neural crest markers, embryonic markers, and hematopoietic markers with the housekeeping gene β-actin. Details of the markers are shown in Table 2.1

Table 2.1: Human gene markers used for PCR amplification. β-actin was used as a housekeeping gene.

Gene Marker	Primer sequence	Annealing Temperature °C	Cycles	Source
CD73	F:5'GTCGCGAACTTGCGCCTGGCCGCCAAG-3' R: 5'-TGCAGCGGCTGGCGTTGACGCACTTGC-3'	65	35	Amr Alraies Cardiff University
CD90	F:5'- ATGAACCTGGCCATCAGCATCG-3' R:5'- CACGAGGTGTTCTGAGCCAGCA-3'	55	35	Amr Alraies Cardiff University
CD105	F:5'-GAAACAGTCCATTGTGACCTTCAG-3' R: 5'-GATGGCAGCTCTGTGGTGTTGACC-3'	65	35	Amr Alraies Cardiff University
CD45	F:5'-GTGACCCCTTACCTACTCACACCACTG-3' R:5'-TAAGGTAGGCATCTGAGGTGTTCGCTG-3'	65	35	Amr Alraies Cardiff University
Oct4	F:5'-AGGAGTCGGGGTGGAGAG-3' R:5'-CGTTTGGCTGAATACCTTCC-3'	55	35	Lindsay Davies Cardiff University
Slug	F:5'- CATACAGCCCCATCACTGTG3' R:5'- CCTGGAGGAGGTGTCAGATG-3'	55	35	Lindsay Davies Cardiff University
hTERT	F:5'- CGGAAGAGTGTCTGGAGCAA-3' R:5'- GGATGAAGCGGAGTCTGGA-3'	55	40	Mantripragada et al., 2008
p53	F:5'- AGACCGGCGCACAGAGGAAG-3' R:5'- CTTTTTGGACTTCAGGTGGC-3'	55	35	Huang et al., 2011
p21^{WAF1}	F:5'- GGATGTCCGTCAGAACCCAT-3' R:5'- CCCTCCAGTGGTGTCTCGGTG-3'	60	35	Mergui et al., 2010
p16^{INK4A}	F:5'- CTTCCTGGACACGCTGGT-3' R:5'- GCATGGTTACTGCCTCTGGT-3'	55	35	Wang et al., 2012
β-actin	F:5'-AGGGCAGTGATCTCCTTCTGCATCCT-3' R:5'- CCACACTGTGCCCATCTACGAGGGGT-3'	65	35	XQ Wei Cardiff University

2.3.5.3 Agarose Gel Preparation

To visualise PCR products a 10µL of sample was loaded on to 1-3 % agarose gels. To prepare agarose gels, 1.4g of agarose powder (Invitrogen, UK) was added to 70mL of 0.5xTBE buffer. Subsequently, agarose was dissolved by microwave heating for 20 s at a time swirling in between until the agarose solution was clear, prior to the addition of 7µl ethidium bromide 10mg/ml (Promega). The gels were poured into a casting tray containing a comb and allowed to set at room temperature, for 30 min. Once set, gels were placed in an electrophoresis tank containing 0.5x TBE buffer. The comb was carefully removed and then 10µl of PCR reaction added to wells, in addition to a 10µl 100 base pair (bp) DNA step ladder (Promega). Loaded gels were subjected to electrophoresis, at 80mV for approximately 45 min, in 1x TBE running buffer. The gel images were captured under UV light (312nm) and analyzed, using the Geldoc programme (BioRad).

2.3.6 Cell Morphology and Determination of Cell Size throughout Their Proliferative Lifespan

The relative cellular morphology and surface areas of DPPCs were compared at early PD, mid PD and at late PD (the total PD achieved by each clone was divided by three, to determine the three PD groups). Serial images of the cells were obtained throughout their proliferative lifespan using a digital camera (Canon PC1234, Tokyo, Japan). The cells were outlined along their peripheral borders and perimeter and the surface area of the cells calculated using ImageJ) processing software. Cellular surface areas was analysed using Excel to identify and compare the variations in the mean cellular surface area throughout the proliferation of DPPCs, and also to assess whether the mean cell area measurements were a true reflection of the overall distribution of cell sizes. The results were presented for individual clones at the three PDs (early, mid and late PDs).

2.3.7 Oxidative Stress Assay

2.3.7.1 Cell Culture

DPPCs at early passage; two clones from patient A, called A31 (the experiment started after 31 days of normal culturing) and A11 (the experiment started after 14

days of normal culture), and one clone from patient B, called B11 (the experiment start after 25 days of normal culture) were seeded at 1×10^5 in T-25 flask and maintained in the absence/presence of sub-lethal doses of H_2O_2 (5, 10, 25, 50, 100, 200μM). Culture medium was changed every two days. Cells were grown to 80–90% confluence and re-plated as described above, until senescence occurred. PDs throughout the culture duration were monitored. Senescence deemed to be achieved when PD <0.5 / week. In addition, images were taken every two days of the morphological changes. mRNA was extracted from each group treatment at early, mid-point, and late stage PDs to assess their triplicate expression of stem cell markers.

2.3.7.2 β-galactosidase (β-gal) Assay

A Senescence Cell Histochemical Kit (Sigma-Aldrich) was used to detect β-galactosidase activity in senescent cells. Cells at selected PDs were seeded in 6 well-plates at $5000/cm^2$ and cultured for 24 h in culture medium. The culture medium was aspirated and the cells washed (x2) with PBS (provided in the Kit) diluted 1:10 in ultrapure water. 1:10 diluted Fixation Buffer (1.5 ml/well) in ultrapure water was added for 7 min at room temperature. Meanwhile 10 ml of Staining Mixture was prepared by mixing 1 ml of prewarmed Staining Solution (in Kit), 0.125ml of Reagent B (in Kit), 0.125ml of reagent C (in Kit), 0.25ml of X-gal solution (in Kit), with 8.50ml of ultrapure water. Following incubation with Fixation Buffer, cells were rinsed (x3) with PBS (1ml/well). Then, Staining Mixture (1ml) was added to each well and incubated at 37^oC at 5% CO_2 overnight, with the plate sealed with parafilm to prevent drying out. Cells were subsequently observed under a light microscope (Nikon eclipse TS100) and blue-stained cells were counted. Finally, the percentage of cells expressing β-galactosidase activity was calculated.

2.3.7.3 DNA Extraction for Telomeres Length Assay

Genomic DNA was isolated using QIAmp® DNA Mini Kit (Qiagen). Firstly, cells from different treatment groups were seeded at $5000/cm^2$ density in T-75 flasks at two different PDs (early and late) and cultured to confluence. Cells were detached from the flask with accutase and centrifuged (1800rpm/5min). The supernatants were discarded and the pellets resuspended in PBS (200ml) and mixed with proteinase K

(20μl) and buffer AL (200μl). Samples were incubated for 10 min at 56°C in a water bath. After incubation, mixtures were briefly centrifuged. 100% ethanol (200ml) was added to each sample and mixed by brief centrifugation for 15 s. The mixtures were transferred to QIAamp Mini Spin Column (in a 2ml collection tube) and centrifuged at 8000rpm for 1min; and the spin column placed in a new 2ml collection tube. Buffer AW1 (500μl) was added to the column and centrifuged at 8000rpm for 1 min and again placed in a new 2ml collection tube prior to addition of buffer AW2 (500μl) to the column and centrifuged at the highest speed (13,300 rpm) for 3 min. The column was placed in new 1.5ml microcentrifuge tube and buffer AE (200μl) was added and left for 1 min at room temperature and then centrifuged at 8000 rpm for 1 min. Finally, DNA yields were measured by absorbance at 260nm in Nanovue (GE. UK). For long-term storage of DNA, the samples were stored in freezer (Indesit, UK) at -20°C.

2.3.7.4 TRF Assay

To determine the telomere length of each DNA samples, Telo TAGGG Telomere Length Assay Kit (Roche, Burgess Hill, UK) was used. Following manufacturer's instructions, each sample of DNA (1μg) was digested with of Hinf1/Rsa1(1μl) and x10 digestion buffer (2μl) in a final volume of 20μl. In addition, a control genomic DNA digest was also established. The DNA samples with enzymes and digestion buffer were incubated at 37°C for 2 h and the reactions terminated by 4μl gel electrophoresis loading buffer. Digested DNA samples were separated by agarose gel electrophoresis with 0.8% gel (highly pure, nucleic acid grade agarose-Agarose MP, Geneflow, UK) in 1x Tris-acetate-EDTA (TAE) buffer containing 0.2μg/ml of ethidium bromide.

For gel electrophoresis, 1μg of DNA digest and 10μl of Digoxigenin (DIG) molecular weight marker were loaded onto each gel and run at 20V, overnight, until the bromophenol blue had separated about 10cm from the starting wells and the gels were removed to perform several treatment processes. The gel was submerged in hydrochloric acid (HCl) solution (Table 2.2) for 10 min, with agitation at room temperature. Gels were rinsed twice with water before being submerged in

Denaturation Solution (Table 2.2) (x2) for 15 min at room temperature; and again rinsed (x2) with water. Finally, the gel was submerged in Neutralisation Solution (Table 2.2) (x2) for 15 min at room temperature, before performing Southern blotting.

For Southern blotting, two pieces of Whatman 3MM paper (Sigma, UK) were used to make a wick gradient. The two pieces of Whatmann paper were placed over a plastic support platform, and wetted with 20x standard sodium citrate (SSC) buffer (Table 2.2). The gel placed face down on the wet Whatmann paper, and covered with SSC-soaked positively charged nylon membrane (Roche). The nylon membrane was covered by 4 pieces 2x SSC-soaked Whatman paper. Finally, a 15cm tall stack of dry cut paper towels was topped with a 100g weight. The entire apparatus was covered to prevent any evaporation and left overnight at room temperature.

The following day, the nylon membrane was fixed by UV-crosslinking for 10 s x2 (Stratalinker, USA) and washed with SSC (Table 2.2) (x2) prior to hybridisation. For hybridisation, all steps were performed in a hybridisation oven (VWR, UK) with the membrane placed in a hybridisation bottle and rotated gently on a rotisserie. Firstly, membranes were placed side up in a hybridisation bottle with 25ml of DIG Easy Hyb (Table 2.2) for 1 h at 42°C, with gentle rotation. This solution was replaced with pre-warmed hybridisation solution (10ml) mixed with 2µl of Telomere probe; and incubated at 42°C for 3 h. Afterwards, the membrane was washed with 25ml of Stringent Wash Buffer I (Table 2.2) (x2) for 5 min at room temperature. Another washing step was performed with 25ml of Stringent Wash Buffer II (Table 2.2) (x2) for 20 min at 50°C, and was lastly washed with 25ml of washing buffer 1x (Table 2.2) for 5 min at room temperature. Subsequently, the membrane underwent several incubations for 30, 30, 15, and 5 min in 25ml: 1x blocking solution, anti-DIG-AP working solution, washing buffer (2x), and 1x detection buffer (Table 2.2) respectively, at room temperature (all solutions provided in the Kit). Finally, the membrane was incubated for 5 min in Substrate Solution (provided in the kit) at room temperature before the membrane was removed from the hybridisation bottle and blotted to remove excess liquid onto 3M Whatman paper and wrapped in Saran. The membrane was inserted in a cassette (Hypercassete,UK)

and exposed for 30 s to a High Performance Chemiluminescence Film (GE,UK). The film was developed using CURIX 60 (AGFA, Mortsel, Belgium).

Table 2.2. Solutions used for TRF assay. Bottles with numbers provided in the kit

TAE Buffer	0.04M Tris-Acetate, 0.001M EDTA pH 8.0
HCl Solution	0.25M HCl
Denaturation Solution	0.5M NaOH, 1.5M NaCl
Neutralisation Solution	0.5M Tris-HCL, 3M NaCl pH7.5
20X SSC	3M NaCl, 0.3M Sodium citrate pH7.0
2X SSC	Dilute 20X SSC 1 :10 with autoclaved distilled water
DIG EasyHyb	Reconstitute the granules (bottle-9-kit) with 64ml of autoclaved distilled water and incubate at 37°C overnight
Stringent wash buffer I	2X SSC, 0.1% Sodium dodecyl sulfate (SDS)
Stringent wash buffer II	0.2X SSC, 0.1% SDS
Blocking Solution 1X	Dilute 10X (bottle 13) 1:10 with malic acid buffer 1X
Malic Acid Buffer 1X	Dilute 10X (bottle 12) 1:10 with autoclaved distilled water
Anti-DIG-AP, Working Solution	Dilute (bottle 14) 1:10,000 with blocking solution
Detection Buffer 1X	Dilute 10X (bottle 15) 1:10 with autoclaved distilled water

2.3.7.5 Densitometry Analysis

To convert the telomeric specific smear on the Southern blot image into mean TRF, the southern blot image was opened using ImageJ software and the image rotated to align vertically and then the colour was inverted to enable analysis. Each lane containing a different DNA sample was analysed separately, before overlaying a box on the image to measure mean density of the telomere specific smear. The size of the box was determined so that it only encapsulated the signal from the individual lane and to allow approximately 30 boxes of the same size to be fitted to each individual lane (Figure 2.1). The background density was calculated using the average density of several boxes that did not contain a telomere specific signal, and subtracted from each box that did have a signal. For each box containing DNA, the mean density (ODi) and corresponding length (Li) using the molecular weight ladders (in kb) at the mid-point of the box was calculated and then substituted into the formula Σ (ODi) / Σ (ODi /Li) to obtain mean TRF length (Kimura et al., 2010).

Figure 2.1. The Southern blot is shown with the telomere specific smear in white. Lane MW contains the size standard ranging from 21.2kb to 1.1kb. The other lanes contain different genomic DNA samples. Lane A31 at 55PDs showed the principles of how the analysis is performed using the ImageJ software.
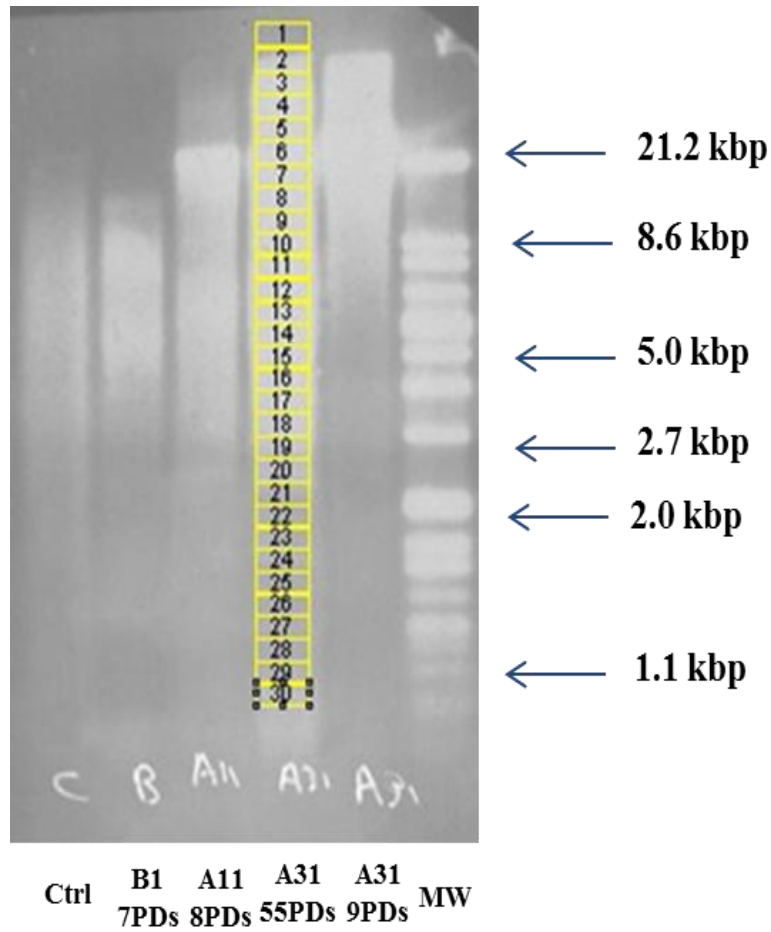
2.4   Results

2.4.1   Characterisation of Cells

2.4.1.1 Cell Colonies

After 6 days of culturing cells on fibronectin pre-coated well, several clones were observed (6 clones from patient A, 1 clone from patient B and 4 clones from Patient C). At day 12, 5 Clones were successfully isolated from patient A, 1 clone from Patient B and 3 clones from patient C). Each clone at day 12 showed crowded, fibroblast cell morphology (Figure 2.2) After isolation, each clone was transferred to be cultured further in 96 well-plates for expansion by transferring to a larger culture vessel at each passage until able to be cultured in T-75 flasks. Several colonies were continued culture and the remainder were cryopreserved until require uses. Cells were cultured until senescence-associated features appeared, as described above.

Figure 2.2. An example of a single clone colony formed after 12 days. The colony was compact and consisted of >32 cells. ×10 magnification, Scale bar 100µm.
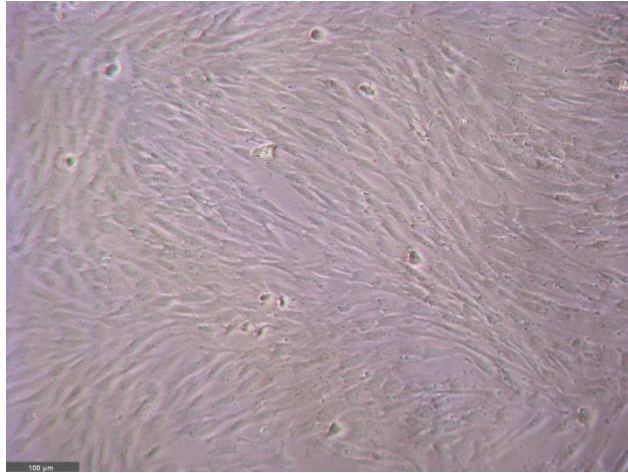
2.4.1.2 Population Doublings (PDs)

There were marked variations in the proliferative capacity between individual clones. Each clone showed significant differences in PDs, when comparisons were performed between clones from the same patient or from different patients. Three separate clones were further cultured until senescence from patient A and one clone from patient B (Figure 2.3). One clone demonstrated a high population doubling (A31) extending beyond 80PDs (almost 300 days), while the other clones from this first patient (A11, A51) demonstrated less than 25PDs under less than 70 days. In contrast, clone B11 from the second patient did not persist beyond 36PDs with less than 85 days in culture.

Figure 2.3. PDs of 4 different clones; 3 clones from patient A (A11, A31, and A51), and one clone from patient B (B11). A31 demonstrated a high population doubling extending beyond 80PDs, while the other clones A11, A51 and B11 demonstrated less than 36PDs.
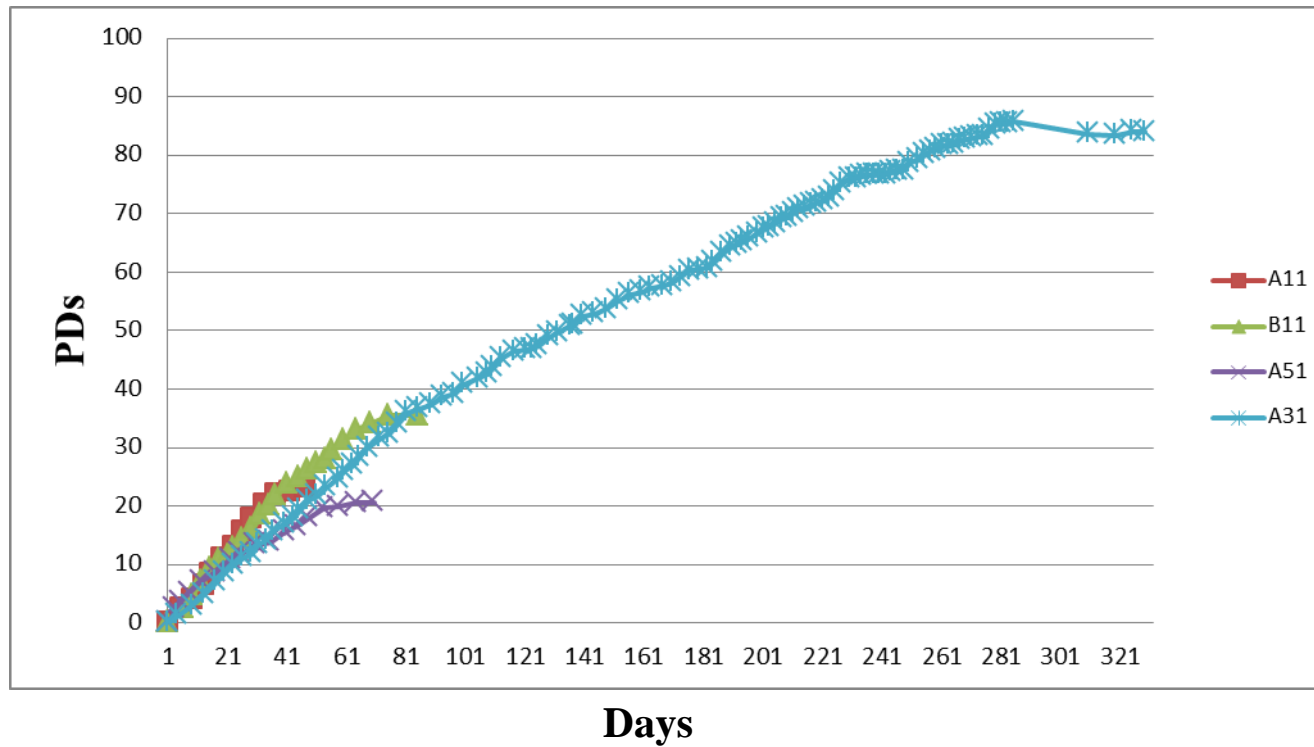
2.4.1.3 Gene Expression

MSC markers CD105, CD90 and CD73 were analysed in three selected clones, two from patient A (A11 and A31) and one clone from patient B (B11) during different periods of their proliferative lifespan. These markers were expressed in all of these clones at early culture (1-10PDs). All markers were lost gradually during their *in vitro* culture expansion. CD105 was the first marker to be lost after 11PDs in clone A11 and after 24PDs in clone A31. Clone A31 all MSCs markers after 60PDs while B11 lost MSCs expression after 24PDs. Further analysis for clone A11 after 24PDs and for clone B11 after 35PDs was not performed as both clones senesced at these time points. Total human RNA was used as a positive control for MSC marker expression of CD73, CD90, and CD105 (Howard-Jones, Thesis). The water and RT-negative experimental controls had no expression (Figure 2.4).

At early culture time points (1-10PDs) other cell markers were also analysed including the hematopoietic cell marker (CD45), an embryonic stem cell marker (Oct4), and the neural crest marker (Slug). CD45 expression was negative while Oct4 and slug were weakly expressed in all clones (Figure 2.5), compared with MSC gene expression (Figure 2.4) and lost completely after 11PDs in all clones. Controls of embryonic markers (HuES09) expressed Oct4, slug and TERT markers. The water and RT-negative experimental controls had no expression.

Expression of the tumour suppressor genes p16, p21 and p53 were investigated at early culture (Figure 2.6) to investigate their effects on cell cycle and proliferation at this stage. p21 gene expression was intensely positive in all clones. The expression of p16 gene was intensely positive in clones; A11 and B11 but was weakly expressed in clone A31. p53 gene was not expressed at all in clone A31 but was strongly expressed in the other 2 clones. Water and RT-negative experimental controls demonstrated no expression.

Figure 2.4. Mesenchymal stem cell gene expression for clones A11, A31, and B11 at specific culture time points. CD105, CD90 and CD73 were gradually lost over 60PDs. β-actin was used as the housekeeping gene. NC refers to no cell available due to cell senescence. Water and RT-negative experimental controls showed no expression.
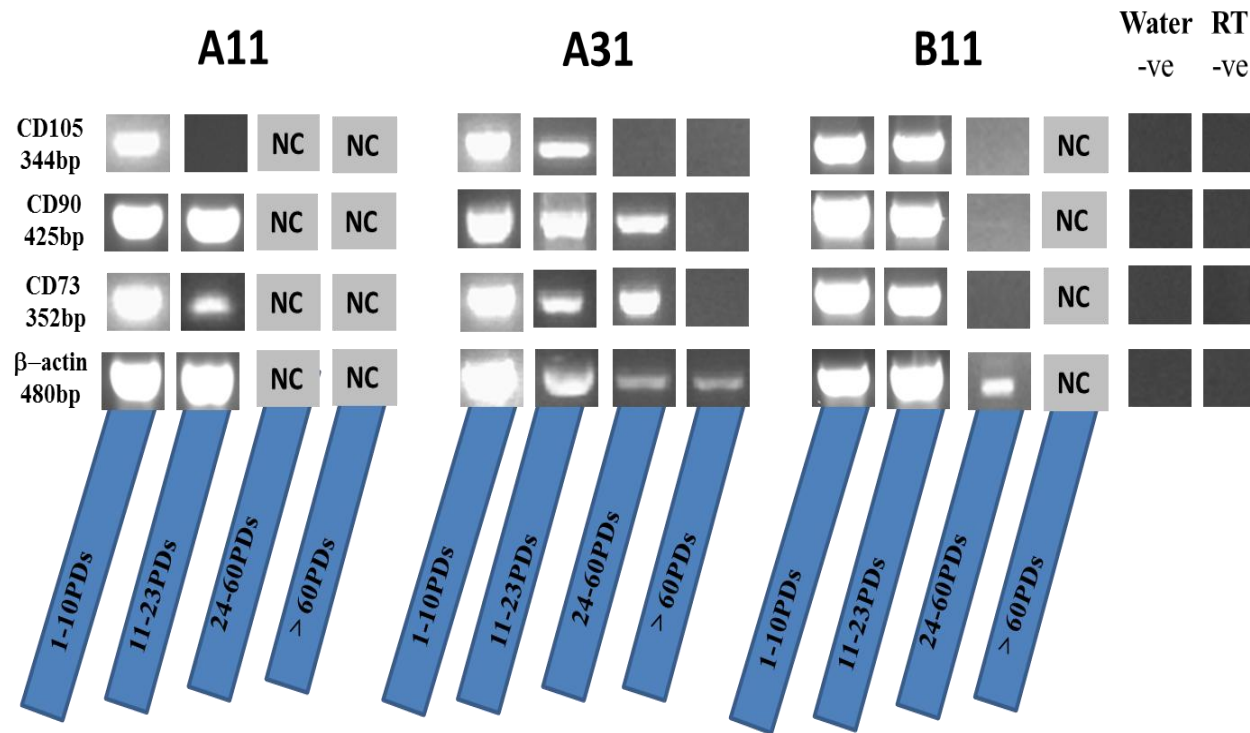
Figure 2.5. Heamapoitic, embryonic and neural crest gene expression for A11, A31, and B11 at early culture (1-10PDs). Hematopoietic cell marker (CD45) was not expressed in all clones. Oct4 and Slug gene expressions were weakly expressed in all clones. β-actin was used as a housekeeping gene. Water and RT-negative experimental controls showed no expression.
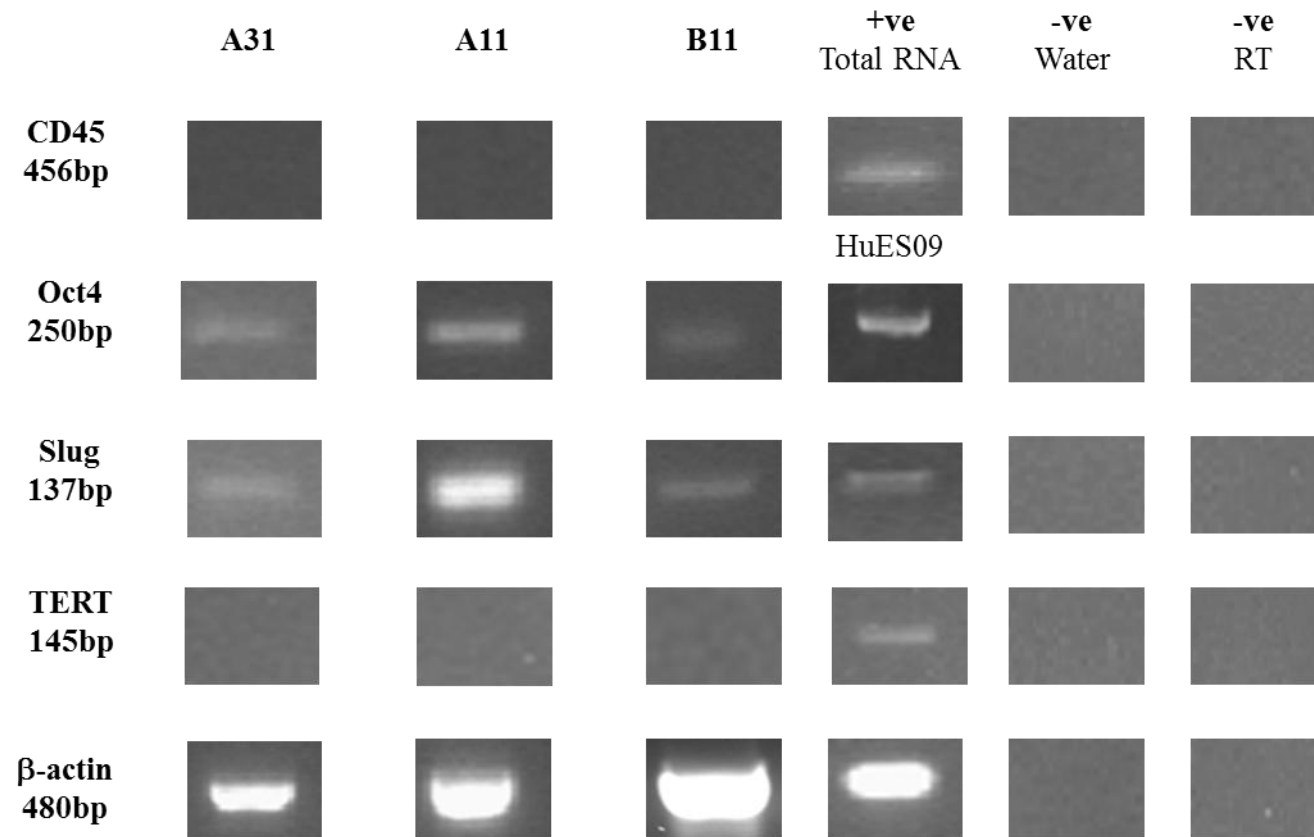
Figure 2.6. Gene expression for tumour suppression markers p16, p21 and p53 in clones A11, A31, and B11 at early culture (1-10PDs). p21 was strongly expressed in all clones. P16 and p53 were expressed intensely in clones A11 and B11 while in clone A31, p16 was weakly expressed and p53 is not expressed at all. β-actin was used as housekeeping gene. Water and RT-negative experimental controls showed no expression.
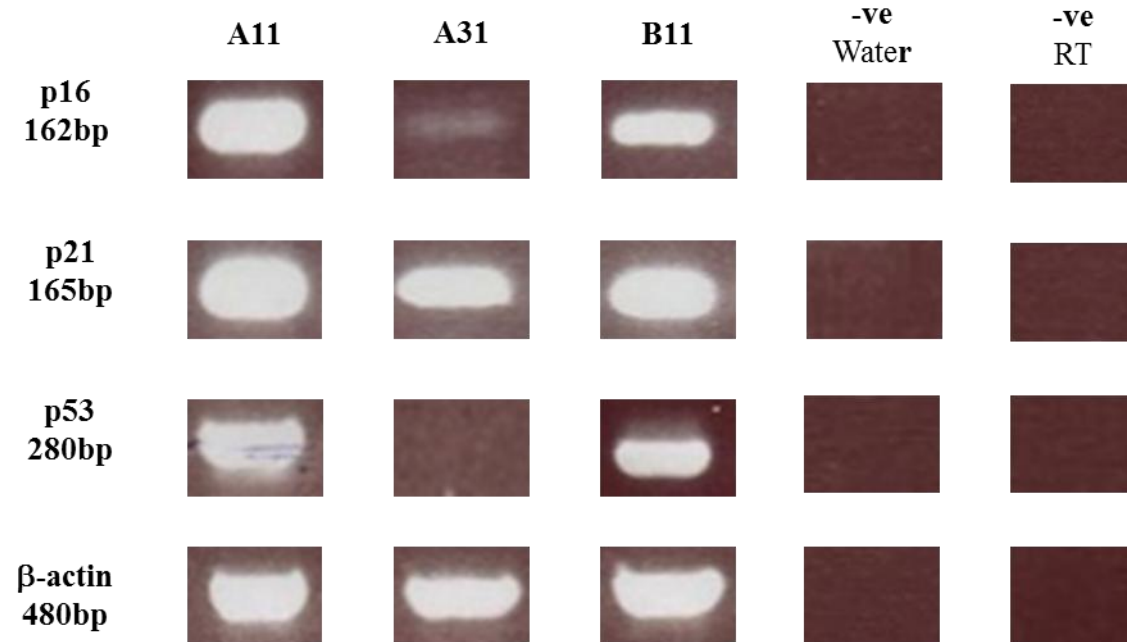
2.4.2 Cellular Morphology of DPPCs throughout Their Proliferative Life Span

To support the PD data, microscopic analysis of DPPC morphology was undertaken throughout proliferation from early PD until senescence. In all clones (A31, A11 and B11) at early PDs (A), cells were morphologically similar with the characteristic long, spindle, bipolar shape as typical fibroblast appearance. Clones A31, A11, B11, are shown in figures 2.9-2.11 respectively. As the cells continued to undergo more PDs, their morphology began to change such that the cells became wider and larger in size, although still maintaining their spindle and bipolar shape at early and late middle PDs (B and C). At the senescence level (D), cells showed a distinct difference in their morphologies. Cells became larger, wider and irregular in shape with loss of polarity and with appearance of stress fibres (stress fibres, shown with arrow).

Figure 2.7. Comparison of the morphological appearance of clone A31 throghout its proliferative lifespan, until senescence. A represents early PD, B represents early mid PD, C represents late mid PD and D represents late PD (stress fibres and wide cells shown with arrow. ×10 magnification, Scale bar 100µm.
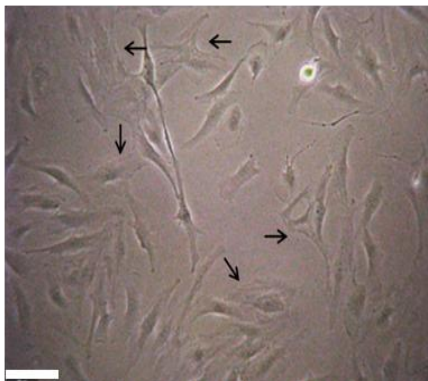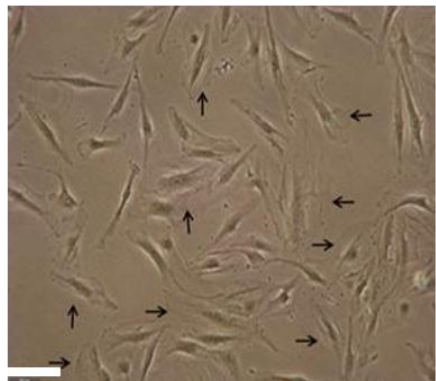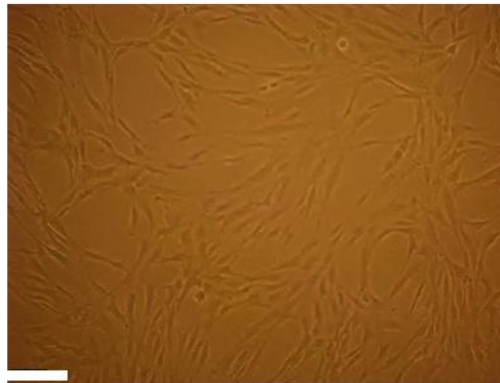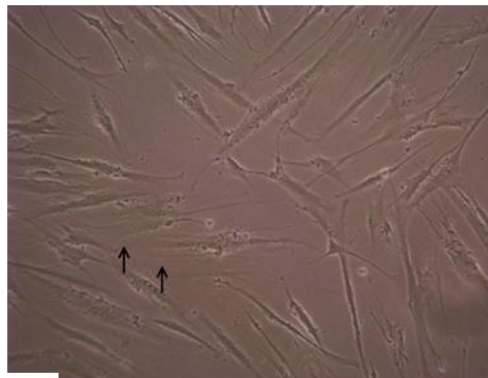
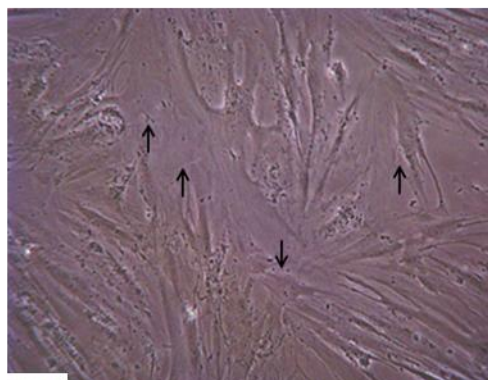A) 3PDs
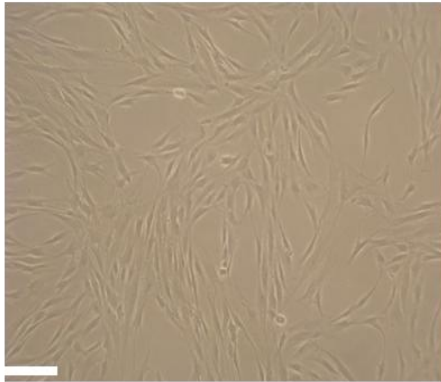
B) 21PDs
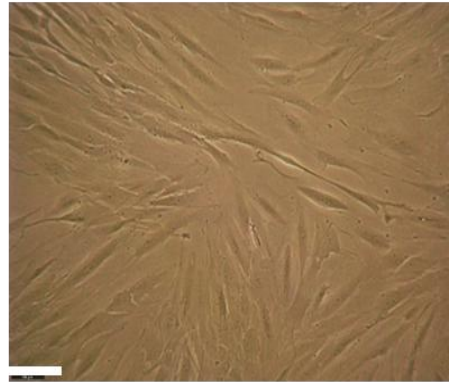
C) 55PDs

D) 85PDs

Figure 2.8. Comparison of the morphological appearance of clone A11 throughout its proliferative lifespan, until senescence. A represents early PD, B mid PD and D represents late PD (stress fibres and wide cells shown with arrow). ×10 magnification, Scale bar 100μm.
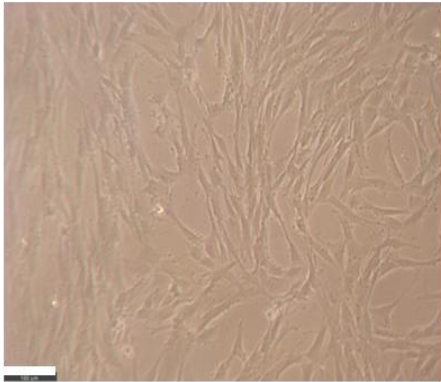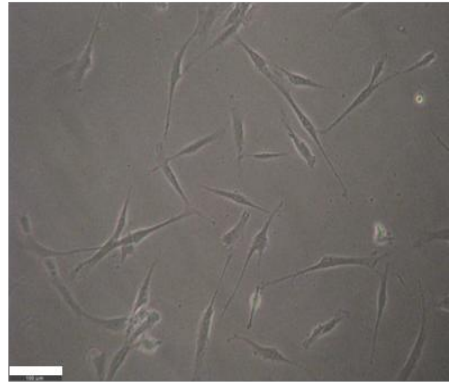
A) 4PDs

B) 15PDs

D) 22PDs

Figure 2.9. Comparison of the morphological appearance of clone B11 throughout its proliferative lifespan, until senescence. A represents early PD, B represents early mid PD, C represents late mid PD and D represents late PD (stress fibres shown with arrow). ×10 magnification, Scale bar 100µm.
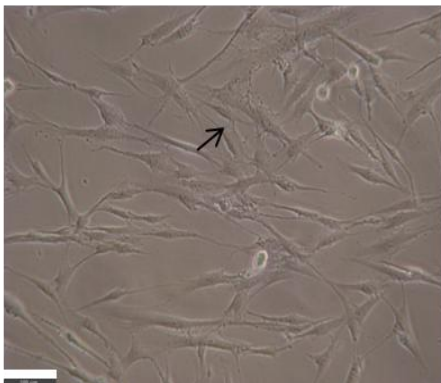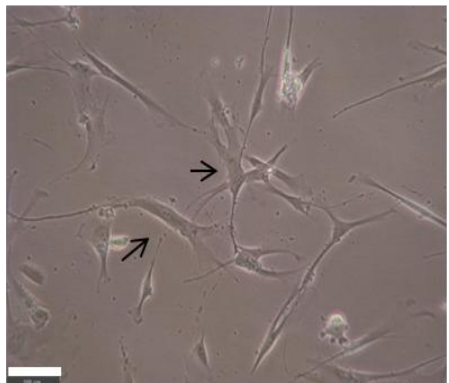
A) 4PDs

B) 18PDs

C) 26PDs

D) 35PDs

2.4.3 Determination of Cell Size of DPPCs throughout Their Proliferative Lifespan

Cell size for all the clones and therefore, their surface area were observed to increase with *in vitro* expansion as was visually clear from the images (Figures 2.7-2.9). This was clearly shown as the cells were narrow and spindle shaped at early PD but became wider and larger when reaching senescence. Cell areas (μm^2) were calculated for 20 cells from different areas in T75 flask (5 images taken from random areas in the T75 flask) (Figure 2.10) and then the mean and standard error mean (SEM) calculated for each individual clone at three PDs (early, mid, and late PDs).

In clone A11, the mean cellular surface area at early PD (4PDs) was 803μm^2 (mean ± 108), which increased at mid PD (15PDs) to 5,060 μm^2 (mean ± 476). At late PD (22PD), the surface area gradually increased so that the mean cellular surface area was 9,885μm^2 (mean ± 1005). In clone A31, the mean at early PD (3PDs) was 815μm^2 (mean ± 51), this mean was increased at mid PD (21PDs) to 4,483μm^2 (mean ± 310). At late PD (85PDs), the surface area gradually increased so that the mean cellular surface area was 9,935μm^2 (mean ± 843). B11 clone demonstrated similar trend of increasing of cell size as the previous clones with the mean cellular surface area at early PD (4PDs) was 813μm^2 (mean ± 56), at mid PD (18PDs) to 1,893μm^2 (mean ± 164) and at late PD (35PDs) was 4,458μm^2 (mean ± 407).

Since there were variation in surface areas between early, mid and late PDs in all clones but no particular pattern, analysis was undertaken by combining the data to identify if each stage of these PDs data (early, mid, late) could have a distinguishing range of surface area. Six different groups of surface areas were established to make a distribution of the cells in all the clones at the three different PDs (Figure 2.11). It was clear that cells from all clones (A11, A31 and B11) at early PD were less than 1500μm^2 surface area. Cells at mid PD from all clones varied between 1500μm^2 to 10,000μm^2. Finally, cells from all clones at late PD contained cells over 1000μm^2 in size.

Figure 2.10. Comparison of the cellular surface areas of DPPCs clones throughout their replicative lifespan. At early PD cells were bipolar and narrow with a small surface area. With progressive proliferation, the cell surface area gradually became larger with a wide and irregular shape. Cells seen were outlined along their peripheral borders to exemplify surface analysis using ImageJ. ×10 magnification, Scale bar 100µm.
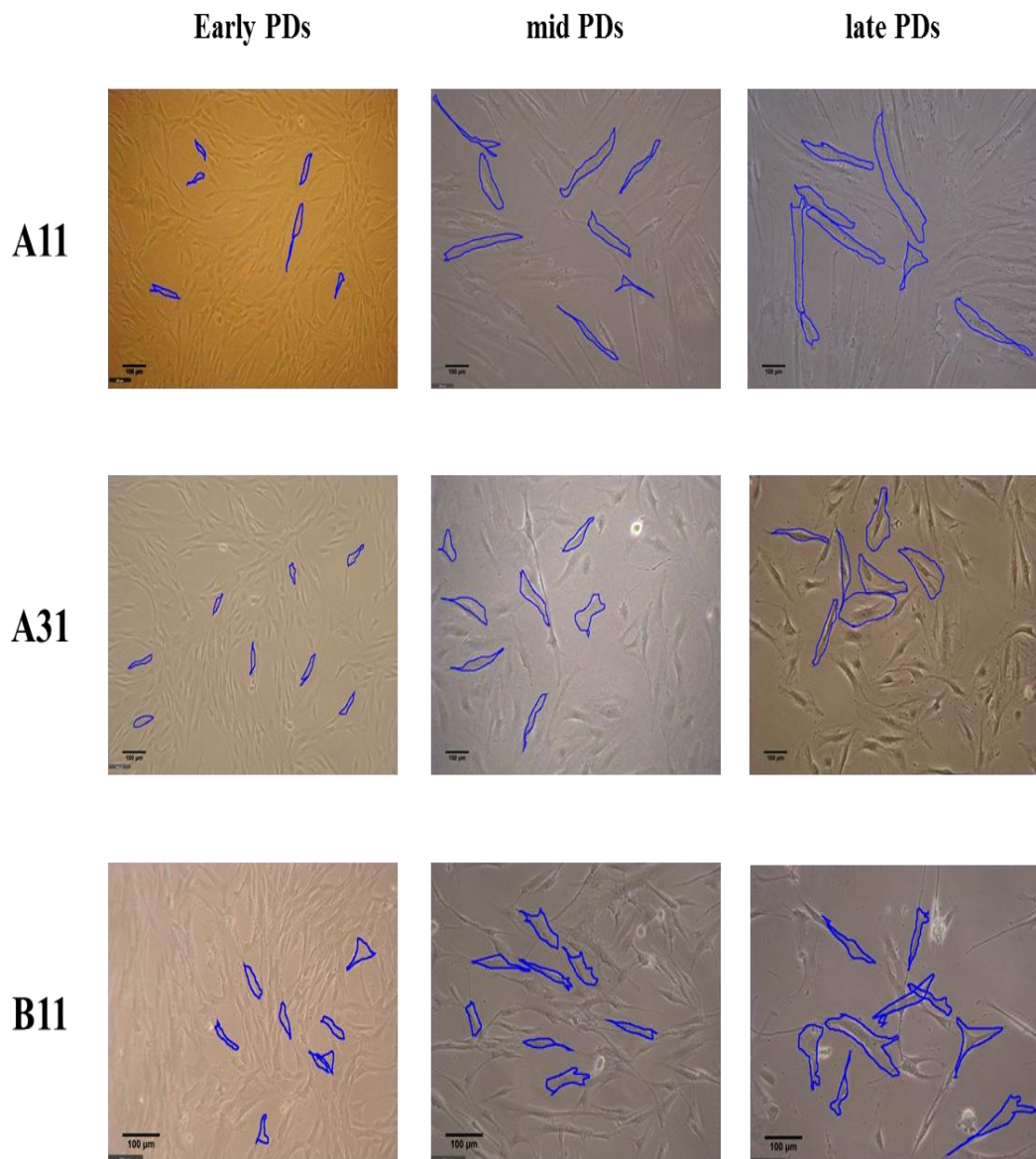
Figure 2.11. The distribution of cell surface area throughout replicative life span of cells. Clones A11, A31, and B11 were analysed collectively. The surface area was obtained from three defined phases (early, mid, and late PDs), with 60 cells were measured for each phase. Cells with <1500μm^2 surface area were collectively at an early PD; cells 1500μm^2-10,000μm^2 surface area were cells at mid PD, and cells > 10,000μm^2 surface area were senescent.
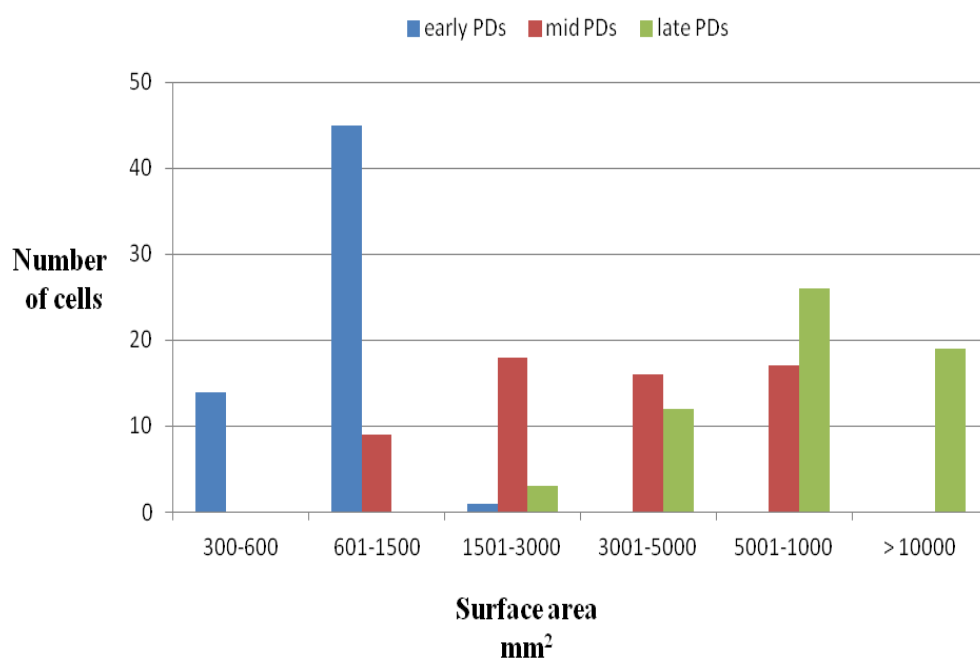
2.4.4　Cell Senescence by β-gal staining

β-galactosidase enzyme is an enzyme associated with cellular senescence and is considered as an indicator of senescent cells if positive staining observed. X gal at pH 6 is converted to blue staining by β- galactosidase that can be visualised using light microscopy. β-galactosidase was performed at early PDs (11PDs for clone A11, 12PDs for clone A31 and 12PDs for clone B11) to confirm their negative expression at this stage, and at very late-stage of culture, when cell PD was less than 0.5 per week. Late-stage was considered after 23PDs for clone A11, 85PDs for clone A31 and 36PDs for clone B11. All the images for the three clones showed a positive staining at late-stage PD for almost 100% of cells and no staining at early PD (Figure 2.12).

Figure 2.12. senescence- associated β-gal activity in populations of clone A11 (11 and 23PDs), A31 (12 and 85PDs), and B11 (12 and 35PDs) suggested all clones have almost 100% positive staining. (β-gal staining shown with arrow) ×10 magnification, Scale bar 100µm.

A11 23PDs

A11 11PDs

A31 85PDs

A31 12PDs

B11 35PDs

B11 12PDs
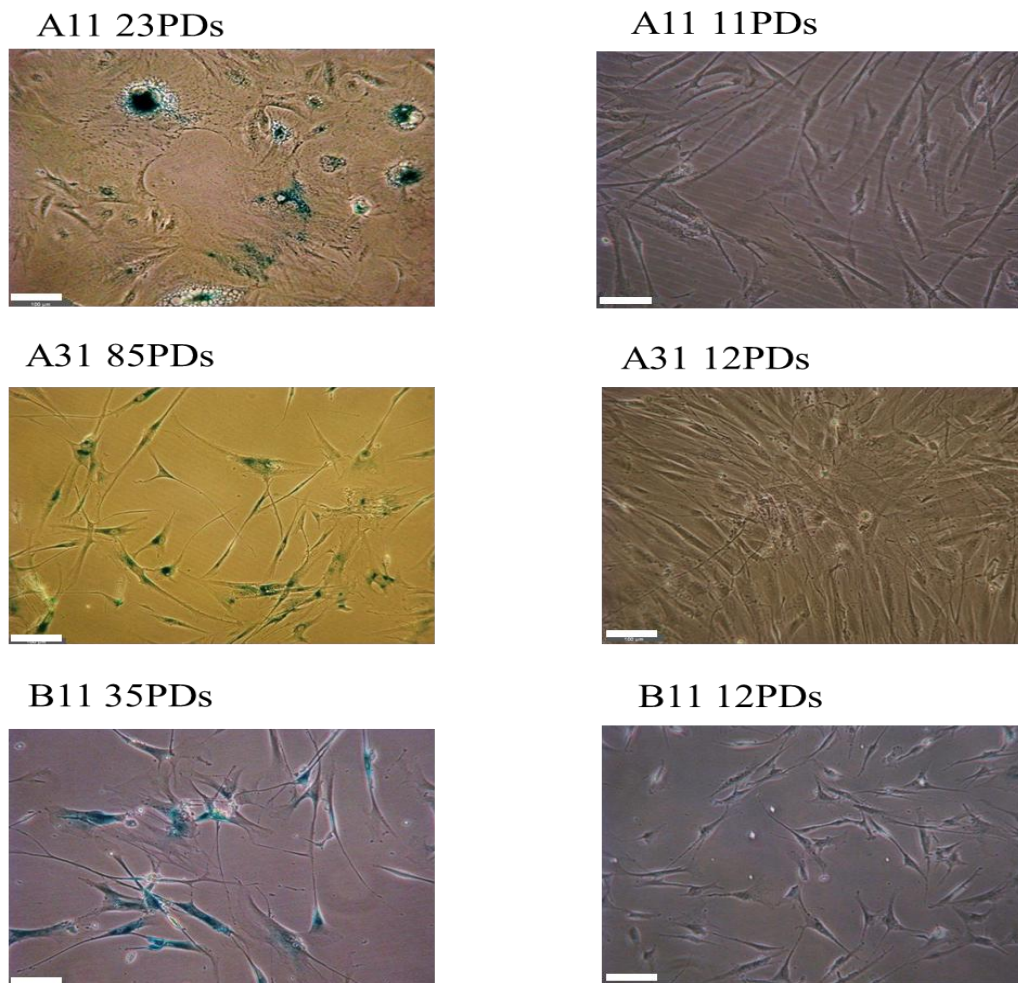
2.4.5   Telomere Length of DPPCs Clones

2.4.5.1 Southern Blot

The average telomere length of 3 selected clones (A11, A31 and B11) was measured using terminal restriction fragment (TRF). Analysis of telomere length was undertaken by southern blots for these clones at mid-early PD (8-14PDs). In addition, clone A31 (55PDs) telomere length was measured at late PD to investigate the effect of aging on telomere length. The southern blot suggested that the highly proliferative clone (A31) had higher smear band than the other clones, and results were quantified by densitometry analysis. Clone A31 at early PD suggested that its smear band started at the same height as the later PD, but the length of the smear band was longer for the later PD, indicating a more heterogeneous population for these cells (Figure 2.13).

2.4.5.2 Densitometry Data Analysis

After determining the mean TRF (Figure 2.1) by using the equation Σ (ODi) / Σ (ODi /Li), the results is shown in Table 2.2. It is clear that clone A31, the highly proliferative clone, had a much longer telomere length, with 18.3Kb compared with clones A11 and B11. Clone A31 at 55PDs appeared to lose significant telomere length compared with its original length at 9PDs with a 11.9Kb shortening.

Figure 2.13. Representative southern blot for three clones (A11, A31 and B11) including Clone A31 at two different PDs (9 and 55PDs) in addition to the kit control (Ctrl) and molecular weight marker (MW).
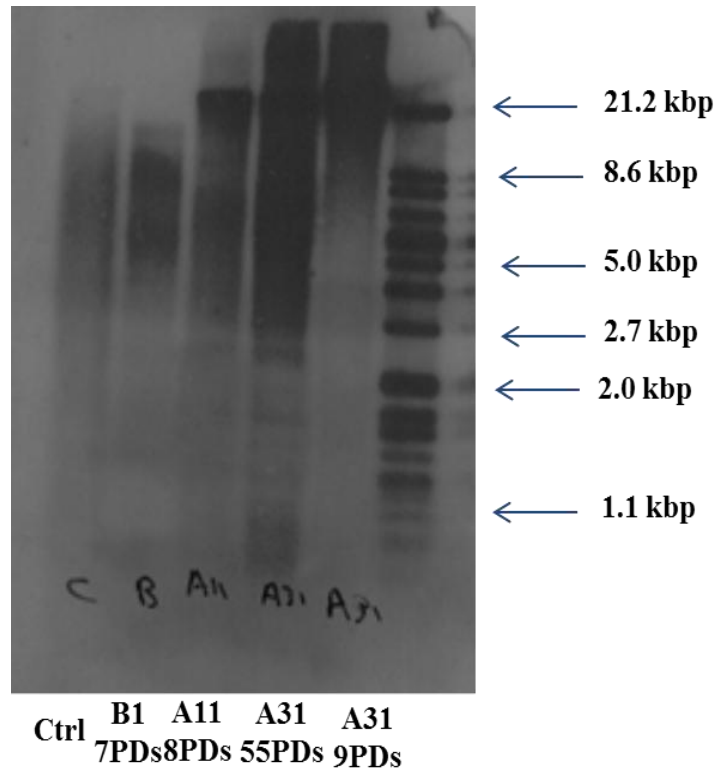

Table 2.2. The mean of telomere length for DPPCs clones calculated from southern blot (Figure 2.15)

Clone	Mean of TRF by Kb
A31 9PDs	18.3
A31 55PDs	6.4
A11 8PDs	5.9
B11 14PDs	5.6

2.4.6   Oxidative Stress Results

2.4.6.1 Population Doublings

The population doubling of DPPCs throughout their proliferative lifespan was also assessed in different H_2O_2 concentrations. At low concentrations of H_2O_2 (5-25μM) population doubling levels for clone A31 were assessed. Based on the resistance of clone A31 to cellular senescence (Figure 2.14), higher H_2O_2 concentrations (50-200μM) were used to assess the susceptibilities of all 3 clones (A31, A11 and B11) to oxidative stress-induced senescence. For the lower concentration, there was almost no difference in the population doubling between controls and the other concentrations as cells in all conditions continued growing for more than 300 days without senescence (Figure 2.14). For the higher concentrations, there were variable differences in each clone but in general, 200μM demonstrated significant reduction and early senescence of all clones. Clone A31 demonstrated more resistance to H_2O_2 at 200μM than other clones. Cells senesced before 100 days in 200μM and then after 160 days for other concentrations (50 and 100μM) (Figure 2.15). On the other hand, clone A11 showed no diversity in population doublings between the different H_2O_2 concentrations (Figure 2.16). Clone B11 at 200μM H_2O_2 senesced after 50 days in culture while cells at 50 and 100μM concentrations senesced after more than 80 days which was similar to the untreated cells (Figure 2.17).

Figure 2.14. Clone A31 at low H$_2$O$_2$ concentrations (0, 5, 10, 25μM). All the treatments including the control exhibited almost the same PD throughout proliferative lifespan until they reach senescence at over 300 days in culture.
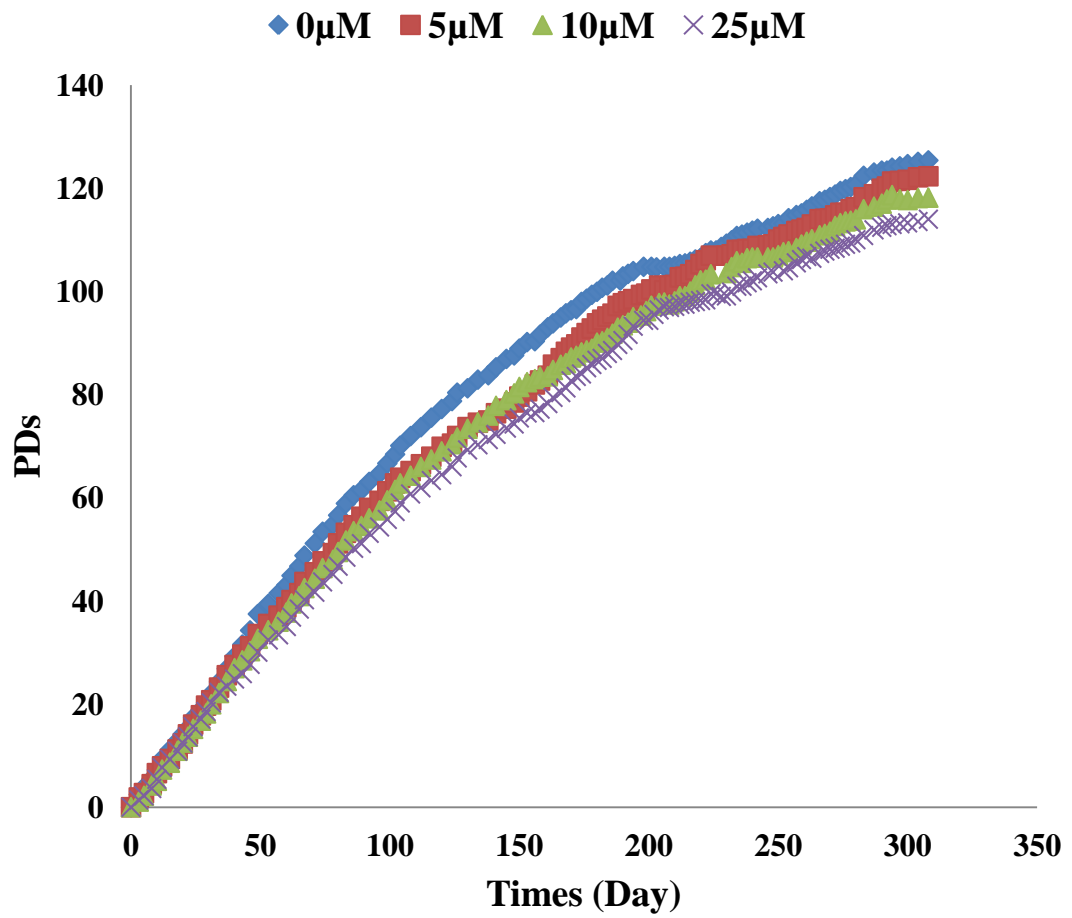
Figure 2.15. Clone A31 at high H_2O_2 concentrations (0, 50, 100, 200μM). Reductions in PD at 100μM and 200μM H_2O_2 concentrations were clear after 50 days, compared with the untreated controls and cells treated with 50μM H_2O_2. PD of cells treated in 50μM only declined compared to untreated control cells at >100 days in culture. Cells cultured in 200μM H_2O_2 senesced at less than 100 days in culture, while cells exposed to other H_2O_2 concentrations maintained proliferative capabilities for more than 150 days.
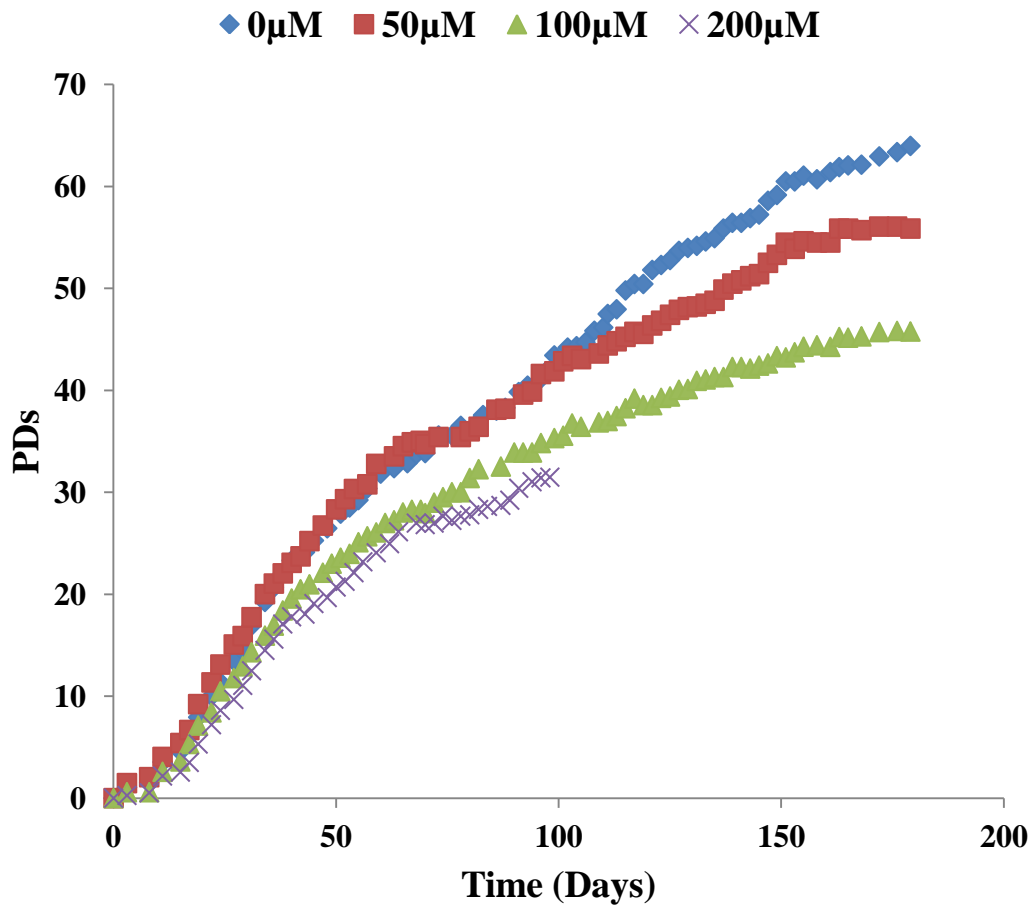
Figure 2.16. Clone A11 at high H_2O_2 concentrations (0, 50, 100, 200μM). There were no differences in PD between the H_2O_2 concentrations during the short period in culture less than 30 days, due to its early senescence. This was also evident with the untreated control.
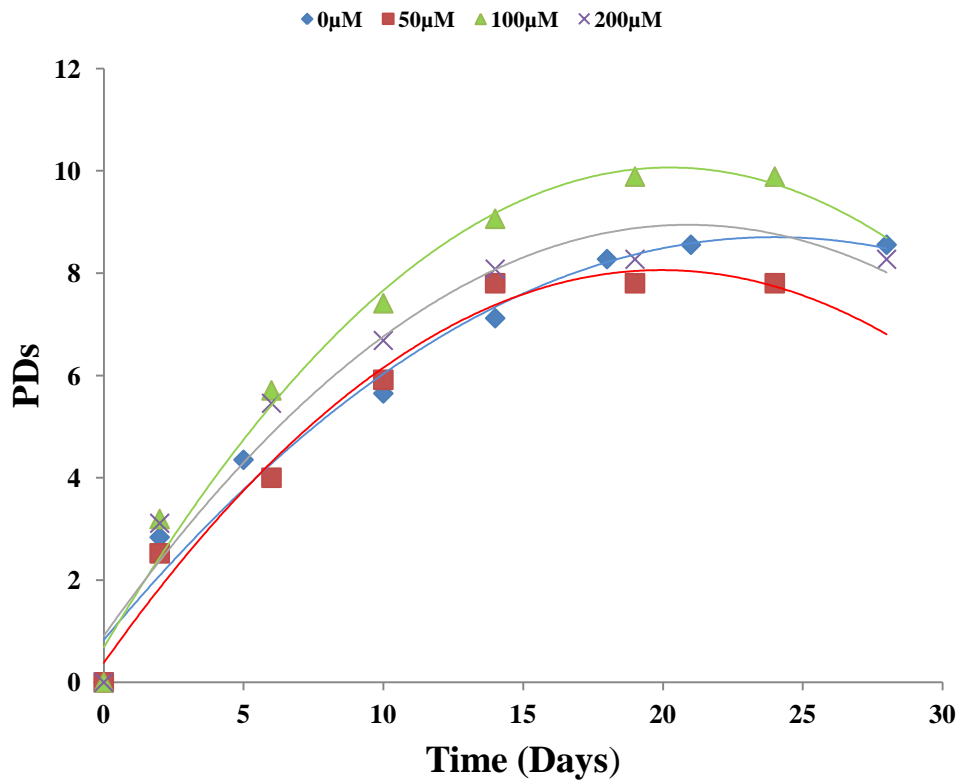
Figure 2.17. Clone B11 (from the second patient) at high H_2O_2 concentrations (0, 50, 100, 200μM) compared to untreated controls over 60 days in culture. The higher concentration (200μM) significantly decreased proliferative capabilities, as cells exhibited lower proliferation within 20 days in culture, and senesced by 50 days. The 100μM H_2O_2 concentration showed a reduction of PD after 30 days, while 50μM concentration has no major effect on PD.
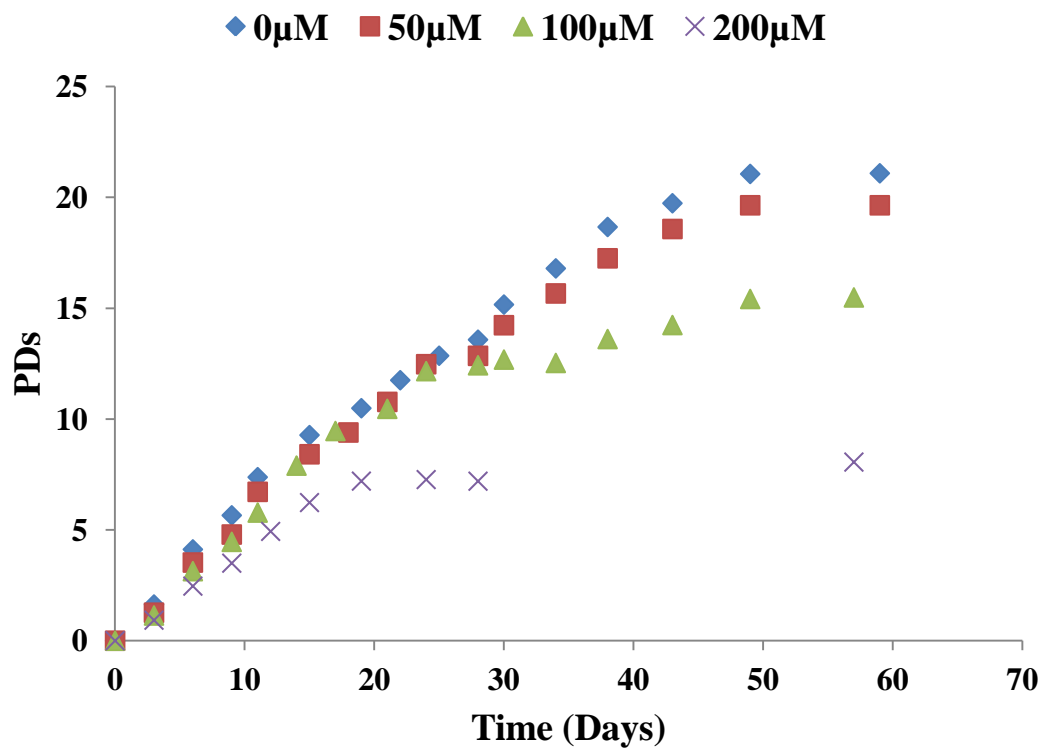
2.4.6.2 Gene Marker Expressions in DPPCs at Different H_2O_2 Concentrations

MSC markers CD105, CD90 and CD73 were analysed in clones A11, A31 and B11 in different concentrations of H_2O_2 (0, 50, 100, 200μM) at the middle period of their treatments 18PDS, 38PDs and 18PDs for A31, A11 and B11 respectively (Figure 2.18). No differences were detected at the MSCs gene expressions in the different concentration of H_2O_2. Water and RT-negative experimental controls demonstrated no expression.

Figure 2.18. Mesenchymal stem cell gene expression for A11, A31, and B11 in different concentrations of H_2O_2 (0, 50, 100, 200μM) at the middle period of their treatments. No differences were detected for MSC gene expression in the different concentrations of H_2O_2. β-actin was used the housekeeping gene. Water and RT-negative experimental controls had no expression.
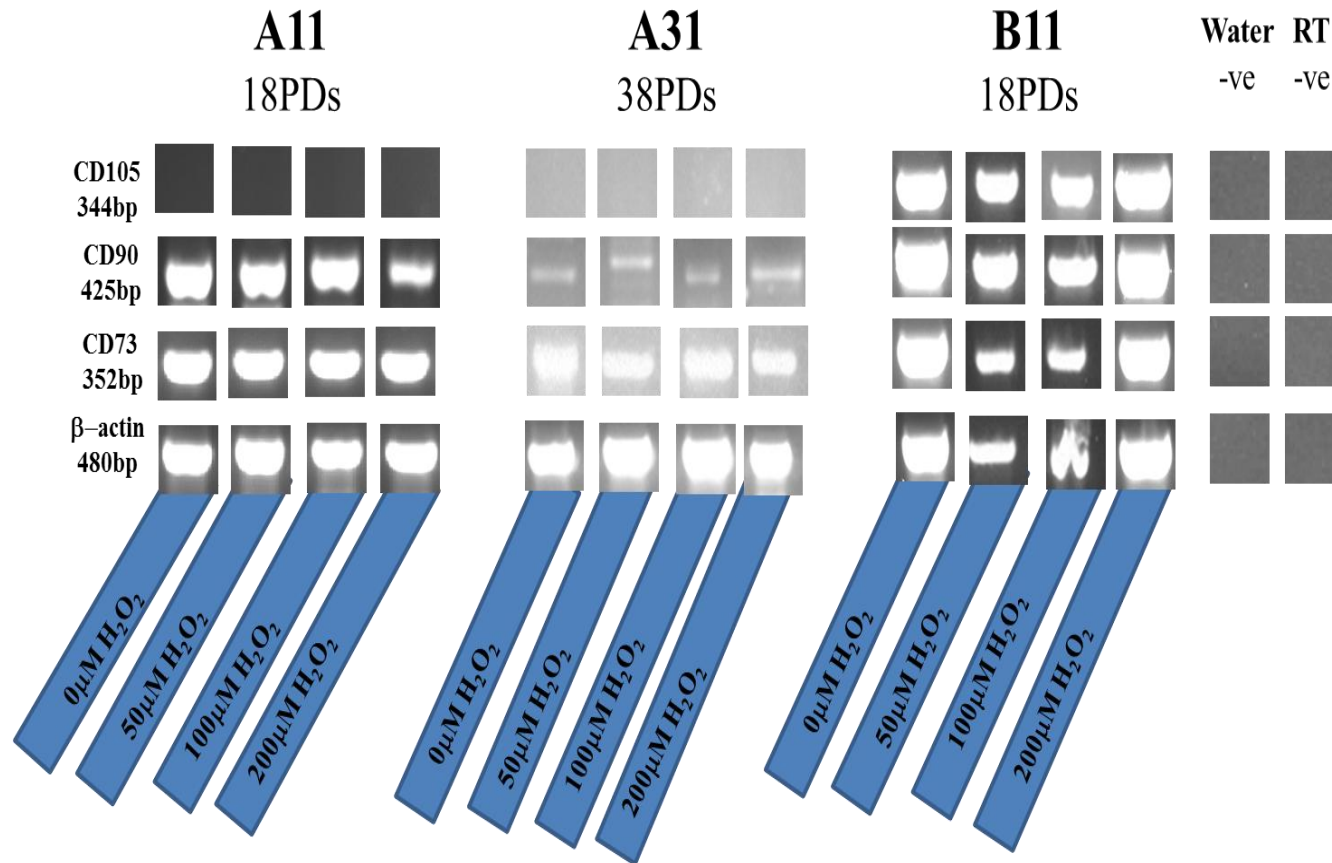
2.4.6.3 Cell Morphology

Microscopic analysis of cellular morphology of the monolayer culture of DPPCs was undertaken throughout proliferation at different concentrations of H_2O_2. At early stages of culture with H_2O_2 treatment, cells did not show any noticeable difference in their morphology at differing concentrations. In later cultures, changes in morphology and size became more apparent between the different concentrations of H_2O_2 figures 2.19 to 2.29. For clone A31, no noticeable difference in cell morphology was observed in cells cultured in all low concentrations of H_2O_2 (0, 5, 10, 25μM) after 1 day, 100 days or 221 days in culture (Figures 2.19 to 2.21), However, cells exhibiting ageing in all concentrations after 221 days became larger, wider and irregular in shape with loss of polarity and with appearance of stress fibers (Figure 2.21).

Clone A31 cultured in higher concentrations of H_2O_2 (0, 50, 100, 200μM) did not show any differences in cell morphology between all these different concentrations after 1 day in culture (Figure 2.22). After 90 days, cells cultured in 200μM H_2O_2 appeared larger with the appearance of stress fibers (Figure 2.23), while after 146 days of culture, cells in the presence of 50 and 100mM H_2O_2 appeared to be more irregular in shape and larger in size compared with non- treated cells which contained few numbers of larger cells (figure 2.24).

Clones A11 and B11 demonstrated similar results as clone A31 at day 1 where no differences appeared in cell morphology between all H_2O_2 concentrations (Figure 2.25 and 2.27). Clone A11 did not show any differences on cell morphology between high H_2O_2 concentrations at day 30, although cells demonstrated senescence morphology (Figure 2.26) as seen in A31 clone (Figure 2.21). For clone B cells in 200μM H_2O_2 after 40 and 60 days, there tended to be more elongated and stressed compared to the other concentrations (Figure 2.28 and 2.29).

Figure 2.19. Comparison of the morphological appearance of clone A31 at different low H_2O_2 concentrations (0, 5, 10, and 25μM) at day 1. All images showed the same size and morphological appearance of cells, with the characteristic long, spindle, bipolar shape.×10 magnification, Scale bar 100μm.

0μM H_2O_2

5μM H_2O_2

10μM H_2O_2

25μM H_2O_2

Figure 2.20. Comparison of the morphological appearance of clone A31 at different low H_2O_2 concentrations (0, 5, 10, and 25μM) at day 100. All the images showed the same size and morphological appearance, with cells started to be wider and larger in size, although still maintaining their spindle and bipolar shape. .×10 magnification, Scale bar 100μm.

0μm H_2O_2
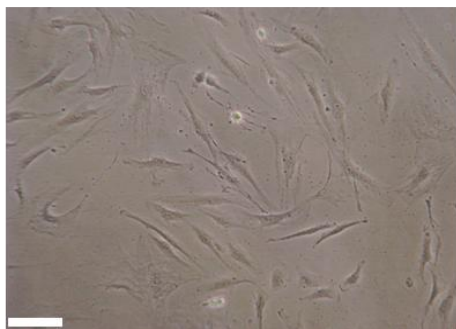
5μm H_2O_2

10μm H_2O_2

25μm H_2O_2

Figure 2.21. Comparison of the morphological appearance of clone A31 at different low H$_2$O$_2$ concentrations (0, 5, 10, and 25µM) at day 221. All the images showed the same size and morphological appearance, with cells became larger, wider and irregular in shape with loss of polarity and with appearance of stress fibers. ×10 magnification, Scale bar 100µm.

0µM H$_2$O$_2$

5µM H$_2$O$_2$

10µM H$_2$O$_2$
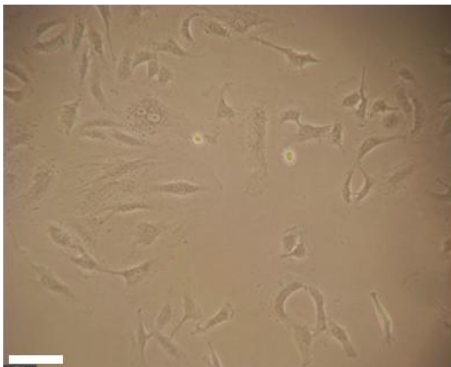
25µM H$_2$O$_2$

Figure 2.22. Comparison of the morphological appearance of clone A31 at different high H_2O_2 concentrations (0, 50, 100, and 200μM) at day 1. All the images showed the same cell size and morphological appearance, with the characteristic long, spindle and bipolar shape. ×10 magnification, Scale bar 100μm.
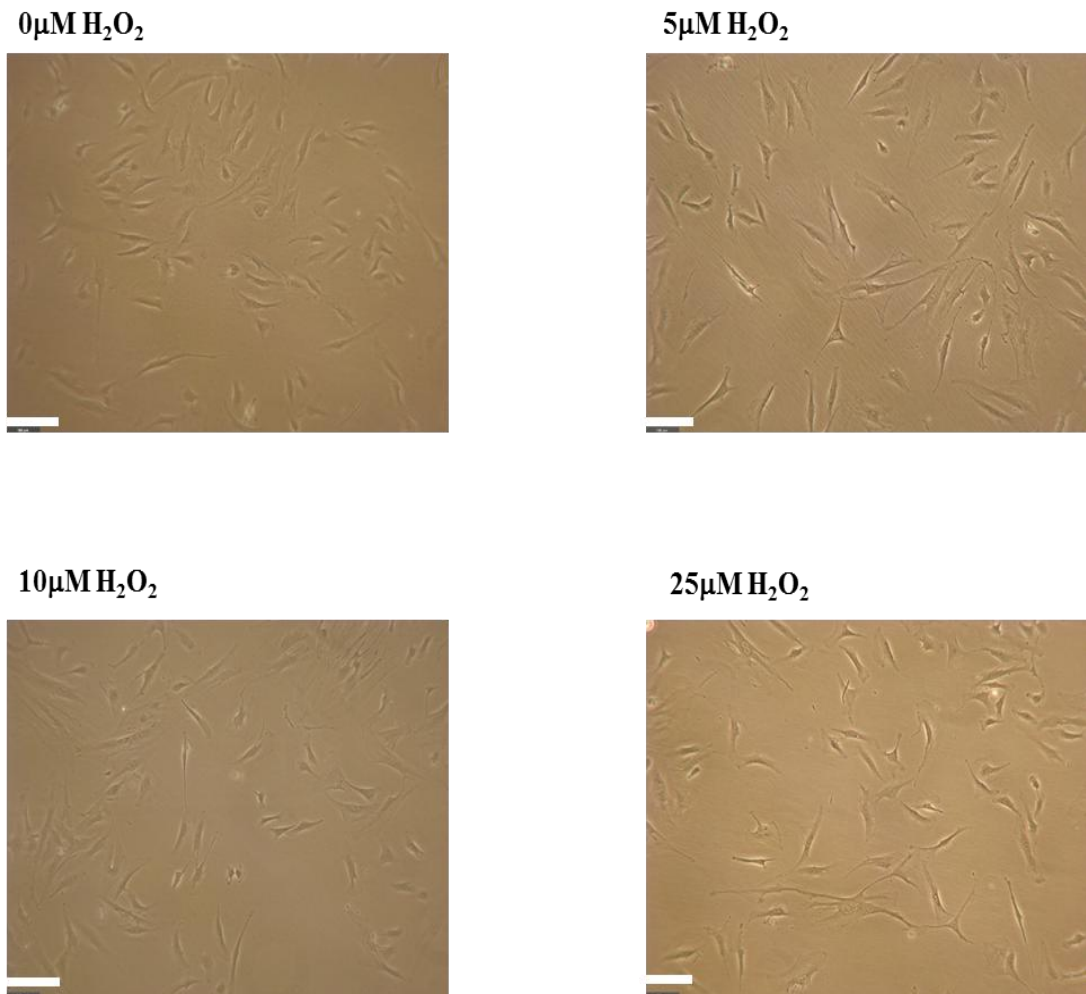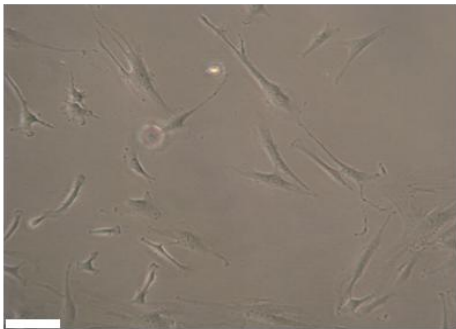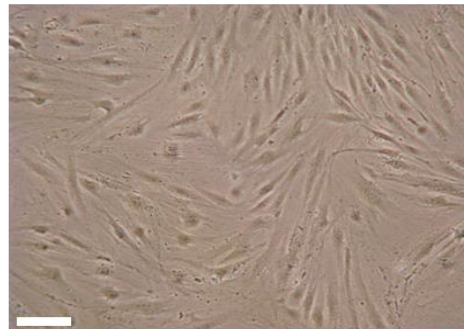
0μM H_2O_2

50μM H_2O_2
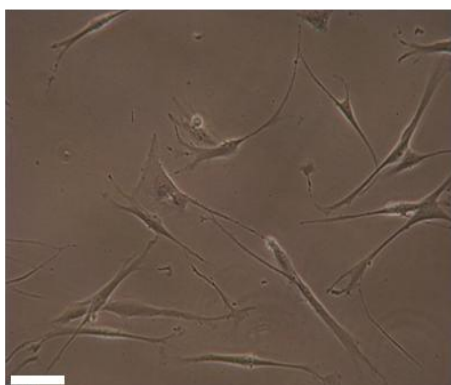
100μM H_2O_2

200μM H_2O_2

Figure 2.23. Comparison of the morphological appearance of clone A31 at different high H_2O_2 concentrations (0, 50, 100, and 200μM) at day 90. The images for 0, 50, 100μM showed similar size and morphological appearance of cells but cells in 200μM were larger, wider and irregular in shape with loss of polarity and appearance of stress fibers. ×10 magnification, Scale bar 100μm.

0μM H_2O_2

50μM H_2O_2

100μM H_2O_2
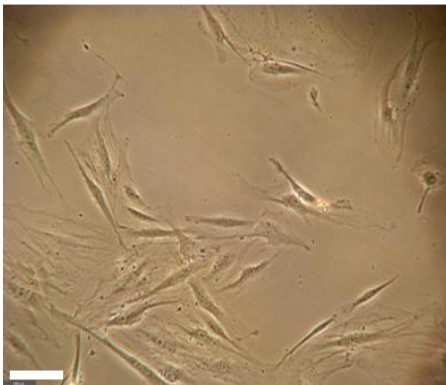
200μM H_2O_2

Figure 2.24. Comparison of the morphological appearance of clone A31 at different high H_2O_2 concentrations (0, 50, 100, and 200μM) at day 146. Most of the cells in the control treatment showed a fibroblastic appearance while cells in 50μM and 100μM H_2O_2 showed more irregularity in shape and increased cell width with more cell fibers visible. ×10 magnification, Scale bar 100μm.

0μM H_2O_2

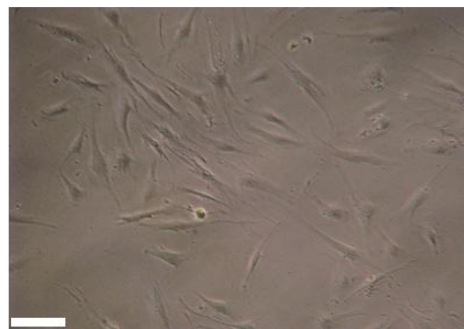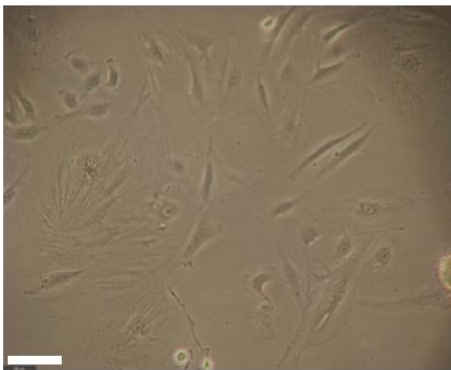50μM H_2O_2

100μM H_2O_2
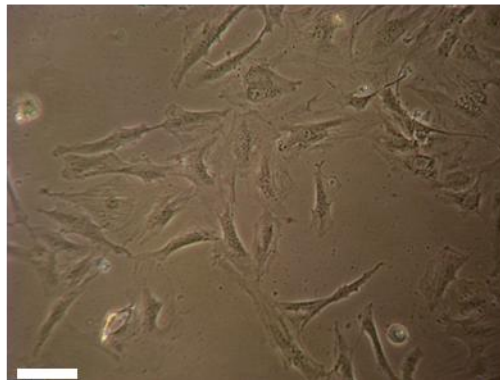
Figure 2.25. Comparison of the morphological appearance of clone A11 at different high H_2O_2 concentrations (0, 50, 100, and 200μM) at day 2. All the images showed the same size and morphological appearance of cells, with the characteristic long, spindle, bipolar shape. ×10 magnification, Scale bar 100μm.
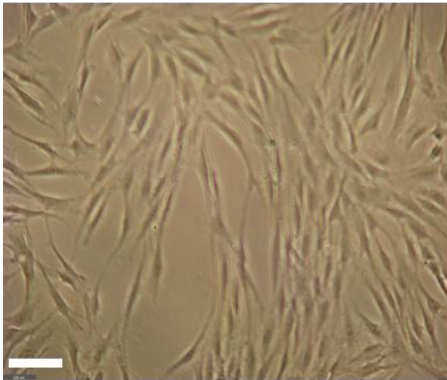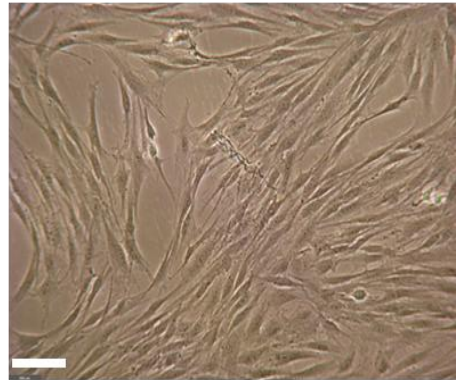
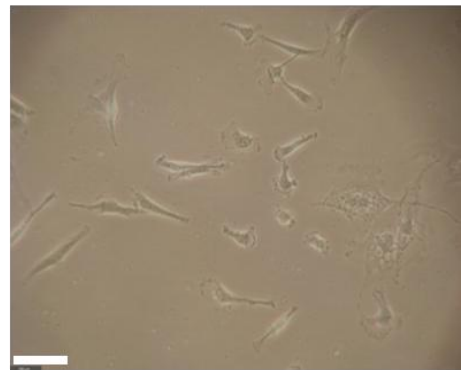0μM H_2O_2

50μM H_2O_2
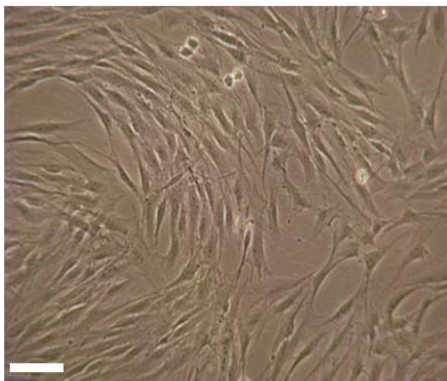
100μM H_2O_2

200μM H_2O_2
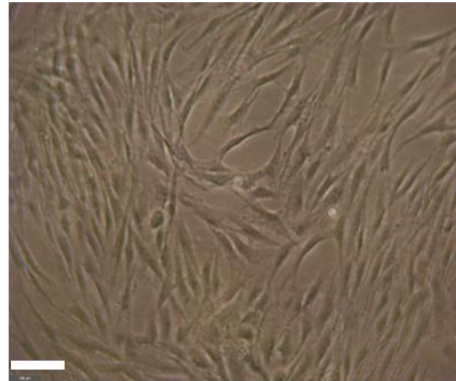
Figure 2.26. Comparison of the morphological appearance of clone A11 at different high H_2O_2 concentrations (0, 50, 100, and 200μM) at day 30. All the images of the all different concentrations showed that the cells increased in size in very short period, 30 days. ×10 magnification, Scale bar 100μm.

0μM H_2O_2

50μM H_2O_2

100μM H_2O_2
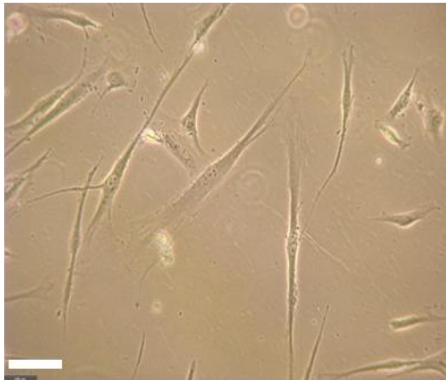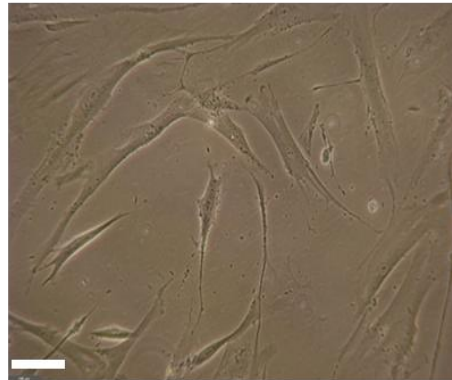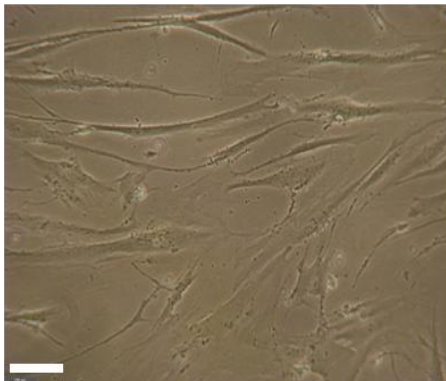
200μM H_2O_2
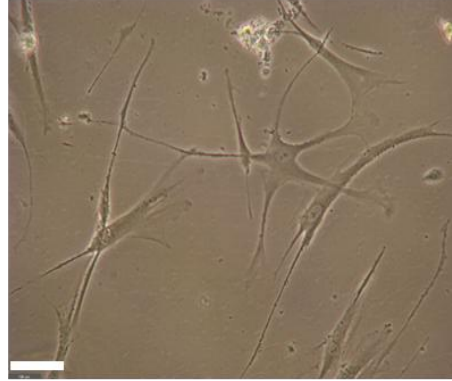
Figure 2.27. Comparison of the morphological appearance of clone B11 at different high H_2O_2 concentrations (0, 50, 100, and 200μM) at day 1. All the images showed the same size and morphological appearance of cells, with the characteristic long, spindle, bipolar shape.. ×10 magnification, Scale bar 100μm.
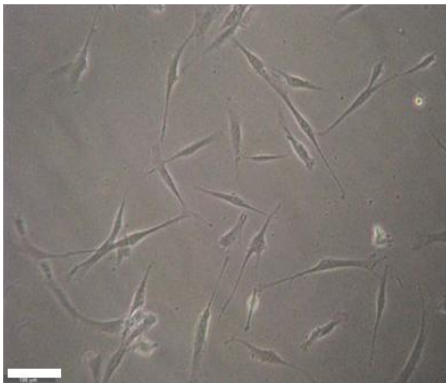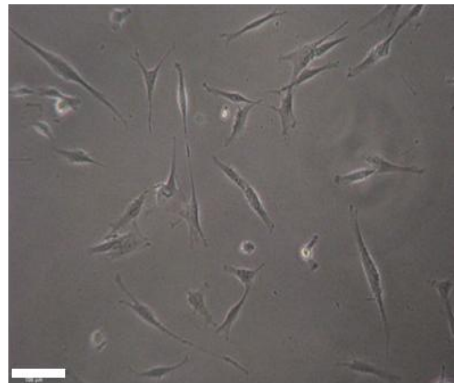
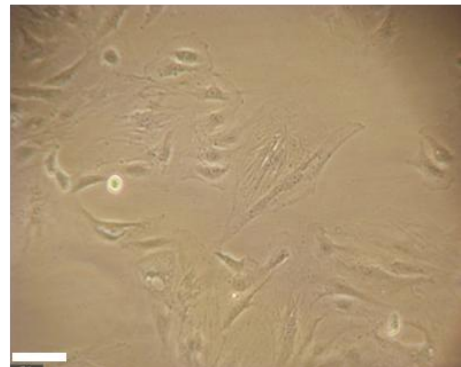0μM H_2O_2

50μM H_2O_2
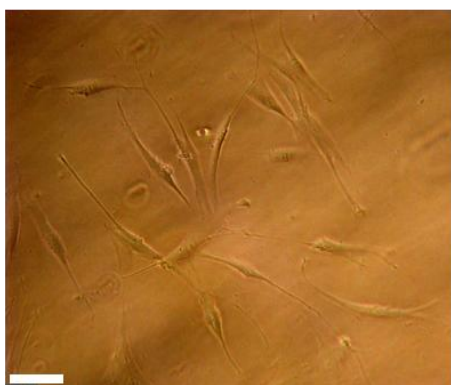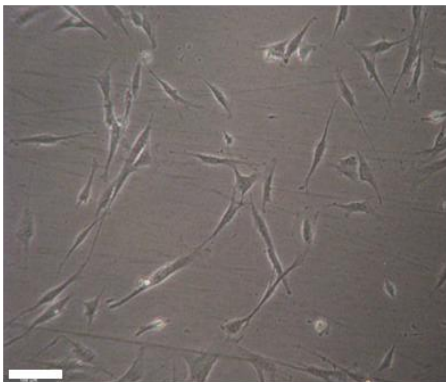
100μM H_2O_2
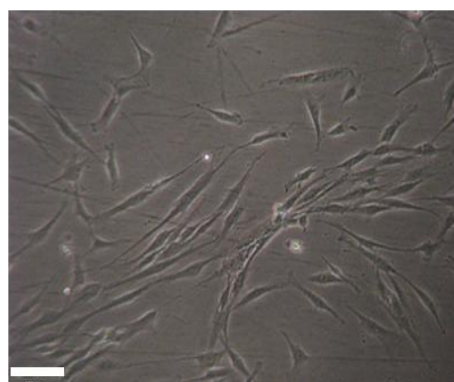
200μM H_2O_2

Figure 2.28. Comparison of the morphological appearance of clone B11 at different high H_2O_2 concentrations (0, 50, 100, and 200μM) at day 40. The images of 0, 50, and 100μM H_2O_2 concentrations showed similar size and morphological appearance, but cells in 200μM H_2O_2 became elongated and stressed. ×10 magnification, Scale bar 100μm.
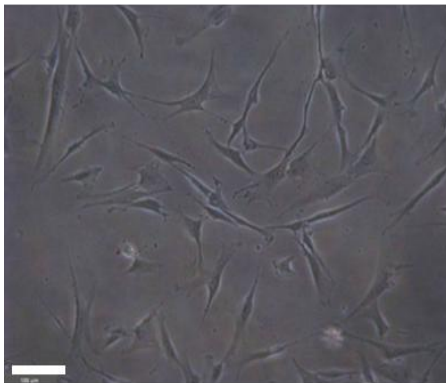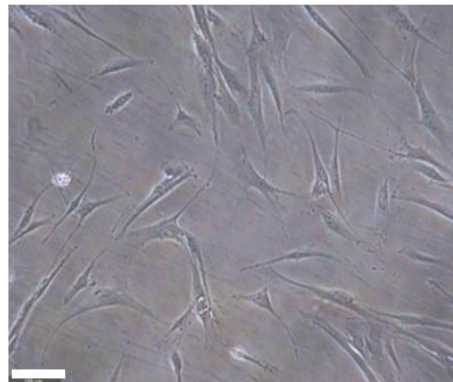
0μM H_2O_2

50μM H_2O_2
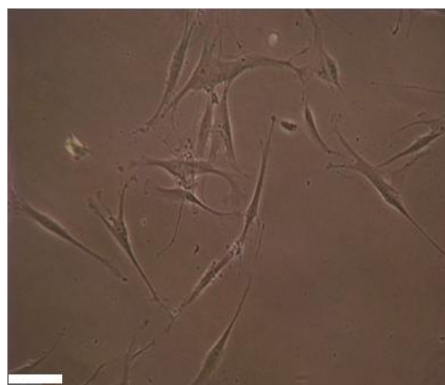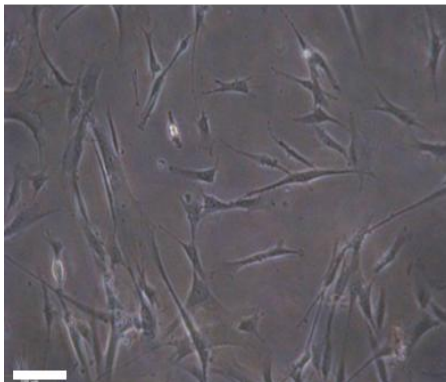

100μM H_2O_2
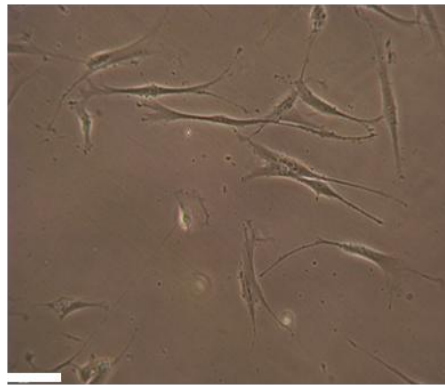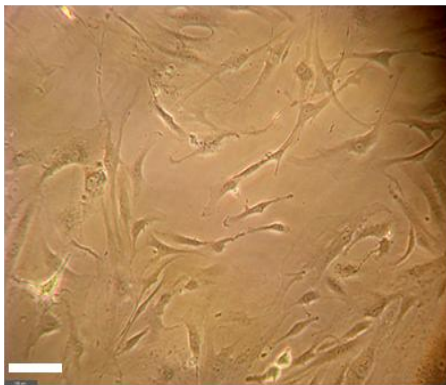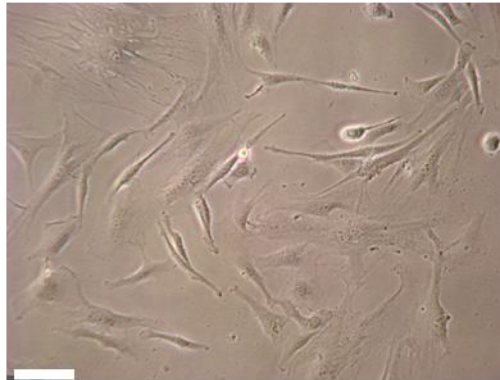

200μM H_2O_2

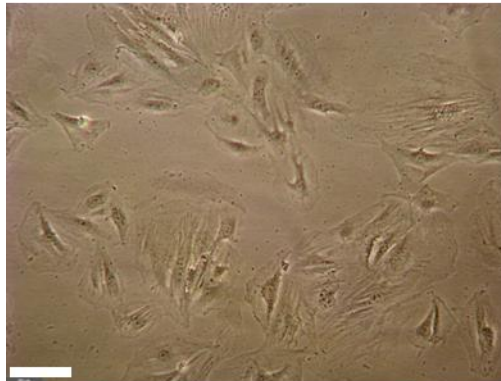**Figure 2.29. Comparison of the morphological appearance of clone B11 at different high H_2O_2 concentrations (0, 50, 100, and 200µM) at day 60. The images of 0, 50, 100µM H_2O_2 showed elongation of the cells while in 200µM H_2O_2 the cells became more stressed. ×10 magnification, Scale bar 100µm.**
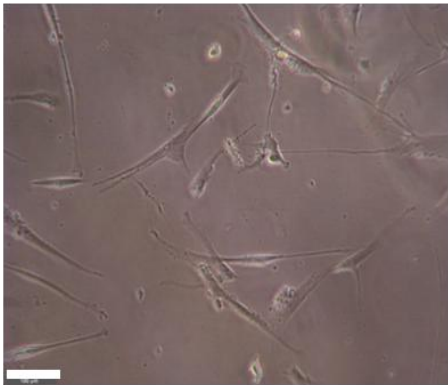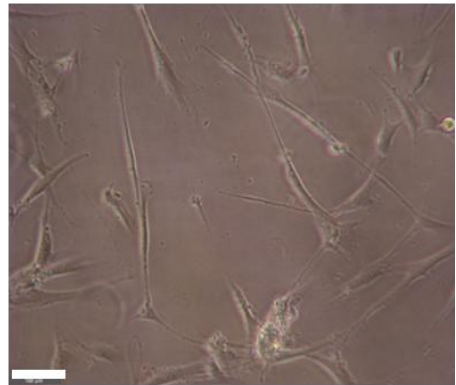
0µM H_2O_2

50µM H_2O_2
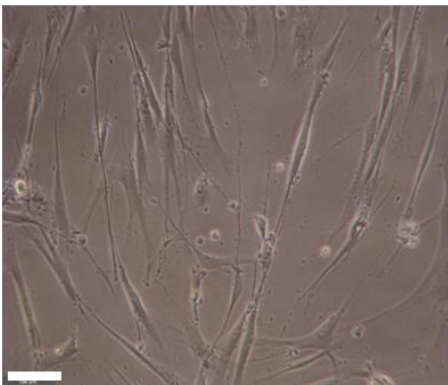
100µM H_2O_2

200µM H_2O_2
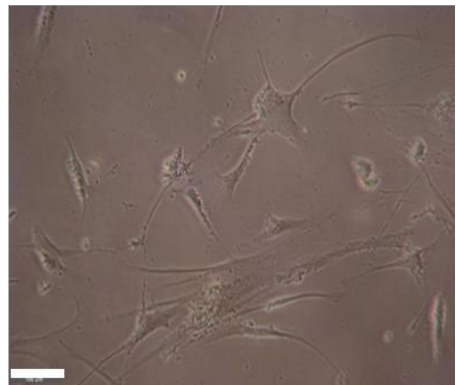
2.4.6.4 Oxidative Stress on Cell Senescence by β-gal Staining

The number of positive (blue) cells for clones A31, A11, and B11 in different H_2O_2 concentrations (0, 50, 100 and 200μM) were counted from 15-20 different areas, seeding triplicate repeats of $38x10^3$ cells in $9.6cm^2$. The triplicate average percentage of positive cells was calculated (Figures 2.30 to 2.34).

50μM and 100μM H_2O_2 appeared to have negligible effect on cell senescence in clone A31, with 45% of cells stained positive with β-gal compared with the control (28% positive β-gal staining). 200μM H_2O_2 demonstrated the largest positive staining, with 61% of cells positive after 128 days of culture (Figure 2.30). In the same conditions after 196 days, there were no cells in 200μM treated cultures as all cells had already senesced. Cells with no treatment or cultured in 50μM H_2O_2 demonstrated similar levels of cell senescence, with 27% of cells β-gal positive, while cells in 100μM H_2O_2 were 53% positive (Figure 2.31).

More than 90% of cells of clone A11 were positively stained following 50 days of culture in different H_2O_2 concentrations (Figure 2.32). Clone B11 showed similar results to Clone A11 after 70 days of culture in the same conditions (Figure 2.34).

Figure 2.30. Comparison senescence- associated β-gal activity in population of clone A31 in different H_2O_2 concentrations (0, 50, 100, and 200μM) after128 days (46PDs). (β-gal staining shown with arrow). ×10 magnification, Scale bar 100μm.

0μM H_2O_2

% of +ve β-gal staining: 28

50μM H_2O_2

% of +ve β-gal staining: 45

100μM H_2O_2

% of +ve β-gal staining: 48

200μM H_2O_2

% of +ve β-gal staining: 61
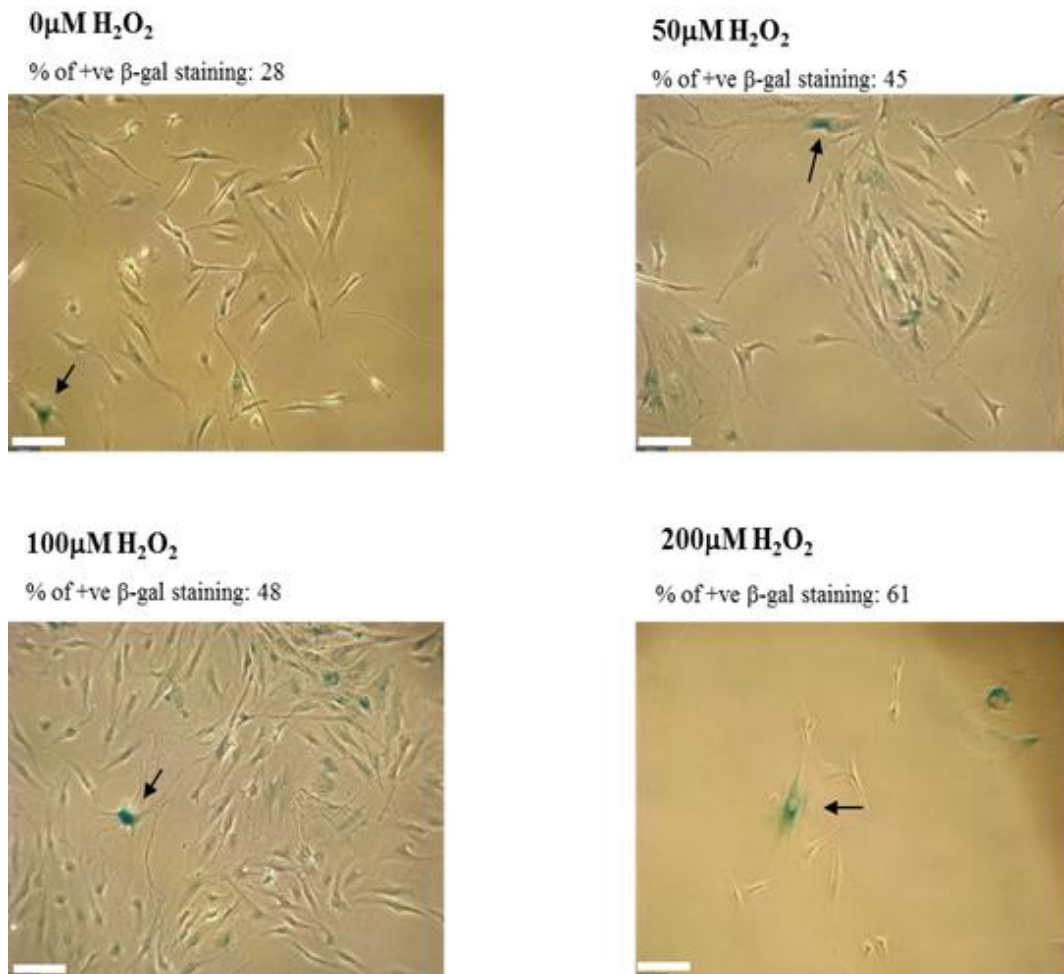
Figure 2.31. Comparison senescence- associated β-gal activity in population of clone A31 in different H_2O_2 concentrations (0, 50 and 100μM) after 196 days (59PDs). (β-gal staining shown with arrow). ×10 magnification, Scale bar 100μm.

0μM H_2O_2

% of +ve β-gal staining: 27

50μM H_2O_2

% of +ve β-gal staining: 28

100μM H_2O_2

% of +ve β-gal staining: 28
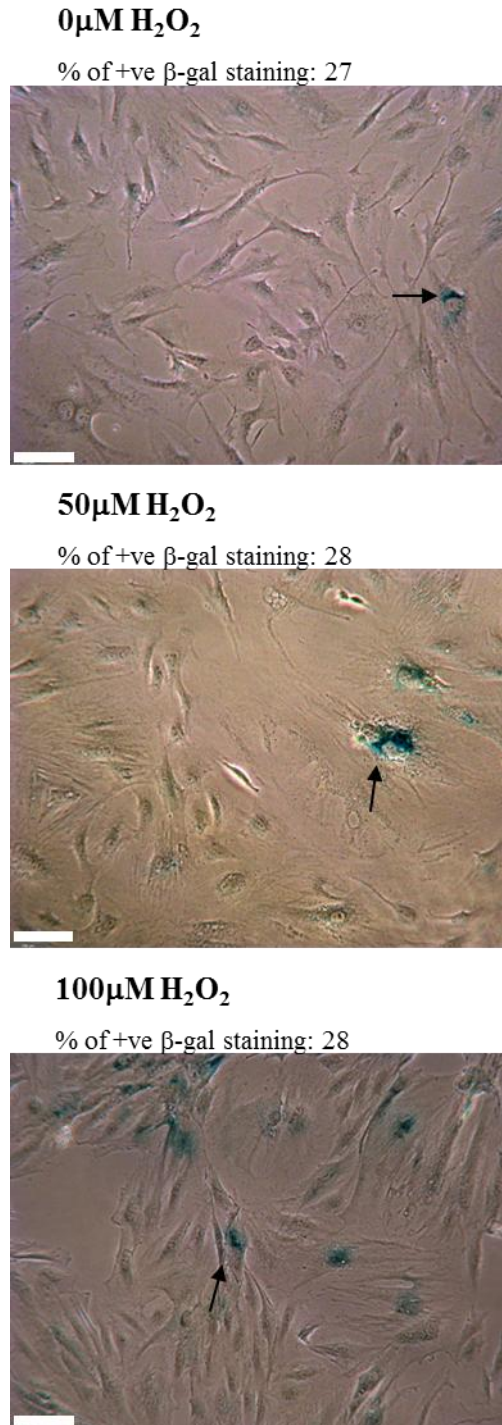
Figure 2.32. Comparison senescence- associated β-gal activity in population of clone A11 in different H$_2$O$_2$ concentrations (0, 50, 100 and 200μM) after 50 days (23PDs). (β-gal staining shown with arrow). ×10 magnification, Scale bar 100μm.

0μM H$_2$O$_2$
% of +ve β-gal staining > 90

50μM H$_2$O$_2$
% of +ve β-gal staining > 90

100μM H$_2$O$_2$
% of +ve β-gal staining > 90

200μM H$_2$O$_2$
% of +ve β-gal staining > 90
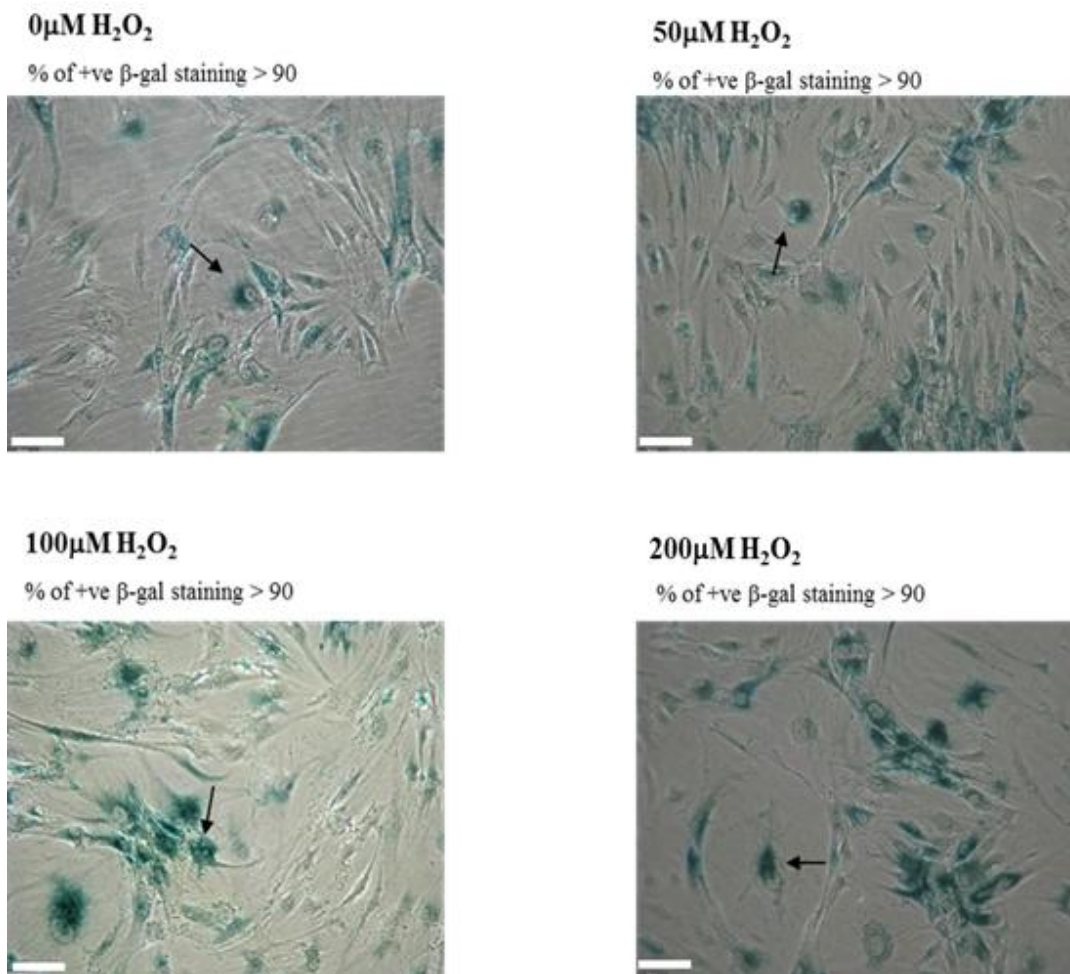
Figure 2.33. Comparison senescence- associated β-gal activity in population of clone B11 in different H_2O_2 concentrations (0, 50, 100 and 200μM) after 50 days. (β-gal staining shown with arrow). ×10 magnification, Scale bar 100μm.

0μM H_2O_2
% of +ve β-gal staining : 20

50μM H_2O_2
% of +ve β-gal staining : 23

100μM H_2O_2
% of +ve β-gal staining : 65

200μM H_2O_2
% of +ve β-gal staining > 90
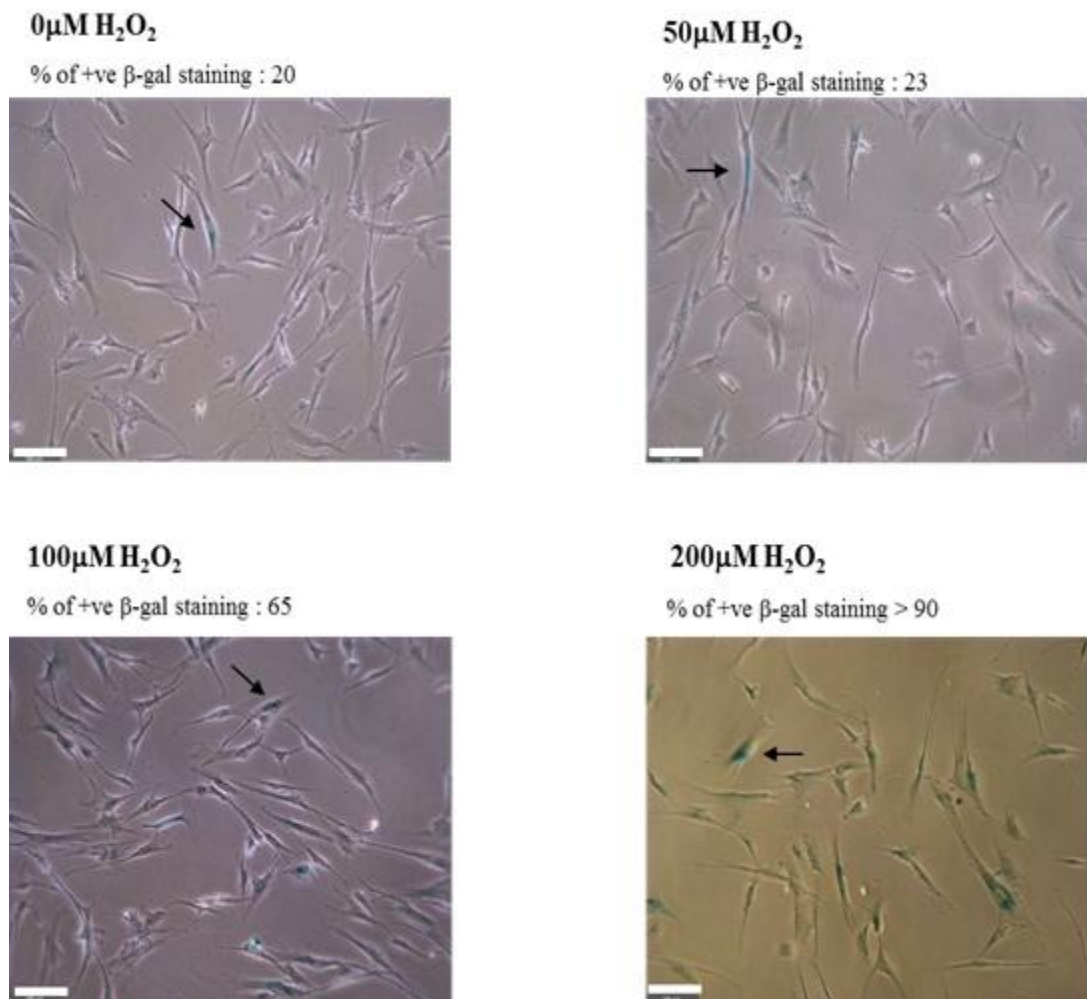
Figure 2.34. Comparison senescence- associated β-gal activity in population of clone B11 in different H_2O_2 concentrations (0, 50, 100 and 200μM) after 70 days. (β-gal staining shown with arrow). ×10 magnification, Scale bar 100μm.

0μM H_2O_2

% of +ve β-gal staining > 90

50μM H_2O_2

% of +ve β-gal staining > 90

100μM H_2O_2
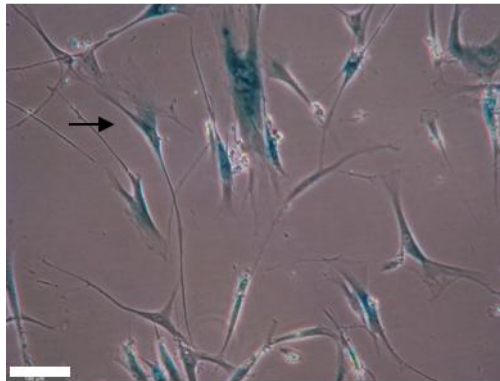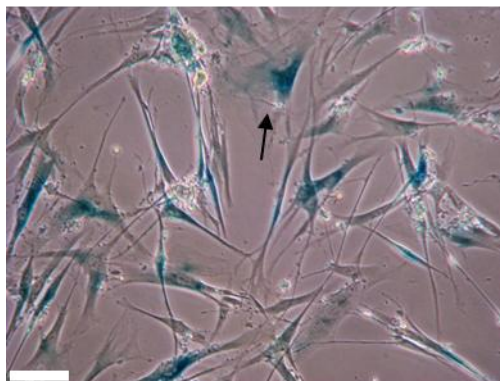
% of +ve β-gal staining > 90
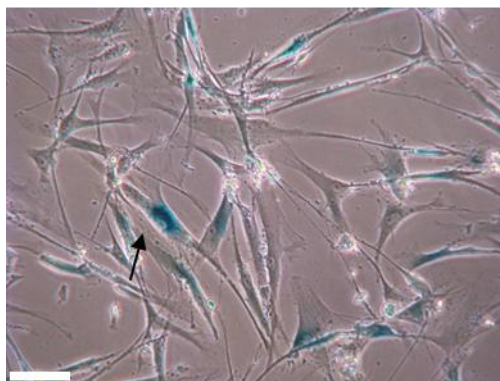
2.4.6.5 Oxidative Stress on Telomeres Length

2.4.6.6 Southern Blot

The average telomere length of 3 selected clones at early PD (A11 at 15PDs, A31 at 18PDs and B11 at 18PDs) in differing H_2O_2 concentrations (0, 50, 100, 200μM) was measured using terminal restriction fragment (TRF) as described in section 2.3.7.5 . Analysis of telomere length was undertaken by southern blots after 30 days of culture in the presence of H_2O_2 which suggested that the density of the smear band in all clones was been affected by different H_2O_2 concentrations. Only clone A11 at 200μM H_2O_2 demonstrated a shorter smear band at the bottom end (Figure 2.35).

2.4.6.7 Densitometry Data Analysis

After determining the mean TRF as shown in figure 2.1 by using the equation Σ (ODi) / Σ (ODi /Li), the results are represented in Table 2.2. The densitometry analysis suggests that clones A31 and B11 have minor differences in telomere length between the different H_2O_2 concentrations, with the maximum difference being less than 1Kb.

Figure 2.35. Representative southern blots for three clones (A11, A31 and B11) in different concentrations of H_2O_2 treatment after around 30 days. The table represents the number indication of each lane.

M	Molecular weight
1	$0\mu M\ H_2O_2$
2	$50\mu M\ H_2O_2$
3	$100\mu M\ H_2O_2$
4	$200\mu M\ H_2O_2$
5	Control Kit
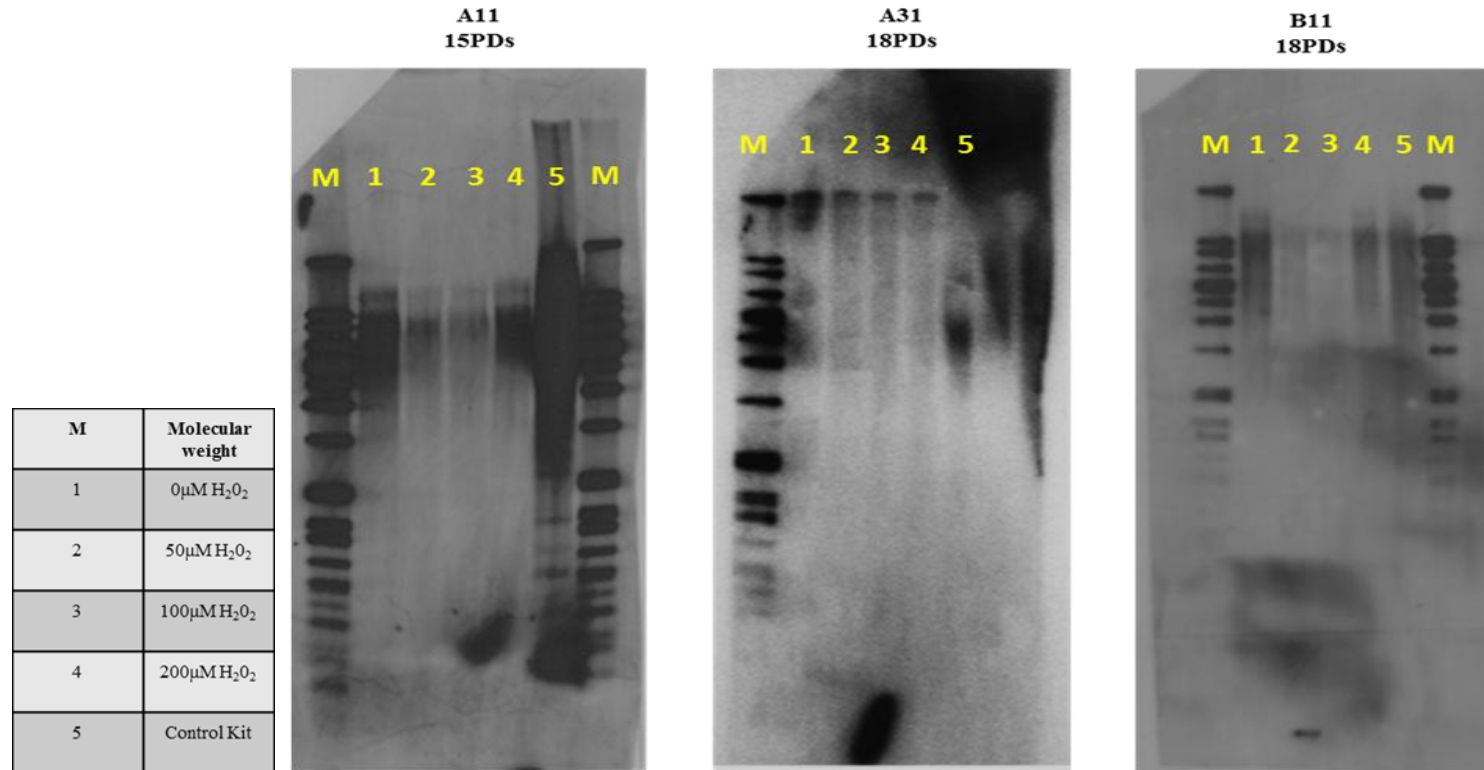
Table 2.2. The mean of telomere length for DPPCs clones calculated from southern blots (Figure 2.35)

Clone	A11				A31				B11			
H_2O_2 concentrations by μM	0	50	100	200	0	50	100	200	0	50	100	200
Telomere length by Kb	4	4.2	4.4	5	17.4	17.6	17.5	17.5	6	5.4	5.5	5.7

2.5   Discussion

Only clone A31 was highly proliferative compared to clones A11 and B11 in this chapter. Proliferation was linked with telomere length, as A31 was highly proliferative and demonstrated longer telomere length. *In vitro* expansion of the clones showed that cultures altered their stemness by loss of stem cell markers, and eventually replicative senescence occurs due to progressive telomere shortening as a result of decreased telomerase activity (Sharpless and DePinho, 2007). Loss of telomerase leads to telomere dependence-senescence of cells. However, when these cells underwent induced senescence by H_2O_2, they showed high resistance. Telomere length was not affected by H_2O_2, and cells underwent telomere independent senescence. The cause of senescence in this situation could be caused by several factors such as DNA damage, accumulation of abnormal protein, or mitochondrial changes (Itahana et al., 2001). The results are explained in detail in the following sections.

Progenitor clones were isolated from human dental pulp based on their adherence to fibronectin. Clones were confirmed as mesenchymal stem cells based on their fibroblastic appearance, expression of triplicate stem cell markers (CD73, CD90 and CD105), lack of expression of haematopoietic antigen CD45 and their ability to differentiate into osteogenic, chondrogenic and adipogenic lineages (Rosenbaum et al., 2008; Kuhn and Tuan, 2009). A total of four clones from two different patients' wisdom teeth; patient A (A11, A31, A51) and patient B (B11) showed different growth kinetics that was represented by PD data until senescence. These variations of PD from the same teeth of the same patient have been reported before (Waddington et al., 2009). Three DPPC A11, A31, and B11 were chosen for further investigation due to their differences. These 3 clones showed different telomere length and ability to resist oxidative stress, which has never been investigated before for this type of cell in the same study. They also exhibited the loss of embryonic and mesenchymal stem cell markers after long-term culture.

In order to use MSCs for clinical therapy they will require considerable *in vitro* expansion, which is shown to be an important factor for the success of the clinical application in bone repair (Quarto et al., 2001) and cartilage repair (Centeno

et al., 2008; Veronesi et al., 2013). However, studies investigating the effect of *in vitro* expansion on MSCs showed that their proliferation capacity and differentiation ability declined with passaging (Banfi et al., 2000; Min et al., 2011) as is shown in this study.

Investigation of the PDs demonstrated that of five different clones, four of them showed less than 36PDs and senesced after less than 85 days, while only one clone (A31) had a high proliferation rate with over 85PDs that senesced after more than 300 days. It has been reported that MSCs from bone marrow are only capable of a maximum 50PDs (Huang et al., 2009b; Tamaki et al., 2012) and they proliferate slower than MSCs from the dental pulp (Alge et al., 2010). These data emphasise the great proliferation rate of DPPCs when compared with other MSCs from other sources that give these cells a potential advantage.

After investigation of mesenchymal, embryonic stem cell and neural markers at different stages during the life span of these 3 clones (A11, A31 and B11), the PCR results showed the expression of these markers during early culture as at 10PDs in clone A31. These markers were gradually lost until they completely disappeared in all the clones. As clone A31 had the longer life span, it also had the longer period of expression of these gene markers with Oct4 being lost first after 10PDs and then CD105 after 24PDs and finally CD73 and CD90 after 60PDs, while for other clones, these markers were lost after short periods of time. It should take in consideration that these clones only survived less than 30PDs. It has been shown before that the level of stem cell markers reduce with time (Patel et al., 2009). Specifically, a study of human MSCs from bone marrow, after culturing for 10 weeks, showed a regression of CD105 and CD73, while CD90 expression stayed constant (Rallapalli et al., 2009). Dental pulp tissues are considered to derive from the cranial neural crest cells (Chai et al., 2000; Miletich and Sharpe, 2004). These cells during embryonic development are associated with embryonic stem antigen, which may explain the ability of the isolated dental pulp progenitor cells (DPPCs) in this study, to express embryonic stem cell markers such as Oct4 (Huang et al., 2009b; Kawanabe et al., 2012). Embryonic stem cell marker Oct4 and neural marker Slug were expressed in the three clones (A11, A31, B11) but were lost at very early stage with less than

10PDs for clone A31. These results are in line with others, where Oct4 is expressed at very low levels in early passage MSCs and disappears at late passage (Boroujeni et al., 2012). However, the real function for Oct4 in MSCs is still debatable, whether it is essential for stemness or it has another function that is different from that in embryonic stem cells (Ulloa-Montoya et al., 2007; Zangrossi et al 2007; Lengner et al., 2008). Furthermore, it has been proposed that detection of Oct4 expression by using RT-PCR is not reliable because it might be a false expression, which is called pseudogene (Liedtke et al., 2007). The expression of neural stem cell markers by these cells wasn't a surprise, taken into account that DPPCs is derived from the neural crest (Chai et al., 2000). Neural markers expression in these cells is proof of successful differentiation into neural lineages (Karaöz et al., 2010; Abe et al., 2012). Also, expression of different markers could be changed during *in vitro* culture due to the components of the culture media. For example, DPPCs cultured in serum-free medium with addition of vascular endothelial growth factor, leads to DPPCs expressing endothelial markers (Karbanová et al., 2011).

The niche of these clones is located or what stage in stem cell development they are could be one of the reasons that explains their different growth kinetic profiles and differentiation ability. It is still not fully known whether these clones are derived from one pluripotent stem cell niche or whether they derive from committed progenitors into specific lineages, due to the lack of specific gene markers of mesenchymal stem cell development (Shi and Gronthos, 2003). It has been suggested that DPPCs are derived from the perivascular niche because they display similar characterisation of pericytes such as expression of CD146 and lack of expression of CD34 in human, the same fibroblastic morphology and their ability to differentiate into osteoblasts, adipocytes and chondrocytes as shown in clone A31 (Shi and Gronthos, 2003). However, it seems not all the dental clones are derived from the perivascular niche. It is suggested, based on staining localisation of embryonic stem cell and mesenchymal stem cell (MSC) markers, that the dental pulp has other locations of DPPCs including; nerve networks in the cell free zone, the innermost pulp layer in the cell rich zone and within outermost pulp layer where all cells from these locations have fibroblast morphology and are positive for the neural marker

nestin (Lizier et al., 2012). The aforementioned may explain the origin of clones A11 and B11 that express CD271 neural marker.

Unlike embryonic stem cells, the MSCs in this study showed a defined proliferation capability with shortening of telomere length. This type of senescence is called replicative senescence (Campisi, 1996). Telomere length is one of the important factors that controls replicative senescence (Harley, 1991). Shortening of telomeres has been linked to the absence of the enzyme telomerase (Zimmermann et al., 2003; Baxter et al., 2004; Parsch et al., 2004). Cellular senescence is also regulated by several tumour suppressor genes including p53, p21 and p16 (Pearson et al., 2000). p53 is activated in response to short telomere length and other stimuli such as DNA damage (Itahana et al., 2001). This explains the positive expression of p53 in the short telomere clones such as A11 and not in the long telomere clone, A31. Also p16 was only expressed in low a proliferative clone that is in line with data from Molofsky et al., (2003). On the other hand, p21 was positively expressed in all the clones; p21 may be considered as a marker of cell senescence and is regulated by p53 or independently of p53 by growth factors and cytokines (El-Deiry et al., 1993). However, p21 appeared to have a dual role in stem cells. In addition to the role of p21 in inducing stem cell senescence in culture, it is also required to maintain stem cell self-renewal because of its positive effects on the cell cycle (Kippin et al., 2005; Ju et al., 2007) and could explain the expression of p21 in all clones at the gene transcription level.

Telomere length varied among the clones with 18.3kb for clone A31, 5.9kb for clone A11 and 5.6kb for clone B11 at early stages of their PD. Telomere length is known to decrease with age, and the telomere length of A31 clone exhibited this decrease during *in vitro* culture being 18.3kb at 9PDs and then 6.4 kb at 55PDs. This shortening in telomere length, which correlated with reduction of proliferative capacity, has been demonstrated in human mesenchymal stem cells from bone marrow (Baxter et al., 2004) and from dental pulp (Mokry et al., 2010).

Telomere length was measured by terminal restriction fragment (TRF), which estimates the average genomic telomere length within a population of cells (Harley et al., 1990; Allsopp et al., 1992). Although TRF is the most widely used method to determine telomere length, there are limitations of this technique such as it only measuring the mean of telomere length of a cell population, and since the telomere length in human cells is extremely heterogeneous, the technique is less sensitive by showing a large area of smear (Aubert et al., 2012). This heterogeneity in smear band was clear in later PD of clone A31 as cells became more heterogeneous, which made it more difficult to estimate the average telomere length. Other disadvantages of TRF was it being labour intensive, costly and it required great amounts of DNA compared with other methods (Kimura et al., 2010). For this reason, extraction of minimal amounts of DNA was difficult at later PD when the proliferation rate was slow, that prevented the comparison of early and mid PDs with late PD. To overcome this problem, single telomere length analysis (STELA) is to be considered for the future work, with picogram range of DNA being enough to evaluate of each single telomere of cell individually (Baird et al., 2003).

Clones are considered senescent when their cell proliferation is less than 0.5PDs per week (Stephens et al., 2003; Dell'Orco et al., 1974). This was confirmed by production of SA β-gal that is used as a marker for aged cells (Dimri et al., 1995). At mid PD (46PDs) and mid-late PD (59PDs) for clone A31, the percentage of cells with positive staining for SA β-Gal was less than 30%. At very late PD (over 85PDs) when cells were considered senescent, the percentage of cells was positive for SA β-Gal increased dramatically to be almost 100% (Figure 2.14). This was similar for the other two clones at this stage when PD was less than 0.5PDs per week with the positive staining of β-gal was almost 100% (Figure 2.14). However, β-gal has been considered a controversial marker to confirm cell senescence because of an increased activity of the enzyme under different conditions other than replicative senescence such as in confluent culture or in cells under serum starvation (Severino et al., 2000; Yang and Hu, 2005). For this reason, β-gal has not been used in this study as an exclusive senescence marker but as co-marker with other cell senescence markers. The morphology of DPPCs throughout their proliferative lifespan was also a useful indicator to assess these cells' senescence. The difference in cellular morphology

was objectively quantified by determining the surface area of the cells by drawing around the cell periphery and calculating the surface area using ImageJ software. *In vitro* aged DPPCs appeared to be bigger in size and more flattened than their ancestors in early passage, this enlargement of cells has been linked with cell ageing (Angello et al., 1989; Karystinou et al., 2009).

Taken together both the telomere smear band and cell size results at late PD, it has been noticed a heterogeneous population of cells where cell size at late PD showed variety of surface areas by displaying a small number of cells with small surface area (less than 3000 μm^2) compared to the majority of cells (more than 5000 μm^2) (Figure 2.13), which indicate that these cells proliferate asymmetrically. This means some cells in the same population reached senescence before others (Ho, 2005), and was supported by telomere lengths when the smear length band was longer indicating various telomere lengths in each cell of clone A31 after considerable time of expansion, 55PDs (Figure 2.15).

Fehrer and Lepperdinger, (2005) reported that stem cells appear to be protected against damage from oxidative stress but without providing experimental data to support this. In this study, data will be provided in terms of proliferation rate, β-gal staining and telomere length. Oxidative stress is continuously produced during the metabolic process of aerobic cells and neutralised by endogenous antioxidant defence system. However the balance between oxidative stress and antioxidant could change due to several causes (Halliwell and Gutteridge, 1990). The increase of oxidative stress is implicated in the cause of diseases and the process of ageing (Finkel and Holbrook, 2000; Valko et al., 2007). Oxidative stress has been linked to cellular ageing by showing decrease in tissue function such as arteries (Brouilette et al., 2003), decrease in proliferation rate, enlargement and flattening of cell morphology; and eventually cell senescence at low doses of H_2O_2 (50-100 μM) in human fibroblast, cell apoptosis at higher doses (300-400μM) (Chen and Ames, 1994; Bladier et al., 1997), and acceleration of telomere attrition in MSCs (Brandl et al., 2011). As has been described, cellular senescence could be telomere-dependent due to the end-replication problem of DNA synthesis that causes telomere shortening

(Harley, 1991). However, in some cases cellular senescence might be independent of telomere length. This could happen due to external causes such as oxidative stress and antioxidant defences system (Von Zglinicki et al., 2000). Cells introduced to mild stress, which still allows cell proliferation, can lead to telomere shortening (Von Zglinicki et al., 1995; Vaziri et al., 1997; Lorenz et al., 2001).

In this study, sub-lethal H_2O_2 (200 μm) insult accelerated the ageing process in A31 and B11 clones. Cell senescence occurred after 50 days in cells cultured in 200μm of H_2O_2 compared with almost 200 days for the non-treated, at 50μm and 100μm concentrations of H_2O_2 in the highly proliferative clone, A31. In B11 clone, cell senescence occurred after 20 days cultured in 200μm of H_2O_2 compared to around 60 days of non-treated cells. In the A11 clone, no obvious difference was observed that is possibly because of the short life of these cells, less than 30 days after the treatment started, which did not give enough time for H_2O_2 to show its effect. Equivalent doses of H_2O_2 have been applied in a previous study with MSCs from human bone marrow but their negative effects were faster compared to the DPPCs (Brandl et al., 2011). Long period treatments of low dose H_2O_2 showed no effect on proliferation rate or cell senescence that is line with the finding in this study (5-50μm H_2O_2) (Figure 2.16).

Sub-lethal H_2O_2 doses (100μm-200μm) in A11 clone seemed to cause effect only in cells with shortest telomere length (Figure 2.37), but this did not cause a difference in the time of cell senescence between the non-treated and 200μm H_2O_2. It is still not clear whether it is the shortest telomere or the mean telomere length that causes cell senescence (Brandl et al., 2011). In A31 and B11 clones the difference in telomere length between the sub-lethal concentrations and non-treated cells was minimal. This in line with the data of PD (Figure 2.17 and 2.18) that shows these two clones after 30 days, did not reveal any difference between the 0μM H_2O_2 and 200μM H_2O_2. Unfortunately, because the TRF technique required a huge amount of DNA, telomere length could not be calculated due to low amounts of cells at later stage of H_2O_2 treatment. Although, literature suggests that there are other mechanical reasons that could make H_2O_2 in 200mm concentration cause cell senescence before

non-treated cells after prolonged days of culture rather than telomere length. Indeed, it has been proven that H_2O_2 causes cellular senescence without reducing the telomere length, which could be explained by the effect of H_2O_2 on cell cycle by increasing p16 protein level (Chen et al., 2001; de Magalhães et al., 2001) or distribution of telomere structure, telomere dysfunction (d'Adda di Fagagna et al., 2003). This confirms that telomere length is not the only reason for cell ageing (Blackburn, 2000).

Cells protect themselves against oxidative stress by several mechanisms. The main mechanism is the antioxidant defence systems including; superoxide dismutase (SOD) (Serra et al., 2003), catalase, and glutathione peroxidase enzymes (Dorval and Hontela, 2003). This was proved by antioxidative in hMSCs, reduced the oxidative stress levels by restoring the antioxidant levels of these cells (Ebert et al., 2006). The work in this chapter demonstrated the remarkable resistance of DPPCs to H_2O_2 compared with other human cells such as fibroblasts (Duan et al., 2005), chondrocytes (Brandl, Hartmann et al., 2011), and MSCs from bone marrow (Brandl et al., 2011). Due to high resistance of DPPCs it could be hypothesis that these cells produce large amounts of catalase or glutathione peroxidase, since it was proven that both enzymes has been increased by H_2O_2 stimulation (Seo et al., 2004). Another reason these cells are resistant to oxidative stress, could be the expression of PPARγ in these cells. PPARγ is believed to act as an anti-inflammatory by removing the activity of ROS (Kim et al., 2012b).

Overall, this chapter showed that DPPCs undergo telomere-dependent senescence. When H_2O_2 was used to induce DPPC senescence however, they were highly resistant to H_2O_2 and the telomere length was not affected. Furthermore, this study showed variations in proliferation capacity of isolated clones from the dental pulp, which could be linked to telomere length, and possibly the different niches that they come from. Further investigations into the aforementioned are in the following chapters.

Chapter 3:

Effects of *In Vitro* Expansion and H_2O_2 on Differentiation Ability of Dental Pulp Progenitor Clones

3.1   Introduction

The multi-potential differentiation capacity of MSCs is the basis for their use in tissue engineering and clinical therapy. However, these cells behave differently in terms of proliferation and differentiation despite their same origin (Liu and Xiao, 2011). Indeed, the previous chapter showed that DPPC clone A31 was highly proliferative, while clones A11 and B11 had low proliferation. This chapter will investigate if there is a connection between differentiation ability and the proliferative capacity, and therefore telomere length. In addition, here a proposed theory will try to explain the reason behind these variations.

The differentiation capacity of dental pulp progenitor cells has been well investigated in the literature. It has been reported that these cells can differentiate into osteoblasts (Zhang et al., 2006; Jo et al., 2007; Graziano et al., 2008; Mangano et al., 2010), adipocytes, chondrocytes (Zhang et al., 2006; Jo et al., 2007; Koyama et al., 2009), oligodendrocytes (Sakai et al., 2012); and along the myogenic pathway (Zhang et al., 2008). To regard the progenitor cells from the dental pulp as mesenchymal stem cells (MSCs), they should differentiate into at least 3 different lineages (osteoblasts, adipocytes and chondrocytes) under standard *in vitro* differentiating conditions (Dominici et al., 2006). The ability of MSCs to differentiate into specific mature cell types is influenced by many factors, such as transcription factors, cytokines, growth factors and extracellular matrix molecules (reviewed in Baksh et al., 2004).

For osteogenic differentiation, the presence of ascorbic acid-2 phosphate, β-glycerophosphate, dexamethasone and foetal bovine serum are required to obtain osteoblastic cell morphology, with the upregulation of alkaline phosphate activity and the deposition of a calcium mineralized extracellular matrix (Barry and Murphy, 2001). In addition, adding growth factors, such as basic fibroblast growth factors

(bFGF) induce osteogenic differentiation by enhancing bone nodule formation (Hanada et al., 1997). There are several markers considered significant for osteogenic differentiation. Runt-related transcription factor 2 (Runx2) is considered the main transcription factor for osteogenic differentiation (Komori, 2010). This has been demonstrated by the absence of bone formation in Runx2 knockout mice (Komori et al., 1997). Other examples of typical bone matrix proteins of osteoblast are; osteocalcin (OCN), osteonectin (ON) and osteopontin (OPN) (Mizuno and Kuboki, 2001; Mori et al., 2011). OCN and OPN are non-collagenous protein, where the former is considered a late marker and the latter as an early marker of osteoblast differentiation (Mizuno and Kuboki, 2001; Vater et al., 2011).

For chondrogenic differentiation, cells must be grown in 3D culture, in serum- free medium with the addition of transforming growth factors-β_1 (TGF- β_1) super-family members. Under these conditions, cells lose their fibroblastic appearance and form a matrix containing aggrecan, type II collagen and the ratio of sulphated glycosaminoglycans is increased. All of these components are observed in the development of human articular cartilage (Barry et al., 2001). One of the main regulators for chondrogenesis is SOX9, which controls the expression of COL2A1 (Lefebvre et al., 1997).

To stimulate MSCs to differentiate into adipocytes, they have first to be grown until confluency in culture medium with serum. At this point, cells begin to change their morphological appearance from fibroblastic to a more spherical shape. Culture medium containing the glucocorticoid dexamethasone, in addition to insulin and indomethacin is required. Dexamethasone induces the accumulation of peroxisome proliferators-activated receptor γ (PPARγ), a major transcription factor in the adipogenesis process, while insulin accelerates triglyceride accumulation (Cui et al., 1997; Shugart and Umek, 1997; Kubo et al., 2000). Under these conditions, several ECM components re-organise and remodel including fibronectin and laminin to form fat cell clusters (Kubo et al., 2000). Lipoprotein lipase (LPL) is then expressed by the mature adipocytes (Goldberg, 1996), which eventually leads to accumulation of intracellular lipid-rich vacuoles that can be stained with oil red O.

Runx2 and PPARγ are the key transcription factors responsible for the osteogenic and adipogenic differentiation. During ageing, the number of bone forming osteoblasts is decreased while the number of adipocytes is increased in the bone marrow. Runx2 is decreased in aged MSCs from bone marrow and leads to negative effect on osteoblast differentiation while PPARγ expression and adipogenesis is increased (Moerman et al., 2004; Huang et al., 2010). Also, it has been shown that, culturing osteoprogenitor cell in serum from postmenopausal women, leads to differentiation of these cells into adipocytes. This suggests that there are components in the serum when women age, which have the ability to influence progenitor cell differentiation to an adipocyte lineages rather than an osteoblast one (Stringer et al., 2007). Determining what factors cause this alteration would be beneficial from tissue engineering point of view in treatment of osteoporosis.

CD73, CD90 and CD105 are the minimal criteria of stem cell markers expression to identify cells as MSCs. However, these markers may not have a direct link with MSC differentiation capacity (Pittenger et al., 1999). Therefore, there are other markers which seem to have a role in the differentiation of progenitor cells such as CD271 (low-affinity nerve growth factor receptor) and CD146 (melanoma cell adhesion molecule). However it is not known if they identify the same cells or a subpopulation of these cells (Tormin et al., 2011). CD146 was linked with progenitor cells that have ability to differentiate into three different lineages (osteogenic, adipogenic and chondrogenic) (Xu et al., 2009). Mikami et al., (2011) showed that CD271 was found in progenitor cells that were not cable to differentiate into these three lineages which may make CD271 marker an important marker to determine differentiation ability of cells.

3.2   Aims

This chapter continues form the data obtained in the previous chapter in terms of the unique character of each clone which has been isolated. In the previous chapter it was found that different clones have different PDs and they responded differently to the oxidative stress, showed different expression markers of cell senescence and different telomere lengths. The effect of aging on these clones in term of proliferation and stem cell marker expressions was also demonstrated. This chapter

will investigate the differentiation ability of each clone; A31, A11 and B11 into osteoblast, chondrocytes and adipocytes and the effect of aging and hydrogen peroxide induced oxidative stress on the osteogenic differentiation for the highly proliferative clone, A31. This assessment will facilitate the process of isolating the best clone for use in tissue engineering.

3.3   Materials and Methods

3.3.1   Cell Source

The isolated DPPC clonal population, A31, A11 and B11 at early PD (30PDs, 17PDs, 25PDs, respectively) in addition to late PD of A31 (75PDs) clones were cultured in adipogenic, chondrogenic and osteogenic induction media, to evaluate the potential of DPPC clones to differentiate along these mesenchymal lineages.

3.3.2   Culture Media

The medium used was the NH stem cell media AdipoDiff, OsteoDiff and ChondroDiff media (Miltenyi Biotec, Surrey, UK) for osteogenic, chondrogenic and adipogenic differentiation, respectively. The medium was thawed and supplemented with 1% antibiotics (100 units/ml penicillin G sodium, 0.1μg/ml streptomycin sulphate and 0.25μg/ml amphotericin; Invitrogen, Paisley, UK). and then aliquoted into samples 20ml for storage at -20$^{\mathrm{o}}$C.

3.3.3   Differentiation Induction Procedures

Details of clonal differentiation into osteogenic, chondrogenic and adipogenic cells are described below. Controls were also performed consisting of DPPCs plated into 2x 6-well plates (Sarstedt, Leicester, UK). These were maintained in culture medium for the same period of differentiation to be used for total RNA extraction and reverse transcription-polymerase chain reaction (RT-PCR). All differentiation studies were performed in triplicate.

3.3.3.1 Adipogenic Differentiation

For the analysis of clonal adipogenic capacity, cells were seeded at 7.5×10^3 cells/cm^2 in 6-well plates and 12-well plates. Cells in 6-well plates were used for RT-PCR and

in 12-well plates for the oil red O analysis. Cells were cultured with AdipoDiff medium and incubated at 37°C, 5% CO_2 for 21 days (as stated in Miltenyi Biotec protocol). The medium was changed every 3 days. On day 21, cells were processed for analysis.

3.3.3.2 Osteogenic Differentiation

For the analysis of clonal osteogenic capacity, cells were seeded at 4.5×10^3 cells/cm^2 in 6-well plates and 12-well plates. Cells in 6-well plates were used for RT-PCR and in 12-well plates for alizarin red staining (Sigma, Dorset, UK) analysis (section 3.2.4.?). Cells were cultured with OsteoDiff medium and incubated at 37°C, 5% CO_2 for 18 days (as stated in Miltenyi Biotec protocol). The medium was changed every 3 days. On day 18, cells were processed for analysis.

3.3.3.3 Chondrogenic Differentiation

For the analysis of clonal chondrogenic capacity, a single cell suspension with 2.5×10^5 cells in 1ml was centrifuged at 150x g for 5 min, to produce a cell pellet in a 15ml polypropylene conical base tube in triplicate (Falcon tube, Sarstedt, Leicester UK). The medium was completely aspirated and replaced with 1ml of ChondroDiff medium before re-centrifugation. The caps of the conical tubes were loosely placed, and the pellets incubated at 37°C, 5% CO_2 for 24 days (as stated in Miltenyi Biotec protocol). The medium was changed every 3 days following centrifugation. On day 24, the pellets were processed for analysis.

3.3.4 Histochemical Analysis

For osteogenic analysis and control cultures, one 12-well plate was washed twice with phosphate buffered saline (PBS) before being fixed with 4% paraformaldehyde (PFA) (Santa Cruz, Texas, USA) for 10 min at room temperature. The PFA was then removed and the fixed cells were washed with PBS (x2). Adipogenic culture analysis and control cultures were washed with 60% isopropanol (x1) for 5 min with gentle agitation. For chondrogenic differentiation, pellet cultures and their controls were washed with PBS (x1), before fixation overnight in 3.7% neutral buffered formalin (in PBS) with gentle agitation. After formalin aspiration, each cell pellet was carefully removed from the conical tube using a thin tip, wrapped in filter paper and

inserted into embedding cassettes for automatic processing (Leica ASP300 S, Leica Microsystem, Milton Keynes, UK). This passed samples through increasing 70%, 90% and 100 % concentrations of ethanol. Samples were paraffin wax embedded and cut into 5µm sections using a sliding microtome (Leica SM2400, Leica Microsystems). Sections were collected on to poly-L-lysine coated glass slides (SuperFrost, Thermo Fisher Scientific, Loughborough, UK) and allowed to dry overnight at 60°C in an incubator (Binder, Germany). Sections were deparaffinised and rehydrated by washing for 10 min with xylene, 5 min with industrial methylated spirits (IMS) and 5 min with water. Sections were circled with immiscible ink using a paraffin pen (Sigma, UK) prior to staining.

3.3.4.1 Alizarin Red S Staining

The osteogenic cultures and its controls were stained with 0.5 ml/well alizarin red S (20g/L dissolved in double distilled water, pH 4.2 for 3 min with gentle shaking. Wells were subsequently washed with running water until the excess stain was removed, left to dry and viewed by light microscopy (Nikon Eclipse TS100).

3.3.4.2 Oil Red O Staining

Oil red O (Sigma, UK) (stock of 3.5g/L dissolved in isopropanol) working stain was prepared fresh by mixing a 4:6 ratio of double distilled water to oil red O stock. This was incubated at room temperature for 10 min on a shaker, before filtering through Whatman grade 42 filter paper (Fisher Scientific, UK). Adipogenic cultures and its controls were stained with 0.5 ml/well working oil red O solution for 10 min at room temperature, with gentle agitation. Wells were subsequently washed with double distilled water and then briefly with 60% isopropanol, before washing again with double distilled water until the excess stain was removed. Sections were left to dry before viewing by light microscopy.

3.3.4.3 Safranin O Staining

Pellet sections were placed in fast green FCF staining solution (1:5000 dilution of 0.1g fast green FCF (Sigma Aldrich, UK) in 500ml double distilled water for 5 min and washed subsequently in 1% acetic acid. For safranin O staining, the washed slide was placed in 0.1% safranin O staining solution (1g/L safranin O, Sigma , UK) in

double distilled for 10 min and was subsequently washed in a 95% ethanol-xylene mixture (1:1). A cover slip was mounted with a drop of glycerol and fastened with nail polish, before viewing by light microscopy.

3.3.5   RT-PCR of DPPC Differentiation

RT-PCR was performed on 6-well plates for osteogenic and adipogenic differentiation cultures and their controls. RT-negative and water negative controls were used and β−actin was used as the housekeeping gene for PCR. The extraction of mRNA and RT-PCR were performed as previously described (Section 2.3.5.1). PCR primers for osteogenic markers OCN and Runx2 and adipogenic markers lipoprotein lipase (LPL) and PPARγ were used. In addition, low-affinity nerve growth factor receptor (LNGFR or CD271) was examined in each clone prior to differentiation. Primer sequences, melting temperatures and product sizes are summarised in Table 3.1.

Table 3.1: Human differentiation gene markers used for PCR amplification. B-actin was used as a housekeeping gene.

Gene Marker	Primer sequence	Annealing Temperature °C	Cycles	Source
Osteocalcin	F:5'-GCAGGTGCGAAGCCCAGCGGTGCAGAG-3' R: 5'-GGGCTGGGAGGTCAGGGCAAGGGCAAG-3'	62	35	Chi Lee Cardiff University
Osteopontin (SPP1)	F:5'- ATCACCTGTGCCATACCA-3' R:5'- CATCTTCATCATCCATATCATCCA-3'	55	35	Maria Stack Cardiff University
peroxisome proliferator-activated receptor γ	F:5'-GCCATCAGGTTTGGGCGGATGCCACAG-3' R: 5'-CCTGCACAGCCTCCACGGAGCGAAACT-3'	62	35	Chi Lee Cardiff University
lipoprotein lipase	F:5'-GCTGGCATTGCAGGAAGTCTGACCAATAA-3' R:5'-GGCCACGGTGCCATACAGAGAAATCTCAA-3'	55	35	Chi Lee Cardiff University
CD271 (LNGFR)	F:5'- CTGCAAGCAGAACAAGCAAG-3' R:5'- GGCCTCATGGGTAAAGGAGT-3'	55	35	Lindsay Davies Cardiff University
β-actin	F:5'-AGGGCAGTGATCTCCTTCTGCATCCT-3' R:5'- CCACACTGTGCCCATCTACGAGGGGT-3'	65	35	XQ Wei Cardiff University

3.4   Results

3.4.1   Osteogenic Differentiation

3.4.1.1 Cell Morphology and Alizarin Red Staining

For clone A31, osteogenic cultures of DPPCs (30PDs) at day 14 were fibroblast-like in morphology, but appeared larger and to form clusters in the calcified area (circled) (Figure 3.1.A), when compared with the control cultures where cells were narrower in morphology and more crowded, (Figure 3.1.B). After 18 days of osteogenic culture, at early PD (30PDs), there was strong alizarin red staining with secreted mineralised calcium nodules scattered in the cells cultured in osteogenic medium (arrowed) (Figure 3.2 A). Mid-point (62PDs) (Figure 3.2 C) and late PD cells (75PDs) (Figure 3.2 E) demonstrated less staining. Control cultures with alizarin red s, at day 18, did not exhibit any stained cells for the 3 different PDs (Figure 3.2 B, D and F).

For clone A11 at early PD (17PDs) there was marked staining of alizarin red (arrowed) (Figure 3.3.A), which was similar to clone A31 at 30PDs (early PD) (Figure 3.2 A). Control cultures exhibited no staining for alizarin red.

Clone B11 at 25PDs showed minimal staining of alizarin red S (Figure 3.4.A), which was significantly less than the staining of Clones A31 at 30PDs and A11 at 17PDs (Figure 3.2.A and 3.3.A) and without region of big cluster. Control culture showed no staining of alizarin red S (Figure. 3.4. B).

Figure 3.1. Exemplar light microscopy of DPPCs (A31 clone at 30PDs) cultured in osteogenic medium for 14 days. (A) Cells appeared larger with clustered areas (indicated by red circle), when compared with control cultures (B) that appeared unclustered. ×10 magnification, Scale bar 100µm.

(A)

(B)
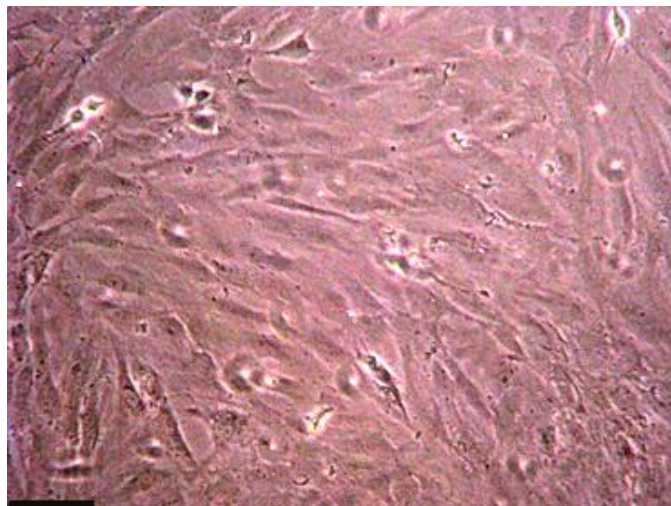
Figure 3.2. Light microscopy of osteogenic cultured cells of A31 clone, stained with alizarin red. Early PD (30PDs) cultured cells demonstrated higher levels of staining with secreted calcium globules at day 18 (A) compared with mid-PD (62PDs) which exhibited less calcium globules (C). Late PD (75PDs) cells were observed to exhibit the least amount of staining (E). Control cultures exhibited no staining at early PD (B), mid PD (D) and late PD (F). ×10 magnification, scale bar 100μm.
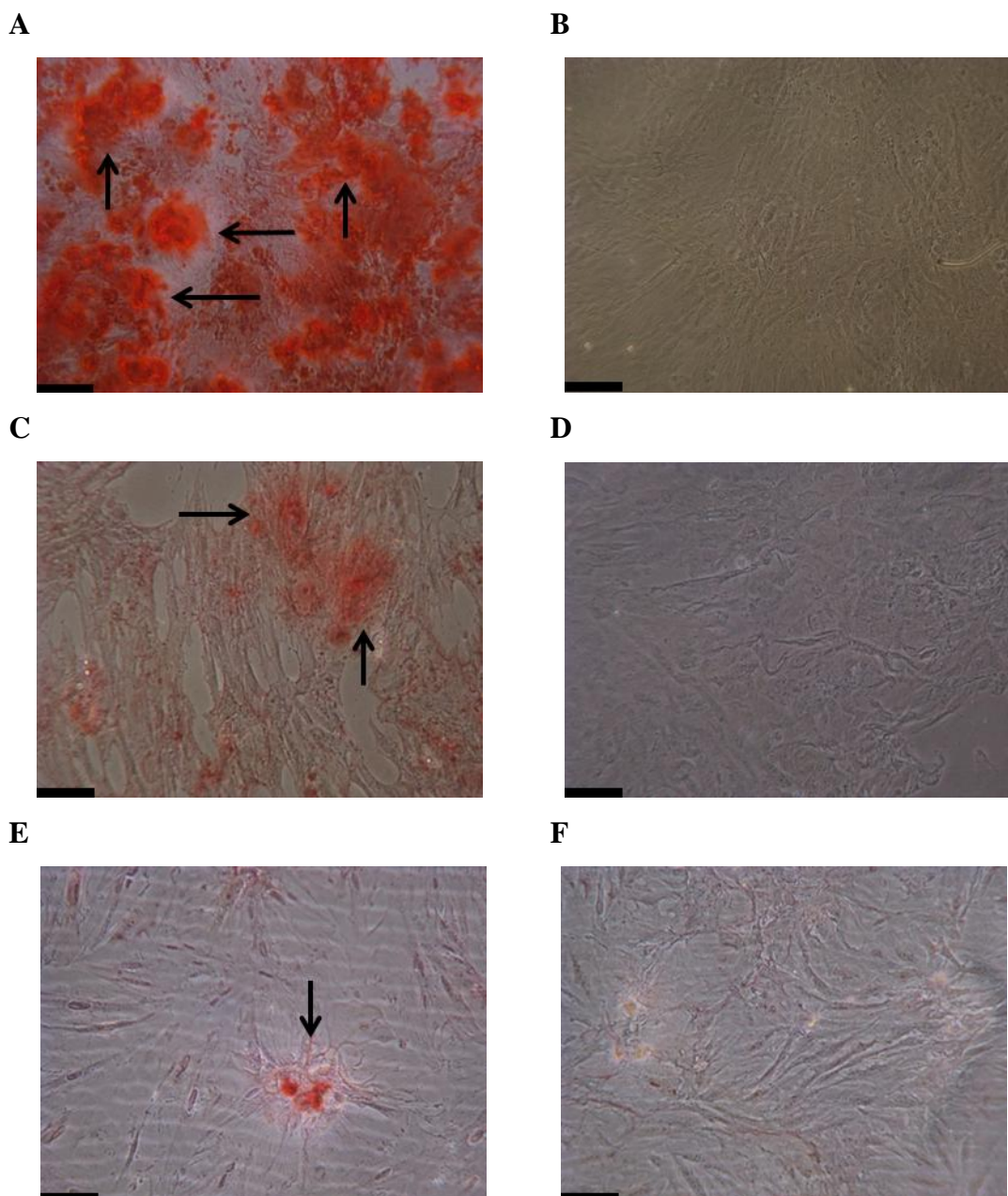
Figure 3.3. Light microscopy of A11 at 17PDs osteogenic cultured cells, stained red with alizarin red (A) that was similar to what was found in early PD of clone A31. no staining was observed with control culture (B). ×10 magnification, scale bar represents 100µm.

(A)
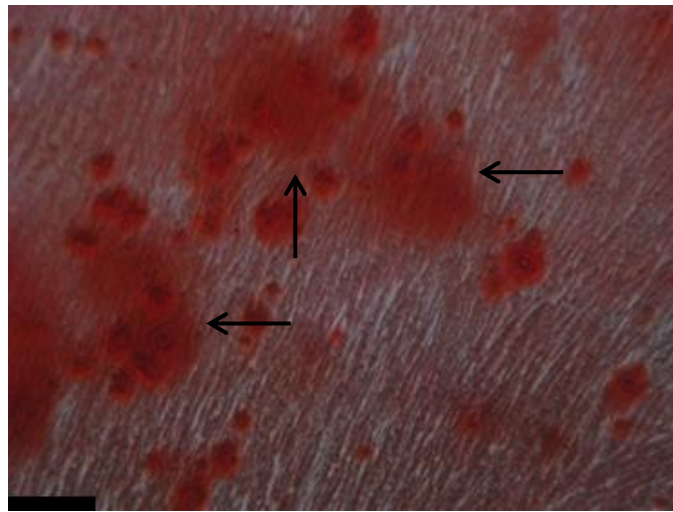
(B)

Figure 3.4. Light microscopy of B11 at 17PDs osteogenic cultured cells, stained with alizarin red S without a specific clustered area (A). Control cultures with no stain observed (B). ×10 magnification, scale bar represents 100μm

(A)
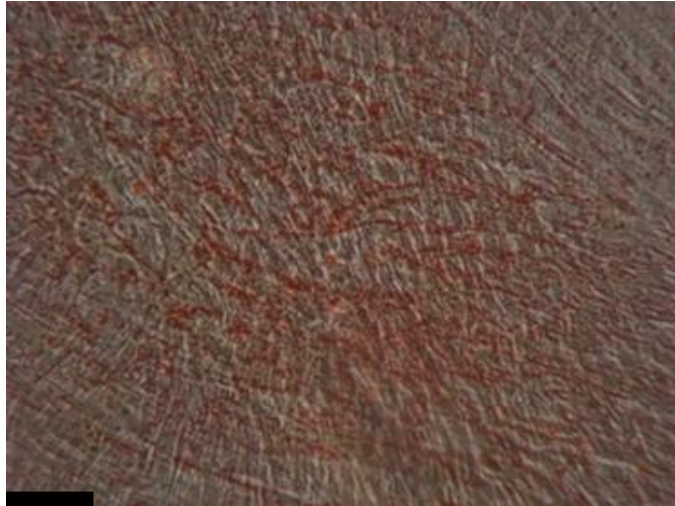
(B)

3.4.1.2 RT-PCR for Osteogenic Differentiation

The RT-PCR for clone A31 late PD (75PDs) of osteogenic cultured cells at day 18 was negative for the 3 osteogenic markers (Runx2, OCN and OPN) (Figure 3.5). The expression of the osteogenic markers was also negative for control cultures at day 18 (Figure 3.5). β-actin housekeeping gene was positive in the all results and RT negative showed no bands.

For all the clones (A31 at 30PDs, A11 at17PDs and B11 at 25PDs), RT-PCR of the osteogenic cultured cells revealed the presence of osteogenic markers Runx2, OCN and OPN at day 18 (Figure 3.6). The day 0 initial culture controls were positive for Runx2 but not OCN and OPN. Day 18 control had the same gene expression as day 0 where Runx2 was positive and OCN and OPN were negative (Figure 3.6).

Clone A31 at early PD in osteogenic medium revealed the presence of osteogeneic markers and high staining of alizarin red which faded gradually with cellular ageing. Furthermore, at later PD, cells cultured in osteogenic medium failed to express all the osteogenic markers. A11 (17PDs) and B11 (25PDs) clones displayed the presence of osteogenic markers in osteogenic culture which was similar to clone A31 at early PD (30PDs).

Figure 3.5. RT-PCR results showed mRNA expression profiles for clone A31 at early (30PDs) and late (75PDs) PDs in osteogenic medium and control culture medium at day 18 for Runx2, OCN and OPN. β-actin was used as a housekeeping gene. Cells at early PD in osteogenic medium expressed the osteogenic markers while at late PD did not express any of the osteogenic markers. Cells in control culture at early PD only expressed Runx2 while in late PD did not express any osteogenic markers.
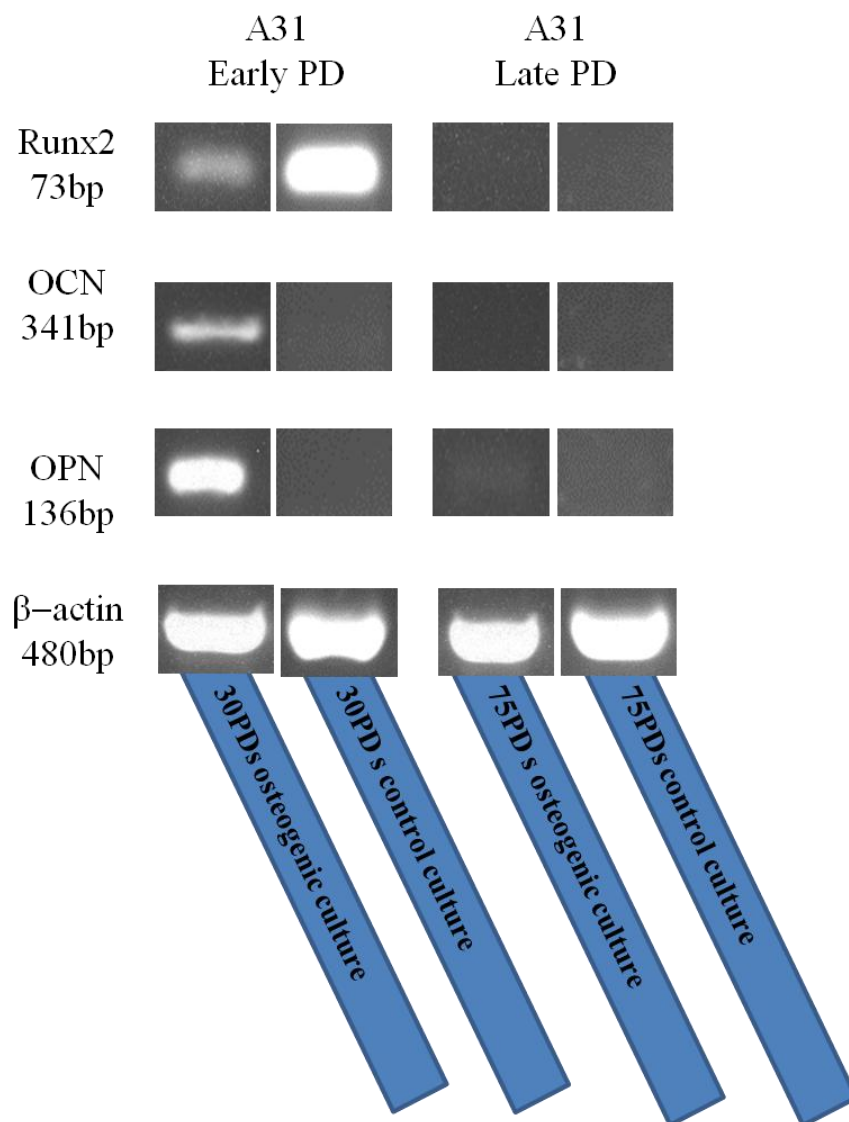
Figure 3.6. RT-PCR results showed mRNA expression profiles for clones; A31 at 30PDs, A11 at 17PDs and B11 at 24PDs in osteogenic medium and control culture medium at day 18 for Runx2, OCN and OPN. β-actin was used as a housekeeping gene. All cells in osteogenic culture expressed the osteogenic markers (Runx2, OCN and OPN). Also, cells in control culture expressed only Runx2.
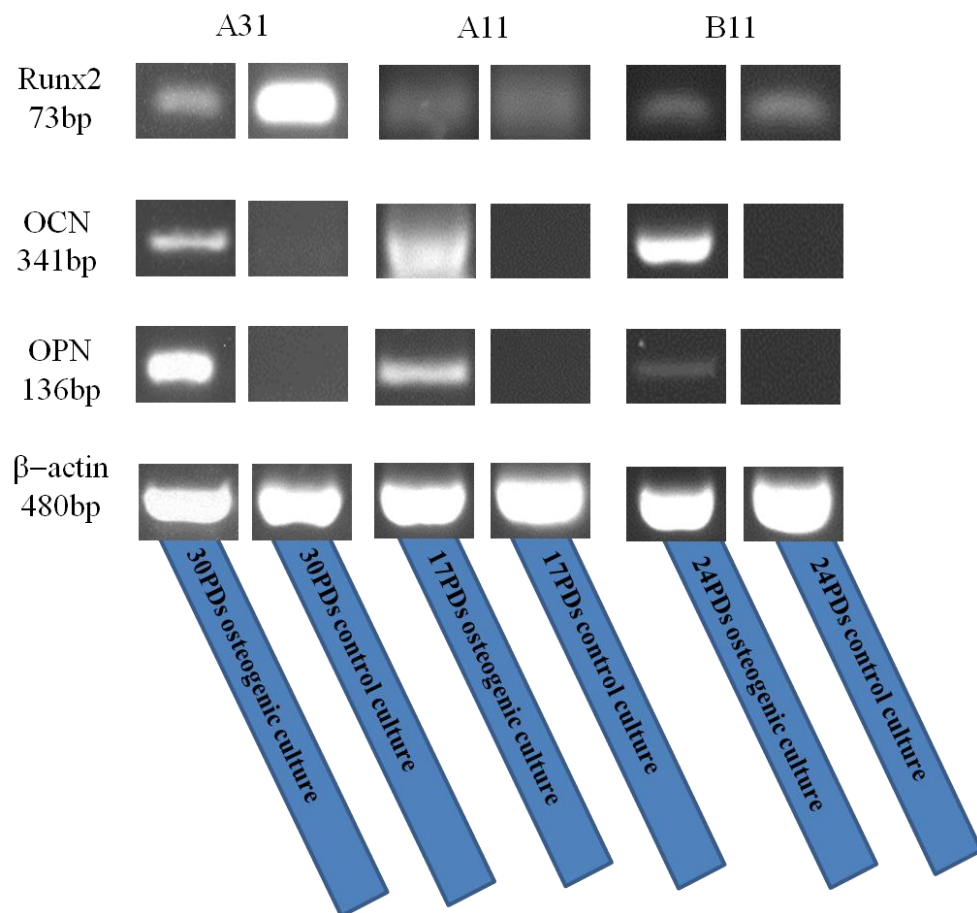
3.4.2 Adipogenic Differentiation

3.4.2.1 Cell Morphology and Oil Red O

For clone A31, adipogenic cultures of DPPCs (62PDs) at day 9 started to secrete fat droplets (arrowed) (Figure 3.7.A), when compared with the control cultures (αMEM with 20% FCS) where cells started to be over-confluent and stressed, (Figure 3.7.B). After 21 days of adipogenic culture, early PD (30 PDs), cells demonstrated small amounts of oil red O staining that revealed the lipid droplet within cells (arrowed) (Figure 3.8.A). At mid-late PD (62PDs), cells demonstrated large amount of oil red O staining present in almost in all the cells revealing the lipid droplet within cells (arrowed) (Figure 3.8.C). At late PD (75PDs), many cells appeared to have died but the remaining cells, did demonstrate oil red O staining of the fat droplets (arrowed) (Figure 3.8.E). Control cultures of A31 clones at the 3 different PD showed no specific staining with some cells tend to lift off the plate due to over-confluency (Figure 3.8. B, D and F).

For both clones A11 (17PDs) and B11 (25PDs), at day 21 in adipogenic culture, no staining of oil red O was observed (Figure 3.9.A. and 3.10.A), along with their control cultures (Figure 3.9.B and 3.10.B).

Figure 3.7. **Light microscopy of DPPCs (clone A31 at 62PDs) cultured in adipogenic medium for 9 days, (A) showed some cells with fat droplet (arrowed), while (B), cells in control cultures after 9 days where cells started to be over-confluent and wider. ×10 magnification, Scale bar 100µm.**

(A)
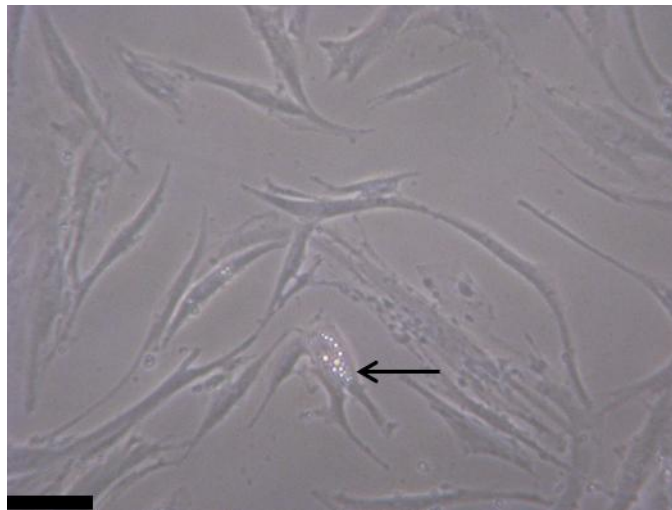
(B)
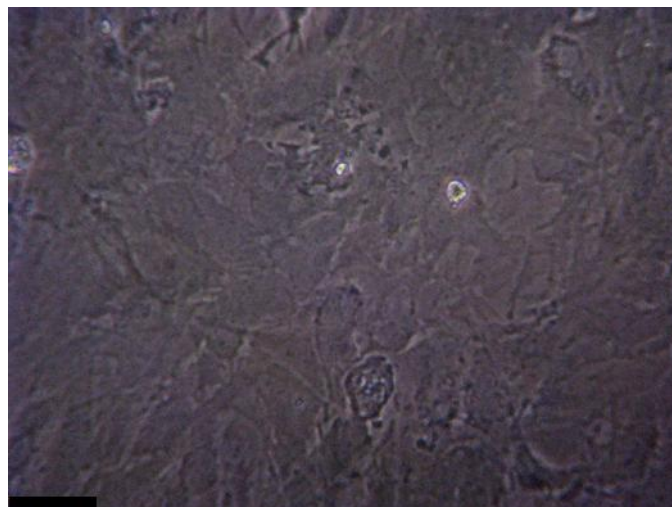
Figure 3.8. Light microscopy of clone A31 adipogenic cultured cells, stained with oil red O for early passage (30PDs) cultured cells showed less fat droplet staining at day 21 (A) compared with mid (62PDs) (C) and late (70PDs) passage (E) which showed more stained fat droplets). No specific stain was observed on control cultures at early (B), mid (D) and late PD (F). ×20 magnification, scale bar represents 100μm.

A   B

C   D

E   F
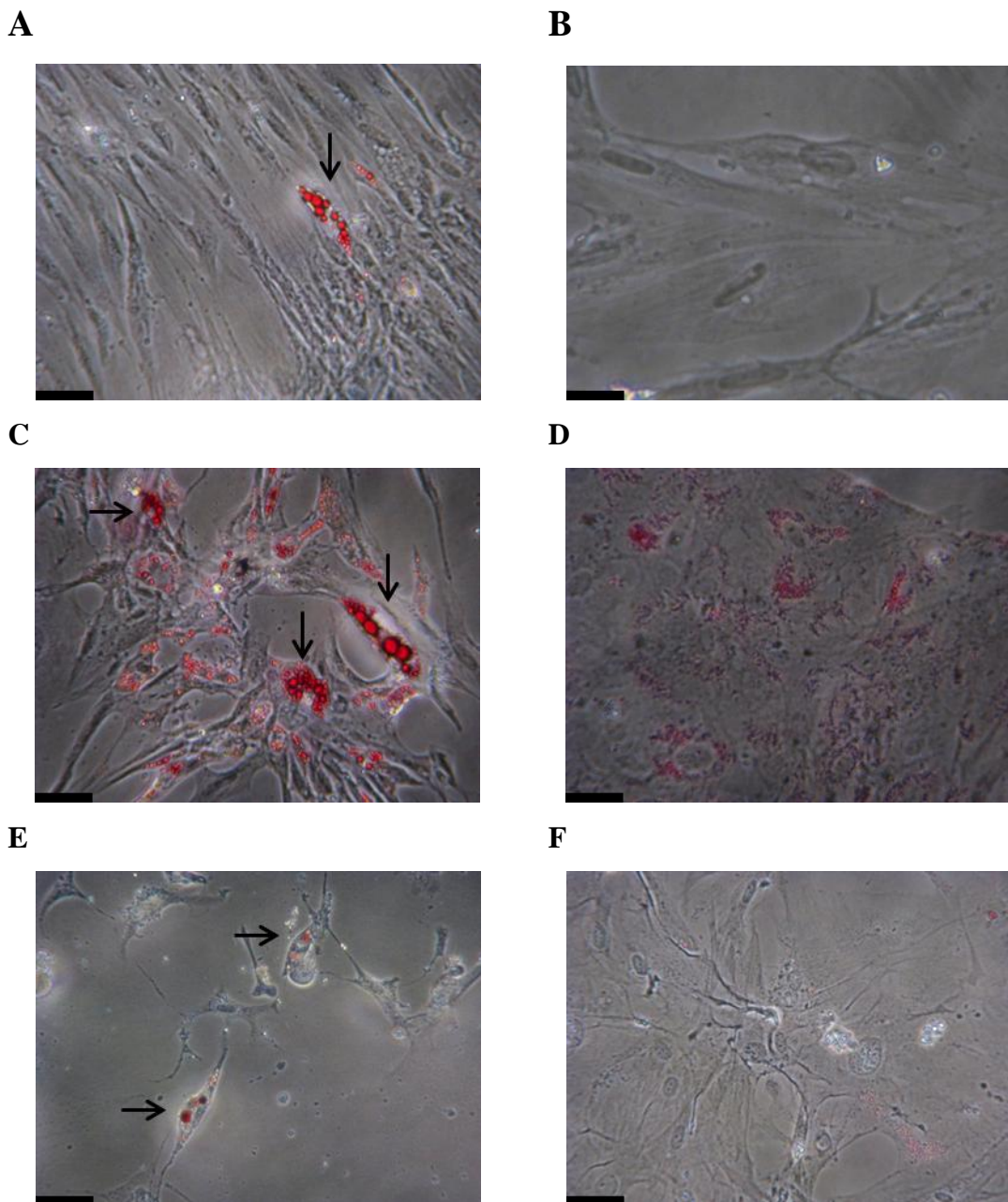
Figure 3.9. Light microscopy of clone A11 adipogenic cultured cells, stained with oil red O showed no fat droplets staining at day 21 (A). Control cultures had no specific stain of fat droplets observed (B). ×10 magnification, scale bar represents 100µm.

A

B
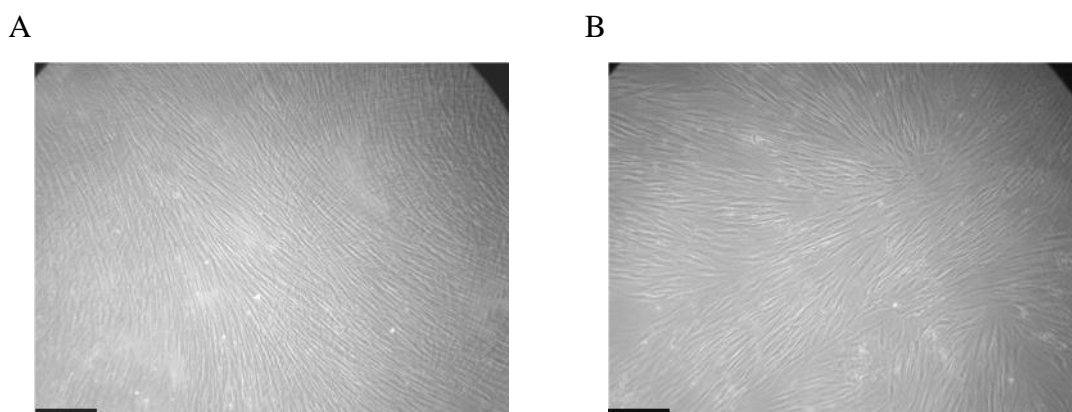
Figure 3.10. Light microscopy of clone B11 adipogenic cultured cells, stained with oil red O showed no fat droplets staining at day 21 (A). Control cultures had no specific stain of fat droplets observed (B). ×10 magnification, scale bar represents 100µm.

A

B
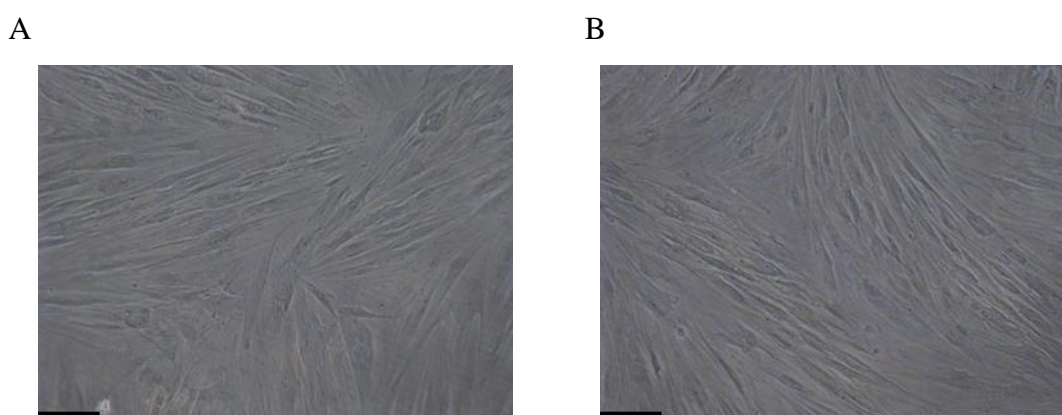
3.4.2.2 RT-PCR for Osteogenic Differentiation

The RT-PCR of the adipogenic cultured cells and the control of clone A31 indicated the presence of adipogenic markers PPARγ at both early (30PDs) and late (75PDs) PDs (Figure3.11) at day 21. LPL gene expression was observed at both PDs (early and late) in the adipogenic cultured cells at day 21, while in the control cultured cells, LPL was negative at early and late PDs (Figure 3.11). Further investigation of RT-PCR, demonstrated the cells cultured in adipogenic culture expressed the osteogenic marker Runx2 at early PD but did not express at late PD. Runx2 expression in the control culture had the same result of the adipogenic culture in both PDs (30 and 75PDs) (Figure 3.11).

For both clones A11 (17PDs) and B11 (25PDs), at day 21 in adipogenic culture, The RT-PCR was positive for PPARγ but not LPL. Similar results of RT-PCR for these two clones were noted for the control cultured cells at day 21, as PPARγ was expressed but not LPL (Figure 3.12). β-actin housekeeping gene was positive in the all results and RT negative showed no bands.

Clone A31 at early and late PDs in adipogenic medium revealed the presence of adipogenic markers which confirmed by staining of oil red O, However the staining was much more in the late PD with the expression of LPL more intense in the late PD. Clones A11 and B11 failed to express LPL which support the negative staining results of oil red O. Cells cultured as control cultures failed to express LPL and were negative for the adipogenic stain.

Figure 3.11. RT-PCR results showed an mRNA expression profile of PPARγ, LPL, Runx2, for clone A31 at early (30PDs) and late (75PDs) in both adipogenic and control culture at day 21. β-actin was used as a house keeping gene. LPL only expressed in the adipogenic culture for both PDs, while Runx2 expressed only in early PD for both cultures medium.

Figure 3.12. RT-PCR results showed an mRNA expression profile of PPARγ and LPL for clones; A31 at 30PDs, A11 at 17PDs and B11 at 25PDs in both adipogenic and control cultures. β-actin was used as a house keeping gene. PPARγ was expressed in all the clones in both adipogenic and control cultures while LPL was only expressed in clone A31 in adipogenic culture.
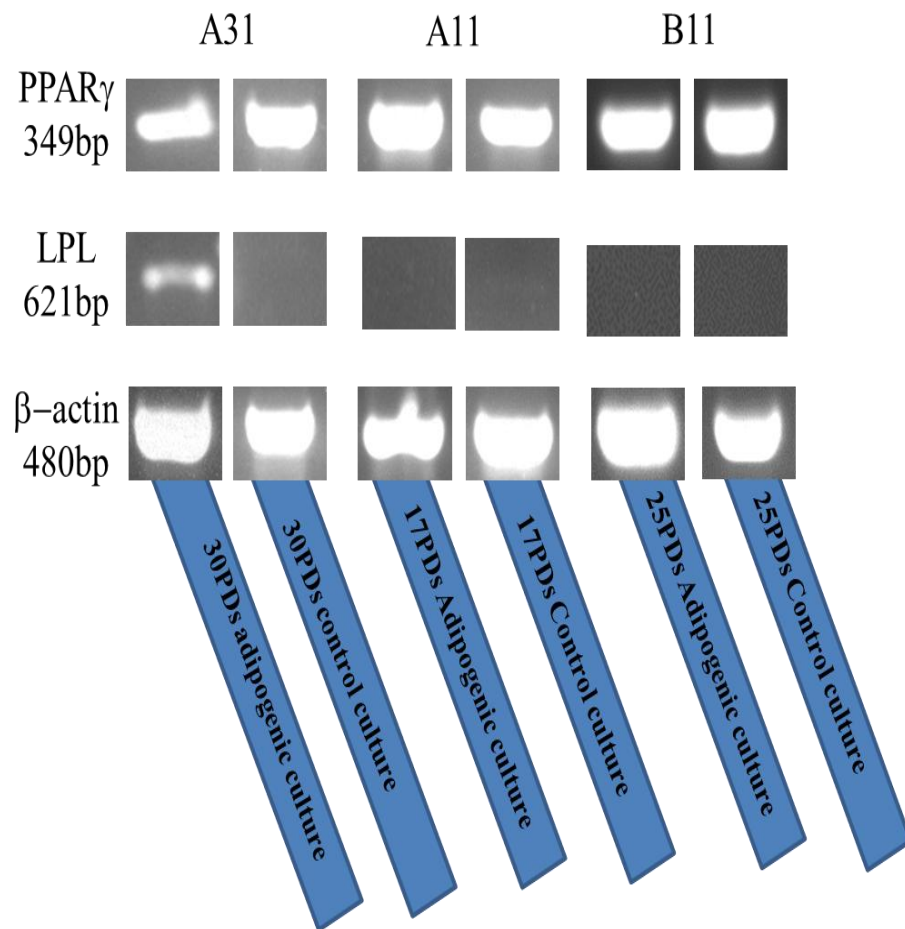
3.4.3   Chondrogenic Differentiation

After culturing the three different clones (A31, A11 and B11) with the ChondroDiff chondrogenic medium, the pellets of cells became rounded after 6 days whereas the control cultures remained as pellets adhered to the bottom of the conical tube. During the process, these rounded pellets became smaller and more rounded, while the control cultures lost their initial pellet appearance and became a mass of cells. At the end of the culture period, day 24 chondrogenic culture pellets appeared very small, rounded and compact and the control cultures were irregular masses of cells (Figure 3.13).

3.4.3.1 Safranin O Staining

After the fixation and sectioning process, clone A31's pellets were strongly stained by Safranin O, while the other two clones had almost no staining observed (Figure 3.14). Control culture pellets failed to be sectioned because cells did not form a rounded tissue as the ChondroDiff chondrogenic medium cultured cells.

Figure 3.13. Photographs of DPPCs pellets cultured in ChondroDiff chondrogenic medium. After 24 days the pellet in chondrogenic medium became rounded (A), whilst the control culture remained as an irregular mass cells (B).

A
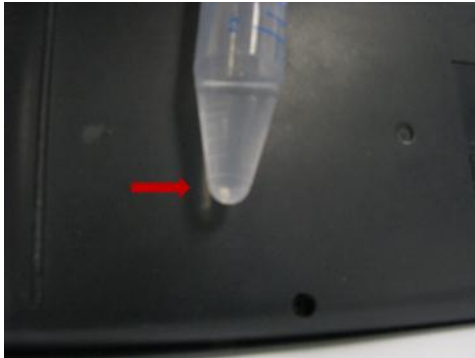
B
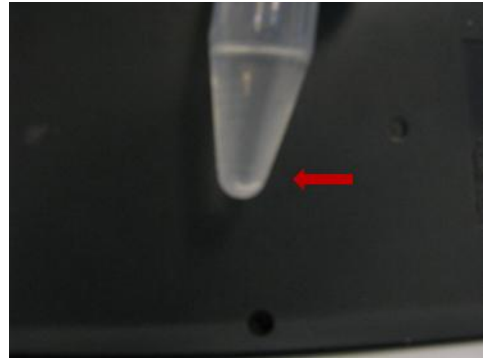
Figure 3.14. Light microscopy at x10 and X40 magnification of clone A31 (A) in chondrogenic cultured cells, stained with Safranin O demonstrated strong staining compared with other clones A11 and B11 (B and C) , scale bar represents 100µm.

Ax10

Ax40

Bx10

Bx40

Cx10

Cx40
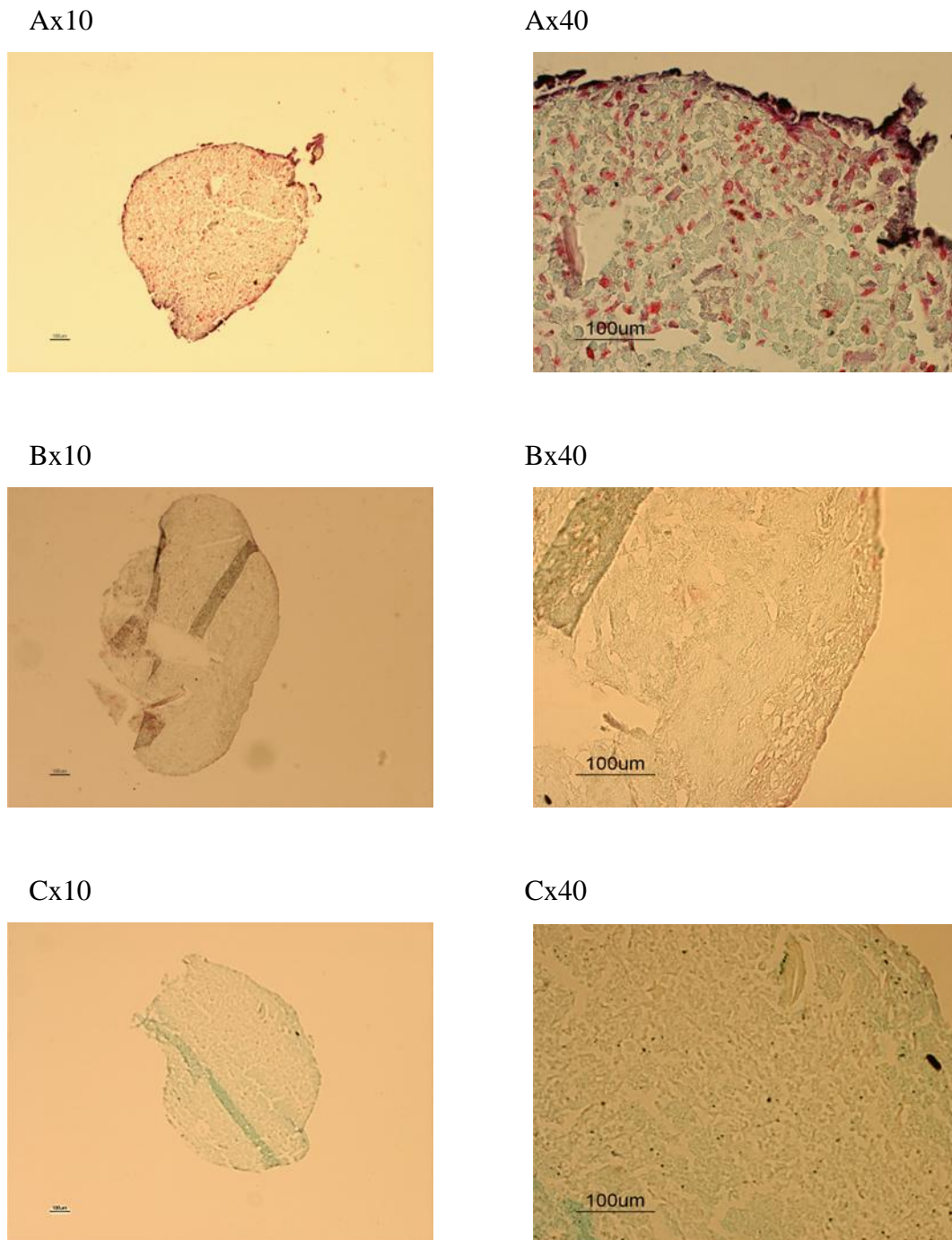
3.4.4 Effects of H$_2$O$_2$ on Osteogenic Differentiation

Clone A31 showed similar staining of alizarin red at all different concentrations (0, 50, 100, 200μM) (Figure. 3.15) of H$_2$O$_2$. Control culture showed no staining of alizarin red S (Figure. 3.16 control). The RT-PCR of the osteogenic cultured cells in the 0 μM concentration of H$_2$O$_2$ was Positive for Runx2, OCN and OPN while cell cultured in 200 μM did not express OCN or OPN (figure 3.17).

Figure 3.15. Light microscopy of A31 osteogenic cultured cells, stained with alizarin red after being cultured under different concentrations of H₂O₂ (0, 50, 100, 200μM). Cells cultured in increasing concentrations of H₂O₂ expressed similar amounts of alizarin red. ×10 magnification, scale bar represents 100μm.

0μM

50μM

100μM
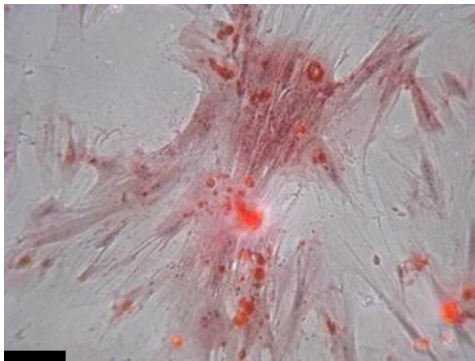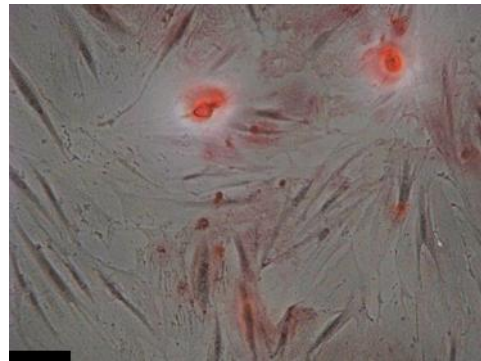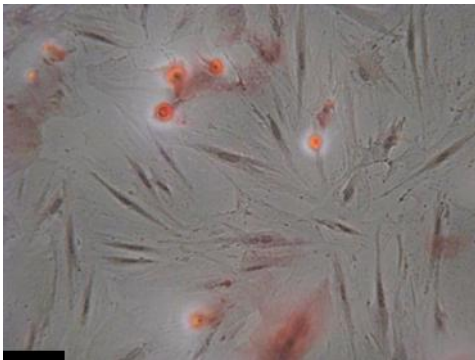
200μM
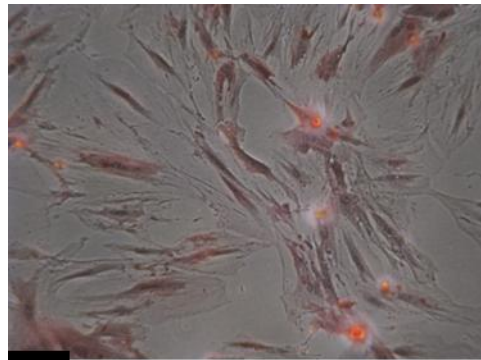
Figure 3.16. The control culture of the previous figure (3.15). No alizarin red staining was observed. ×10 magnification, scale bar represents 100μm.

0μM -control

50μM -control

100μM -control
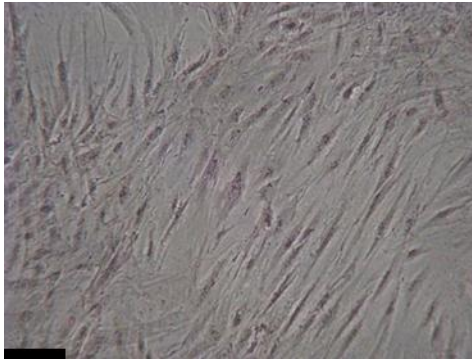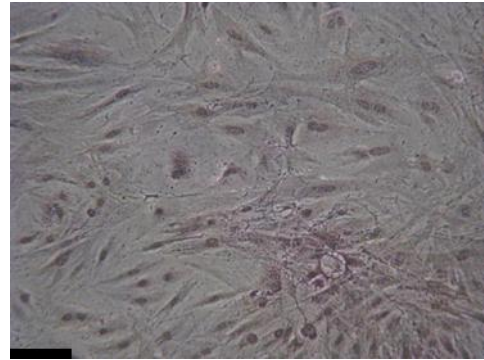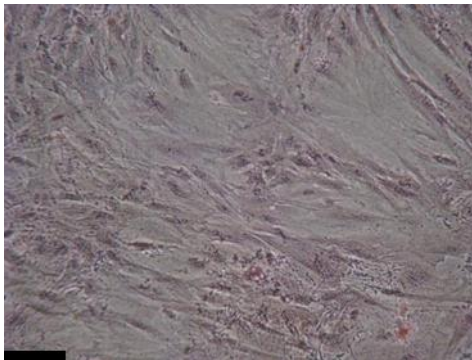
200μM -control
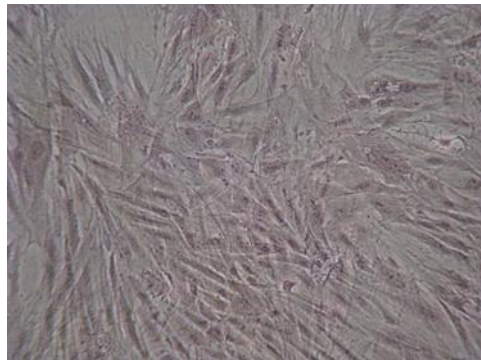
Figure 3.17. RT-PCR for 0 μm and 200μm concentrations of H_2O_2 in osteogenic culture and in control culture for Runx2, OCN and OPN. OCN and OPN were only expressed on 0 μm concentration of H_2O_2 while Runx2 was positive in all of them. β-actin was used as a house keeping gene.
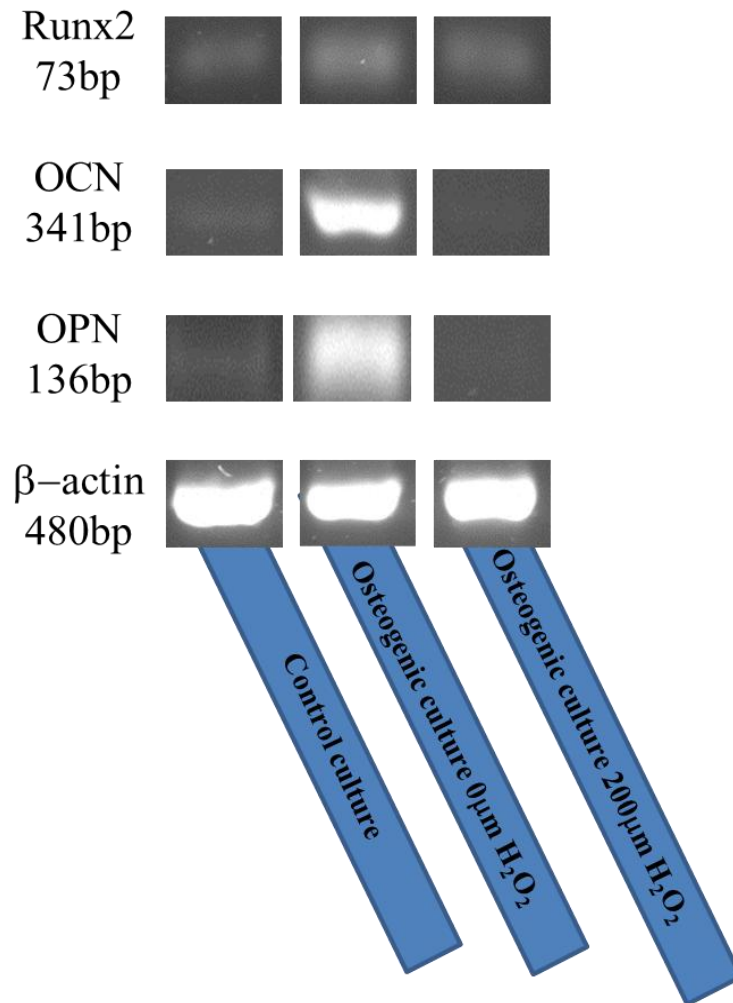
3.4.5   CD271 Expression

All the clones were investigated for CD271 marker expression prior to differentiation. Clone A31 at 30PDs did not express this marker, while A11at 17PDs and B11 at 25PDs did express CD271 (Figure 3.18).
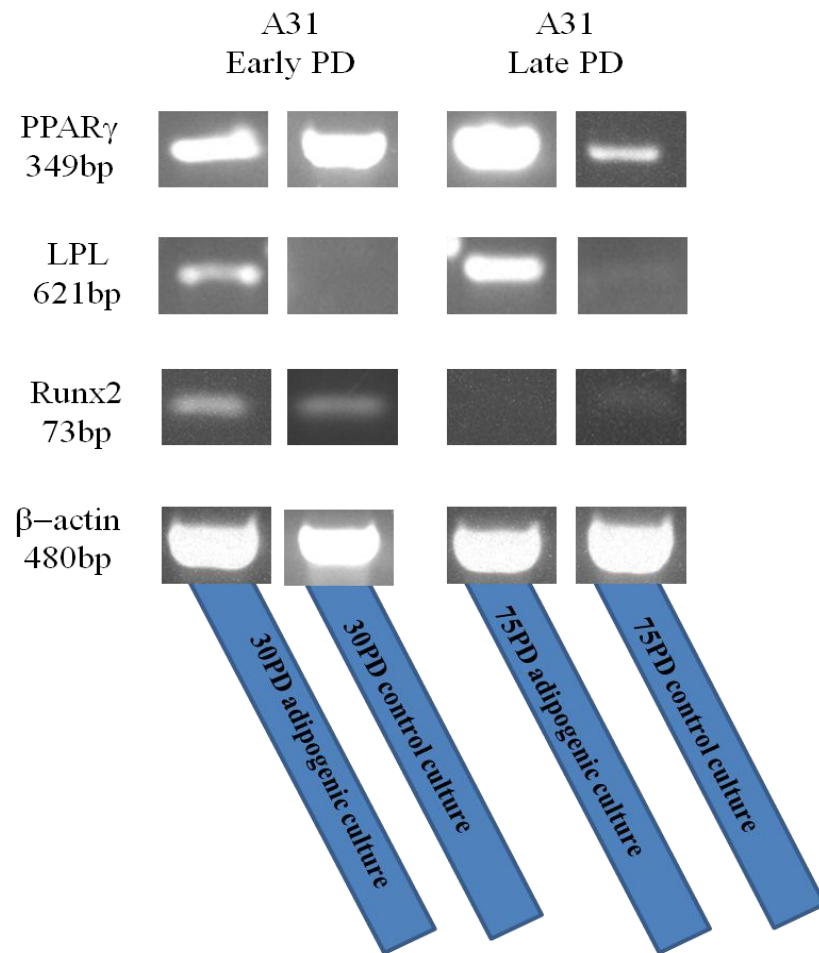
Figure 3.18. RT-PCR results showed an mRNA expression profile of CD271 for clones; A31 at 30PDs, A11 at 17PDs and B11 at 25PDs. CD271 was expressed by clones A11 and B11 but not A31. . β-actin was used as a house keeping gene.
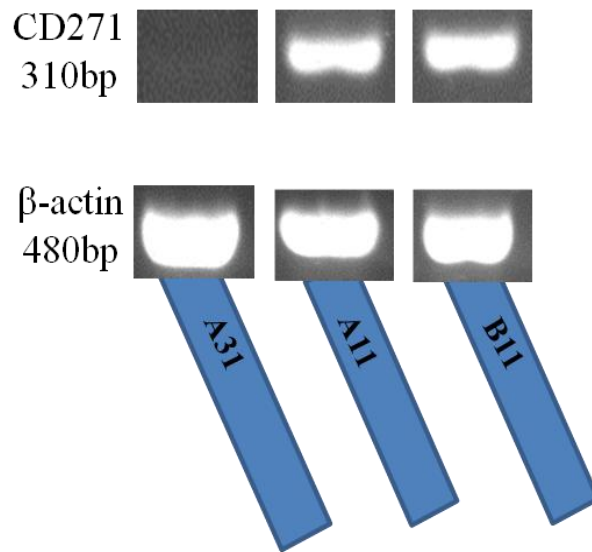
3.5   Discussion

This chapter clearly linked the highly proliferative clone, A31 that has a long telomere length with the ability to differentiate into three different lineages i.e. osteogenic, chondrogenic, and adipogenic. While the low proliferative clones, A11 and B11, that have short telomere lengths, were more committed and only differentiated into osteoblasts. In addition, CD271 marker was only expressed in clones A11 and B11, the clones that differentiated into one lineage, indicating CD271 expression marker could be used to distinguish between multipotent and unipotent clones. Furthermore, *in vitro* expansion of the clones affected their differentiation ability into osteoblasts in favour of adipocyte differentiation. Finally, as seen from the previous chapter H_2O_2 had no effects on clones, it also appears in this chapter H_2O_2 had no effect on ability of clones to differentiate into osteoblasts.

The results of clonal analyses in terms of differentiation potential have been discussed extensively in the literature and are supported by the findings of this work. Many papers show that clonal populations of DPPCs are able to differentiate into the three lineages, but appear to be from a small percentage of overall numbers of isolated clones, which is less than 5% of the total population (Halleux et al., 2001; Okamoto et al., 2002; Russell et al., 2010). The data in this study demonstrated that all three clones (A31, A11, B11) differentiated into an osteogenic phenotype, while A31 clone (the highly proliferative clone) alone was able to differentiate into three different lineages (osteoblast, chondrocytes, and adipocytes). This is in line with data presented by Halleux *et al* (2001), where 24 designated clones differentiated into osteogenic lines, while 17/24 and 18/24 clones differentiated into chondrogenic and adipogenic lineages, respectively. The preferable differentiation of these clones into osteogenic lineages may be due to their source of origin as pulp cells are indicated to express bone markers (Gronthos *et al.,* 2002). It is also worthy to note that although these studies perform their experiments on clones, methods of isolation or culture medium were different from those described in this study, such as isolation of cells based on their stem cell marker expression, and culture of clones in Dulbecco's modified Eagle's medium (DMEM). Whereas here, clones were isolated by fibronectin adhesion assay, and alpha minimum essential medium, respectively. Indeed, different methods of isolation could result in different population of cells.

Cells isolated by enzymatic dissociation showed better differentiation ability into osteogenic lines than cells isolated by direct outgrowth (Bakopoulou et al., 2011).

The reason behind the variety of the clones in terms of differentiation ability is still not fully understood. Some studies have linked variations to the expression levels of cell surface markers such as CD146 (Russell et al., 2010) or CD271 (Mikami et al., 2011). The reason behind different stem cell marker expression could be due to their different locations. DPPCs that express CD146 marker are suggested to be from a perivascular niche (Shi and Gronthos, 2003), while DPPCs that express CD271 marker suggests that the niche is of a nerve network origin within the cell-free zone (Lizier et al., 2012). The relationship between CD146 expression and differentiation ability was proportional, while for CD271, differentiation was inversely related to the differentiation ability (Russell et al., 2010; Mikami et al., 2011). In this study, A31 clone, the only clone with multiple differentiation ability, was the only clone to not express CD271. Although A11 clone is from the same patient as A31 clone, it did express CD271. This may indicate different niches from which these clones were isolated. Another theory which supports the reason of the variations in both differentiation and proliferation between the clones is asymmetric division of the stem cell. Adult stem cells have the ability for self-renewal and differentiate into multiple cell lineages, with short life-spans. To achieve self-renewal capabilities and differentiation functions, stem cells divide slowly and symmetrically to produce an identical daughter cell with low proliferative capacity and multipotential differentiation. Some of these adult stem cells go on to divide asymmetrically and give rise to one identical daughter cell and another progenitor cell called a transit amplifying (TA) cell. TA cells have a high proliferative potential and low differentiation ability and give rise to more committed progenitors with reduced proliferative potential (Figure 1.1), and eventually produce terminal differentiated cells (Alison et al., 2002; Ho, 2005). Asymmetrical division could give one explanation of the reasons that cause different characteristics between isolated clones of DPPCs. Here, clone A31 was the only clone that had both characteristics with highly proliferative and multipotential differentiation, probably because of asymmetrical division of stem cells that led to this clone to have both populations i.e. stem cells and TA cells. While clones A11 and B11 were more committed

progenitors with low proliferation capacity and commitment to differentiate only into osteoblasts.

For osteogenic differentiation, alizarin red staining was shown in all isolated DPPCs clones (A11, A31 and B11). Alizarin red is used to demonstrate the calcium deposition nodules (Koch et al., 2007). In addition, several bone specific genes (Runx2, OCN, and OPN) were expressed in these clones after induction in osteogenic medium for 18 days. Runx2 controls the expression of many tooth and bone related genes and regulate the differentiation of MSCs into osteoblasts (Lian et al., 2006). OCN gene expression is recognized to occur at a late stage of osteoblastic differentiation (Mizuno and Kuboki, 2001). OPN is a major non-collagenous protein produced by differentiated osteoblasts, and BSP is considered as a specific marker for osteoblasts (Mizuno and Kuboki, 2001). Runx2 was detected in early passage cells in all clones in normal and osteogenic medium, but OCN and OPN were only detected in cells cultured in osteogenic medium. As such, the expression of Runx2, OCN, and OPN with alizarin red staining, confirmed the osteogenic differentiation of all three DPPCs clones. At late PD, Runx2 was not detected in neither normal nor osteogenic cultured medium cells. Therefore, OCN and OPN expression was absent. Losing Runx2 with ageing indicated loss of the ability of these cells to differentiate into bone, which has been previously reported (Banfi et al., 2000); and may explain the deterioration of bone in elderly patients with osteoporosis where Runx2 is suppressed by PPARγ (Moerman et al., 2004).

Clone A31 demonstrated its differentiation ability into an adipogenic lineage by morphological changes and expression of specific adipogenic genes. The main morphological change was the accumulation of lipid rich vacuoles within cells which is a sign of successful differentiation of MSCs into adipocytes (Pittenger et al., 1999; Jaiswal et al., 2000; Huang et al., 2009b). In addition, clone A31 adipogenic differentiated cells expressed PPARγ, the key factor for MSC differentiation into adipocytes (Muruganandan et al., 2009). PPARγ was shown in all the clones, for both adipogenic and control cultures, while LPL was only identified in clone A31 after culturing in adipogenic medium; which was also the only clone to have the positive staining of oil red O. This is due to the fact that adipocytes and osteoblasts

141

share the same origin progenitor cells, while only pre-osteoblastic cells differentiate into osteoblast, but not into adipocytes (Shakibaei el al, 2012). Furthermore, LPL is downstream from PPARγ and so is mainly expressed in mature adipocytes, in order to increase the generation of fatty acid (Yoke Yin et al., 2010). This explains the presence of oil red O staining with the expression of LPL in the only clone differentiated into adipocytes (A31 clone).

It has been reported that *in vitro* ageing, which means passaging cells during cell culture, has greater effects on MSCs, in term of proliferation and differentiation, than *in vivo* ageing (Fickert et al., 2011; Kim et al., 2012b). Due to the need of considerable stem cell expansion *in vitro* for DPPCs to produce sufficient cell numbers to characterise these cells and for the therapeutic use in the future (Thirumala et al., 2013), an investigation of the effect of *in vitro* ageing was performed. In this study, the highly proliferative clone A31 showed more ability to differentiate along the osteogenic pathway and less ability to differentiate into adipocytes at early PD. However, A31 lost its osteogenesis ability at late PD in favour of adipogenesis. The lack of Runx2 has been shown before that it prevents the osteogenic differentiation (Komori et al., 1997), which is similar to what has been found in clone A31 at late PD. Comparing this to an *in vivo* model, osteoblasts and adipocytes are derived from mesenchymal stem cells in bone marrow (Bianco et al., 2001), based on two main transcription factors; Runx2 for osteogenic differentiation and PPARγ for adipogenic differentiation (Kim et al., 2012b). PPARγ acts as suppressor of Runx2 and osteoblast phenotype. With ageing, the expression of PPARγ increases which leads more MSCs to terminally differentiated adipocytes, rather than osteoblasts. These results may explain the reason of the appearance of fatty marrow with advancing age (Moerman et al., 2004). Furthermore, decreases in the differentiation capabilities with ageing seem to co-ordinate with the loss of the stem cell marker expression that has been shown in chapter 2. It is noteworthy to point that what is consider as early PDs in this thesis could not be the same in other studies such as in Deng et al., (2001) where early PD was at passage 2.

For the chondrogenic differentiation clones, highly proliferative clone A31 showed high potential to differentiate into cartilaginous tissue by using chondrogenic

medium in 3D culture, in the form of pellet culture (Johnstone et al., 1998). The specimens were stained with Safranin O to stain proteoglycans, which are major proteins in cartilage (Schmitz et al., 2010). In addition the transcription factor, Sox9, is also a major component of the cartilage (Shirasawa et al., 2006), was detected in this clone. Low proliferative clones (A11 and B11) showed almost no ability to differentiate into cartilaginous tissue. This again may be due to the origin of these clones, as described previously.

H_2O_2 is used to accelerate cellular senescence at concentrations that are non-lethal to cells. As oxidative stress-induced senescence had no effects on the telomere lengths, H_2O_2 did not have an effect on the differentiation capacity of the highly proliferative clone A31 in terms of mineralisation, which was shown by Alizarin red staining and the expression of gene marker, Runx2. However, the expression of OCN and OPN were negative only in the highest concentration, 200μm. This proves that the expression of these two markers does not co-ordinate with mineralisation, in line with previous studies (Beck et al., 1998; Addison and McKee, 2010). Even though Runx2 is considered as a regulator for OCN and OPN, however it is not the only regulator of these genes, which means that H_2O_2 may have an effect on other regulators that lead to OCN and OPN not being expressed, such as homeodomain proteins, exogenous phosphate or ascorbate could react with H_2O_2 (Goralczyk et al., 1998; Hassan et al., 2004). Oxidative stress via H_2O_2 has been linked to loss of bone density with ageing in both men and women (Basu et al., 2001), but it did not show that in this study. This may be due to the time exposure of H_2O_2 was not enough to cause effects on the mineralisation process.

In conclusion, this chapter has demonstrated that only the highly proliferative clone (A31) was able to differentiate into osteogenic, chondrogenic and adipogenic lineages, which makes it the likeliest candidate for tissue engineering. Although, clone A11 is from the same patient as A31 but it did not show the same results as A31. This could be due the different niche where these clones arise from or what stage of development these cells are as shown in figure 1.1 Given their low levels in dental pulp cell populations, this means finding better ways to isolate and characterise these clones is a crucial step before using these MSC clones for

therapeutic applications. Furthermore, *in vitro* expansion of the cells has its effect on the clone differentiation ability, which could explain the differences that occurs in humans during ageing, such as increase of fat in bone marrow, at the expense mineralised of bone status.

Chapter 4:

Identification of Clonal Dental Pulp Variations Using Raman Spectroscopy

4.1   Introduction

There are ever-increasing demands on the therapeutic usage of mesenchymal stem cells (MSCs), which means further investigation regarding cell characteristics and behaviour is needed (Pijanka et al., 2010). This is because MSCs have no specific markers and their behaviour differs, based on the species, site of origin and maturity. However, to analyse these cells, this may require fixation, staining and drying steps that damage cellular characteristics, or structural features and does not provide the real-time chemical information from living human stem cells. This calls for investigations to develop non-destructive applications to characterise cells. One of these methods is Raman Spectroscopy (Moody et al., 2010).

Raman spectroscopy is a biochemical characterisation method based on the inelastic scattering of monochromatic light. When the incident light is scattered from a molecule or crystal, most photons are elastically scattered. Only a very small fraction of photons (approximately 1 in 10^7 photons) are scattered inelastically, i.e. with a frequency different from that of the incident photons. This inelastic scattering is called the Raman effect (Advanced physics Laboratory, 2006). The monochromatic light that is used in Raman spectroscopy is a laser, whose wavelength can vary from the visible to the infrared region of the electromagnetic spectrum. The theoretical physics behind Raman spectroscopy is that photons scatter at the same angle as the incident angle, due to the vibration of the molecules and atoms. When the wavelength of the scattered Raman photon is lower than that of the incident photon, it is termed anti-Stokes scattering. In contrast, when the wavelength of the scattered Raman photon is higher than that of the incident photon, so-called Stoke scattering occurs (Figure 4.1). There are many Raman band assignments that have been identified for human cell components. Table 4.1 shows some of these bands (Chan et al., 2009). The energy difference between the incident and scattered photons is numerically calculated as Raman shift in wave numbers (cm^{-1}), through the following equation: $V = 1/\lambda_{incident} - 1/\lambda_{scattered}$ where λ is the wavelength in cm.

Figure 4.1. Energy level diagram for Raman scattering. (a) Stokes scattering and (b) anti-Stokes scattering. (Image taken from Advanced Physics Laboratory, 2006).
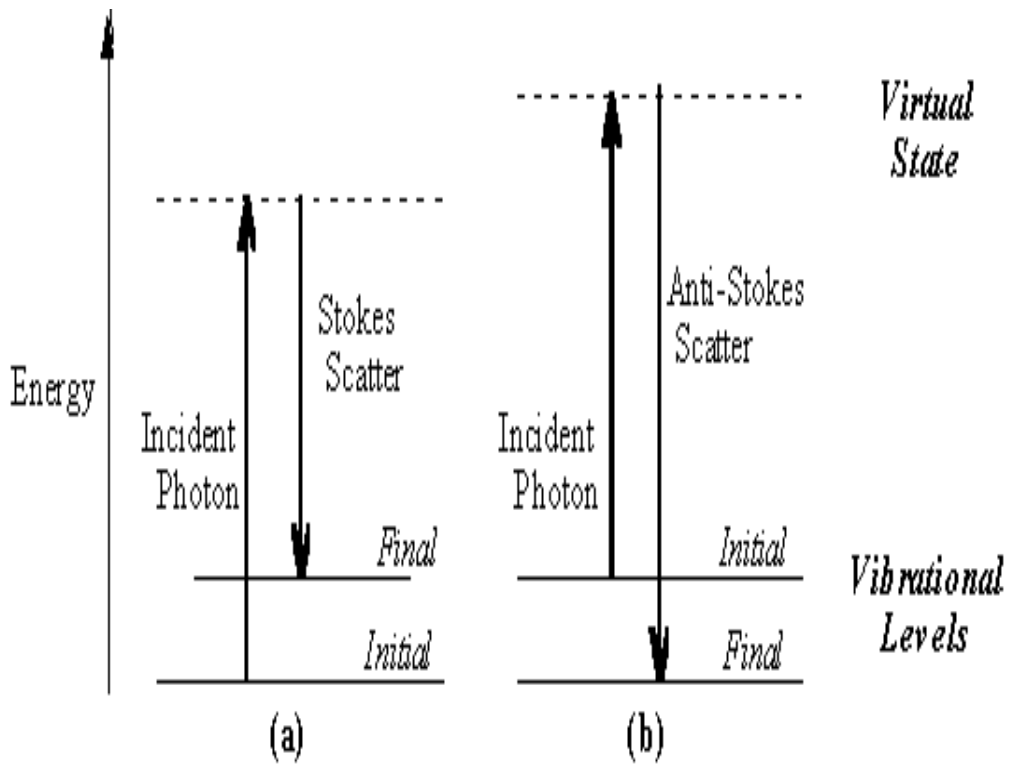
Table 4.1 Raman peak wavenumbers and their assignments

Wavenumber cm^{-1}	Assignment
3328	Amide A: N–H and O–H stretching vibrations of polysaccharides, proteins
3129	Amide B: N–H stretching vibrations of proteins
3015	Olefinic =CH stretching: unsaturated lipids, cholesterol esters
2960	CH$_3$ antisymmetric stretching: lipids, protein side chains
2920	CH$_2$ antisymmetric stretching: mainly lipids
2875	CH$_3$ symmetric stretching: protein side chains, lipids
2850	CH$_2$ symmetric stretching: mainly lipids
1720–1745	C=O stretching vibrations of lipids (triglycerides and cholesterol esters)
1710–1716	C=O antisymmetric stretching: RNA and purine base
1705–1690	C=O antisymmetric stretching vibrations: RNA, DNA
1654	Amide I: C=O (80%) and C–N (10%) stretching, N–H (10%) bending vibrations: proteins a-helix
1630–1640	Amide I: C=O (80%) and C–N (10%) stretching, N–H (10%) bending vibrations:proteins β-structure
1610, 1578	C4-C5 and C=N stretching in imidazole ring of DNA, RNA
1515	Aromatic tyrosine ring
1540–1550	Amide II: N–H (60%) bending and C–N (40%) stretching vibrations: proteins α-helix
1530	Amide II: N–H (60%) bending and C–N (40%) stretching vibrations: proteins β-structure
1467	CH$_2$ bending vibrations: lipids and proteins
1455	CH$_3$ bending and CH$_2$ scissoring vibrations: lipids and proteins
1370–1400	COO– symmetric stretching and CH$_3$ bending vibrations: lipids, proteins
1330–1200	Amide III: proteins
1230–1244	PO$_2{}^-$ antisymmetric stretching vibrations: RNA, DNA and Phospholipids
1090-1080	PO$_2{}^-$ symmetric stretching vibrations: RNA, DNA
996	RNA stretch and bend ring of uracil

Table is adapted from Aksoy and Severcan, 2012.

Vibrational investigation of the biomedical properties of specimens has been applied before using infrared (IR) absorption spectroscopy (Miura and Thomas, 1995). However, water is a strong IR absorbing medium. The advantage of Raman spectroscopy over IR spectroscopy is that the Raman peak of water is far from the fingerprint region (600-2000cm^{-1}) of most of living biological systems (Thomas, 1999). Other advantages of Raman spectroscopy are its ability to examine samples at different physical states, (solutions, suspensions, precipitates, gels, fibres, etc.) and its non-destructive and label-free nature (Thomas, 1999). On the other hand, one of the disadvantages of Raman spectroscopy is the weakness of the Raman signal. For this reason, improvements to Raman spectroscopy techniques are being sought, such as sample preparation, illumination or scattered light detection (Kachynski et al., 2008).

4.1.1 Applications of Raman Spectroscopy

Raman spectroscopy has been used to identify and measure the cellular responses, such as cell-cell interaction, cell-matrix interaction, cell metabolism and senescence (Notingher, 2007). For example, it is possible to identify cell death based on the cellular response to toxic agents that produce distinct biochemical fingerprints in the Raman spectra of cells. This fingerprint is related to the intrinsic molecular composition of the cell. Ricin and sulphur mustard were used as the toxic agents and Raman spectroscopy showed high sensitivity to damaged cells with 99% accuracy (Notingher, 2007).

The uniqueness of the Raman fingerprints of cells and tissues is beneficial in different biomedical applications, such as the analysis of chemical composition (DNA, RNA, lipids and proteins), molecular markers, the measurement of biological functions (enzymatic activity and lipid intake), diagnosis of diseases (cancers) and *in vivo* endoscopies (Wachsmann-Hogiu et al., 2009). Most structurally informative bands occur in the range between 500-1800cm^{-1}, such as protein and nucleic acid with the exception of the hydrogenic stretch molecules which generates wavenumbers at 2400-3600cm^{-1} Raman interval (Thomas, 1999). Figure 4.2 shows the Raman spectrum of P22 virus by using Raman Spectrum excited by argon laser at 514.5nm. Water has been used as a buffer at its wavelength between 3000-3700cm^{-1}.

Figure 4.2. Raman spectrum at 514.5nm excitation of P22 virus in H_2O buffer at 20°C. Bottom trace showed the complete spectrum, including H_2O solvent (3000–3700cm⁻¹) and aliphatic C -H stretch modes of viral protein and DNA (~2900cm⁻¹). Most of the bands occurred in the 600-1800cm⁻¹, including DNA backbone range between 830 and 1039cm⁻¹. The figure is adapted from (Thomas, 1999).
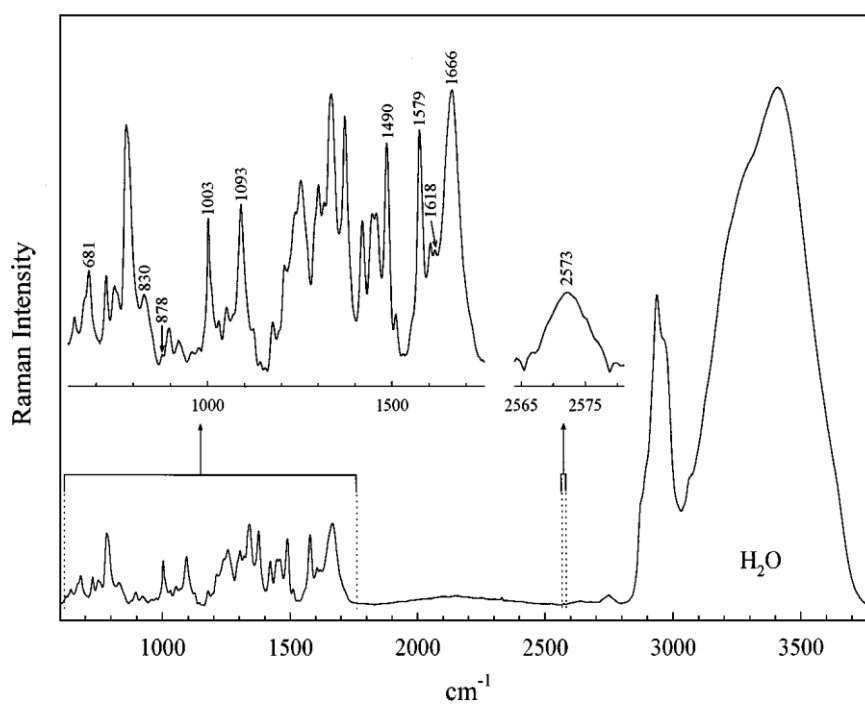
Raman spectroscopy has also been used to distinguish between different types of cells. It has been reported that human embryonic stem cells (hESCs) show a higher Raman intensity in the lipid region (peaks at 2920, 2850 and 1740cm^{-1}), when compared to human MSCs (Pijanka el al, 2010). This difference could help distinguish between multipotent and pluripotent stem cells, based on their lipid contents. This suggests Raman spectroscopy can separate stem cells from their derivatives, based on DNA and RNA contents, because their levels drop significantly during stem cell differentiation. The decrease of RNA to protein ratio was clearly shown in in murine neural stem cells during differentiation to glial cells (Ghita et al., 2012). Another benefit of Raman spectroscopy in stem cells therapy is the detection and avoidance of teratomas by successful separation of stem cells from their derivatives. This is because with uncharacterised stem cells, there is a possibility of having mixed populations containing different types of cell, especially during the necessary culture expansion that led some of these cells to undergo differentiation. This type of heterogeneous population may cause teratoma and cancer (Chan et al., 2009; Downes et al., 2011).

Data analysis forms a very important part of Raman spectroscopy. One of the most commonly used statistical analyses with high potential to separate signals that have different intensities in the Raman spectra is Principal Component Analysis (PCA) (Hasegawa et al., 2000). PCA is a multvariate statistical analysis method based on non-parametric data that converts a collection of observations of probably connected variables into a group of values of linearly unconnected variables, called principal components (Massart et al., 1998). PCA is mathematically defined as "an orthogonal linear transformation that transforms the data to a new coordinate system such that the greatest variance by any projection of the data comes to lie on the first coordinate (called the first principal component), the second greatest variance on the second coordinate, and so on" (Jolliffe, 2002). PCA has been broadly used in Raman spectroscopy to distinguish between different tissues, especially between normal and diseased tissues, such as non-diseased skin tissue and basal cell carcinoma (Martin et al., 2004), to identify T and B lymphocytes of normal and leukemic patients (Chan et al., 2008); and to discriminate between live and apoptotic cells, such as in human

gastric cancer cells (Yao et al., 2009). However, PCA does not provide any chemical information, but only reveals differences between samples (Ong et al., 2012).

4.2   Aims

Characterisation of adult stem cells is vital to regenerative medicine. As it has been shown in the previous chapters, clones isolated from dental pulp behave differently according to the different methods of characterisation used, such as stem cell marker expression, population doubling level (PD), differentiation ability and telomere length. However, these methods are time consuming, which might also be destructive for the stem cells.

For this reason, Raman spectroscopy was used to investigate if it could be used as a quick non-invasive method to characterise dental pulp progenitor cells (DPPCs) prior to their use in stem cell-based therapies. Raman spectroscopy was also used to investigate if the biochemical signatures of DPPCs are different from their successors following differentiation into chondrocytes.

4.3   Material and Methods

4.3.1   Cell Source

Cultures of the isolated DPPC clonal populations at early PD (A31 at 18PDs, A11 at 8PDs and B11 at 7PDs) in addition to mid-late A31 PD at 60PDs were thawed from liquid nitrogen and prepared for Raman spectroscopy by washing first in α-MEM medium and subsequently in PBS. Cells were centrifuged at 1,800 rpm (Labofuge 400, Thermo Scientific, USA) for 5 min to form a pellet, and further 1 ml of 90% industrial methanol solution (IMS) was added and left overnight at -80°C.

4.3.2   Raman Spectroscopy

4.3.2.1 Experimental Raman Set Up

The Raman Microspectroscope used in this chapter was built by Dr. Elisabetta Canetta at Cardiff School of Bioscience (Figure 4.3). The microscope of the Raman system is an Eclipse Ti-U inverted microscope Nikon equipped with a 20x (NA = 0.75) dry objective. The laser source is a diode pumped solid-state (DPSS) laser,

operating at 532nm and with a maximum power of 50mW (Lasever, Ningbo, China). The laser beam passes through a clean-up filter (Semrock-Laser 2000, Ringstead, UK) which transmits ≥90% of the laser beam at 532nm, in order to remove any optical noise from non-lasing (i.e. plasma) lines and spontaneous emissions. To fulfil the back-aperture (4.37mm) of the 20x (NA 0.75) objective of the microscope, the nominal laser beam size 1/e2 of 2mm was expanded 3 times. At this size, a 1:3 beam expander composed of two visible achromat lenses of focal lengths f = +75mm (Thorlabs, Ely, UK) and f = -25mm (Thorlabs, UK) was used along with a scan lens of f = 100mm (Thorlabs, UK), as the tube lens focal length for Nikon microscopes is ~200mm. The laser beam is reflected from a dichroic beam splitter (Semrock-Laser 2000, UK) and focused onto the sample by an objective lens.

The Raman scatter from the sample was collected by the same objective lens and transmitted through the same dichroic beam splitter. It then passed through a Steinheil triplet achromat lens with a magnification of 1:1 and f = 50mm (Edmund Optics, York, UK), followed by a confocal slit that can open up to 6mm (Thorlabs, UK) and another Steinheil triplet achromat lens 1:1. The confocal slit was kept open to its maximum (i.e. 6mm) and confocality achieved using the slit of the spectrometer. A bi-convex lens of f = 25mm (Thorlabs, UK) was placed in front of the confocal slit in order to image the sample onto the grating of the spectrometer.

Before entering the spectrometer the Raman scatter, passed through a long-pass filter (Semrock-Laser 2000, UK), in order to reject any Rayleigh scatter travelling with the Raman scatter, so that only the latter enters the spectrometer. The spectrometer is an iHR550 Jobin Yvon (Horiba, Kyoto, Japan) equipped with a 600 grooves/mm grating (spectral resolution 4 cm^{-1}) and a spectroscopy CCD camera (model Newton, Andor, USA). The Raman system is entirely enclosed for safety reasons.

4.3.2.2 Raman Sample Preparation

The sample chamber used in the Raman experiments was made using a 80-μm deep vinyl spacer between a quartz slide (1 mm in thickness) and a quartz coverslip (200 μm in thickness) (UQG, Cambridge, UK). Cell suspensions (20μl) were placed inside

the chamber and the cells allowed to sediment onto the inverted quartz coverslip for ~30 min, before commencing the Raman experiments.

4.3.2.3 Raman Experiments

Single cell standard spectra were acquired from 20 fixed cells from each clone and measured over a range of $600cm^{-1}$ to $1800cm^{-1}$. Ten spectra were measured from the central region of the cells (nucleus) and another ten spectra were measured from the peripheral region of cells (cytoplasm and membrane), to obtain average spectra representing each cell type. The background spectra were also acquired at a 20x objective (N.A. =0.7). The laser power on the sample during signal acquisition was ~36mW with each spectrum collected in the range from 500 to $2100cm^{-1}$ (grating 150 grooves/mm) with an integration time of 60 s. The laser beam, during acquisition, was focused on the cell nucleus. At the beginning of each Raman session, the dark current of the Andor camera was measured.

Figure 4.3. Raman Microspectroscopy setup used in this study (built by Dr. Elisabetta Canetta).
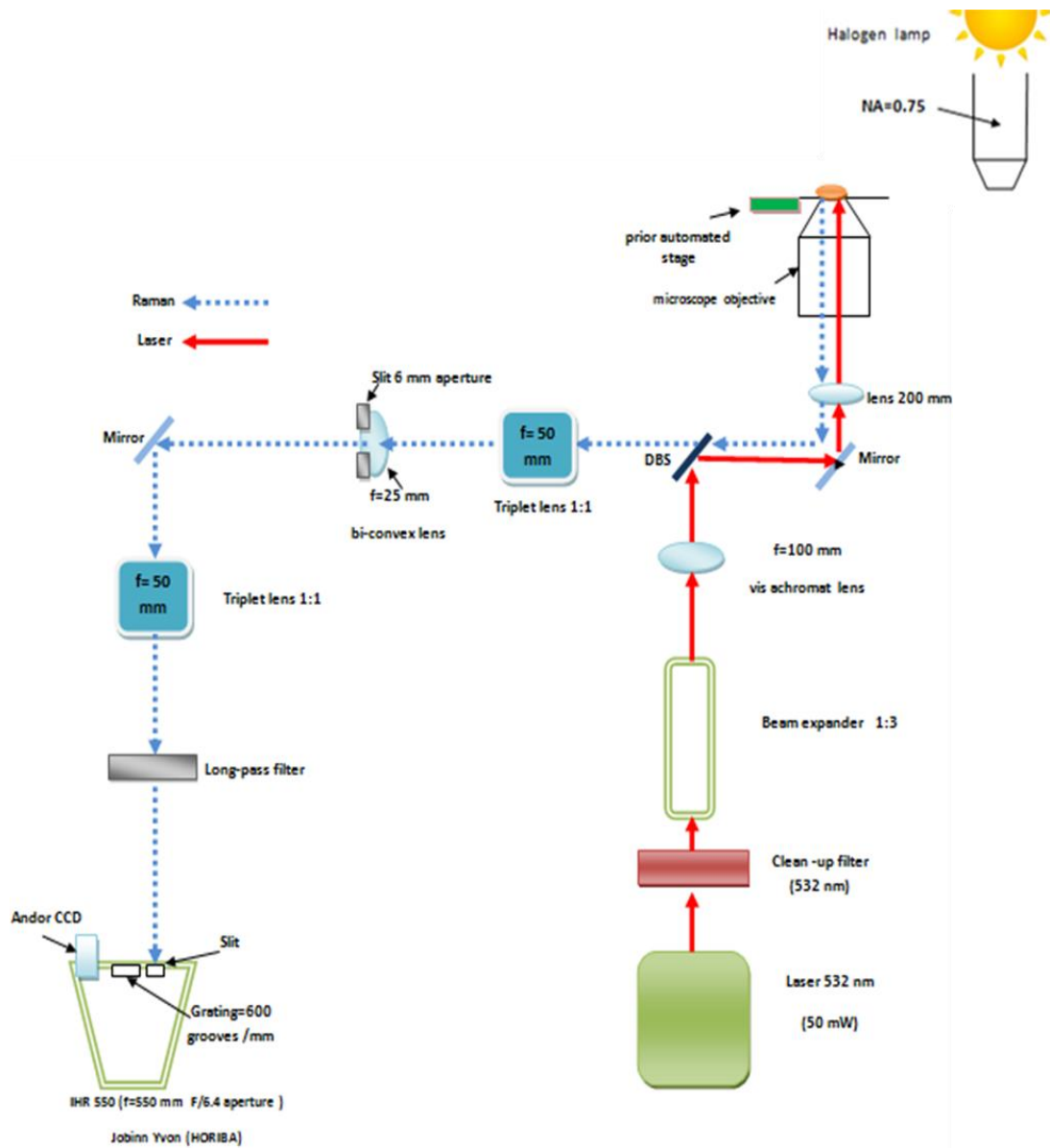
4.3.3 Data Analysis

4.3.3.1 Calibration of the Spectrometer Using a Neon Lamp

To convert the Raman spectra acquired from pixels to wavenumbers, the spectrometer needed to be calibrated. For this, a clear neon lamp (RS, Corby, UK) was used. The neon lamp was inserted inside the condenser of the Ti-U Nikon microscope, in order to achieve a homogenous illumination of the sample area. Neon spectra were taken at centre wavelength positions of 600nm (Figure 4.4).

The neon spectra in pixels were compared with neon spectra in wavelength found in literature. The pixel–wavelength experimental data were fitted with a linear fit (Figure 4.5).

Figure 4.4. Neon spectrum obtained at a 600nm wavelength position of the iHR550 spectrometer, using a 150 grooves/mm grating.
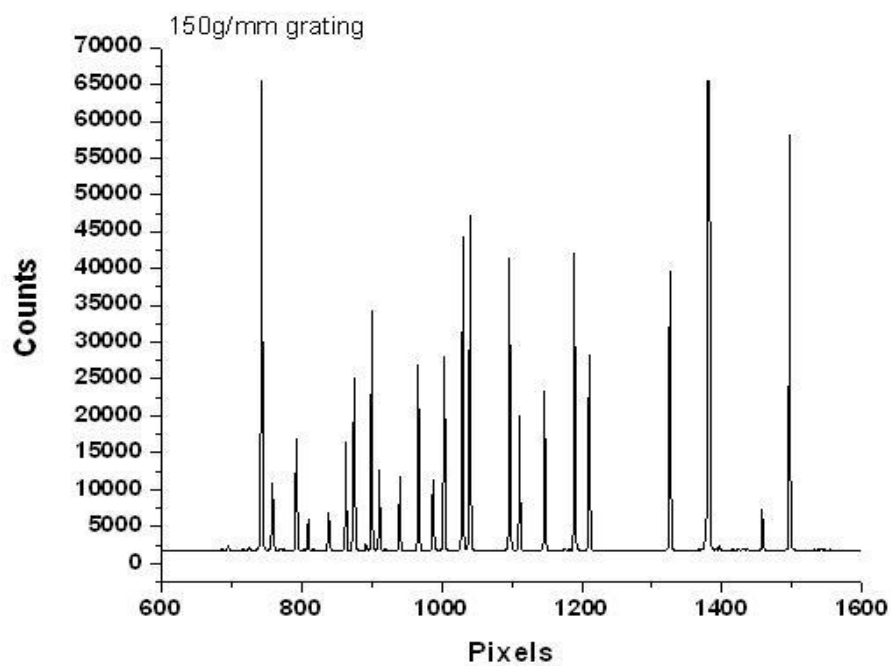
Figure 4.5. Linear fit of the neon spectra pixel data versus wavelength.
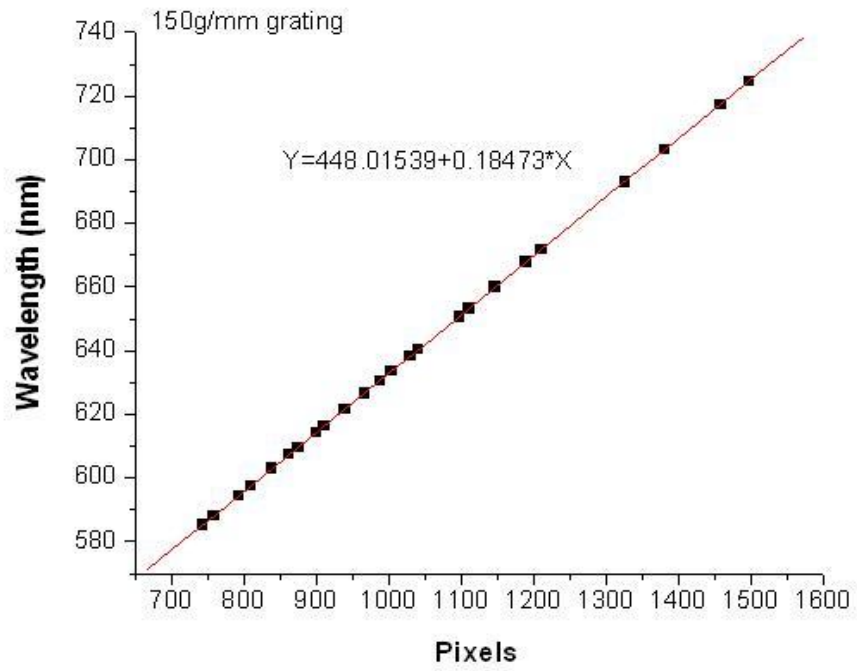
4.3.3.2 Spectral Analysis

The Raman spectra were analysed using Origin v. 7 (OriginLab, Northampton, USA). The average of the 20 Raman spectra for each individual cell and the dark current was subtracted from each average. The same procedure was adopted for the background spectra. The average background was then subtracted from the average Raman spectrum of the samples for fluorescence suppression. The main peaks of the Raman spectra for each clone were assigned by comparing them to the reference peaks based on (Notingher, 2007).

4.3.3.3 Multivariate Statistical Analysis

To achieve clonal classification, the Raman spectra were investigated using PCA. PCA extracts the relevant information from the original data and generates a new set of variables, called principal components (PC). This has been used to build an algorithm, based on the PCA scores to relate the Raman spectra findings, where the PC are related to the most important variation that occurs in all spectra, in this study they were PC3 and PC4. This was achieved by using prcomp function in the R package.

4.4   Results

4.4.1   Comparisons between Dental Pulp Progenitor Cell's Clones

Raman spectroscopy allowed vibrational characterisation of 3 clones; A31 at 18PDs and 60PDs, A11 at 8PDs and B11 at 7PDs, without staining. All spectra had been normalised to the area of the peak at 1450cm^{-1}, to enable the direct comparison of data (Chan et al., 2009). Figure 4.6 shows the Raman spectra of these clones in the spectral range 600 to 1800cm^{-1}. The spectra contains the typical Raman peaks assigned to DNA nucleic acids at 729, 789, 834, 858, 1092, 1167cm^{-1}, those assigned to proteins at 1245 and 1680cm^{-1}; and CH deformation at 1450cm^{-1}. Differences were found at 1056cm^{-1} assigned to RNA ribose C–O vibration, which was only visible with the clone A31 at 18PDs; and 958cm^{-1} assigned to phenylalanine. Comparing the different Raman spectra showed that the spectral intensity of A31 at 18PDs was much higher than A31 at 60PDs and the other clones (Figure 4.6). Table 4.2 shows in detail the bands present in each clone and Table 4.3 shows the

percentage of intensity of each band of A31 at 60PDs, A11 at 8PDs and B11 at 7PDs, compared with A31 at 18PDs. Taking selected band which are responsible for cell growth (Figure 4.7), it is clear that clone A31 at 18PDs has higher intensity peaks compared with the other clones.

PCA discriminated Raman spectra of DPPCs clones. In particular, PC3 and PC4 were used because they captured the most significant variance among the clones (Figure 4.8). The scatter plot using scores of PC3 and PC4 of the Raman spectra of the 3 DPPCs clones (A31 18PDs, A11 8PDs, B11 7PDs), in addition to A31 at 60PDs (Figure 4.9), demonstrates that A11 and B11 overlap almost exactly indicating that their Raman fingerprints are similar. A31 at 18PDs and A31 at 60PDs did not overlap at all, indicating a large difference in their fingerprints. Furthermore, both A31 populations are widely spread and do not overlap with A11 and B11, further confirming difference in their signatures.

Figure 4.6. Mean Raman spectra obtained from three clones (A31 at 18PDs, A11 at 8PDs and B11 at 7PDs) in addition to Raman spectra obtained for A31 at 60PDs. These spectra are displayed in the fingerprint range from 600 to 1800cm^{-1}. All data was detected as relative intensities in arbitrary units (a.u.). The strongly dominated bands have been highlighted and the corresponding wavenumbers given. The regions 1-5 are the main regions where the main differences between the clones were observed. All spectra have been normalised to the area of peak (1450cm$^{-1)}$) to enable fairer, robust- comparisons of data.
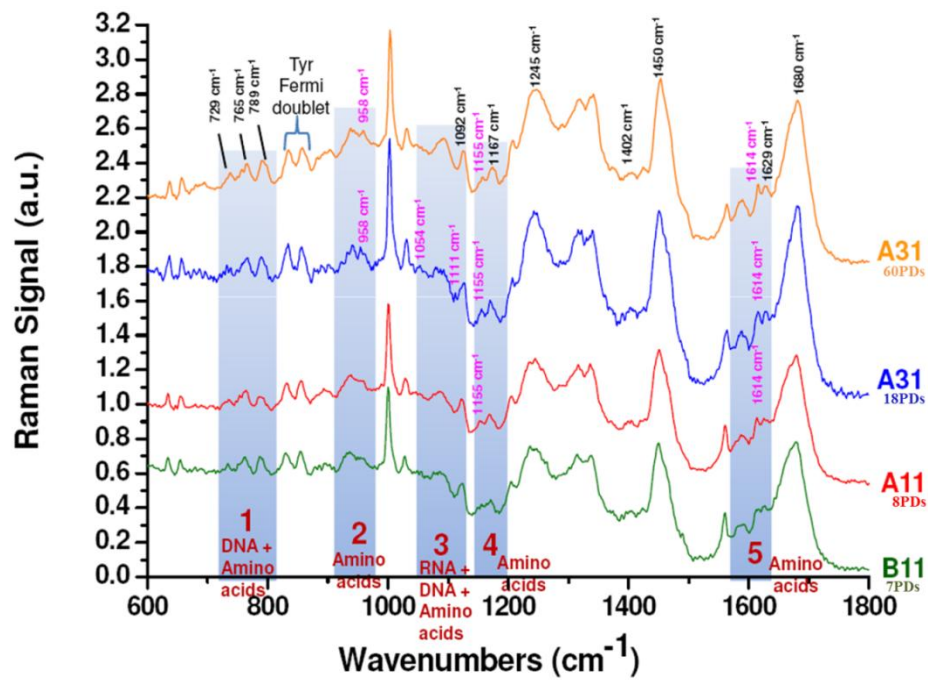
Table 4.2. Highlights of the dominating peaks with their assignments from Figure 4.6. The major differences with the high proliferating A31 clone at 18PDs were the presence of phenylalanine (958cm^{-1}) and RNA (1054cm^{-1}) which were not visible in A31 at 60PDs; or clones A11, and B11.

Wavenumber (cm^{-1})	A31 60PDs	A31 18PDs	A11 8PDs	B11 7PDs	Assignment	
729	√	√	√	√	Ring breathing of adenine (DNA)	1
765	√	√	√	√	Ring breathing Tryptophan (proteins)	
789	√	√	√	√	DNA backbone - PO$_2^-$ symmetric stretching	
834	√	√	√	√	Tyrosine ring breathing vibration	
858	√	√	√	√	Tyrosine Fermi resonance doublet with 834	
958	√	√			C-C stretching (phenylalanine)	2
1054		√			RNA ribose C-O vibration	3
1092	√	√	√	√	DNA PO$_2^-$ backbone symmetric stretching	
1111		√			Tyrosine	
1155	√	√	√		Tyrosine	4
1167	√	√	√	√	Isoleucine	
1245	√	√	√	√	Amide III (β-sheet, protein)	
1402	√	√	√	√	Cβ rocking (arginine)	
1450	√	√	√	√	C-H deformations vibr. (in all components of cell)	
1614	√	√	√		Tyrosine	
1629	√	√	√	√	Serine	5
1680	√	√	√	√	Amide I- C=O vibrations of polypeptide backbone	

Table 4.3. The percentage of intensity of major bands of A31 at 60PDs, A11 at 8PDs and B11 at 7PDs, compared with A31 at 18PDs, with their assignments. 1054 and 958cm⁻¹ bands were only detected in A31 at 18PDs.

Wavenumbers (cm⁻¹)	Assignment	Difference percentage compared to A31 at 18PDs
729	Adenine (DNA)	A31 at 60PDs ~ 6% lower A11 at 8PDs ~ 40.3% lower B11 at 7PDs ~ 39.9% lower
789	DNA	A31 at 60PDs ~ 10.2% lower A11 at 8PDs ~ 46.4% lower B11 at 7PDs ~ 31.3% lower
1092	DNA	A31 at 60PDs ~ 4.8% lower A11 at 8PDs ~ 30.2% lower B11 at 7PDs ~ 21.4% lower
1167	Isoleucine	A31 at 60PDs ~ 23.6% lower A11 at 8PDs ~ 25.7% lower B11 at 7PDs ~ 39.2% lower
1245	Amide III (β-sheet)	A31 at 60PDs ~ 23.8% lower A11 at 8PDs ~ 44.2% lower B11 at 7PDs ~ 45.4% lower
1402	Thymine	A31 at 60PDs ~ 48.3% lower A11 at 8PDs ~ 41.5% lower B11 at 7PDs ~ 35.8% lower
1450	Proteins and Lipids	A31 at 60PDs ~ 5.6% lower A11 at 8PDs ~ 31% lower B11 at 7PDs ~ 32.2% lower
1629	Serine	A31 at 60PDs ~ 40.2% lower A11 at 8PDs ~ 41.1% lower B11 at 7PDs ~ 51% lower
1680	Amide III	A31 at 60PDs ~ 15.2% lower A11 at 8PDs ~ 40.7% lower B11 at 7PDs ~ 39.3% lower

Figure 4.7. Highlights of the intensity of peaks responsible for cell growth, derived from Figure 4.6. Clone A31 had higher intensities for all of these peaks, compared to A11 and B11 clones.
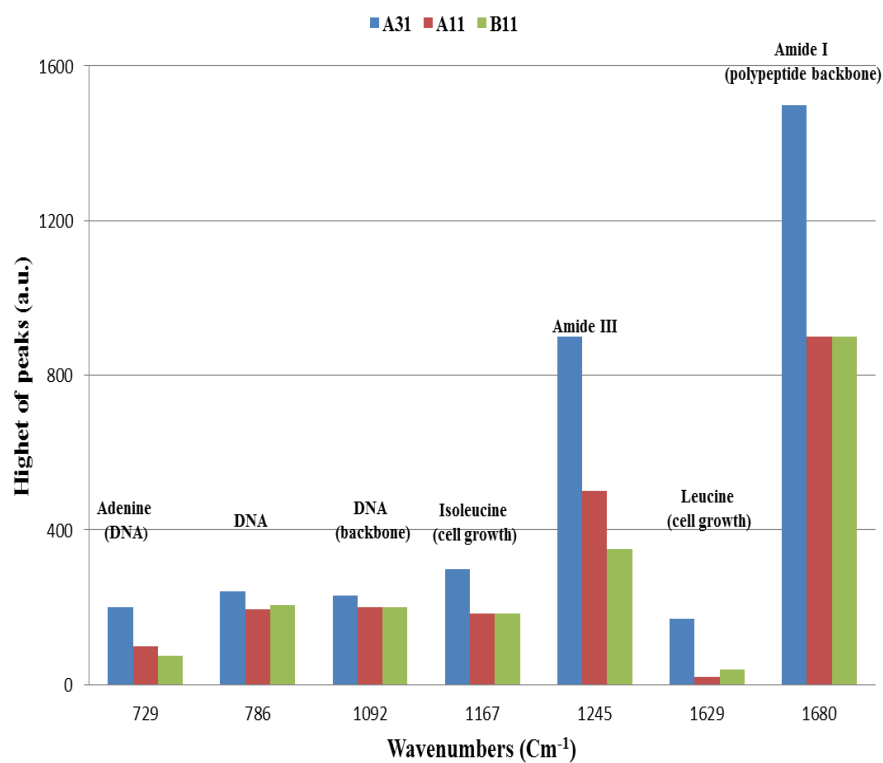
Figure 4.8. (A) PC3 and (B) PC4 of the Raman spectra showed the Raman contribution inter-sample variation, attributed to the cellular changes that distinguish the samples.

(A)

(B)
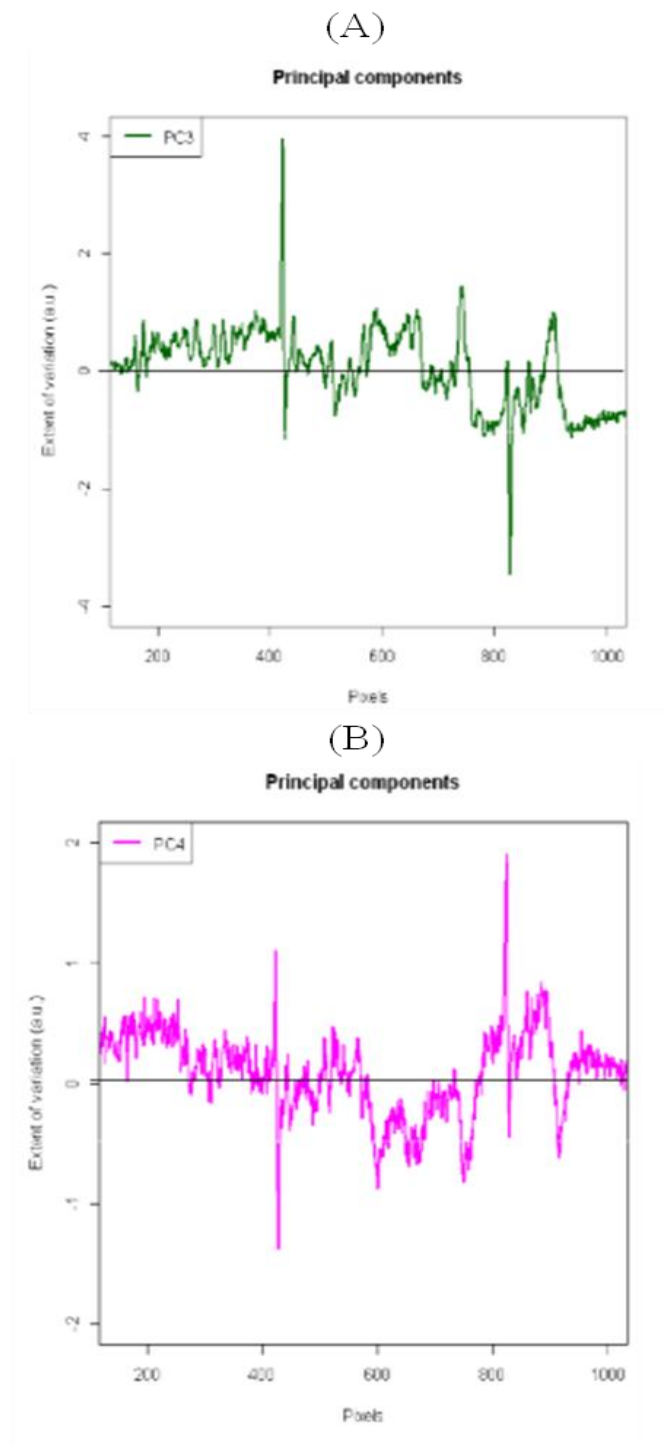
Figure 4.9. PCA dot plots were widely spread and showed three clearly distinguishable areas depicted as red and green (B11 and A11), blue (A31 at 18PDs) and orange (A31 at 60PDs).
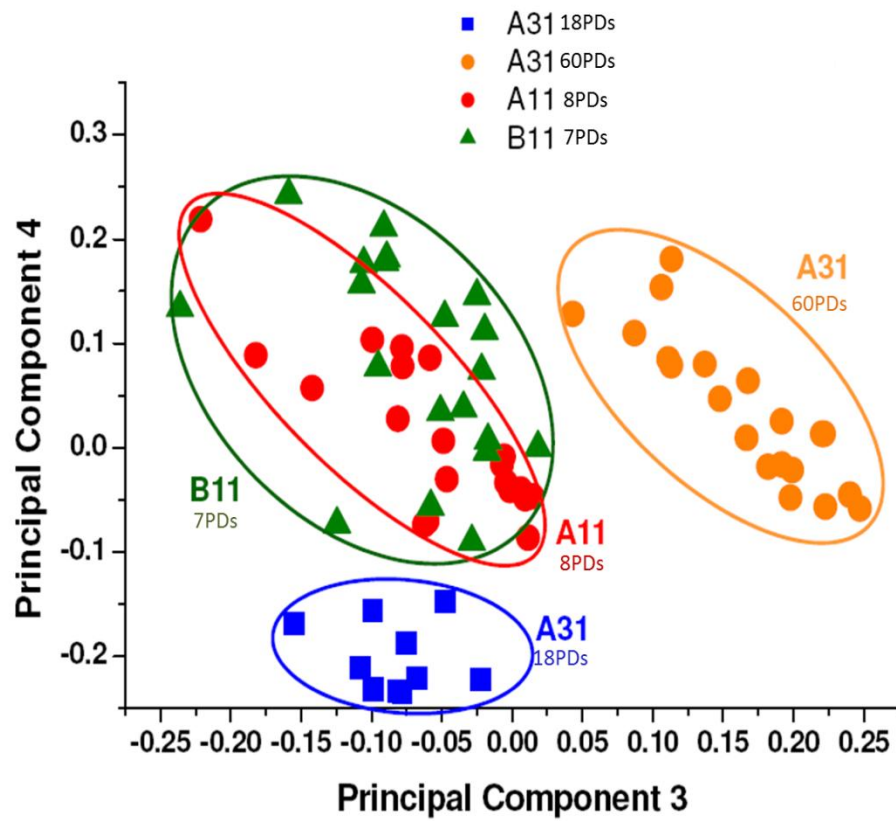
4.4.2 Comparisons between A31 Clone and Its Derivatives (Chondrocytes)

Raman spectroscopy also allowed the vibrational characterisation of clone A31 at 18PDs, before and after differentiation into chondrocytes. All spectra were normalised to the area of the peak at 1450cm^{-1}, to enable a fairer comparison of the data (Chan et al., 2009). Figure 4.10 shows Raman spectra of A31 and its derivative in the spectral region 600 - 1800cm^{-1}. The spectra show differences, where some peaks are present only in the progenitor (788cm^{-1} and 1095cm^{-1}), while other peaks were only observed in differentiated cells (chondrocytes). These included 945,1466, 1560, 1616 and 1730cm^{-1}. Table 4.4 shows in detail the presence of each band in each clone and to which biochemical compounds it refers.

Figure 4.10. Mean Raman spectra obtained for clone A31 at 18PDs and after chondrogenic differentiation. These spectra are displayed in the fingerprint range from 600cm^{-1} to 1800cm^{-1}. All data were detected as relative intensities in arbitrary units (a.u.). The strongly dominated bands have been highlighted with their numbers. All spectra were normalised to intensity of peak 1450cm^{-1} to enable direct comparison of data.
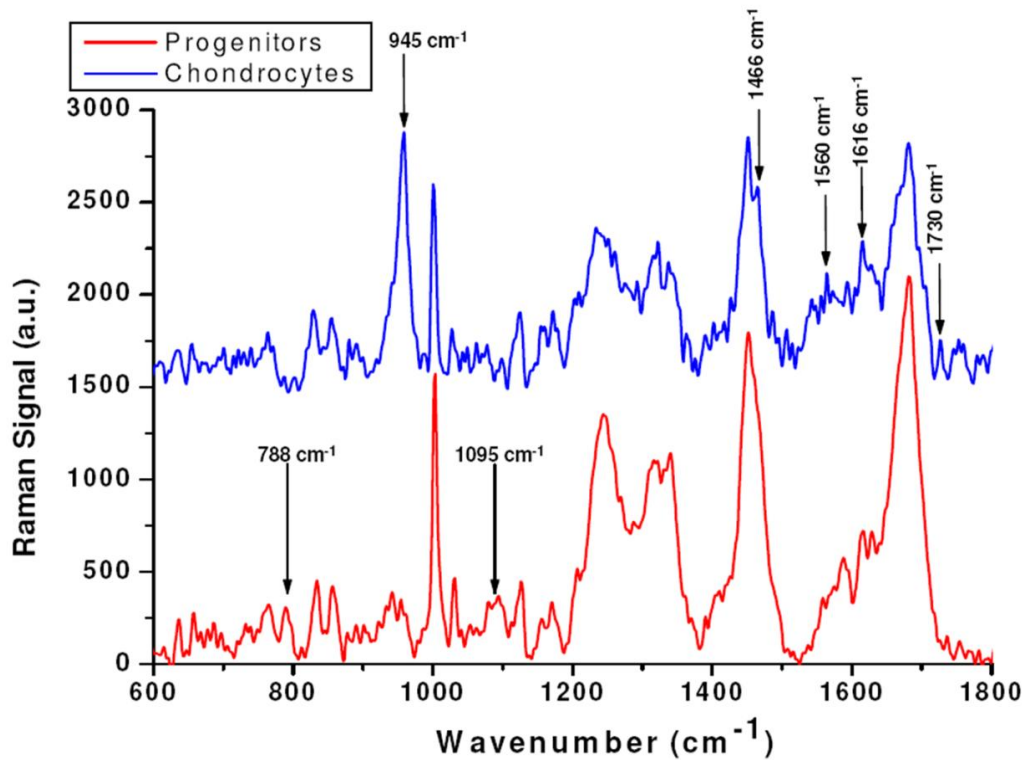
Table 4.4. Dominating peaks with their assignments from Figure 4.10. The major differences with undifferentiated clone A31 at 18PDs were the presence of DNA bands at 788 and 1094cm^{-1}, while chondrogenic differentiation showed the presence of protein bands at 945, 1466, 1560, 1616 and 1730cm^{-1}.

Wavenumber (cm^{-1})	Progenitor	Chondrocyte	Assignment
788	√		O-P-O str. DNA
945		√	C-C BK str. α-helix
1095	√		PO$_2^-$ str.
1466		√	CH def.
1560		√	C=C aromatic ring (Tyr, Trp)
1616		√	Amide I
1730		√	C=O ester

4.5   Discussion

For the first time, the differences between the DPPCs clones isolated from the same tissue is confirmed in term of intensity of peaks at specific waves number by Raman spectroscopy. These wavenumbers were based on DPPCs biochemical features which will help to discriminate between MSCs clones to identify best clones to use in tissue engineering.

The clinical use of stem cells in tissue engineering needs to develop criteria for distinguishing the best MSCs from other cells to be used for stem cell therapy. Currently, identification of MSCs needs an extensive *in vitro* expansion that may affect the behaviour of these cells (Harkness et al., 2012). Raman spectroscopy is a non-invasive, rapid and sensitive technique that has been used to investigate stem cell characteristics (Chan and Lieu, 2009; Downes et al., 2010). In this study, the possibility of using Raman spectroscopy as a sensitive method for quick identification of different clonal DPPCs has been investigated. Differences in spectral peak intensities were been observed between the clones.

Cell components consist mainly of water, proteins, nucleic acids, lipids and carbohydrates (Cooper, 2000). Differences in one or all of these components between cells may provide further evidence of their behaviour and ability to proliferate and differentiate. Cells can contain more than 1000 various molecules. These molecules include different sugars, amino acids, fatty acids, proteins and nucleic acids, where each one will have a specific fingerprint spectrum in the wavenumber range 400-1800cm^{-1}. This range contains virtually all of the basic vibrational information on a protein or nucleic acid molecule, which gives a promising potential to detect the different between clones in the shortest, non-invasive way possible (Thomas, 1999; Dukor, 2002; Swain and Stevens, 2007). These fingerprints may also probe chemical compositions and structural changes in tissues and cells in real-time. This could also help to discriminate ageing cells and dead cells (Chan et al., 2008).

In general, the results (Figure 4.6) showed that the Raman spectrum of each clone contains many bands, where each band represents a distinct molecular vibration. Over the range of Raman shifts shown, characteristic peaks include those

representing essential amino acids, such as adenine group vibrations around 729cm^{-1} ,tryptophan around 765cm^{-1}, tyrosine at 843cm^{-1}, isoleucine at 1167cm^{-1} , arginine at 1402cm^{-1} and serine at 1629cm^{-1}; which have all been found in the clones, including the later PD for clone A31. The existence of all these amino acids in each clones confirms that they are fundamental factors in building the cell components, such as DNA, RNA and proteins (Alberts et al., 2008). Little is known about the precise function of these amino acids on MSCs behaviour, such as proliferation and differentiation, but it appears that all the mentioned amino acids have a function on stem cell proliferation (Higuera et al., 2012). However, the intensity of these peaks was different between the clones (Table 4.3), which indicates different concentrations of these amino acids. These differences would appear to reflect differences in their proliferation. For example, serine was almost double in clone A31 at 18PDs compared to the other clones or the same clone at later PD. It has been found, that cells with higher serine content are also more active, as serine regulates cell proliferation in progenitor cells (Saito et al., 2012). Changes in the Raman spectra that can be accredited to differences in the proliferative status of the cells are clearly evident in Figure 4.6. These conclusions are supported by the results in Table 4.3, which demonstrated that for clone A31, the highly proliferative clone, a higher DNA content was observed, compared with the low proliferative clones, A11 and B11. Furthermore, Figure 4.7 highlighted the bands that may be involved in cell growth. It was clear that clone A31 has higher peaks than the other clones. It has been observed in rat liver cells that increasing DNA synthesis will stimulate cell proliferation (Abanobi et al., 1982). Furthermore, cells at later PD showed less DNA content than earlier PD for clone A31, to confirm DNA damage or loss in cells with ageing (Beckman and Ames, 1998).

Only the high proliferating clone A31 at early PD showed the presence of tyrosine at 1111cm^{-1}. Tyrosine was found in different wavenumbers as it exists in different isoforms. This finding was interesting as the role of tyrosine in stem cells has been suggested to maintain the undifferentiated state and the proliferation of progenitor cells (Anneren, 2008). As such, tyrosine could possibly be used as a marker for highly proliferative clones. In addition, phenylalanine was only found in the highly proliferative clone in both early and late PDs. Although the role of

phenylalanine has been described as inhibiting cell proliferation (Oberdoerster et al., 2000), phenylalanine is a precursor for tyrosine. This may indicate that phenylalanine is only converted to tyrosine in early DPPCs by phenylalanine hydroxylase, but not in later DPPCs. (Hernández et al., 2010; Müller et al., 2012). These findings could be linked to the decreased proliferation of late PD of clone A31, as oxidative stress increases with age and leads to defects in phenylalanine hydroxylase (Brouilette et al., 2003). For example, the disease called phenylketonuria, results from an increase of phenylalanine in the blood due to a defect in phenylalanine hydroxylase, which is accompanied with a increase in oxidative stress, and reduction in antioxidant defence (Vargas et al., 2011). Another notable difference was the representative Raman markers for RNA ($1054cm^{-1}$), which was only visible in A31 at early PD but not at later PD, and not shown at all in clones A11 and B11. This Raman marker may indicate the ability of a cells differentiation capacity, as only clone A31 at early PD underwent differentiation into 3 different lineages. As such, RNA delivers amino acids and is shown to have an influence in inducing differentiation of stem cells (Tan et al., 2011).

PCA was used to compare spectral features of the clones. It showed a separation between the highly proliferative clone (A31) and low proliferative clones (A11 and B11). PCA also demonstrated a separation between clone A31 at early PD and later in higher order PCAs (PCA3 and PCA4). This was apparent in (Figure 4.9), where clones A11 and B11 overlapped almost exactly suggesting that their Raman fingerprints are similar, even if they were isolated from 2 different patients. In contrast, clone A31 at early PD and late PD did not overlap at all, suggesting large differences in their fingerprints. Moreover, A31 at early late PD did not overlap with A11 and B11 clones, further confirming differences in their signatures. It is noteworthy that all clusters are reasonably compact, indicating good level of homogeneity in the data sets (i.e. Raman spectra of each data set are quite similar to each other). This method of characterization was compared with the population doublings and differentiation data from previous chapters to confirm that PCA can be effectively used as a quick, non-invasive method to discriminate between DPPCs and possibly other MSC sources.

Raman spectroscopy was also used to study the signature differences between the progenitor cells and their derivatives. In this case, chondrocytes were compared to their undifferentiated form for clone A31. Changes in the Raman spectra were observed. Results demonstrated that the protein level was higher and DNA level was lower in chondrocytes, compared to the undifferentiated progenitor cells. This was observed in the Raman spectra (Figure 4.10) by the presence of prominent protein bands in the chondrocytes including amide I (around 1660cm-[1]), CH_2 (around 1466cm-[1]) and a-helix (935cm[1]) (de Mul et al., 1984; McManus et al., 2011), in addition to presence of prominent DNA bands in progenitor cells at 788cm[1] and 1095cm[1] peaks (de Mul et al., 1984). These results confirm that the relative amount of protein is higher following chondrogenic differentiation (McManus et al., 2011). This means that this technique can be used to confirm DPPCs differentiation.

This study showed that Raman spectroscopy is a quick method which can discriminate between clones, based on their biochemical features to select of the ideal clone for tissue engineering as several recent studies have demonstrated that Raman activated cell sorting is achievable (Chan et al.,2009). The PCA technique was also successful in achieving clonal classification, which matches with the results of other methods in the previous chapters. In addition, the results presented here show that Raman spectroscopy can be used to detect biochemical changes that occur as a result of changes in differentiation, which make it easier to distinguish between MSCs and their derivatives, especially that there are no specific markers to sort these cells out from their neighbours.

Chapter 5:

Type I Collagen Gel Interaction with DPPCs

5.1   Introduction

The extracellular matrix (ECM) plays a critical role in regulating stem cell functions that includes proliferation, migration, and differentiation into different lineages (Campbell et al., 1985; Flaim et al., 2005; Kihara et al., 2006). ECM remodelling is regulated through synthesis and degradation. ECM components play an important role in regulating mechanical properties of the ECM, and consists of intrinsic matrix proteins such as collagen (*e.g.* types I, II, III and IV), glycoproteins (fibronectin and laminin), proteoglycans (aggrecan, decorin, and biglycan), and elastin (Jean et al., 2011). Collagen type IV is essential for basement membrane stability (Pöschl et al., 2004). The dental pulp contains a progenitor stem cell population that is vital for the repair of the tissue. Dental pulp progenitor cells (DPPCs) exist within and interacts with the ECM. Many studies however, investigate the potential of cultured progenitor cells *in vitro* without considering the ECM role during expansion. Collagen gel could provide a unique way to study the interaction of DPPCs with the ECM such as the effect of collagen contraction and its influence on cell proliferation and morphology, which is not possible in routine cell culture surfaces. The collagen status (attached and detached) is found to have important roles in fibroblast proliferation (Butt et al., 1995; Riddle et al., 2005; Yamamoto et al., 2005; Stops et al., 2010), chondrogenic differentiation (Steward et al., 2013), and controlling fibroblast shape and alignment (Eastwood et al., 1998). The ECM interacts with cells physically and functionally *via* cell surface receptors such as integrins, which provide the ECM-cell link (Desgrosellier and Cheresh, 2010). These integrins can also activate matrix metalloproteinases (MMPs) that have major roles in ECM remodelling (Deryugina et al., 2001). Such ECM remodelling plays an important role in disease progression (Messent et al., 1998). Seeding DPPCs in collagen gels will hopefully contribute towards a better understanding of the behaviour of DPPCs during different environmental conditions, such as quiescent conditions within the niche, or pulpal inflammation.

5.1.1 Collagen

Collagens are the most abundant family of proteins in the human body and the major structural element in connective tissues. They provide strength and structural integrity for tissues. Collagen is composed of a triple helix of three polypeptide chains. Each of the 3 α chains forms an extended left handed helix, supercoiled around a central axis in a right handed manner and stabilised by interchain hydrogen bond. The amino acid composition of the three α chains is either identical or different, depending on collagen type. Each α chain is 300nm in length and contains approximately 1000 amino acids, which is characterised by repetitious polypeptide chains, glycine-X-Y, where X and Y position is often occupied by proline and hydroxyproline (Gelse et al., 2003).

There are 28 types of collagens which have been identified in the human body so far. Types I, II, III and V collagen are the main types that compine the essential collagen components in bone, cartilage, tendon, skin and muscle (Smith and Rennie, 2007). Collagen type I is the most well-known type of collagen. It is the major form of organic mass in bone and the main types of collagen in tendon, skins, ligaments, cornea and other tissues. In bone, it provides load bearing, tensile strength and stiffness (Gelse et al., 2003). Collagen type I is the major fibrous component in the dental pulp with addition to collagen type III (Linde, 1985). Furthermore, collagen type I regulates dental pulp cells gene expressions. e.g. it down-regulate dentin matrix protein-1 (Dmp-1) and up-regulates osteocalcin mRNA levels (Mizuno et al., 2003).

Culturing cells in collagen gel is not a novel idea. In 1972, Elsdale and Bard cultured fibroblast cells in a model of collagen matrices (Elsdale and Brad, 1972). These 3D collagen gels induced morphological changes in the fibroblasts that mimicked cell morphology *in vivo*. Since then, collagen gels became the favourite choice to provide possibly the most physiological and biomimetic environment in which stromal cellular function can be studied (Lee et al., 2011). Other advantages of collagen gel: biocompatibility, adhesion, suturable, highly porous, combination with other material such as demineralised bone powder, transuded by fluid pressure, (Glowacki J, Mizuno, 2008) and collagen fibrous network, allows researchers

excessive use in tissue engineering. In addition, with the surrounding medium fluid, cells are permitted to migrate and interact with each other naturally as they would within the ECM (Lee et al., 2011). Collagen gels have already been approved for use as tissue engineered skin in clinics (Trent and Kirsner, 1998). Additionally, cultured MSC's collagen gels enhanced osteogenic differentiation, showing better result than fibrin glue and alginate as substrate (Oh et al., 2012). In this chapter, collagen type I gel will be utilised for the culture and assessment of DPPCs in term of cell morphology and matrix metalloproteinases (MMPs) production.

Cell characteristics such as morphology, signalling and proliferation, within collagen matrices, vary depending on the physical state of collagen such as mechanical stress. Fibroblasts within stressed collagen develop isometric tension and contract once the gels are detached, which provides a similar model to wound contraction. In contrast, fibroblasts in attached, stressed gels tend to proliferate, whereas cells in relaxed gel became quiescent which may be explained by reducing signalling through extracellular-signal-regulated kinase (ERK) (Cukierman et al., 2002).

5.1.2   Matrix Metalloproteinases (MMPs)

ECM remodelling plays a vital role in many cellular events, such as cell migration, proliferation and development. It also plays a role in the pathological events, such as inflammation and wound healing (Vargova et al., 2012). ECM degradation occurs through the actions of different groups of proteolytic enzymes, classified based on their structure and catalytic mechanism. These enzymes are MMPs, serine proteinases, cysteine proteinases and aspartic proteinases, which are produced by many types of cells (Barrett et al., 1998). Although collagen is resistant to most proteolytic enzymes and has a long half-life *in vivo*, MMPs produced by many cells such as fibroblasts and odontoblasts in many events such as participate in dentin matrix organisation or even dental caries that leads of degrading collagen type I (Hannas et al., 2007; Sabeh et al., 2009). MMPs are a family of zinc-dependent enzymes which collectively can degrade almost all major ECM components (Kähäri and Saarialho-Kere, 1997) . There are over 24 members of the MMP family recognised in humans (Lee and Murphy, 2004). All MMPs members have a pro-

domain and a catalytic domain. MMPs are generally secreted as inactive enzymes until the propeptide has been removed by proteolysis. During proteolytic activation, the pro-domain is first cleaved generating an MMP intermediate, which is followed by cleavage of the remnants of the prodomain by the MMP intermediate itself, or by other active proteinases, generating the fully active MMP (Lee and Murphy, 2004).

MMP activation and inactivation is regulated by a number of factors, such as the expression of inflammatory cytokines, growth factors and tissue inhibitors of MMPs (TIMPs) (Dasu et al., 2003). Mechanical force also plays a role in the regulation of MMP expression, where a relationship between actin cytoskeletal organisation and MMP-2 activation has been found through the regulation of the membrane-tethered metalloenzyme (MT1-MMP) (Sanka et al., 2007). Collagenases (MMP-1, MMP-8 and MMP-13) together with gelatinases (MMP-2 and MMP-9) can degrade collagen, in addition to being able to activate growth factors and other MMP zymogens (Shiomi et al., 2010). Like all MMPs, gelatinases need to be activated by proteolytic removal of the N-terminal proenzyme domain. For pro-MMP-9, activation occurs by cleavage through soluble proteinases, such as MMP-3 and plasmin, while pro MMP-2 is converted to its active form by a mechanism mediated by TIMP-2 and MT1-MMP (Ries et al., 2007). Human MSCs travel from their niche in response to different stimuli, such as injury, via type I collagen. Invasion of collagen is performed by secreting MMP-2 that is activated by MT1-MMP (Lu et al., 2010).

5.2   Aims

The objective of this chapter was to determine whether collagen matrices will act as a native ECM environment for DPPCs by assessing proliferation, morphology and MMPs production by seeded high and low proliferative DPPCs.

5.3   Materials and Methods

5.3.1   Preparation of Gelatinase-Free, Foetal Calf Serum

Gelatinases, MMP-2 and MMP-9, were removed from foetal calf serum. Briefly, gelatin Sepharose 4B (GE Healthcare, Amersham, UK), was added to foetal calf

serum at a ratio of 1:5; and mixed for 18 h at 4°C. Following centrifugation at (1000g/5 min), supernatants were removed from the gelatin Sepharose pellet and sterilised through 0.22µm membrane filter (Elkay, Basingstoke, UK) (Azzam and Thompson, 1992).

5.3.2 Preparation of 3D Collagen Matrices and Culture

Equal volumes of αMEM (Invitrogen, Paisley, UK) were added to the same amount of type I rat tail collagen (First Link, Wolverhampton, UK) to make up 1mg/ml concentration of collagen. This solution was neutralised by the drop wise addition of 5M sodium hydroxide until a change of colour (yellow to pink). Subsequently, 1ml of the collagen mixture was poured into each well of 12-well plate and left at 37°C, 5% CO$_2$ for 45 min for the collagen matrices to solidify. After detachment, DPPCs clones (A31, A11) at different population doubling levels (PDs) were suspended in αMEM, containing 20% gelatinase-free, foetal calf serum. Cells at 5x10^4/ml gelatinase-free, αMEM were added to the collagen matrices that already were made in the 12-well plates. For detached collagen gels, collagen was detached using a filter tip.

The degree of lattice contraction was quantified from 3 separate lattice diameter measurements performed on each of the 3 replicate samples, at days 1, 2, 4, 6, and 12. The average collagen contraction values obtained were expressed as % reduction in matrices diameter, compared to the matrices diameters, at 0h. Conditioned medium surrounding the matrices was also collected from each individual well for the analysis of gelatinase production and activity at the same time-points as the matrices measurements.

5.3.3 Cell Morphology Using Light and Fluorescence Microscope

Cellular morphology was compared in different types of culture conditions (plastic surface attached collagen and detached collagen) by light microscopy with serial images captured using a digital camera (Canon PC1234, Japan). The actin cytoskeleton of cells was stained with phalloidin-FITC (Sigma-Aldrich, Poole, UK) to determine cellular morphology. The cells were washed with phosphate buffered saline (PBS) and fixed with 1ml/well 4% paraformaldyhyde (PFA, Santa Cruz,

Dallas, USA) and incubated for 10 min at room temperature. The PFA was aspirated and washed twice with 1ml/well PBS at 5 min interval. The PBS was aspirated before the cells were treated with 1ml/well 0.3% Triton-X100 (Sigma-Aldrich) for 30min, with gentle shaking at room temperature. The Triton-X100 was aspirated and the cells washed twice with Tris-buffered saline (TBS, pH7.5). The cells were blocked with 1ml/well of 1% fraction V bovine serum albumin (BSA, Fisher Scientific, Loughborough, UK) in TBS (1% BSA-TBS) for 1 h at room temperature with gentle shaking. The blocking buffer was removed before the addition of 1ml/well Phalloidin-FITC (20μg/mL, Sigma-Aldrich) in 1% BSA-TBS; and incubated for 1 h at 4°C with gentle shaking and under darkness. The stain was aspirated and cells washed twice with 1ml/well TBS at 5 min interval. Images were captured using an ultra violet (UV) microscope (Olympus AX70 with a Digital Eclipse DXM1200 digital camera attachment, Tokyo, Japan). The images were captured using the Automatic Camera Tamer (ACT-1) control software (Nikon Digital, Tokyo, Japan) at 373nm/456nm (FITC).

5.3.4   Scanning Electron Microscopy (SEM)

The morphology of the collagen scaffolds was captured in collaboration with Nafiseh Badiei (Swansea University) using a Hitachi S4800 Scanning Electron Microscope (Hitachi, Japan) operated at 10kV. To prepare the sample for SEM, collagen gels were fixed with 2.5% glutaraldehyde (Agar Scientific, Stansted, UK) in 0.1M Cacodylate buffer for 2 h at room temperature and then washed 3 times with 0.1M Cacodylate buffer. The fixed samples were dehydrated in a graded ethanol series: 30%, 50%, 70%, and 100% for 15 min each and finally allowed to dry overnight. The dried hydrogels were sputter-coated and SEM images were taken at multiple locations across the sample.

5.3.5   Determination of Cell Numbers Within Collagen Lattices

DPPCs were recovered at days 1, 2, 4, 6 and 12 from 4 collagen matrices by enzymatic degradation as previously described by Stephens et al. (1996). Lattices were solubilised by incubation for 120 min at 37ºC with 400 μL of PBS containing 2 mg/mL Collagenase A.   This was followed by incubation with 100 μL of 0.05% (w/v) Trypsin/0.53mM EDTA for 20 min at 37ºC.   The cells were recovered by

centrifugation and viable cell numbers determined using a 0.02% (w/v) Trypan Blue solution, and a direct counting was undertaken in a Neubauer haemocytometer.

5.3.6 Assessment of Matrix Metalloproteinase Activity

To measure the relative amount of pro- and active- MMP-2 and -9 produced by 2 different DPPCs clones at early and late PDs, gelatin zymography was performed (Stephens et al., 2004). Equal volumes (25μl) of conditioned medium mixed with same volume of loading buffer (Table 5.1) were separated by SDS-polyacrylamide gel electrophoresis (SDS-PAGE) on pre-cast 10% gelatin zymography gels (Ready Gel 10% Gelatin Zymogram Gels, Bio-Rad Laboratories Ltd, Hemel Hempstead, UK). The gel was run at 20mA (Bio-Rad Mini-Protean 3 Electrophoresis Cell). SDS was removed from gels by washing in 2.5% Triton X-100 solution (Sigma), at room temperature, for 1h. MMPs were activated by incubation in Activation buffer (Table 5.1), at $37^{o}C$ overnight. Gels were stained with 0.05% Coomassie Blue (Table 5.1), destained in Destaining solution (Table 5.1) and gel images captured by using a Scanjet 3300c (Hewlett-Packard, USA). The relative amounts of pro- and active- MMP-2 and MMP-9 was confirmed by the appearance of clear bands at comparable molecular weights to MMP-2 and MMP-9 standards.

5.3.7 MMPs Data Analysis

To convert the intensity of each band of MMPs into quantitative data (numbers), the gel zymography images were opened using image J software. Each band was selected and then density of the band was calculated. Each process was performed on 3 separate occasions. The average values and standard error of mean (SE represented as ±) were determined using Microsoft Excel. Samples were compared using analysis of variance (ANOVA). *p-values* below 0.05 were considered statistically significant at a 95% confidence interval by using GraphPad InStat3 software.

Table 5.1. Gelatin Zymography Solutions

Running Buffer (x5, stock solution; 2000mL) Adjust pH to 8.3 with HCl. When required, stock solution was diluted 1:5 with ddH$_2$O.	Reagent	Amount
	Tris (Sigma)	30.2g
	Glycine (Sigma)	188g
	SDS (Sigma)	10g
	ddH$_2$O	2000mL

Loading Buffer (200mL) Adjust to pH 6.75 with HCl. Dilute to 200mL with ddH$_2$O.	Reagent	Amount
	Tris (Sigma)	1.15g
	Glycerol (Sigma)	20mL
	ddH$_2$O	35mL
	SDS	4g
	Bromophenol Blue (Sigma)	0.002g

Activation Buffer (1000mL) Adjust pH to 7.8 with HCl.	Reagent	Amount
	Tris (Sigma)	6.06g
	Calcium Chloride (Sigma)	0.74g
	Sodium Chloride (Sigma)	8.8g
	ddH$_2$O	1000mL

Coomassie Blue (stock solution; 500mL)	Reagent	Amount
	Methanol (Fisher Scientific)	250mL
	ddH$_2$O	250mL
	Coomassie Blue (Sigma)	1.25g

Coomassie Blue (working solution; 250mL)	Reagent	Volume (mL)
	Coomassie Blue stock solution	50
	Methanol (Fisher Scientific)	88
	Glacial acetic acid (Fisher Scientific)	24
	ddH$_2$O	88

Destain solution (1000mL)	Reagent	Volume (mL)
	Methanol (Fisher Scientific)	50
	Glacial acetic acid (Fisher Scientific)	75
	ddH$_2$O	875

5.4 Results

5.4.1 Cellular Proliferation

The average values gained for DPPCs clonal (A11 at 17PDs and A31 at 30PDs and 80PDs) proliferation upon culture over 12 days for cells cultured in attached collagen (Attached), detached collagen (Detached) and on the surface of 12-well plates (Monolayer), are shown in Figure 5.1. For attached collagen, all the DPPC's clones had similar numbers of cells for the first 4 days, approximately $7x10^4$ cells/well. After 4 days, A31 cells at 30PDs and A11 at 17PDs began to proliferate until they reached approximately 20 $x10^4$ by day 6. At day 12, both A31 (30PDs) and A11 (17PDs) cells decreased in number, with A11 showing a greater tendency to decrease than A31 (30PDs). A31 (80PDs) did not show proliferation during the 12 day culture period. On detached collagen gel, A11 and A31, both at early and late PDs, did not show a significant increase in cell number during the 12 day period. In monolayer culture, the three progenitor clones showed similar trends of cell number as with the attached collagen, with the exception that A31 (30PDs) at day 12 remained nearly the same as the cell number at day 6. Further investigation using ANOVA (Table 5.2) showed that a significant differences on cell numbers of clone A31 early PD (30PDs) and late PD (80PDs) when cells cultured on monolayer and or on attached collagen with p value <0.05 after 6 days of culture while there were no significant differences between the different clone (A11 and A31), (p value > 0.05).

Figure 5.1. Number of clonal cells (A11 at 17PDs, and A31 at 30PDs and 80PDs) on A) attached collagen, B) detached collagen, and C) monolayer, over 12 days in culture (N=3, average ± SE). After 4 days, cell numbers on A and C started to increase while B demonstrated no change in cell number over 12 days in culture.

A-) Attached

B-) Detached

Legend: A11 17PDs ◆ — A3130PDs ■ — A31 80PDs ▲
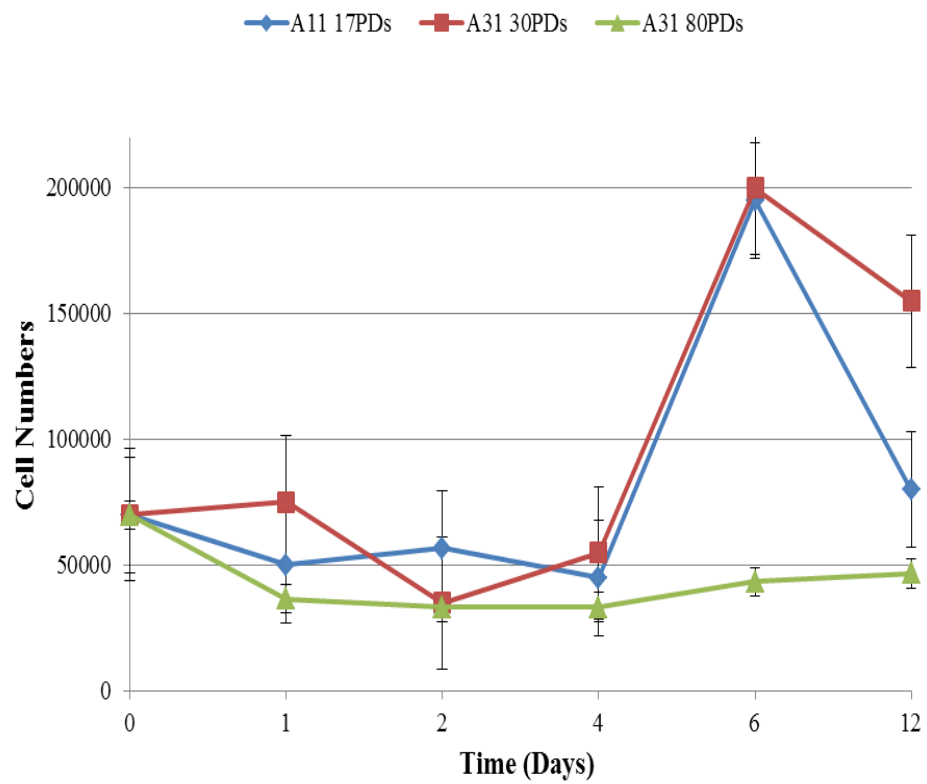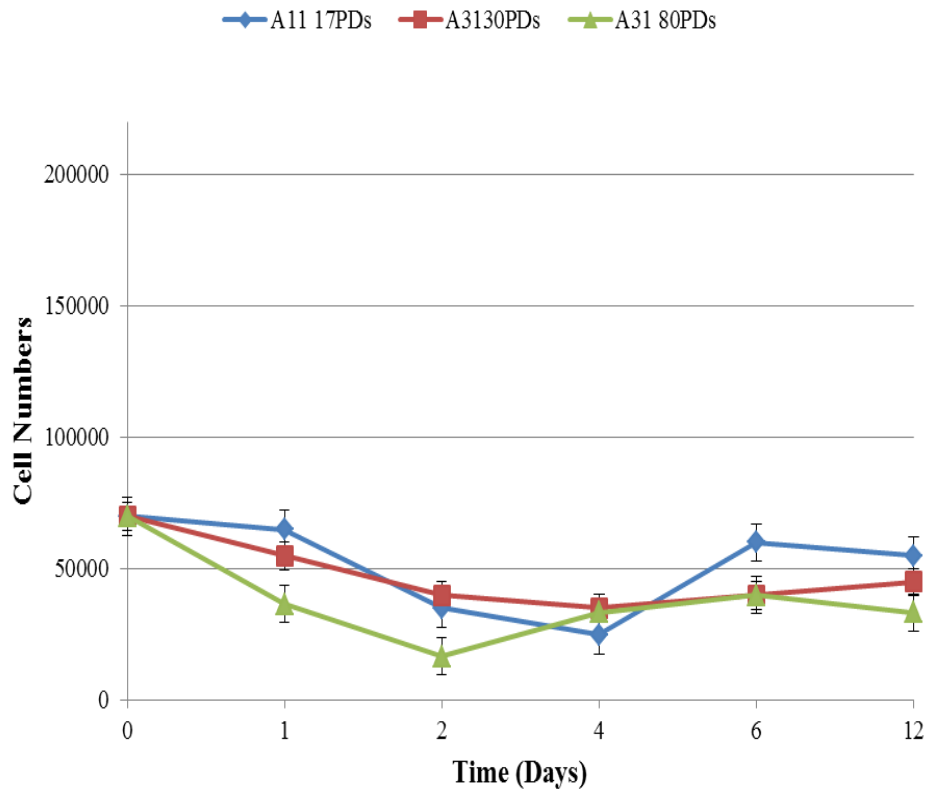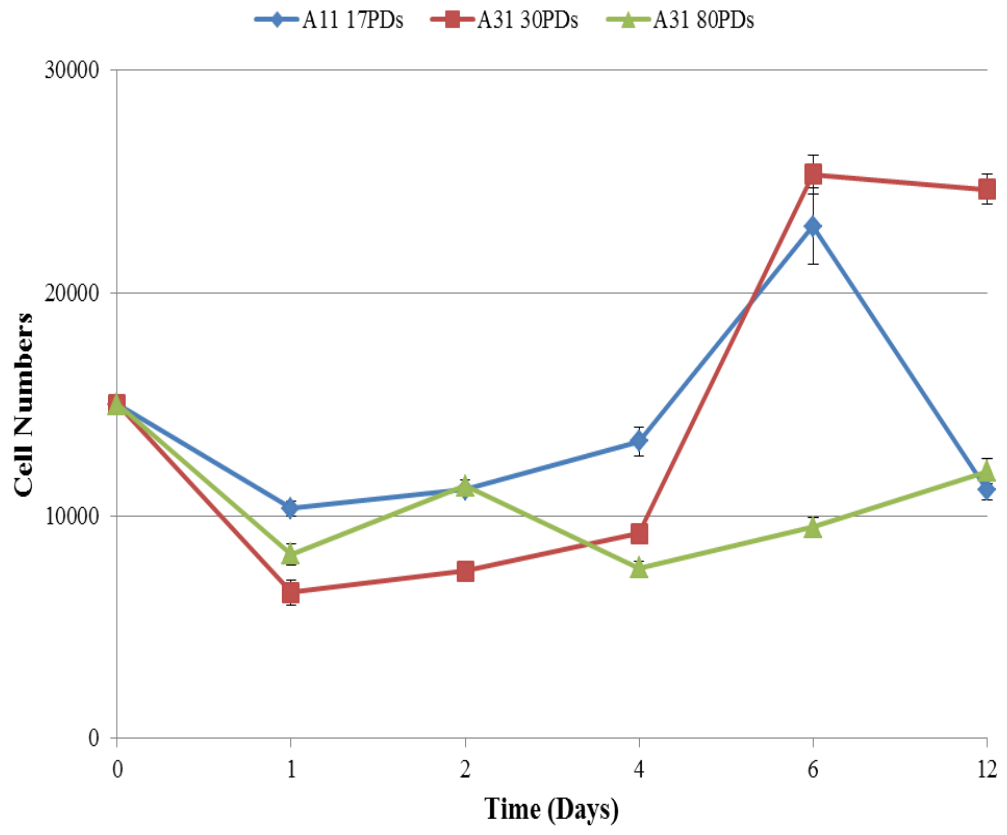
C-) Monolayer

Table 5.2. Sums of significant p values for cell numbers from Figure 5.1. comparing clone A31 at 30PDs in 3 different culture (monolayer, attached and detached collagen gel) with clone A31 at 80PDs and clone A11 at 17PDs in the same culture condition over 12 days. * = p<0.05, non-significant (ns) = p>0.05.

		Monolayer A11 17PDs	Monolayer A31 80PDs	Attached A11 17PDs	Attached A31 80PDs	Detached A11 17PDs	Detached A31 80PDs
Day1	Monolayer A31 30PDs	ns	ns				
	Attached A31 30PDs			ns	ns		
	Detached A31 30PDs					ns	ns
Day2	Monolayer A31 30PDs	ns	ns				
	Attached A31 30PDs			ns	ns		
	Detached A31 30PDs					ns	ns
Day4	Monolayer A31 30PDs	ns	ns				
	Attached A31 30PDs			ns	ns		
	Detached A31 30PDs					ns	ns
Day6	Monolayer A31 30PDs	ns	*				
	Attached A31 30PDs			ns	*		
	Detached A31 30PDs					ns	ns
Day12	Monolayer A31 30PDs	ns	ns				
	Attached A31 30PDs			ns	ns		
	Detached A31 30PDs					ns	ns

5.4.2   Cellular Morphology

For cell morphology, A31 (30PDs) and A11 (17PDs) cells in attached and detached collagen did not exhibit any morphological differences, compared to cells in monolayer (Figure 5.2). There were also no morphological differences between cells cultured in monolayer surface and the attached collagen, following staining with phalloidin-FITC (Figure 5.2A and B, respectively). Cells under both conditions exhibited very clear actin filaments with fibroblastic appearance, while cells cultured on detached collagen appeared to lose the fibroblast appearance with less prominent actin filaments (Figure 5.2C).

The microscopic structure of acellular collagen gels obtained by SEM showed a fibrillar network consisting of cross-linked fibers (Figure 5.3). The SEM analysis of A31 (30PDs) cells on collagen gels obtained showed that these cells attached to the collagen fibre at day one (Figure 5.4A) and showed better representative example of cells interacting with collagen matrices after 12 days, by demonstrating entanglement of matrix fibrils with cell extensions and putting out pseudopodia-like outgrowths (arrowed) (Figure 5.4B).

Figure 5.2. Phalloidin-FITC actin cytoskeletal staining for clone A31 at 30PDs in monolayer culture (A), attached collagen (B), and detached collagen (C). ×10 Magnification. Scale bar 500μm.

(A)
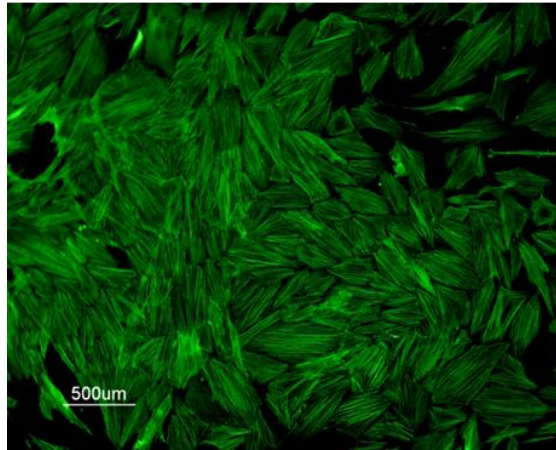
(B)
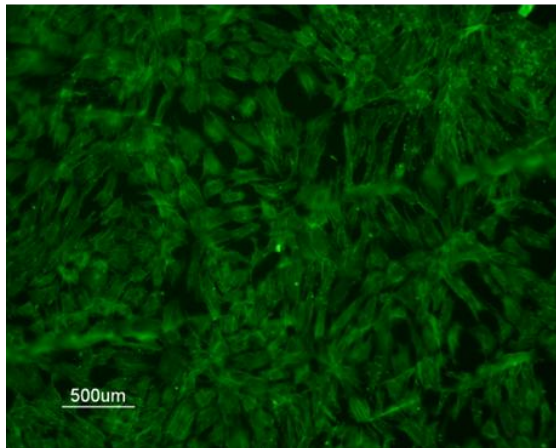
(C)
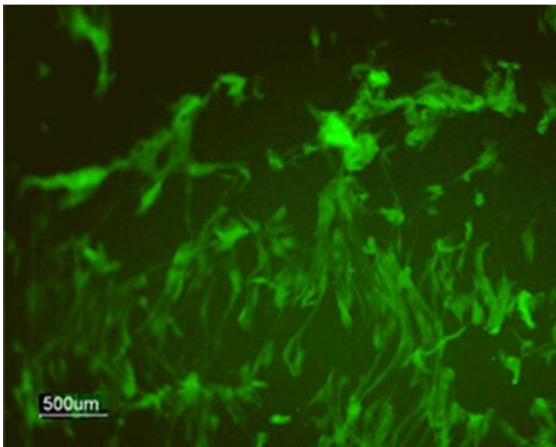
Figure 5.3. SEM images of control acellular collagen gels. The collagen fibrillar meshwork is clearly visible. Images are shown in different magnifications (A) x1100, (B) x4000, (C) x10,000 and x (D) 15,000).
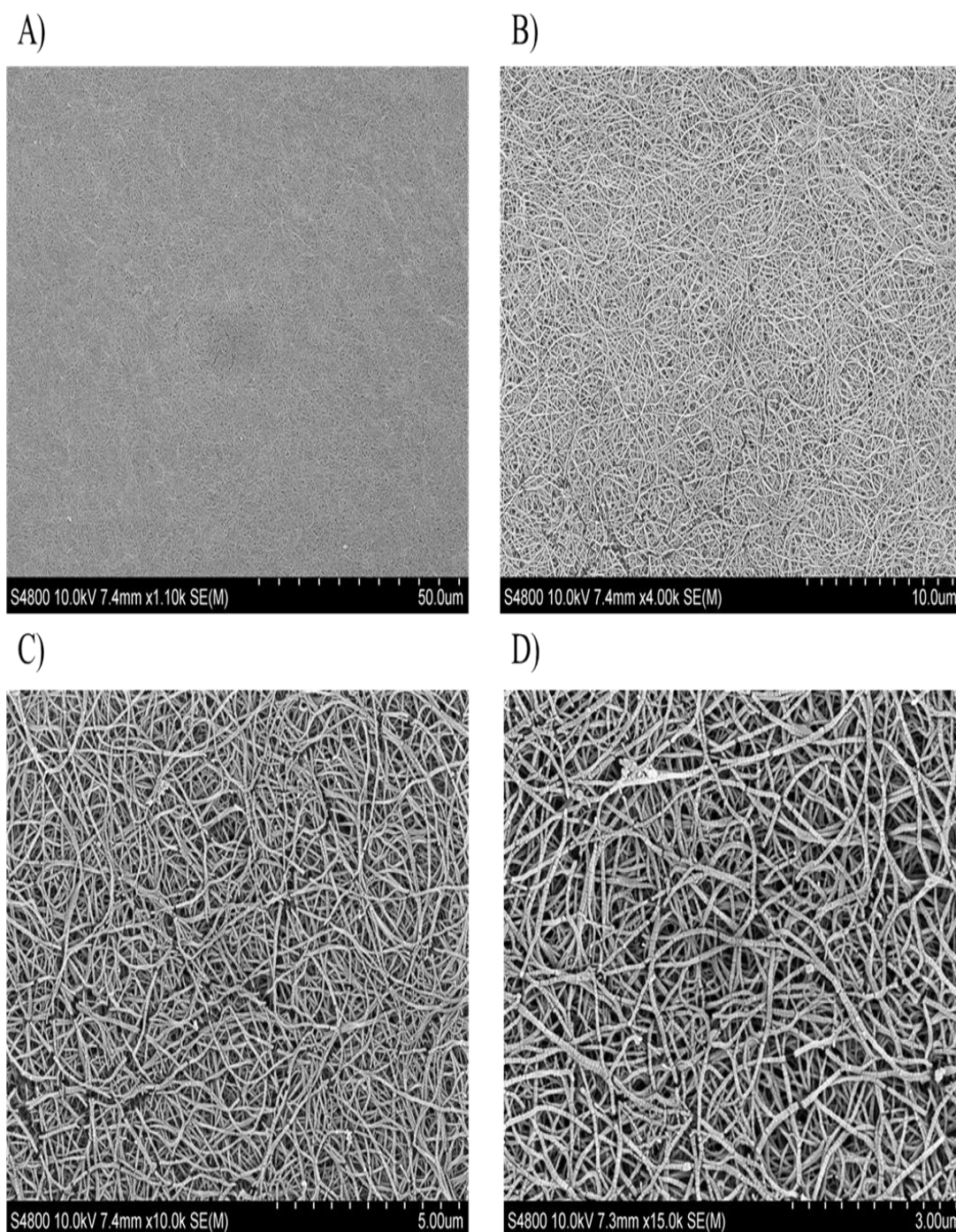
Figure 5.4. SEM images of clone A31 30PDs seeded in collagen gel after 1 day (A) and 12 days (B). pseudopodia-like outgrowths arrowed. Images are shown in different magnifications.

A) x700

S4800 10.0kV 7.4mm x700 SE(M)   50.0um

A) x2500

S4800 10.0kV 7.5mm x2.50k SE(M)   20.0um

B) x1100

S4800 10.0kV 9.5mm x1.10k SE(U)   50.0um

B) x3500

S4800 10.0kV 9.5mm x3.50k SE(U)   10.0um
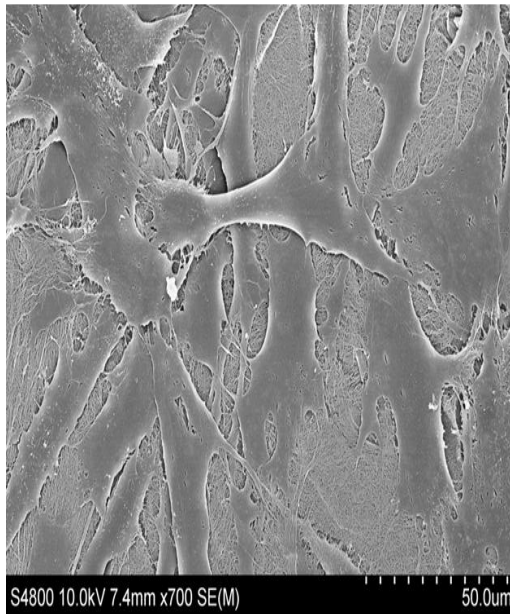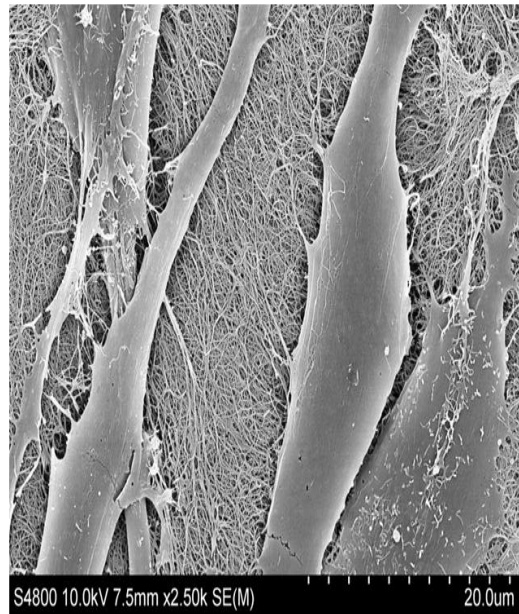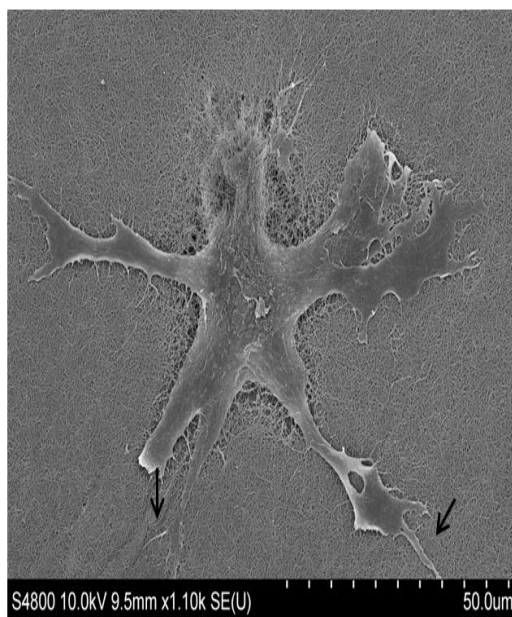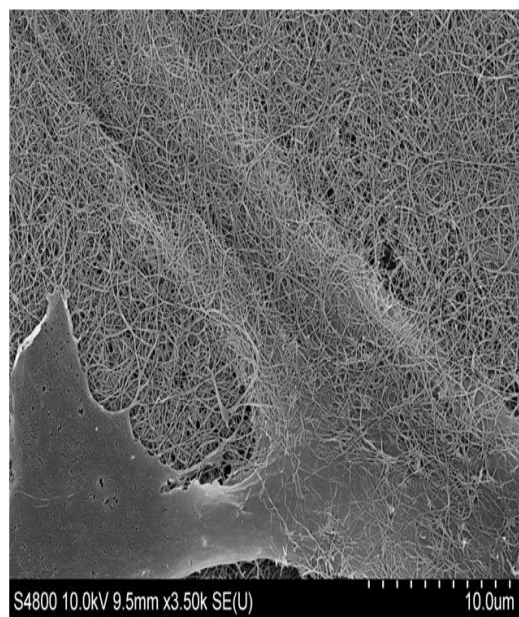
5.4.3   Collagen Gel Contraction

Collagen gel contraction images for clone A31 (30PDs) over 12 days in culture are shown in Figure 5.5.   Average collagen gel contraction values, expressed as % reduction in gel diameter, for DPPCs clones for 12 days period are shown in Figure 5.7. As expected, cells from all clones in attached collagen did not show any contraction (data not shown), as the collagen remain attached to the well during the 12 day period. Cells in detached collagen showed variable contraction rates, which increased over time. For both clones A11 (17PDs) and A31 at early PD (30PDs), cells displayed gradual contraction from day 1 to day 4, where clone A31 (30PDs) displayed more contraction (54% left of its original size) than A11 (65% left of its original size). At day 6, when cell numbers increased, collagen continued to shrink with A11 showing more contraction at this point than A31 (30PDs). By day 12, collagen reduced in size to 29% and 34% from their original size at day 0 for clone A11 and A31 (30PDs), respectively. In contrast, clone A31 at late PD (80PDs) displayed almost no shrinkage over the first 6 days and the collagen size reduced to only 74% from its original size by day 12 (Figure 5.6). Further investigation using ANOVA (Table 5.3) showed a significant difference in collagen contraction between early PD and late PDs of clone A31 with p value < 0.001 while no significant difference observed between the different clones (A31 and A11), with p value > 0.05.

Figure 5.5. Example of detached collagen contraction of clone A31 at 30PDs that can be easily visualised over 12 days in culture.
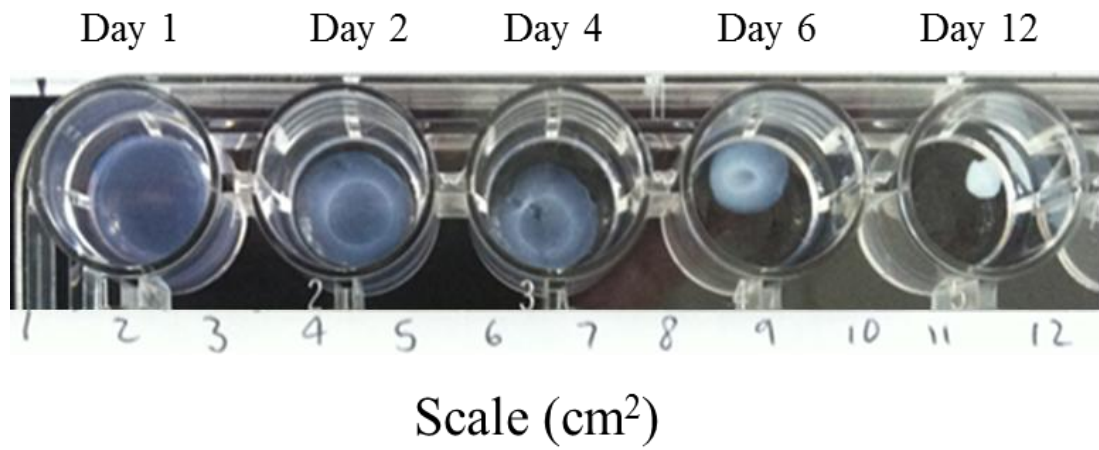
Figure 5.6. Average type I collagen lattice contraction (N=3, average ± SE), expressed as % reduction in lattice diameter, upon culture in detached collagen for clones A11 (17PDs) and A31 (30PDs and 80PDs).
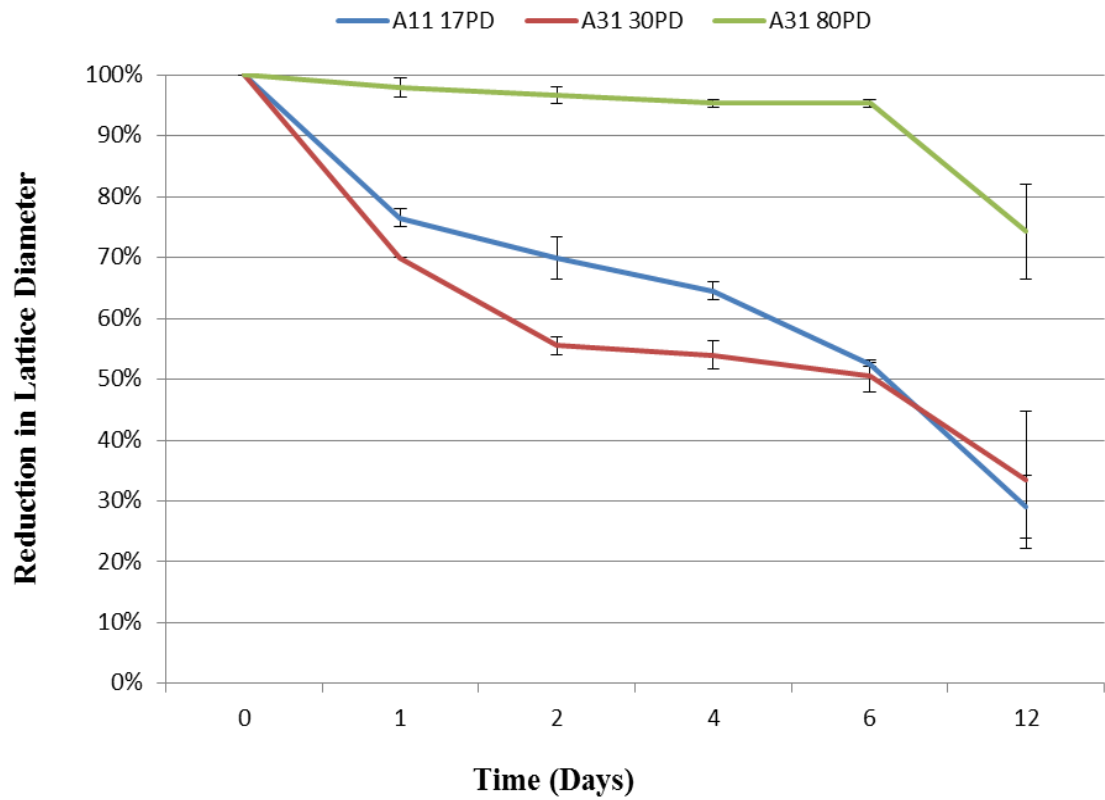
Table 5.3. Sums of significant p values for collagen lattice contraction from Figure 5.6. comparing the contraction of collagen of clone A31 at 30PDs with clone A31 at 80PDs and clone A11 at 17PDs over 12 days in culture. ** = p<0.01, *** = p<0.001, non-significant (ns) = p>0.05.

		A11 17PDs	A31 80PDs
Day1	A31 30PDs	ns	***
Day2	A31 30PDs	ns	***
Day4	A31 30PDs	ns	***
Day6	A31 30PDs	ns	***
Day12	A31 30PDs	ns	**

5.4.4 Dental Pulp Progenitor Cells and Matrix Metalloproteinase Synthesis

MMP gelatin zymography analyse of conditioned media collected from clones A11 (17PDs), A31 (30PDs) and A31 (80PDs) in detached collagen and monolayer culture over a 12 days period, are shown in Figure 5.7. MMP zymography analysis from the band intensity demonstrated that pro-MMP-2 was detectable in all clones under all conditions. It also demonstrated that active-MMP-2 was only detectable in detached collagen after day 4. Clone A31 at 80PDs showed less MMP activity, compared with other clones. MMP-2 expression for all the clones in different environments increased gradually over time (Figure 5.8 A,B and C). MMP-9 was detected only in clone A31 at later PD (80PDs), with more MMP-9 activity at later PD than earlier PD (30PDs) in monolayer culture. Furthermore, conditioned medium from clone A31 (30PDs) in detached collagen showed more MMP-9 activity over time than in monolayer culture (Figure 5.9).

By determining p-values for the production of pro-MMP-2 (Table 5.4), it was clear that a significant difference between all the clones in monolayer was evident, with p values < 0.001 from day 2 until day 12. In detached collagen, there was a significant difference in clone A31 between early PD (30PDs) and late PD (80PDs) over the 12 days period. However comparing clone A31 at 30PDs with clone A11 at 17PDs showed significance different only at day 4 and 6 when active-MMP-2 started to be produced.

Figure 5.7. Zymography gels showed pro-MMP-2 running at molecular weight (Mw) 72kDa, active-MMP-2 running at Mw of 62kDa and MMP-9 enzymes running at Mw of 92kDa, obtained from clones A31 (30PDs and 80PDs) and A11 (17PDs) from detached collagen and monolayer conditioned medium, over 12 days in culture.
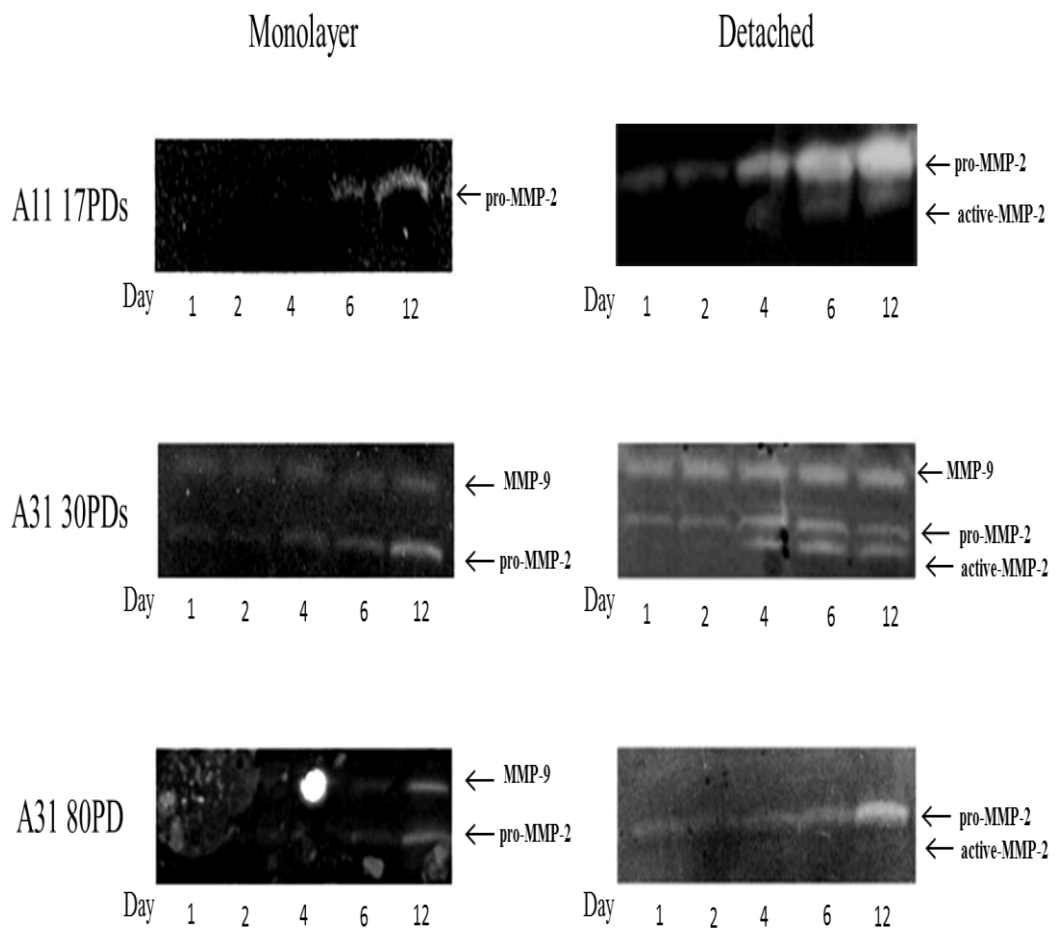
Figure 5.8. Quantitative analysis of pro-MMP-2 bands of the zymography gel obtained from conditioned medium of monolayer and detached collagen of A) A11 (17PDs), B) A31 (30PDs) and C) A31 (80PDs) (N=3, average ± SE). * = p<0.05, ** = p<0.01, *** = p<0.001, non-significant (ns) = p>0.05.

(A) A11 (17PDs)
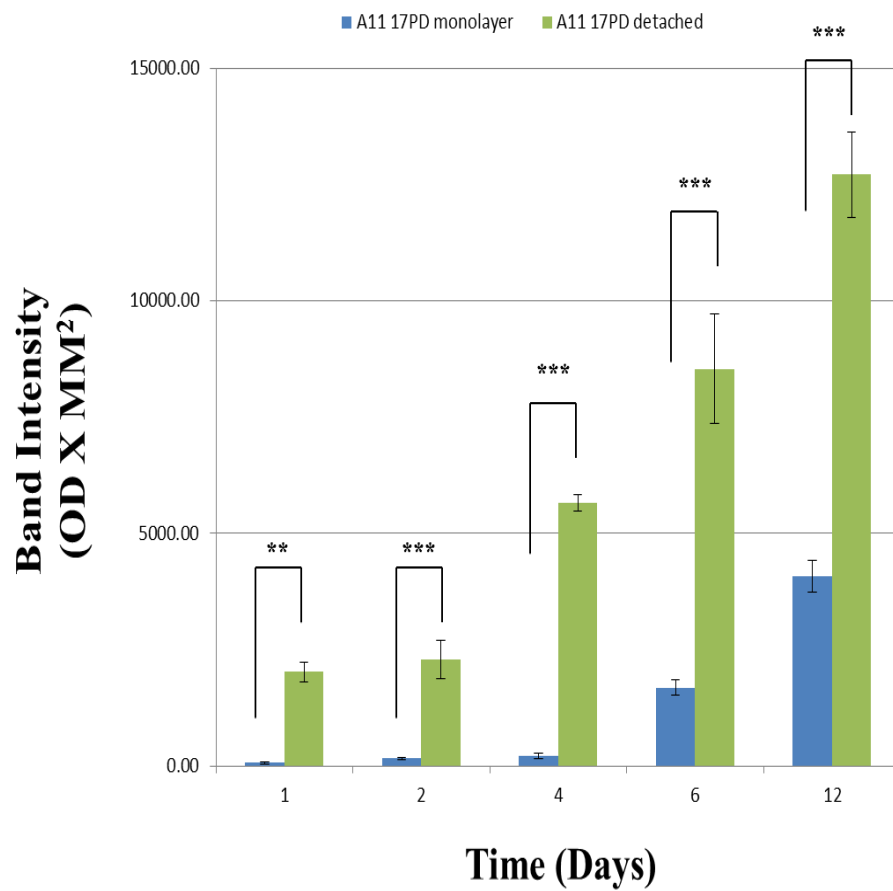
(B)   A31 (30PDs)
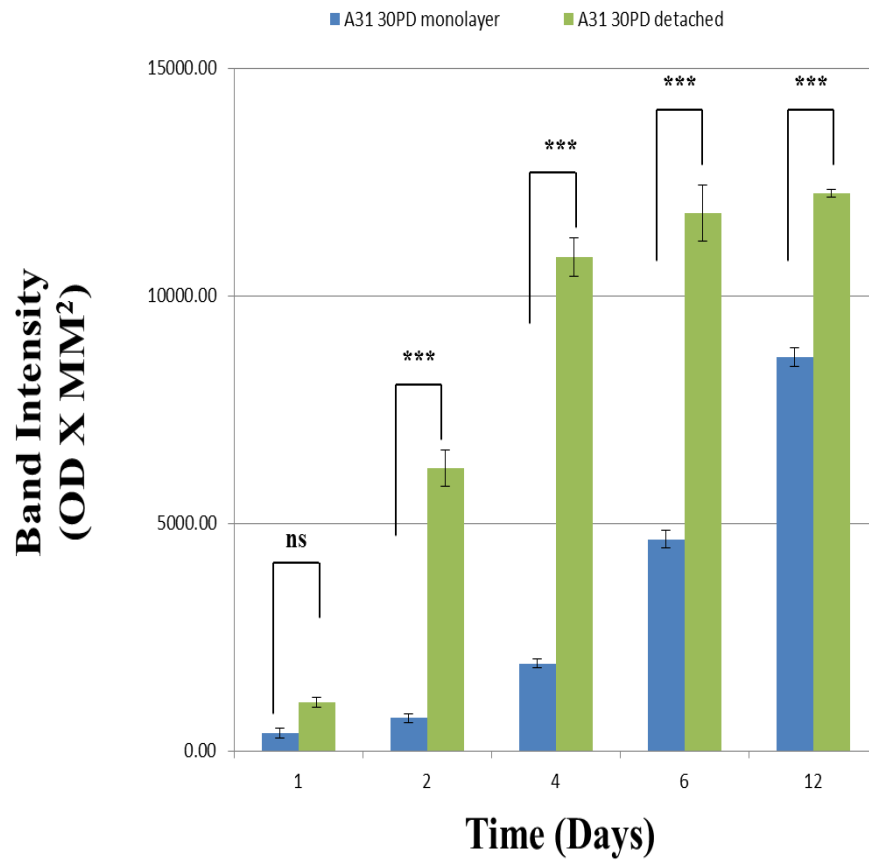
(C)   A31 (80PDs)
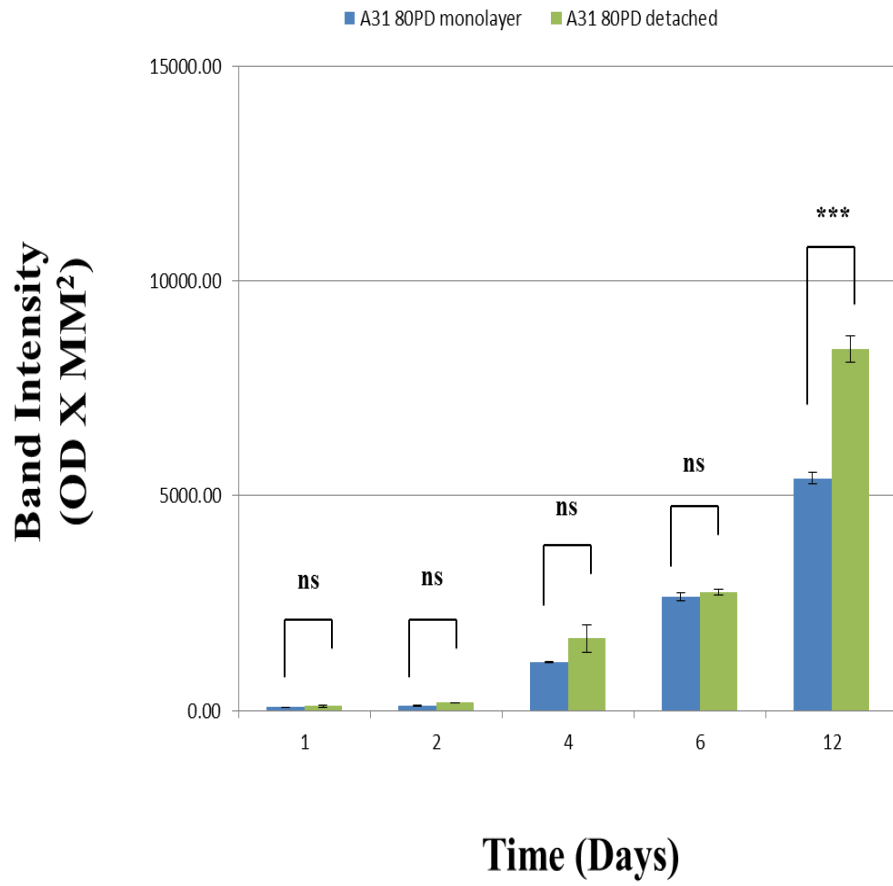
Figure 5.9. Quantitative analysis of MMP-9 bands of the zymography gel obtained from conditioned medium of monolayer clone A31 (30PDs and 80PDs) and detached collagen of A31 (30PDs). (N=3, average ± SE). * = p<0.05, ** = p<0.01, *** = p<0.001, non-significant (ns) = p>0.05.
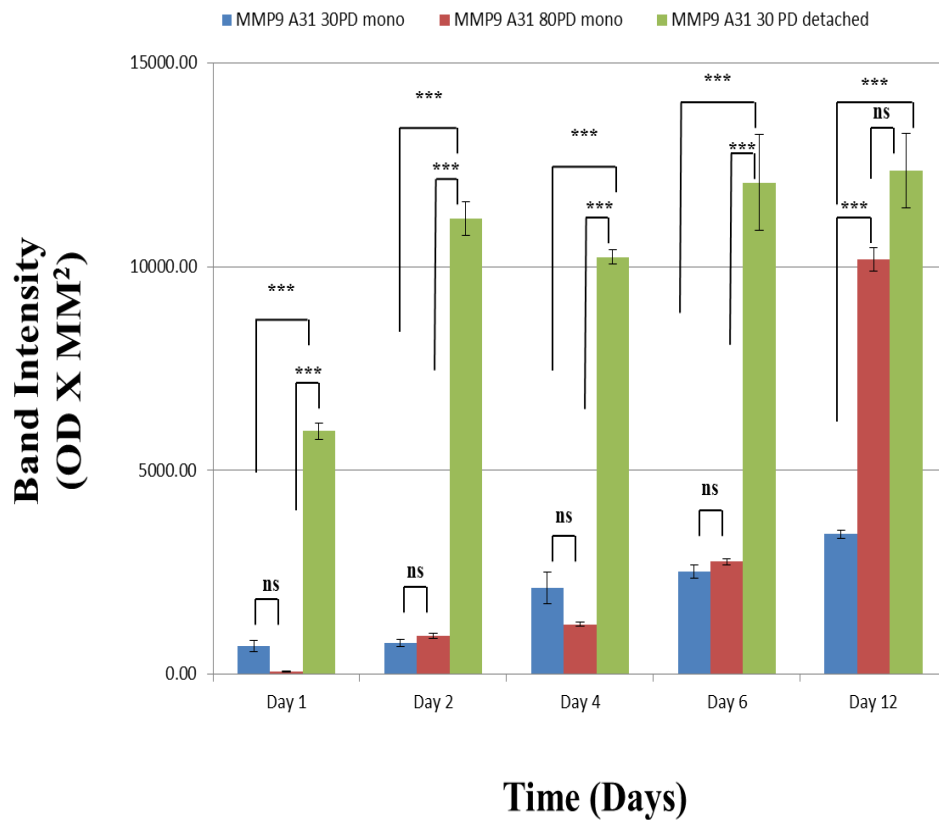
Table.5.4 Sums of significant p values for pro-MMP-2 from Figure 5.7. Compares pro-MMP2 synthesis from clone A31 at 30PDs in 2 different conditions (monolayer and detached collagen gel) with production of pro-MMP-2 in clones A31 at 80PDs and A11 at 17PDs, in the same conditions over 12 days in culture. ** = p<0.01, *** = p<0.001, non-significant (ns) = p>0.05.

		Monolayer A11 17PD	Monolayer A31 80PD	Detached A11 17PD	Detached A31 80PD
Day1	Monolayer A31 30PD	**	**		
Day1	Detached A31 30PD			ns	**
Day2	Monolayer A31 30PD	***	***		
Day2	Detached A31 30PD			ns	***
Day4	Monolayer A31 30PD	***	***		
Day4	Detached A31 30PD			***	***
Day6	Monolayer A31 30PD	***	***		
Day6	Detached A31 30PD			***	***
Day12	Monolayer A31 30PD	***	***		
Day12	Detached A31 30PD			ns	***

5.5   Discussion

This chapter illustrated that collagen gels, attached and detached, could potentially mimic the basic niche of DDPCs in different conditions, quiescent and proliferative respectively. Cells in attached collagen gel tend to proliferate the same as on a plastic surface, where active MMP-2 was not synthesised. On the other hand, DPPCs on detached collagen did not proliferate, and synthesised active MMP-2. For this reason, detached gel could mimic the quiescent stage in the dental pulp, while attached collagen gel could mimic the pulp in response to stimuli such as inflammation. The collagen gel interaction with DPPCs will help in understanding cell responses to ECM components, which is proved to play an important role in cell differentiation and tissue mineralisation (Kim et al., 2012a; Coyac et al., 2013). This work sheds light on collagen gel, which may be an intriguing material to use as a scaffold in tissue engineering.

The PD data showed differences in proliferation of DPPCs between culturing on plates compared to culturing these cells on collagen gels. There was also a clear difference when comparing the behaviour of DPPCs on floating collagen gels, compared to attached gels. Currently, there is much evidence that cells respond differently when cultured in collagen constructs in comparison to cell culture plates which has been credited to the similarities of collagen environment with the natural ECM (Butcher and Nerem, 2004). Mechanical forces, such as gravity, tension and fluid shear stress, influence the behaviour of cells under physiological and pathological conditions. In addition, the force generated by the cells themselves may influence many biological processes of stem cells, such as proliferation and differentiation (Wang and Thampatty, 2008). It has been shown that mechanical loading is essential for differentiation of fibroblasts into myofibroblasts (Arora et al., 1999) and mechanical forces can induce the differentiation of MSCs into functional osteoblasts, by enhancing alkaline phosphatase (ALP) activity and the mRNA expression of other osteogenic marker genes (Zhao et al., 2008).

In attached collagen gels, cells developed isometric tension by forming actin prominent stress fibers and demonstrated cell extensions attached to matrix fibrils and began to put pseudopodia-like outgrowths to help in their movement or

attachment on the collagen (Gabbay et al., 2006). DPPCs have also shown the ability to proliferate on the attached collagen, due to mechanical stresses in line with other findings (Riddle et al., 2005; Yamamoto et al., 2005; Stops et al., 2010). The proliferation for both clones A11 and A31 at early PDs began after a lag period of approximately 4 days, following which they proliferated rapidly. The cell number began to decrease after 12 days, possibly due to cells reaching the maximum numbers to survive in the collagen gel, suggesting cells were over-confluent. Clone A31 at late PD only exhibited no or low proliferation as was expected at this stage of PD as cells were senescent. Cells cultured on detached collagen showed minimal or no proliferation during the 12 day period for clones A11 and A31, in line with other findings (Rosenfeldt and Grinnell, 2000; Hadjipanayi et al., 2009). Said studies showed that fibroblasts do not proliferate in floating collagen as they are arrested in G0 phase of the growth cycle. Both clones, A31 and A11, when in monolayer revealed the same pattern of proliferation rate on attached collagen. The main reason cells tend to proliferate on attached collagen and tend to be quiescent in floating collagen is still not fully understood. It could be explained by signalling through the extracellular signal-regulated kinases (ERK pathway). ERK or MAP kinases belonging to a group of proteins that are activated in response to a number of stimuli, such as growth factors, neurotransmitters and environmental stresses such as heat shock (Pages et al., 1993) or mechanical stresses (Ruwhof and van der Laarse, 2000). These control cell growth, as ERK kinase seems to be essential during G1 progression for triggering entry into the S phase of the cell cycle (Pages et al., 1993). A study had shown that ERK signalling decreases in detached collagen (Fringer and Grinnel, 2001). This decrease was linked with the absence of isometric tension which results in the lack of actin stress fibers as shown by Phalloidin-FITC staining. It is also worth mentioning that in monolayer, the ERK pathway is regulated mostly by growth factors, such as platelet-derived growth factor (PDGF), and cell adhesion (Fringer and Grinnel, 2001). Taken together, the attached collagen could mimic the phase of injury when cells of granulation tissue proliferate under isometric tension, as in skin wounds (Clark, 1993; Grinnel et al., 1999). This could explain what happens to the DPPCs in response to injury in the tooth. Upon injury, DPPCs are recruited from their niche where they are engrafted in high numbers at the wound site, and stimulate a cascade of complex and as yet unclarified events (Mitsiadis et al.,

2011). Furthermore, cells in detached collagen could mimic the quiescent phase of cells on their microenvironment which is a common stem cell niche feature (Ema and Suda, 2012).

Cellular functions within tissues are firmly regulated by the tissue microenvironment, which consists of an extracellular matrix that is metabolised potentially by MMPs (Shiomi et al., 2010). These proteolytic enzymes play an important role in many cellular events, such as cell proliferation and migration (Vargova et al., 2012). Furthermore, hMSCs, in response to signalling cascades, tend to mobilise from their niche to penetrate the affected host site and subsequently differentiate into the appropriate specific type of cells (Lu et al., 2010). Several MMPs are expressed in human dental pulp including MMP-2 and MMP-9, where they are involved in dentine matrix organisation during dentinogenesis and also during pathological conditions, such as dental caries where MMP-2 and MMP-9 contribute to degradation of the organic matrix of teeth (Palosaari et al., 2003; Mazzoni et al., 2007). The natural ability of DPPCs to remodel their ECM environment by activating proteolytic enzymes (MMP-2 and MMP-9) was evaluated by gelatin zymography (Toth et al., 2012). There are many resemblances in MMP-2 and MMP-9 in structure and substrates, but they differ in terms of regulation and activation. For example, MMP-2 is activated by MMP-1, MMP-7, MMP-13, MMP-14, MMP-15, MMP-16, MMP-17, MMP-24 or MMP-25, while MMP-9 activated by MMP-2 itself or by MMP-1 (Visse and Nagase, 2003). In general, MMP-2 is produced in a wide range of cell types, including fibroblasts, endothelial cells, keratinocytes, and macrophages, while MMP-9 is produced mainly in leukocytes and other cell types in response to stimuli, such as inflammation (Whatling et al., 2004; Xue and Jackson, 2008). For example, human lung fibroblasts do not produce MMP-9 in monolayer or in collagen gels, but only produce MMP-9 when stimulated by cytokines (Kamio et al., 2010). Controversially, cell stress has been shown to be one of the factors that upregulate and downregulate MMP gene expression (Mudera et al., 2000; Sternlicht and Werb, 2001; Karamichos et al., 2007). Therefore, a relationship could be established between cell proliferation, which is also affected by cell stress, and MMPs production. The relationship appeared to be an inverse one

between the cell proliferation rate and the presence of the MMP inhibitor, as in the fibroblast (Bott et al., 2010).

Data from this study has shown that the physical state of the collagen gel influences cell proliferation. It also demonstrated the physical state regulated MMP production, which caused collagen shrinkage over time. In monolayer culture, there was an expression of pro-MMP-2 by both clones (A11 and A31) that increased gradually over time, especially after day 4, suggesting the increase was related to cell number. In monolayer culture no expression of active-MMP2 was detected, while in detached collagen active-MMP-2 was detected, which indicated that MMP-2 activation was induced by the ECM, collagen type I. The amount of pro-MMP-2 produced by cells in detached collagen gels was much higher than in monolayer cultures. This could be because cells in detached collagen have less tension than in monolayer and it has been found that a decrease in cell tension may lead to an increase in the expression of MMP-2 (Howard et al., 2012). MSCs function has been shown to be regulated by MMP activity (Kasper et al., 2007; Glaeser et al., 2010; Lu et al., 2010; Lozito and Tuan, 2011). Human bone marrow mesenchymal stem cells have been found to constitutively produce MMP-2 *in vitro* to organise the basement membrane (Ries et al., 2007). hMSCs that have MMP-2 gene knock-down lose their invasion ability into affected site (Ries et al., 2007). This may explain the reason why cells of both clones reduced in number in late PD as cells also tend to lose their stemness by age (Stolzing et al., 2008) as demonstrated in chapter 2. Furthermore, MMP-9 production was only detected in clone A31 in both monolayer and in detached collagen. In detached collagen gels, the production of MMP-9 remained constant during the 12 day period, while it increased gradually in monolayer culture. MMP-9 production by clone A31 in detached collagen gel was greater than in monolayer, which could be due to the cell numbers. However, comparing early PD (30PDs) with late PD (80PDs) of clone A31, found that late PD produced more MMP-9 even when it had less cell numbers. Another explanation why the expression of MMP-9 was highest at the late PD, was that cells were almost senescent, which confirms the link between MMP-9 and cell senescence (Cao et al., 2013).

This chapter has demonstrated that detached collagen gels appear to be regulated by MMP-2 only and not MMP-9. Also demonstrated was increased type I collagen lattice contraction, which was mediated by increased pro-MMP-2 expression/activity whereby active-MMP-2 started to appear (Azzam and Thompson, 1992; Gilles et al., 1997; Theret et al., 1999; Rupp et al., 2008). This regulatory mechanism could be important for MSCs to keep them in their quiescent state in their physiological stem cell niche and to activate their differentiation in the case of injury (Kasper et al., 2007). MMP-9 was only expressed in the highly proliferative clone, which could be connected to what stage of commitment these cells are in as described in chapter 2. Furthermore, it is known that hMSCs express very low level of MMP-9 under normal conditions (Ries et al., 2007), which may suggest that they are linked to the clonal variation. However, more investigation is needed such as examining the expression of MMP-2 and MMP-9 at a gene level and expression of tissue inhibitor of metalloproteinases (TIMPs), especially as MSCs from bone marrow express high levels of TIMPs (Lozito and Tuan, 2011). Therefore, it is important in the future to study TIMPs expression levels in monolayer, attached collagen and detached collagen.

Overall, the objective of this chapter was to determine whether collagen matrices will act as a native ECM environment for DPPCs, by assessing DPPCs proliferation, morphology and MMPs production. However, the initial data showed that the physical state will play an important role in these properties. The attached collagen seems to be successful to obtain cell proliferation and morphology of these cells, but not detached collagen. Recently, a study on DPPCs seeded on collagen gel found that culturing these cells on collagen will enhance their differentiation ability. However, in order to do so, the collagen was compressed to make it resemble to the natural matrix environment (Coyac et al., 2013). This means further investigations are needed to compare between all these different physical states of the collagen and their subsequent effects on cell morphology and cell differentiation to allow clinicians to benefit from the combination of DPPCs with collagen gels for the clinical repair of osseous and dental defects.

Chapter 6:
Discussions

6.1 General Discussion

This thesis set out to better identify dental pulp progenitor cells (DPPCs) clones most efficient for tissue engineering. Previous studies have showed the existence of different mesenchymal stem cells (MSCs) clones only in terms of proliferation ability and differentiation capacity, without demonstrating possible reasons for clonal variation; despite identical gene expression of selected MSCs (CD29, CD44, CD90, CD105, and CD166) (Gronthos et al., 2002; Mareddy et al., 2007; Jeon et al., 2011). In addition, use of heterogeneous stem cell populations is likely to produce an unpredictable biological activity such as inefficiency of differentiation into specific lineages or differentiation into undesirable cell types (Roy et al., 2006; Müller et al., 2010). Thus, from efficacy and safety points of view, ability to identify homogenous MSCs clones will be more beneficial for clinical application. Hereon, a highly proliferative clone (A31) was identified, and for the first time the highly proliferative clone was linked with other preferable properties for tissue engineering. These properties include long telomere length, higher resistance to H_2O_2 with delayed senescence, ability to differentiate into three different lineages (i.e. adipogenic, osteogenic, and chondrogenic), absence of tumor suppression genes (p53 and p16^{INK4a}) and of neural marker CD271. On the other hand, low proliferative clones (A11 and B11) were linked with short telomere length, less resistance to H_2O_2 and cell senescence, ability to differentiate only into osteogenic lineage, and expression of tumor suppression genes (p53 and p16) and marker CD271. As such, generating well-defined cell populations from stem cells will advance tissue engineering therapies (Karystinou et al., 2009). In order to reach this goal to identify such a desirable clone, extensive *in vitro* expansion was needed. Such expansion altered DPPCs stemness by loss of stem cell markers, loss of telomere length, differntial differentiation ability (favouring adipogenesis over osteogenesis), and eventual replicative senescence. The process of expansion is also costly and time consuming. For this reason, a different method was investigated to identify clonal differences. Raman spectroscopy was used to identify a quick and non-invasive method to

discriminate between clones, based on their attributed DNA, RNA, and amino acid contents, relative to proliferation and differentiation status. Raman spectroscopy successfully showed that the highly proliferative clone (A31) had a completely different fingerprint, based on biochemical features, compared with low proliferative clones. Lastly, the behaviour of high and low proliferative clones on type I collagen was assessed. DPPCs in detached collagen caused collagen contraction irrespective of clonal type, by synthesising active MMP-2, which is not expressed on a plastic culture surface. In addition, DPPCs in detached collagen did not proliferate, which may mimic a quiescent state in the dental pulp. On the other hand, DPPCs in attached collagen gel tended to proliferate, which may mimic the pulps response to stimuli such as inflammation. MMP-9 expression was only seen in the highly proliferative clone, and expression level was the same on both collagen and plastic environments. This expression level of MMP-9 increased at late PDs, which may indicate an MMP-9 role in cell senescence, and distinguish such an advantageous clone from others less so. Thus collagen gel is an intriguing material to assess DPPCs behaviour in 3D culture, for use in cell-therapy.

It is now well-acknowledged that individual mesenchymal stem cells (MSCs) colonies, from the same tissue including dental pulp, exhibit different behaviour and differentiation capacities (Gronthos et al., 2002; Guilak et al., 2006; Karystinou et al., 2009). However, none of these previous studies compared isolated colonies from the same tissue or the same donor and subsequently linked proliferative capacity with differentiation ability and telomere length. In this thesis, three clones were isolated from wisdom teeth of the same patient A11, A31, and A51, and another clone from different patient, B11. Only one clone, A31 proliferated for more than 80PDs while others only proliferated for less than 40PDs (Figure 2.3). For this reason, clone A31 was taken forward with another clone from the same patient (A11), with the other clone from the second patient (B11), to address the reasons behind these differences. In addition, the subsequent impact of such variations in proliferative capabilities on clonal differentiation and regenerative potential were also examined. The highly proliferative clone showed the ability to differentiate into three different lineages: osteoblasts (Figure 3.2), adipocytes (Figure 3.8) and chondrocytes (Figure 3.14), while the low proliferative clones (A11 and B11) were only differentiated into

osteoblasts (Figure 3.3 and Figure 3.4). The reasons behind the ability of clone A31 to differentiate into the three different lineages could be down to the asymmetric division of the stem cell as will described in the next paragraph.

Adult stem cells are capable of self-renewal and differentiation into multiple cell lineages, with short life-spans. To achieve self-renewal capabilities and differentiation functions, stem cells divide slowly and symmetrically to produce an identical daughter cell with low proliferative capacity and multipotential differentiation. Some of these adult stem cells go on to divide asymmetrically and give rise to one identical daughter cell and another progenitor cell called a transit amplifying (TA) cell. TA cells have a high proliferative potential and low differentiation ability and give rise to more committed progenitors with reduced proliferative potential (Figure 1.1), which eventually produce terminal differentiated cells (Alison et al., 2002; Ho, 2005). Asymmetrical division could give one explanation of the reasons that cause different characteristics between isolated clones of DPPCs. Here, clone A31 was the only clone that had both characteristics with highly proliferation and multipotential differentiation, probably because of asymmetrical division of stem cells that led to this clone to have both populations i.e. stem cells and TA cells. This hypothesis supports the telomere data presented here as clone A31 had longer telomeres throughout culture, while at later PD it showed a long smear band indicative of the existence of two populations, possibly showing stem cell with longer telomeres and TA cells with shorter telomeres. In addition, the clones A11 and B11 were unipotent and displayed less division potential and shorter telomere lengths, possibly as they could be considered to be the more committed progenitor cells. Another result that supports this theory is the expression of senescence marker p53. This marker was expressed in short telomere clones which suggested that clone A11 is a later stage version of clone A31 as they are from the same patient (Hao et al., 2013). One of the differences between the clones is the expression of p16 gene that was expressed only in the low proliferative clones, which gives support to the asymmetrical stem cell division theory by way of explanation for the differences between clones. The expression of p16 gene could be another beneficial way to help researchers distinguish between high and low proliferative

colonies, as it has been shown that enhancing expression of p16 leads to a decrease in the proliferation capacity of stem cells in mice (Molofsky et al., 2003).

Another theory that could explain the differences between the clones, is the niche in which DPPCs reside. DPPCs are proposed to be located in different niches within the pulp, such as the perivascular region (Huang et al., 2009b), within capillaries and nerve networks of the cell free zone (Lizier et al., 2012), or subodontoblastic cell-rich layer of the dental pulp (Hosoya et al., 2012). This might bestow different characteristics such as different stem cell gene expression profile. In this study, expression of the selected stem cell markers was the same for all the clones except the expression of the CD271 gene. CD271 was expressed in low proliferative clones (A11 and B11), which suggests that low proliferative clones were derived from the nerve networks in cell free zone within the dental pulp, as CD271 is considered a neural tissue marker (Lizier et al., 2012) . More stem cell markers gene expressions need to be investigated for A31, A11 and B11 clones for their respective expression profiles, such as CD146 that is linked to progenitor cells raised from the perivascular niche (Shi and Gronthos, 2003). Such experimentation will help to investigate if such genes could be linked to either highly proliferative clone (A31) or low proliferative clones (A11 and B11). Moreover, CD271 has conflicting results in terms of it's expression in MSCs, based on the tissue it is raised from. MSCs with positive expression of CD271 from bone marrow differentiate into osteogenic, adipogenic and chondrogenic lineages, while MSCs from umbilical cord do not show an indication of any differentiation (Watson et al., 2013). Furthermore, CD271 is found to inhibit differentiation of deciduous dental pulp stem cells (Mikami et al., 2011). In line with the data presented here, the only clone that did not show expression of CD271 marker was the multipotent clone, A31. This means that clones which express CD271 isolated from dental pulp could be excluded from use in tissue engineering. Finally, another consideration is the epigenetic regulation of stem cells, which is deeply involved in their development and differentiation (Liu and Xiao, 2011). Chromatin-modifying activities, including methylation and phosphorylation organise the suppression or activation of gene expression, such as Runx2, SOX9 and PPARγ, which control the stem cell differentiation along osteogenic, chondrogenic and adipogenic lineages, respectively. These regulatory

mechanisms suggest that epigenetics might provide an important role in stem cell differentiation (Kelly and Jacobs, 2010; Li et al., 2010).

The differences between the three clones were supported by the data from the Raman spectroscopy (Chapter 4). Indeed, the initial results displayed that highly proliferative clone (A31) had a completely different fingerprint based on their biochemical features compared with low proliferative clones (A11 and B11). The low proliferative clones also had very similar fingerprints with one other. The only peaks found in clone A31 were $1111cm^{-1}$ and $958cm^{-1}$, which corresponds to tyrosine and phenylalanine, respectively. These two peaks could be used as markers in Raman spectroscopy to distinguish between high proliferative and low proliferative clones. Raman spectroscopy data was analysed by the principal component analysis (PCA), where low proliferative clones overlapped each other while clone A31 had a completely distinguishable and separate area (Figure 5.7). Raman spectroscopy was also used as a marker of chondrogenic differentiation for clone A31, which may help in distinguishing stem cells from their derivatives. Spectra from chondrocytes highlighted bands that were characteristic of proteins that included amide I ($1616cm^{-1}$) and C=O ester ($1730cm^{-1}$). While non-differentiated cells highlighted a band characteristic of DNA, the $C_{5'}$-O-P-O-$C_{3'}$ phosphodiester bonds in DNA ($788cm^{-1}$) (Table 4.4). Successful separation of stem cells from their derivatives will help to isolate a pure population for tissue engineering, by avoiding a heterogeneous population that is indicated to lead to teratoma and cancer (Chan et al., 2009; Downes et al., 2011).

In order to use DPPCs in cell therapy, *in vitro* cell expansion is needed. This expansion may have an effect on the quality of the cells eventually obtained. It has been reported that MSCs lose their multipotentiality, proliferation ability and capability to differentiate to bone during expansion *in vitro* (Banfi et al., 2000; Min et al., 2011). MSCs have a finite proliferative life-span, which means they will undergo replicative senescence during long-term culture *in vitro*. Replicative senescence is characterised by gradual reduction in proliferation rate, morphological changes, loss of function and reduction in their telomere length (Bonab et al., 2006). There are many studies into the effects of *in vitro* expansion of MSCs (Banfi et al.,

2000; Stenderup et al., 2003; Bonab et al., 2006; Brandl et al., 2011; Kim et al., 2012b). None of these studies however, look at the long term and simultaneous effects on proliferation, differentiation, telomere length, stem cell marker expression, cell senescence and H_2O_2 senescence on DPPCs. Indeed, this thesis showed the effect of long term *in vitro* culture on DPPCs from different aspects. Firstly, the stem cell population doubling levels (PDs) decreased following 280 days culture for clone A31, and less than 100 days for the other clones (A11, B11, and A51) (Figure 2.5). Secondly, the expression of embryonic and mesenchymal stem cell markers was gradually lost with increasing PDs, until they completely disappeared in all clones (Figure 2.6). Despite the loss of stem cell markers, clones were still capable of proliferation. Previous work shows that DPPCs loss their mesenchymal stem cell markers as early as twenty-five passages (Kerkis et al., 2006). The loss of these markers during *in vitro* culture is still not fully understood, but it may be due to cells not having the same environment as they have in their original niche, which leads cells undergoing spontaneous differentiation followed by senescence (Patel et al. 2009). Thirdly, DPPCs lost their ability to differentiate into an osteogenic lineage at late PD (Figure 3.2), in favour of an adipogenic lineage (Figure 3.8), which was supported by decreased Runx2 bone gene expression and increased PPARγ adipogenic gene expression. A study by D'Ippolito *et al* (1999) found that MSCs from bone marrow lose their capacity to differentiate into osteoblasts during aging. MSCs from bone marrow tend to differentiate into adipocytes, much like when bone marrow is partially replaced by adipocytes in human aging, which is believed to cause some forms of osteoporosis whereby Runx2 is suppressed by PPARγ (Moremen et al., 2004; Fehrer and Lepperdinger, 2005). Finally, the other effect of *in vitro* expansion on DPPCs was replicative senescence. Replicative senescence was witnessed by morphological alterations (Figures 2.9, 2.10, 2.11), positive staining of β-galactosidase enzyme (Figure 2.14), and shortening of the telomere length (Figure 2.15); which was also supported by absence of human telomerase reverse transcriptase (hTERT) of these cells (Figure 2.7). In addition to telomere shorting, DNA damage accumulation could be another mechanism supporting replicative senescence (Gharibi and Hughes, 2012). Little is known however about replicative senescence in MSCs. Telomere shortening and accumulation of DNA damage leads to activation of tumour suppressor p53 and its downstream p21, and induction of the

cyclin-dependent kinase inhibitor p16^{INK4a} (reviewed in Sperka et al., 2012). p53 and p16^{INK4a} were expressed at early PD in low proliferative clones (A11, B11) but not in the highly proliferative clone (A31) (Figure 2.8). These findings lend support to the theory of asymmetric division whereby clone A11 is later-stage MSC of clone A31. Overall, this thesis reported a link between replicative senescence, reduction in stemness related genes, loss of MSCs self-renewal, and loss of differentiation potential, as reported in other type of MSCs (Liu et al., 2004; Alves et al., 2010; Cheng et al., 2011), and a link between tumour suppression gene markers (p16 and p53) with the differences between the isolated clones.

The stem cell environment changes widely during stem cell lifespan and has an effect on stem cell behaviour and shape (Hao et al., 2013). ECM contributes to stem cells behaviour because cells that attach to a substrate have been shown to exert contractile forces, resulting in tensile stresses in the cytoskeleton. The relationship between cells, environment and mechanical stiffness or elasticity of this ECM have a major influence on cell activities such as migration, apoptosis and proliferation (Guilak et al., 2009). For this reason, an investigation of the effect of an artificial type I collagen ECM, was conducted. Results demonstrated that DPPCs in floated collagen did not proliferate. This may represent the quiescent stage of stem cell *in vivo,* while DPPCs in attached collagen proliferate in similar way when on the surface of a flask. This may represent the state of stem cells when they respond to stress, such as an inflammation. Stem cells rest in their quiescent stage for most of their lifespan *in vivo* (Fehrer and Lepperdinger, 2005) and are activated through signals, such as the ERK pathway in response to stimuli such as inflammation (Pages et al., 1993), in order to endorse repair and regeneration process (Fehrer and Lepperdinger, 2005). In response to the ERK signalling pathway, MSCs mobilise from their niche into an affected site by penetrating the ECM, which includes collagen type I, *via* increased matrix metalloproteinase (MMP) expression (Lu et al., 2010). Indeed, this thesis showed that active MMP-2 is only demonstrated in cells cultured in floating collagen, which underwent contraction, unlike cells cultured on a plastic surface (Figure 5.8). This confirms that MMP-2 activity plays an important role in matrix remodelling by DPPCs, and possibly in migration as shown by MSCs from bone marrow (De Becker et al., 2007). MMP-9 was only detected in clone A31,

which might be linked to the clonal variation. This MMP-9 did not increase with time in detached collagen as MMP-2 did, which suggests that only active MMP-2 had a role in collagen organisation by DPPCs. MMP-9 expression also was higher expressed in late PD (80PDs) than in early PD (30PDs), which suggests that MMP-9 has role in cell senescence (Cao et al., 2013).

In conclusion, this thesis identified key reasons behind variations in DPPCs clones. The data confirmed clonal variations in DPPC proliferative capacity and the onset of senescence, identified by reductions in PD, altered morphology, increased senescence associated β-galactosidase staining and senescence marker (p53/p21^{WAF1}/p16^{INK4A}) expression. Highly proliferative clone was capable of >80PDs *in vitro*, while low proliferating clones only achieved <40PDs. Although it was shown that hTERT expression is not responsible for clonal variation in proliferative capabilities, this study is the first to identify that highly a proliferative clone can possess inherently longer telomeres (>15kb, by Telomere Restriction Fragment Length analysis) than low proliferative clones, which maintains stem cell marker (CD73, CD90 and CD105) expression for longer. Early senescence and stem cell marker loss in low proliferative clones further leads to impaired osteogenic and chondrogenic lineage differentiation at earlier PD, unlike highly the proliferative clone. Therefore, the preferred highly proliferative/regenerative DPPC clones could be exploited for tissue repair/regeneration purposes. These findings with the addition of Raman spectroscopy results, will ultimately help into developing methods for the selective screening/isolation of highly proliferative/regenerative clones from whole dental pulp, thereby permitting greater cellular expansion for *in vitro/in vivo* assessment and eventual clinical use.

6.2   Future Works

The work described in this thesis has begun to explore the use of Raman spectroscopy as a quick non-invasive tool for the selective screening and isolation of highly proliferative clones from dental pulp for therapeutic use. Raman spectroscopy however, is to be considered an additional supporting method, as the isolation of such a desirable clone is likely to require several techniques. A number of approaches could be used as quick way to identify highly proliferative clones. For example, single telomere length analysis (STELA) is one of these approaches.

STELA is a novel PCR-based technique for the analysis of telomere length from single chromosome ends. The exquisite sensitivity of this technique allows the detection and characterisation of single telomeric molecules, thereby revealing the full spectrum of telomere lengths (including ultra-short telomeres). Importantly, STELA only requires small numbers of cells (500+), and thus can determine telomere length very early (≈5PDs) in the proliferative lifespan of cells. Another example relies on proposed genes involved in DPPC proliferation and senescence (Mehrazarin et al., 2011); of which there are many genes critical to stem cell function not yet characterized. Here differences in the expression of CD271 in DPPCs clones were seen. A plethora of other genes however need to be investigated such as CD146 (proposed stem cell niche marker), and BMI-1 (regulator of tumour suppression genes p16 and p53; as found here in low proliferative clones). For this reason use of *Affymetrix* Microarrays, a quartz chip for analysis of DNA microarrays (Perez-Iratxeta et al., 2005), will permit quick scanning for the presence of particular genes in a biological sample (Perez-Iratxeta et al., 2005). Such microarrays could complete clonal characterisation and identify candidate genes for enhanced/reduced proliferation and regenerative potential.

The work in this thesis on the interaction of DPPCs with type I collagen gel is only a stepping stone for further investigation of the role of ECMs in regulating DPPCs function. Future works need to be done in this area firstly includes, investigating whether cells penetrate collagen vertically by using confocal microscopy to confirm that this environment is truly a 3D culture model. Secondly, investigation of 3D culture to enhance differentiation ability of cells, by measuring expression of specific markers at protein level using Western blot. Finally, an important focus is the MMP-9 role in the highly proliferative clone, by inhibiting expression of MMP-9 via TIMP-1, and the potential effect upon DPPC behaviour on collagen and plastic surfaces.

References.

Abanobi SE, Lombardi B, Shinozuka H. 1982. Stimulation of DNA synthesis and cell proliferation in the liver of rats fed a choline-devoid diet and their suppression by phenobarbital. *Cancer Res* 42(2), pp. 412-5.

Abe S, Hamada K, Miura M, Yamaguchi S. 2012. Neural crest stem cell property of apical pulp cells derived from human developing tooth. *Cell Biol Int* 1; 36(10), pp. 927-36.

Advanced Physics Laboratory. 2006, Feb.

Addison WN, McKee MD. 2010. Inositol hexakisphosphate inhibits mineralization of MC3T3-E1 osteoblast cultures. *Bone* 46(4), pp. 1100-7.

Agata H, Asahina I, Watanabe N, Ishii Y, Kubo N, Ohshima S, Yamazaki M, Tojo A, Kagami H. 2010. Characteristic change and loss of *in vivo* osteogenic abilities of human bone marrow stromal cells during passage. *Tissue Eng Part A* 16(2), pp. 663-73.

Airas L, Hellman J, Salmi M, Bono P, Puurunen T, Smith DJ, Jalkanen S. 1995. CD73 is involved in lymphocyte binding to the endothelium: characterization of lymphocyte-vascular adhesion protein 2 identifies it as CD73. *J Exp Med* 182(5), PP. 1603-8.

Akkouch A, Zhang Z, Rouabhia M. 2013. Engineering bone tissue using human dental pulp stem cells and an osteogenic collagen-hydroxyapatite-poly(-lactide-co-{varepsilon}- aprolactone) scaffold. *J Biomater Appl*, May 2 (ahead of print).

Aksoy C and Severcan F. 2012. Role of Vibrational Spectroscopy in Stem Cell Research. *Spectroscopy: An International Journal* 27 (3), pp. 167–184.

Alberts B, Johnson A, Lewis J, Raff M, Roberts K, Walter P. 2008. Molecular Biology of the Cell. *New York: Garland Science* 5th.

Alge DL, Zhou D, Adams LL, Wyss BK, Shadday MD, Woods EJ, Gabriel Chu TM, Goebel WS. 2010. Donor-matched comparison of dental pulp stem cells and bone marrow-derived mesenchymal stem cells in a rat model. *J Tissue Eng Regen Med* 4(1), PP. 73-81.

Alison MR, Poulsom R, Jeffery R., Dhillon AP, Quaglia A, Jacob, J, Novelli M, Prentice G., Williamson J and Wright NA. 2000. Hepatocytes from non-hepatic adult stem cells; *Nature* 20;406(6793):25.7.

Alison MR, Poulsom R, Forbes S, Wright NA. 2002. An introduction to stem cells. *J Pathol* 197(4), p. 419-23.

Alliot-Licht B, Hurtrel D, Gregoire M. 2001. Characterization of alpha-smooth muscle actin positive cells in mineralized human dental pulp cultures. *Arch Oral Biol* 46(3), pp. 221-8.

Allsopp RC, Vaziri H, Patterson C, Goldstein S, Younglai EV, Futcher AB, Greider CW, Harley CB. 1992. Telomere length predicts replicative capacity of human fibroblasts. *Proc Natl Acad Sci U S A* 1; 89(21), pp. 10114-8.

Alongi DJ, Yamaza T, Song Y, Fouad AF, Romberg EE, Shi S, Tuan RS, Huang GT. 2010. Stem/progenitor cells from inflamed human dental pulp retain tissue regeneration potential. *Regen Med* 5(4), pp. 617-31.

Alp NJ, Mussa S, Khoo J, Cai S, Guzik T, Jefferson A, Goh N, Rockett KA, Channon KM. 2003. Tetrahydrobiopterin-dependent preservation of nitric oxide-mediated endothelial function in diabetes by targeted transgenic GTP-cyclohydrolase I overexpression. *J Clin Invest* 112(5), pp. 725-35.

Altman GH, Horan RL, Lu HH, Moreau J, Martin I, Richmond JC, Kaplan DL. 2002. Silk matrix for tissue engineered anterior cruciate ligaments. *Biomaterials* 23, pp. 4131-41.

Alves H, Munoz-Najar U, De Wit J, Renard AJ, Hoeijmakers JH, Sedivy JM, Van Blitterswijk C, De Boer J. 2010. A link between the accumulation of DNA damage and loss of multi-potency of human mesenchymal stromal cells. *J Cell Mol Med* 14(12), pp. 2729-38.

Alves H, Mentink A, Le B, van Blitterswijk CA, de Boer J. 2013. Effect of antioxidant supplementation on the total yield, oxidative stress levels, and multipotency of bone marrow-derived human mesenchymal stromal cells. *Tissue Eng Part A* 19(7-8), pp. 928-37.

Ames BN, Shigenaga MK, Hagen TM. 1993. Oxidants, antioxidants, and the degenerative diseases of aging. *Proc Natl Acad Sci U.S.A*. 90, pp. 7915-7922.

Anderlini P, Rizzo JD, Nugent ML, Schmitz N, Champlin RE, Horowitz MM. 2001. Peripheral blood stem cell donation: an analysis from the International Bone Marrow Transplant Registry (IBMTR) and European Group for Blood and Marrow Transplant (EBMT) databases. *Bone Marrow Transplant* 27, pp. 689-692.

Andreou I, Tousoulis D, Tentolouris C, Antoniades C, Stefanadis C. 2006. Potential role of endothelial progenitor cells in the pathophysiology of heart failure: clinical implications and perspectives. *Atherosclerosis* 189(2), pp. 247-54.

Andriantsitohaina R, Duluc L, García-Rodríguez JC, Gil-del Valle L, Guevara-Garcia M, Simard G, Soleti R, Su DF, Velásquez-Pérez L, Wilson JX, Laher I. 2012. Systems biology of antioxidants. *Clin Sci* (*Lond)* 1;123(3), pp.173-92.

Angello JC, Pendergrass WR, Norwood TH, Prothero J. 1989. Cell enlargement: one possible mechanism underlying cellular senescence. *J Cell Physiol* 140(2), pp. 288-94.

Annerén C. 2008. Tyrosine kinase signalling in embryonic stem cells. *Clin Sci (Lond)* 115(2), pp. 43-55.

Arai F and Suda T. 2007. Maintenance of quiescent hematopoietic stem cells in the osteoblastic niche. *Ann N Y Acad Sci* 1106, pp. 41-53.

Arora PD, Narani N, McCulloch CA. 1999. The compliance of collagen gels regulates transforming growth factor-beta induction of alpha-smooth muscle actin in fibroblasts. *Am J Pathol* 154(3), pp. 871-82.

Arthur, A., Shi, S., Zannettino, A.C., Fujii, N., Gronthos, S., Koblar, S.A. 2009. Implanted adult human dental pulp stem cells induce endogenous axon guidance. *Stem Cells* 27(9), pp. 2229-37.

Asahara T, Murohara T, Sullivan A, Silver M, van der Zee R, Li T, Witzenbichler B, Schatteman G, Isner JM. 1997. Isolation of putative progenitor endothelial cells for angiogenesis. *Science* 14;275(5302), pp. 964-7.

Ashton BA, Allen TD, Howlett CR, Eaglesom CC, Hattori A, Owen ME. 1980. Formation of bone and cartilage by marrow stromal cells in diffusion chambers *in vivo. Clin Orthop* 151, pp. 294–307.

Atala A. 2012. Tissue engineering of reproductive tissues and organs. *Fertil Steril* 98(1), pp. 21-9.

Atari M, Caballé-Serrano J, Gil-Recio C, Giner-Delgado C, Martínez-Sarrà E, García-Fernández DA, Barajas M, Hernández-Alfaro F, Ferrés-Padró E, Giner-Tarrida L. 2012. The enhancement of osteogenesis through the use of dental pulp pluripotent stem cells in 3D. *Bone* 50(4), pp. 930-41.

Aubert G, Hills M, Lansdorp PM. 2012. Telomere length measurement-Caveats and a critical assessment of the available technologies and tools. *Mutat Res* 1;730(1-2), pp. 59-67.

Azzam HS and Thompson EW. 1992. Collagen-induced activation of the M(r) 72,000 type IV collagenase in normal and malignant human fibroblastoid cells. Cancer Res 15;52(16), pp. 4540-4.

Baird DM, Rowson J, Wynford-Thomas D, Kipling D. 2003. Extensive allelic variation and ultrashort telomeres in senescent human cells. *Nat Genet* 33(2), pp. 203-7.

Bakopoulou A, Leyhausen G, Volk J, Tsiftsoglou A, Garefis P, Koidis P, Geurtsen W. 2011. Assessment of the impact of two different isolation methods on the osteo/odontogenic differentiation potential of human dental stem cells derived from deciduous teeth. *Calcif Tissue Int* 88(2), pp. 130-41.

Baksh D, Song L, Tuan RS. 2004. Adult mesenchymal stem cells: characterization, differentiation, and application in cell and gene therapy. *J Cell Mol Med* 8(3), pp. 301-16.

Ballinger SW, Van Houten B, Jin GF, Conklin CA, Godley BF. 1999. Hydrogen peroxide causes significant mitochondrial DNA damage in human RPE cells. *Exp Eye Res* 68(6), pp. 765-72.

Banfi A, Muraglia A, Dozin B, Mastrogiacomo M, Cancedda R, Quarto R. 2000. Proliferation kinetics and differentiation potential of ex vivo expanded human bone marrow stromal cells: Implications for their use in cell therapy. *Exp Hematol* 28(6), pp. 707-15.

Barboni E, Gormley A. M, Pliego Rivero F. B, Vidal M, and Morris R. J.1991. Activation of T lymphocytes by cross-linking of glycophospholipid-anchored Thy-1 mobilizes separate pools of intracellular second messengers to those induced by the antigen-receptor/CD3 complex. *Immunology* 72, pp. 457–463.

Barrett, AJ, Rawlings, ND, Woessner, JF (Eds.). 1998. Handbook of Proteolytic Enzymes. *Academic Press, London, U.K.*

Barry F, Boynton RE, Liu B, Murphy JM. 2001. Chondrogenic differentiation of mesenchymal stem cells from bone marrow: differentiation-dependent gene expression of matrix components. *Exp Cell Res* 15;268(2), pp. 189-200.

Barry FP and Murphy JM. 2004. Mesenchymal stem cells: clinical applications and biological characterization. *Int J Biochem Cell Biol* 36(4), pp. 568-84.

Basu S, Michaëlsson K, Olofsson H, Johansson S, Melhus H. 2001. Association between oxidative stress and bone mineral density. *Biochem Biophys Res Commun* 19;288(1), pp. 275-9.

Baxter MA, Wynn RF, Jowitt SN, Wraith JE, Fairbairn LJ, Bellantuono I. 2004. Study of telomere length reveals rapid aging of human marrow stromal cells following *in vitro* expansion. *Stem Cells* 22(5), pp. 675-82.

Bayreuther K, Francz PI, Gogol J, Hapke C, Maier M, Meinrath HG. 1991. Differentiation of primary and secondary fibroblasts in cell culture systems. *Mutat Res* 256(2-6), pp. 233-42.

Beck GR Jr, Sullivan EC, Moran E, Zerler B. 1998. Relationship between alkaline phosphatase levels, osteopontin expression, and mineralization in differentiating MC3T3-E1 osteoblasts. *J Cell Biochem* 1;68(2), pp. 269-80.

Beckman KB and Ames BN. 1998. The free radical theory of aging matures. *Physiol Rev* 78(2), pp. 547-81.

Ben-Porath I and Weinberg RA. 2005. The signals and pathways activating cellular senescence. *Int J Biochem Cell Biol* 37(5), pp. 961-76.

Bendall, Sean C, Stewart, Morag H, Bhatia, Mickie. 2008. Human embryonic stem cells: lessons from stem cell niches *in vivo*. *Regenerative medicine* 3(3), pp. 365-376.

Beniash E, Deshpande AS, Fang PA, Lieb NS, Zhang X, Sfeir CS. 2011. Possible role of DMP1 in dentin mineralization. *J Struct Biol* 174(1), pp. 100-6.

Beningo KA, Dembo M, Wang YL. 2004. Responses of fibroblasts to anchorage of dorsal extracellular matrix receptors. *Proc Natl Acad Sci U S A* 101(52), pp. 18024-9.

Bennett JH, Joyner CJ, Triffitt JT, Owen ME. 1991. Adipocytic cells cultured from marrow have osteogenic potential. *J Cell Sci* 99, pp. 131–139.

Bergsma JE, Rozema FR, Bos RR, Boering G, de Bruijn WC, Pennings AJ. 1995. *In vivo* degradation and biocompatibility study of *in vitro* pre-degraded as-polymerized polyactide particles. *Biomaterials* 16(4), pp. 267-74.

Bianco P, Riminucci M, Gronthos S, Robey PG. 2001. Bone marrow stromal stem cells:nature, biology, and potential applications. *Stem* 19(3), pp. 180-92.

Blackburn EH. Telomere states and cell fates. 200. *Nature* 2;408(6808), pp. 53-6.

Bladier C, Wolvetang EJ, Hutchinson P, de Haan JB, Kola I. 1997. Response of a primary human fibroblast cell line to H_2O_2: senescence-like growth arrest or apoptosis? *Cell Growth Differ* 8(5), pp. 589-98.

Blau H.M, Brazelton T. R, and Weimann J.M. 2001. The evolving concept of a stem sell:entity or function? *Cell* 105, pp. 829–841.

Bonab MM, Alimoghaddam K, Talebian F, Ghaffari SH, Ghavamzadeh A, Nikbin B. 2006. Aging of mesenchymal stem cell *in vitro*. *BMC Cell Biol* 10, pp. 7:14.

Bongso A and Tan S. 2005. Human blastocyst culture and derivation of embryonic stem cell lines. *Stem Cell Rev* 1(2), pp. 87-98.

Boonen KJ and Post MJ. 2008. The muscle stem cell niche: regulation of satellite cells during regeneration. *Tissue Eng Part B Rev* 14(4), pp. 419-31.

Boroujeni M.E, Gowda P, Johnson J, Rao J, Saremy S. 2012. The proliferation and differentiation capacity of bone marrow derived- human mesenchymal stem cells in early and late doubling. *Asian Journal of Biochemistry* 7: 27-36.

Bott K, Upton Z, Schrobback K, Ehrbar M, Hubbell JA, Lutolf MP, Rizzi SC. 2010. The effect of matrix characteristics on fibroblast proliferation in 3D gels. *Biomaterials* 31(32), pp. 8454-64.

Brandl A, Meyer M, Bechmann V, Nerlich M, Angele P. 2011a. Oxidative stress induces senescence in human mesenchymal stem cells. *Exp Cell Res* 1;317(11), pp. 1541-7.

Brandl A, Hartmann A, Bechmann V, Graf B, Nerlich M, Angele P. 2011b. Oxidative stress induces senescence in chondrocytes. *J Orthop Res* 29(7), pp. 1114-20.

Bränvall k, Bergman K, Wallenquist U, Svahn S, Bowden T, Hilborn J, Forsberg-Nilsson. 2007. Enhanced neuronal differentiation in a three-dimensional collagen-Hyaluronan matrix. *Journal of Neuroscience Research* 85, pp. 2138-46.

Brooke G, Cook M, Blair C, Han R, Heazlewood C, Jones B, Kambouris M, Kollar K, McTaggart S, Pelekanos R, Rice A, Rossetti T, Atkinson K. 2007. Therapeutic applications of mesenchymal stromal cells. *Semin Cell Dev Biol* 18(6), pp. 846-58.

Brouilette S, Singh RK, Thompson JR, Goodall AH, Samani NJ. 2003. White cell telomere length and risk of premature myocardial infarction. *Arterioscler Thromb Vasc Biol* 1;23(5), pp. 842-6.

Bryan TM and Reddel RR. 1997. Telomere dynamics and telomerase activity in *in vitro* immortalised human cells. *Eur J Cancer* 33(5), pp. 767-73.

Bühring HJ, Treml S, Cerabona F, de Zwart P, Kanz L, Sobiesiak M. 2009. Phenotypic characterization of distinct human bone marrow-derived MSC subsets. *Ann N Y Acad Sci* 1176, pp. 124-340.

Bundesen LQ, Scheel TA, Bregman BS. 2003. Ephrin-B2 and EphB2 regulation of astrocyte-meningeal fibroblast interactions in response to spinal cord lesions in adult rats. *J Neurosci* 23, pp. 7789 –7800.

Bunnell, B.A., Flaat, M., Gagliardi, C., Patel, B., and Ripoll, C. 2008. Adipose-derived stem cells: isolation, expansion and differentiation. *Methods* 45(2), pp. 115-20.

Butcher JT and Nerem RM. 2004. Porcine aortic valve interstitial cells in three-dimensional culture: comparison of phenotype with aortic smooth muscle cells. *J Heart Valve Dis* 13(3), pp. 478-86.

Butt RP, Laurent GJ, Bishop JE. 1995. Mechanical load and polypeptide growth factors stimulate cardiac fibroblast activity. *Ann N Y Acad Sci* 27;752, pp. 387-93.

Calvi LM, Adams GB, Weibrecht KW, Weber JM, Olson DP, Knight MC, Martin RP, Schipani E, Divieti P, Bringhurst FR, Milner LA, Kronenberg HM, Scadden DT. 2003. Osteoblastic cells regulate the haematopoietic stem cell niche. *Nature* 23;425(6960), pp. 841-6.

Camargo CH, Camargo SE, Valera MC, Hiller KA, Schmalz G, Schweikl H. 2009. The induction of cytotoxicity, oxidative stress, and genotoxicity by root canal sealers in mammalian cells. *Oral Surg Oral Med Oral Pathol Oral Radiol Endod* 108(6), pp. 952-60.

Campbell A, Wicha MS, Long M. 1985. Extracellular matrix promotes the growth and differentiation of murine hematopoietic cells *in vitro. J Clin Invest* 75(6), pp. 2085-90.

Campisi J.1996. Replicative senescence: an old lives' tale? *Cell* 23;84(4), pp. 497-500.

Campisi J, d'Adda di Fagagna F. 2007. Cellular senescence: when bad things happen to good cells. *Nat Rev Mol Cell Bi*ol 8(9), pp. 729-40.

Cao L, Wang H, Wang F, Xu D, Liu F, Liu C. 2013. Aβ-induced senescent retinal pigment epithelial cells create a proinflammatory microenvironment in AMD. *Invest Ophthalmol Vis Sci* 1;54(5):3738-50.

Caplan AI. 1991. Mesenchymal stem cells. *J Orthop Res* 9, pp. 641–650.

Case J, Ingram DA, Haneline LS. 2008. Oxidative stress impairs endothelial progenitor cell function. *Antioxid Redox Signal* 10(11), pp. 1895-907.

Cavalcanti BN, Lage-Marques JL, Rode SM. 2003. Pulpal temperature increases with Er:YAG laser and high-speed handpieces. *J Prosthet* 90, pp. 447–51.

Centeno CJ, Busse D, Kisiday J, Keohan C, Freeman M, Karli D. 2008. Regeneration of meniscus cartilage in a knee treated with percutaneously implanted autologous mesenchymal stem cells. *Med Hypotheses* 71(6), pp. 900-8.

Chai Y, Jiang X, Ito Y, Bringas P Jr, Han J, Rowitch DH, Soriano P, McMahon AP, Sucov HM. 2000. Fate of the mammalian cranial neural crest during tooth and mandibular morphogenesis. *Development* 127(8), pp. 1671-9.

Challen GA, Boles N, Lin KK and Goodell MA. 2009. Mouse Hematopoietic Stem Cell Identification and Analysis. *Cytometry Part A* 75A, pp. 14-24.

Chamberlain G, Fox J, Ashton B, Middleton J. 2007. Concise review: mesenchymal stem cells: their phenotype, differentiation capacity, immunological features, and potential for homing. *Stem Cells* (11), pp. 2739-49.

Chambers, I., Colby, D., Robertson, M., Nichols, J., Lee, S., Tweedie, S and Smith, A. 2003. Functional expression cloning of Nanog, a pluripotency sustaining factor in embryonic stem cells. *Cell* 113, pp. 643–655.

Chan JW, Taylor DS, Lane SM, Zwerdling T, Tuscano J, Huser T. 2008. Nondestructive identification of individual leukemia cells by laser trapping Raman spectroscopy. *Anal Chem* 15;80(6), pp. 2180-7.

Chan JW, Lieu DK, Huser T, Li RA. 2009. Label-free separation of human embryonic stem cells and their cardiac derivatives using Raman spectroscopy. *Anal Chem* 15;81(4), pp. 1324-31.

Chang SW, Lee SI, Bae WJ, Min KS, Shin ES, Oh GS, Pae HO, Kim EC. 2009. Heat stress activates interleukin-8 and the antioxidant system via Nrf2 pathways in human dental pulp cells. *J Endod* 35(9), pp. 1222-8.

Chaussain C, Eapen AS, Huet E, Floris C, Ravindran S, Hao J, Menashi S, George A. 2009. MMP2-cleavage of DMP1 generates a bioactive peptide promoting differentiation of dental pulp stem/progenitor cell. *Eur Cell Mater* 12, pp. 18:84-95.

Chen Q and Ames BN. 1994. Senescence-like growth arrest induced by hydrogen peroxide in human diploid fibroblast F65 cells. *Proc Natl Acad Sci U S A* 10;91(10), pp. 4130-4.

Chen QM, Prowse KR, Tu VC, Purdom S, Linskens MH. 2001. Uncoupling the senescent phenotype from telomere shortening in hydrogen peroxide-treated fibroblasts. *Exp Cell Res* 1;265(2), pp. 294-303.

Chen X and Li Y. 2009 Role of matrix metalloproteinases in skeletal muscle: migration, differentiation, regeneration and fibrosis. *Cell Adh Migr* 3(4), pp. 337-41.

Cheng JX and Xie X. 2007. Coherent Anti-Stokes Raman Scattering Microscopy: Instrumentation, Theory, and Applications. *J. Phys. Chem. B* 108 (3), pp. 827–840.

Cheng H, Qiu L, Ma J, Zhang H, Cheng M, Li W, Zhao X, Liu K. 2011. Replicative senescence of human bone marrow and umbilical cord derived mesenchymal stem cells and their differentiation to adipocytes and osteoblasts. *Mol Biol Rep* 38(8), pp. 5161-8.

Chesa PG, Rettig WJ, Thomson TM, Old LJ, Melamed MR. 1988. Immunohistochemical analysis of nerve growth factor receptor expression in normal and malignant human tissues. *J Histochem Cytochem* 36(4), pp. 383-9.

Cho SW, Jeon O, Kim JE, Gwak SJ, Kim SS, Choi CY, Kim DI, Kim BS. 2006. Preliminary experience with tissue engineering of a venous vascular patch by using bone marrow-derived cells and a hybrid biodegradable polymer scaffold. *J Vasc Surg* 44(6), pp. 1329-40.

Chung IH, Yamaza T, Zhao H, Choung PH, Shi S, Chai Y. 2009. Stem cell property of postmigratory cranial neural crest cells and their utility in alveolar bone regeneration and tooth development. *Stem* 27(4), pp. 866-77.

Clark RA. 1993. Biology of dermal wound repair. *Dermatol Clin* 11(4), pp. 647-66.

Cooper GM. 2000. The cell: A molecular approach 2nd edition.

Copelan EA. 2006. Hematopoietic stem-cell transplantation. *N Engl J Med* 27;354(17), pp. 1813-26.

Coyac BR, Chicatun F, Hoac B, Nelea V, Chaussain C, Nazhat SN, McKee MD. 2013. Mineralization of dense collagen hydrogel scaffolds by human pulp cells. *J Dent Res* 92(7), pp. 648-54.

Cui Q, Wang GJ, Balian G. 1997. Steroid-induced adipogenesis in a pluripotential cell line from bone marrow. *J Bone Joint Surg Am* 79, pp. 1054–63.

Cukierman E, Pankov R, Yamada KM. 2002. Cell interactions with three-dimensional matrices. *Curr Opin Cell Biol* 14(5), pp. 633-9.

Cukierman E, Pankov R, Stevens DR, Yamada KM. 2001. Taking cell–matrix adhesions to the third dimension. *Science* 294, pp. 1708-1712.

D'Adda di Fagagna F, Reaper PM, Clay-Farrace L, Fiegler H, Carr P, Von Zglinicki T, Saretzki G, Carter NP, Jackson SP. 200. A DNA damage checkpoint response in telomere-initiated senescence. *Nature* 13;426(6963), pp. 194-8.

D'Autréaux B and Toledano MB. 2007. ROS as signalling molecules: mechanisms that generate specificity in ROS homeostasis. *Nat Rev Mol Cell* 8(10), pp. 813-24.

D'Ippolito G, Schiller PC, Ricordi C, Roos BA, Howard GA. 1999. Age-related osteogenic potential of mesenchymal stromal stem cells from human vertebral bone marrow. *J Bone Miner Res* 14(7), pp. 1115-22.

Daar AS and Greenwood HL. 2007. A proposed definition of regenerative medicine. *J Tissue Eng Regen Med* 1(3), pp. 179-84.

Dasu MR, Barrow RE, Spies M, Herndon DN. 2003. Matrix metalloproteinase expression in cytokine stimulated human dermal fibroblasts. *Burns* 29(6), pp. 527-31.

Dawson E, Mapili G, Erickson K, Taqvi S and Roy K. 2008. Biomaterials for stem cell differentiation. *Advanced Drug Delivery Reviews* 60, pp. 215-228.

Dayem A, Choi HY, Kim JY, Cho SG. 2010. Role of Oxidative Stress in Stem, Cancer, and Cancer Stem Cells. *Cancers 2*(2), pp. 859-884.

De Becker A, Van Hummelen P, Bakkus M, Vande Broek I, De Wever J, De Waele M, Van Riet I. 2007. Migration of culture-expanded human mesenchymal stem cells through bone marrow endothelium is regulated by matrix metalloproteinase-2 and tissue inhibitor of metalloproteinase-3. *Haematologica* 92(4), pp.440-9.

De Magalhães JP, Chainiaux F, Remacle J, Toussaint O. 2002. Stress-induced premature senescence in BJ and hTERT-BJ1 human foreskin fibroblasts. *FEBS Lett* 17;523(1-3), pp. 157-62.

De Mul F, van Welie A, Otto C, Mud J, Greve, J. 1984. Micro-Raman spectroscopy of chromosomes. *Journal of Raman Spectroscopy* 15(4), pp. 268-272.

Defawe OD, Kenagy RD, Choi C, Wan SY, Deroanne C, Nusgens B, Sakalihasan N, Colige A, Clowes AW. 2005. MMP-9 regulates both positively and negatively collagen gel contraction: a nonproteolytic function of MMP-9. *Cardiovasc Res* 1;66(2), pp. 402-9.

Dell'Orco RT, Mertens JG, Kruse PF Jr. 1974. Doubling potential, calendar time, and donor age of human diploid cells in culture. *Exp Cell Res* 15;84(1), pp. 363-6.

Deng W, Obrocka M, Fischer I, Prockop DJ. 2001. *In vitro* differentiation of human marrow stromal cells into early progenitors of neural cells by conditions that increase intracellular cyclic AMP. *Biochem Biophys Res Commun* 23;282(1), pp. 148-52.

Denham M, Conley B, Cole T.J and Mollard R. 2005.Stem cells: an overview chapter 23, unit 23.1.

Dernbach E, Urbich C, Brandes RP, Hofmann WK, Zeiher AM, Dimmeler S. 2004. Antioxidative stress-associated genes in circulating progenitor cells: evidence for enhanced resistance against oxidative stress. *Blood* 1;104(12), pp. 3591-7.

Deryugina EI, Ratnikov B, Monosov E, Postnova TI, DiScipio R, Smith JW, Strongin AY. 2001. MT1-MMP initiates activation of pro-MMP-2 and integrin alphavbeta3 promotes maturation of MMP-2 in breast carcinoma cells. *Exp Cell Res* 15;263(2), pp. 209-23.

Desgrosellier JS and Cheresh DA. 2010. Integrins in cancer: biological implications and therapeutic opportunities. *Nat Rev Cancer* 10(1), pp. 9-22.

Dhingra S, Sharma AK, Singla DK, Singal PK. 2007. p38 and ERK1/2 MAPKs mediate the interplay of TNF-alpha and IL-10 in regulating oxidative stress and cardiac myocyte apoptosis. *Am J Physiol Heart Circ Physiol* 293(6), pp. 524-31.

Digirolamo, C.M., Stokes, D., Colter, D., Phinney, D.G., Class, R., Prockop, D.J. 1999. Propagation and senescence of human marrow stromal cells in culture: a simple colony-forming assay identifies samples with the greatest potential to propagate and differentiate. *Br. J. Haematol* 107, pp. 275–281.

Dimri GP, Lee X, Basile G, Acosta M, Scott G, Roskelley C, Medrano EE, Linskens M, Rubelj I, Pereira-Smith O, et al. 1995. A biomarker that identifies senescent human cells in culture and in aging skin *in vivo. Proc Natl Acad Sci U S A* 26;92(20), pp. 9363-7.

Discher DE, Mooney DJ, Zandstra PW. 2009. Growth factors, matrices, and forces combine and control stem cells. *Science* 26,324(5935), pp. 1673-7.

Dissanayaka WL, Zhan X, Zhang C, Hargreaves KM, Jin L, Tong EH. 2012. Coculture of dental pulp stem cells with endothelial cells enhances osteo-/odontogenic and angiogenic potential *in vitro. J Endod* 38(4), pp. 454-63.

Dominici M, Le Blanc K, Mueller I, Slaper-Cortenbach I, Marini F, Krause D, Deans R, Keating A, Prockop Dj, Horwitz E. 2006. Minimal criteria for defining multipotent mesenchymal stromal cells. *The International Society for Cellular Therapy position statement*. Cytotherapy 8(4), pp. 315-7.

Dorval J and Hontela A. 2003. Role of glutathione redox cycle and catalase in defense against oxidative stress induced by endosulfan in adrenocortical cells of rainbow trout (Oncorhynchus mykiss). *Toxicol Appl Pharmacol* 15;192(2), pp. 191-200.

Downes A, Mouras R, Elfick A. 2010. Optical spectroscopy for noninvasive monitoring of stem cell differentiation. *J Biomed Biotechnol* 2010, article ID 101864.

Downes A, Mouras R, Bagnaninchi P, Elfick A. 2011. Raman spectroscopy and CARS microscopy of stem cells and their derivatives. *J Raman Spectrosc* 42(10), pp. 1864-1870.

Drummond-Barbosa D. 2008. Stem cells, their niches and the systemic environment: an aging network. *Genetics*180(4), pp. 1787-97.

Duan J, Duan J, Zhang Z, Tong T. 2005. Irreversible cellular senescence induced by prolonged exposure to H_2O_2 involves DNA-damage-and-repair genes and telomere shortening. *Int J Biochem Cell Biol* 37(7), pp. 1407-20.

Dukor RK. 2002. Vibrational spectroscopy of the detection of cancer. Handbook of vibrational spectroscopy, in: applications of vibrational spectroscopy in live and natural Sciences, Five volume set, John Wiley&Sons LTD, pp. 3335–3361.

Duque C, Hebling J, Smith AJ, Giro EMA, Oliveira MF and De Souza Costa CA. 2006. Reactionary dentinogenesis after applying restorative materials and bioactive dentin matrix molecules as liners in deep cavities prepared in nonhuman primate teeth. *Journal of Oral Rehabilitation* 33, pp. 452–461.

Eastwood M, Mudera VC, McGrouther DA, Brown RA. 1998. Effect of precise mechanical loading on fibroblast populated collagen lattices: morphological changes. *Cell Motil Cytoskeleton* 40(1), pp. 13-21.

Ebert R, Ulmer M, Zeck S, Meissner-Weigl J, Schneider D, Stopper H, Schupp N, Kassem M, Jakob F. 2006. Selenium supplementation restores the antioxidative capacity and prevents cell damage in bone marrow stromal cells *in vitro. Stem Cells* 24(5), pp. 1226-35.

El-Deiry WS, Tokino T, Velculescu VE, Levy DB, Parsons R, Trent JM, Lin D, Mercer WE, Kinzler KW, Vogelstein B. 1993. WAF1, a potential mediator of p53 tumor suppression. *Cell* 19;75(4), pp. 817-25.

Eliasson P and Jönsson JI. 2010. The hematopoietic stem cell niche: low in oxygen but a nice place to be. *J Cell Physiol* 222(1), pp. 17-22

Elsdale T and Bard J. 1972. Collagen substrata for studies on cell behavior. *J Cell Biol* **54**, pp. 626-637.

Ema H and Suda T. 2012. Two anatomically distinct niches regulate stem cell activity. *Blood* 120(11), pp. 2174-81.

Evans MD, Dizdaroglu M, Cooke MS. 2004. Oxidative DNA damage and disease: Induction, repair and significance. *Mutat Res* 567, pp. 1-61.

Fattman CL, Schaefer LM, Oury TD. 2003. Extracellular superoxide dismutase in biology and medicine. *Free Rad Biol Med* 35, pp. 236-256.

Fedorovich NE, Haverslag RT, Dhert WJ, Alblas J. 2010. The role of endothelial progenitor cells in prevascularized bone tissue engineering: development of heterogeneous constructs. *Tissue Eng Part A* 16(7), pp. 2355-67.

Fehrer C and Lepperdinger G. 2005. Mesenchymal stem cell aging. *Exp Gerontol* 40(12), pp. 926-30.

Feng J, Mantesso A, De Bari C, Nishiyama A, Sharpe PT. 2011. Dual origin of mesenchymal stem cells contributing to organ growth and repair. *Proc Natl Acad Sci U S A* 19;108(16), pp. 6503-8.

Fickert S, Schröter-Bobsin U, Gross AF, Hempel U, Wojciechowski C, Rentsch C, Corbeil D, Günther KP. 2011. Human mesenchymal stem cell proliferation and osteogenic differentiation during long-term ex vivo cultivation is not age dependent. *J Bone Miner Metab* 29(2), pp. 224-35.

Finkel T and Holbrook NJ. 2000. Oxidants, oxidative stress and the biology of ageing. *Nature*. 408(6809), pp. 239-47.

Fitzgerald M, Chiego DJ Jr, Heys DR. 1990. Autoradiographic analysis of odontoblast replacement following pulp exposure in primate teeth. *Arch Oral Biol* 35(9), pp. 707-15.

Flaim CJ, Chien S, Bhatia SN. 2005. An extracellular matrix microarray for probing cellular differentiation. *Nat Methods* 2(2), pp. 119-25.

Flores I and Blasco MA. 2010. The role of telomeres and telomerase in stem cell aging. *FEBS Lett* 10;584(17), pp. 3826-30.

Flores I, Benetti R, Blasco MA. 2006. Telomerase regulation and stem cell behaviour. *Curr Opin Cell Biol* 18(3), pp. 254-60.

Forsberg EC and Smith-Berdan S. 2009. Parsing the niche code: the molecular mechanisms governing hematopoietic stem cell adhesion and differentiation. *Haematologica* 94(11), pp. 1477-81.

Frei B, Yamamoto Y, Niclas D, Ames BN. 1988. Evaluation of an isoluminol chemiluminescence assay for the detection of hydroperoxides in human blood plasma. *Anal Biochem* 15;175(1), pp.120-30.

Friedenstein AJ, Petrakova KV, Kurolesova AI, Frolova GP. 1968. Heterotopic of bone marrow; Analysis of precursor cells for osteogenic and hematopoietic tissues. Transplantation 6, pp. 230–247.

Friedenstein AJ, Chailakhjan RK, Lalykina KS. 1970. The development of fibroblast colonies in monolayer cultures of guinea-pig bone marrow and spleen cells. *Cell Tissue Kinet* 3(4), pp. 393-403.

Friedenstein AJ, Latzinik NW, Grosheva AG, Gorskaya UF. 1982. Marrow microenvironment transfer by heterotopic transplantation of freshly isolated and cultured cells in porous sponges. *Exp Hematol* 10(2), pp. 217-27.

Friedenstein AJ, Chailakhyan RK, Gerasimov UV. 1987. Bone marrow osteogenic stem cells: *In vitro* cultivation and transplantation in diffusion chambers. *Cell Tissue Kinet* 20, pp. 263–272.

Fringer J and Grinnell F. 2001. Fibroblast quiescence in floating or released collagen matrices: contribution of the ERK signaling pathway and actin cytoskeletal organization. *J Biol Chem* 17;276(33), pp. 31047-52.

Fuchs E, Tumbar T and Guash G. 2004. Socializing with the neighbors: stem cells and their niche. *Cell* 116(6), pp. 634-7.

Gabbay JS, Heller JB, Mitchell SA, Zuk PA, Spoon DB, Wasson KL, Jarrahy R, Benhaim P, Bradley JP. 2006. Osteogenic potentiation of human adipose-derived stem cells in a 3-dimensional matrix. *Ann Plast Surg* 57(1), pp. 89-93.

Gafni Y, Turgeman G, Liebergal M, Pelled G, Gazit Z, Gazit D. 2004. Stem cells as vehicles for orthopedic gene therapy. *Gene Ther* 11(4), pp. 417-26.

Gala K, Burdzińska A, Idziak M, Makula J, Pączek L. 2011. Characterization of bone-marrow-derived rat mesenchymal stem cells depending on donor age. *Cell Biol Int* 35(10), pp. 1055-62.

Gelse K, Pöschl E, Aigner T. 2003. Collagens-structure, function, and biosynthesis. *Adv Drug Deliv Rev* 28;55(12), pp. 1531-46.

Gharibi B and Hughes FJ. 2012. Effects of medium supplements on proliferation, differentiation potential, and *in vitro* expansion of mesenchymal stem cells. *Stem Cells Transl Med* 1(11), pp. 771-82.

Ghita A, Pascut FC, Mather M, Sottile V, Notingher I. 2012. Cytoplasmic RNA in undifferentiated neural stem cells: a potential label-free Raman spectral marker for assessing the undifferentiated status. *Anal Chem* 3;84(7), pp. 3155-62.

Giannoni E, Buricchi F, Raugei G, Ramponi G, Chiarugi P. 2005. Intracellular reactive oxygen species activate Src tyrosine kinase during cell adhesion and anchorage-dependent cell growth. Mol Cell Biol 25(15), pp. 6391-403.

Gilles C, Polette M, Seiki M, Birembaut P, Thompson EW. 1997. Implication of collagen type I-induced membrane-type 1-matrix metalloproteinase expression and matrix metalloproteinase-2 activation in the metastatic progression of breast carcinoma. *Lab Invest* 76(5), pp. 651-60.

Giorgio M, Trinei M, Migliaccio E, Pelicci PG. 2007. Hydrogen peroxide: a metabolic by-product or a common mediator of ageing signals? *Nat Rev Mol Cell Biol* 8(9), pp. 722-8.

Glaeser JD, Geissler S, Ode A, Schipp CJ, Matziolis G, Taylor WR, Knaus P, Perka C, Duda GN, Kasper G. 2010. Modulation of matrix metalloprotease-2 levels by mechanical loading of three-dimensional mesenchymal stem cell constructs: impact on *in vitro* tube formation. *Tissue Eng Part A* 16(10), pp. 3139-48.

Glowacki J and Mizuno S. 2008. Collagen scaffolds for tissue engineering. Biopolymers 89(5), pp. 338-44.

Gluckman E, Broxmeyer HA, Auerbach AD. 1989. Hematopoietic reconstitution in a patient with Fanconi's anemia by means of umbilical-cord blood from an HLA-identical sibling. *N Engl J Med* 321, pp. 1174-1178.

Goldberg IJ. 1996. Lipoprotein lipase and lipolysis: central roles in lipoprotein metabolism and atherogenesis. *J Lipid Res* 37(4), pp. 693-707.

Goldberg M, Farges JC, Lacerda-Pinheiro S, Six N, Jegat N, Decup F, Septier D, Carrouel F, Durand S, Chaussain-Miller C, Denbesten P, Veis A, Poliard A. 2008. Inflammatory and immunological aspects of dental pulp repair. Phar*macol Res* 58(2), pp. 137-47.

Gonzalo S, Jaco I, Fraga MF, Chen T, Li E, Esteller M, Blasco MA. 2006. DNA methyltransferases control telomere length and telomere recombination in mammalian cells. *Nat Cell Biol* 8(4), pp. 416-24.

Goralczyk R, Appold A, Luz A, Riemann S, Strauss PG, Erfle V, Schmidt J. 1998. Establishment and characterization of osteoblast-like cell lines from retrovirus (RFB MuLV)-induced osteomas in mice. *Differentiation* 63(5), pp. 253-62.

Goshima J, Goldberg VM, Caplan AI. 1991. The origin of bone formed in composite grafts of porous calcium phosphate ceramic loaded with marrow cells. Clin Ortho Rel Res 269, pp. 274-283.

Góth L. 2008. Catalase deficiency and type 2 diabetes. *Diabetes Care* 31(12), e93.

Graziano A, d'Aquino R, Cusella-De Angelis MG, De Francesco F, Giordano A, Laino G, Piattelli A, Traini T, De Rosa A, Papaccio G. 2008. Scaffold's surface geometry significantly affects human stem cell bone tissue engineering. *J Cell Physiol* 214(1), pp. 166-72.

Graziano A, d'Aquino R, Laino G, Papaccio G. 2008. Dental pulp stem cells: a promising tool for bone regeneration. *Stem Cell Rev* 4(1), pp. 21-6.

Grinnell F, Zhu M, Carlson MA, Abrams JM. 1999. Release of mechanical tension triggers apoptosis of human fibroblasts in a model of regressing granulation tissue. *Exp Cell Res* 1;248(2), pp. 608-19.

Grinnell F. 2000. Fibroblast-collagen-matrix contraction: growth-factor signalling and mechanical loading. *Trends Cell Biol* 10(9), pp. 362-5.

Gronthos S, Mankani M, Brahim J, Robey PG, Shi S. 2000. Postnatal human dental pulp stem cells (DPSC) *in vitro* and *in vivo*. *Proc Natl Acad Sci USA* 97, pp. 13625-13630.

Gronthos S, Brahim J, Li W, Fisher LW, Cherman N, Boyde A, DenBesten P, Robey PG, Shi S. 2002. Stem cell properties of human dental pulp stem cells. *J Dent Res* 81(8), pp. 531-5.

Guilak F, Lott KE, Awad HA, Cao Q, Hicok KC, Fermor B, Gimble JM. 2006. Clonal analysis of the differentiation potential of human adipose-derived adult stem cells. *J Cell Physiol* 206(1), pp. 229-37.

Guilak F, Cohen DM, Estes BT, Gimble JM, Liedtke W, Chen CS. 2009. Control of stem cell fate by physical interactions with the extracellular matrix. *Cell Stem Cell* 2009 2;5(1), pp. 17-26.

Guo Y, Costa R, Ramsey H, Starnes T, Vance G, Robertson K, Kelley M, Reinbold R, Scholer H, Hromas R. 2002. The embryonic stem cell transcription factors Oct-4 and FoxD3 interact to regulate endodermal-specific promoter expression. *Proc Natl Acad Sci U S A* 19;99(6), pp. 3663-7.

Gurtner GC, Callaghan MJ, Longaker MT. 2007. Progress and potential for regenerative medicine. *Annu Rev Med* 58, pp. 299-312.

Halleux C, Sottile V, Gasser JA, Seuwen K. 2001. Multi-lineage potential of human mesenchymal stem cells following clonal expansion. *J Musculoskelet Neuronal Interact* 2(1), pp. 71-6.

Hadjipanayi E, Mudera V, Brown RA.2009. Close dependence of fibroblast proliferation on collagen scaffold matrix stiffness. *J Tissue Eng Regen Med* 3(2):77-84.

Halliwell B and Gutteridge JM. 1990. Role of free radicals and catalytic metal ions in human disease: an overview. *Methods Enzymol* 186, pp. 1-85.

Halliwell B, Gutteridge JM, Cross CE. 1992. Free radicals, antioxidants, and human disease: Where are we now? *J Lab Clin Med* 119, pp. 598-620.

Halliwell B, Clement MV, Long LH. 2000. Hydrogen peroxide in the human body. *FEBS Lett* 1;486(1), pp. 10-3.

Halliwell B. 2012. Free radicals and antioxidants: updating a personal view. *Nutr Rev* 70(5), pp. 257-65.

Hanada K, Dennis JE, Caplan AI. 1997. Stimulatory effects of basic fibroblast growth factor and bone morphogenetic protein-2 on osteogenic differentiation of rat bone marrow-derived mesenchymal stem cells. *J Bone Miner Res* 12(10), pp. 1606-14.

Hannas AR, Pereira JC, Granjeiro JM, Tjäderhane L. 2007. The role of matrix metalloproteinases in the oral environment. *Acta Odontol Scand* 65(1), pp. 1-13.

Hao H, Chen G, Liu J, Ti D, Zhao Y, Xu S, Fu X, Han W. 2013. Culturing on Wharton's jelly extract delays mesenchymal stem cell senescence through p53 and p16INK4a/pRb pathways. *PLoS One* 8(3):e58314.

Harley C, Futcher B, Greider C. 1990. Telomeres shorten during ageing of human fibroblasts. *Nature* 345, pp. 458–460.

Harley CB. 1991. Telomere loss: mitotic clock or genetic time bomb? *Mutat Res* 256(2-6), pp. 271-82.

Harkness L, Novikov SM, Beermann J, Bozhevolnyi SI, Kassem M. 2012. Identification of abnormal stem cells using Raman spectroscopy. *Stem Cells Dev* 10;21(12), pp. 2152-9.

Harman D. 1956. Aging: a theory based on free radical and radiation chemistry. *J Gerontol*. 11(3), pp. 298-300.

Hasegawa T, Nishijo J, Umemura J. 200. Separation of Raman spectra from fluorescence emission background by principal component analysis. *Chem. Phys* 317, pp. 642-646.

Hassan MQ, Javed A, Morasso MI, Karlin J, Montecino M, van Wijnen AJ, Stein GS, Stein JL, Lian JB. 2007. Dlx3 transcriptional regulation of osteoblast differentiation: temporal recruitment of Msx2, Dlx3, and Dlx5 homeodomain proteins to chromatin of the osteocalcin gene. *Mol Cell Biol* 24(20), pp. 9248-61.

Hayflick L and Moorhead PS. 1961. The serial cultivation of human diploid cell strains. *Exp Cell Res* 25, pp. 585-621.

He T, Peterson TE, Holmuhamedov EL, Terzic A, Caplice NM, Oberley LW, Katusic ZS. 2004. Human endothelial progenitor cells tolerate oxidative stress due to intrinsically high expression of manganese superoxide dismutase. *Arterioscler Thromb Vasc Biol* 24(11), pp. 2021-7.

He F, Yang Z, Tan Y, Yu N, Wang X, Yao N, Zhao J. 2009. Effects of Notch ligand Delta1 on the proliferation and differentiation of human dental pulp stem cells *in vitro. Arch Oral Biol* 54(3), pp. 216-22.

Henle ES, Han Z, Tang N, Rai P, Luo Y, Linn S. 1999. Sequence-specific DNA cleavage by Fe2+-mediated fenton reactions has possible biological implications. *J Biol Chem* 8;274(2), pp. 962-71.

Hernández B, Pflüger F, Adenier A, Kruglik SG, Ghomi M. 2010. Vibrational analysis of amino acids and short peptides in hydrated media. VIII. Amino acids with aromatic side chains: L-phenylalanine, L-tyrosine, and L-tryptophan. *J Phys Chem B* 25;114(46), pp. 15319-30.

Hesse E, Hefferan TE, Tarara JE, Haasper C, Meller R, Krettek C, Lu L, Yaszemski MJ. 2010. Collagen type I hydrogel allows migration, proliferation, and osteogenic differentiation of rat bone marrow stromal cells. *J Biomed Mater Res A* 94(2), pp. 442-9.

Higuera GA, Schop D, Spitters TW, van Dijkhuizen-Radersma R, Bracke M, de Bruijn JD, Martens D, Karperien M, van Boxtel A, van Blitterswijk CA. 2012. Patterns of amino acid metabolism by proliferating human mesenchymal stem cells. *Tissue Eng Part A* 18(5-6), pp. 654-64.

Hiyama E and Hiyama K. 2007. Telomere and telomerase in stem cells. *Br J Cancer* 10;96(7), pp. 1020-4.

Ho AD. 2005. Kinetics and symmetry of divisions of hematopoietic stem cells. *Exp Hematol* 33(1), pp. 1-8.

Hoffman L.M and Carpenter M.K. 2005. Characterization and culture of human embryonic stem cells. *Nature Biotechnology* 23(6), pp. 699-708.

Hołowiecki J. 2008. Indications for hematopoietic stem cell transplantation. *Pol Arch Med Wewn* 118(11), pp. 658-63.

Honda MJ, Imaizumi M, Tsuchiya S, Morsczeck C. 2010. Dental follicle stem cells and tissue engineering. *J Oral Sci* 52(4), pp. 541-52.

Hosoya A, Hiraga T, Ninomiya T, Yukita A, Yoshiba K, Yoshiba N, Takahashi M, Ito S, Nakamura H. 2012. Thy-1-positive cells in the subodontoblastic layer possess

high potential to differentiate into hard tissue-forming cells. *Histochem Cell Biol* 137(6), pp. 733-42.

House M, Sanchez CC, Rice WL, Socrate S, Kaplan DL. 2010. Cervical tissue engineering using silk scaffolds and human cervical cells. *Tissue Eng Part A* 16(6), pp. 2101-12.

Howard EW, Crider BJ, Updike DL, Bullen EC, Parks EE, Haaksma CJ, Sherry DM, Tomasek JJ. 2012. MMP-2 expression by fibroblasts is suppressed by the myofibroblast phenotype. *Exp Cell Res* 1;318(13), pp. 1542-53.

Hu YF, Gourab K, Wells C, Clewes O, Schmit BD, Sieber-Blum M. 2010. Epidermal neural crest stem cell (EPI-NCSC)- mediated recovery of sensory function in a mouse model of spinal cord injury. *Stem Cell Rev* 6(2), pp. 186-98.

Huang GT, Sonoyama W, Chen J, Park SH. 2006. *In vitro* characterization of human dental pulp cells: various isolation methods and culturing environments. *Cell Tissue Research* 324, pp. 225–36.

Huang E, Lian X, Chen W, Yang T and Yang L. 2009a. Characterization of rat hair follicle stem cells selected by vario magnetic activated cell sorting system. *Acta Histochem Cytochem* 30;42(5), pp. 129-36.

Huang GT, Gronthos S, Shi S. 2009b. Mesenchymal stem cells derived from dental tissues vs. those from other sources: their biology and role in regenerative medicine. *J Dent Res*, 88(9), pp. 792-806.

Huang J, Zhao L, Xing L, Chen D. 2010. MicroRNA-204 regulates Runx2 protein expression and mesenchymal progenitor cell differentiation. *Stem Cells* 28(2), pp. 357-64.

Huang WY, Yang PM, Chang YF, Marquez VE, Chen CC. 2011. Methotrexate induces apoptosis through p53/p21-dependent pathway and increases E-cadherin

expression through downregulation of HDAC/EZH2. *Biochem Pharmacol* 15;81(4), pp. 510-7.

Hubbel, J.A. 1995. Biomaterials in tissue engineering. *Biotechnology* 13, 565

Hutmacher DW. 2000. Scaffolds in tissue engineering bone and cartilage. *Biomaterials* 21(24), pp. 2529-43.

Hwang, Y.S, Randle, W.L, Bielby, R.., Polak, J.M, Mantalaris, A. 2006. Enhanced derivation of osteogenic cells from murine embryonic stem cells after treatment with HepG2 conditioned medium and modulation of the embryoid body formation period: application to skeletal tissue engineering. *Tissue Eng* 12 (6), pp. 1381-92.

Ibarretxe G, Crende O, Aurrekoetxea M, García-Murga V, Etxaniz J, Unda F. 2012. Neural crest stem cells from dental tissues: a new hope for dental and neural regeneration. *Stem Cells Int* 2012:103503.

Ikada Y. 2006. Challenges in tissue engineering. *J R Soc Interface* 22;3(10), pp. 589-601.

Inaba M and Yamashita YM. 2012. Asymmetric stem cell division: precision for robustness. *Cell Stem Cell* 5;11(4), pp. 461-9.

Ingram DA, Krier TR, Mead LE, McGuire C, Prater DN, Bhavsar J, Saadatzadeh MR, Bijangi-Vishehsaraei K, Li F, Yoder MC, Haneline LS. 2007. Clonogenic endothelial progenitor cells are sensitive to oxidative stress. *Stem Cells* 25(2), pp. 297-304.

Iohara K, Nakashima M, Ito M, Ishikawa M, Nakasima A, Akamine A. 2004. Dentin regeneration by dental pulp stem cell therapy with recombinant human bone morphogenic protein 2. *Journal of Dental Research* 83, pp. 590–5.

Itahana, K., Dimri, G., Campisi, J. 2001. Regulation of cellular senescence by p53. *Eur. J. Biochem* 268, pp. 2784–91.

Jaiswal RK, Jaiswal N, Bruder SP, Mbalaviele G, Marshak DR, Pittenger MF. 2000. Adult human mesenchymal stem cell differentiation to the osteogenic or adipogenic lineage is regulated by mitogen-activated protein kinase. *J Biol Chem* 31;275(13), pp. 9645-52.

Javazon EH, Beggs KJ, Flake AW. 2004. Mesenchymal stem cells: paradoxes of passaging. *Exp Hematol* 32(5), pp. 414-25.

Jean C, Gravelle P, Fournie JJ, Laurent G. 2011. Influence of stress on extracellular matrix and integrin biology. *Oncogene* 16;30(24), pp. 2697-706.

Jiang H and Grinnell F. 2005. Cell-matrix entanglement and mechanical anchorage of fibroblasts in three-dimensional collagen matrices. *Mol Biol Cell* 16(11), pp. 5070-6.

Jeon MS, Yi TG, Lim HJ, Moon SH, Lee MH, Kang JS, Kim CS, Lee DH, Song SU. 2011. Characterization of mouse clonal mesenchymal stem cell lines established by subfractionation culturing method. *World J Stem Cells* 26;3(8), pp. 70-82.

Jo Y-Y, Lee H-J, Kook S-Y, Choung H-W, Park J-Y, Chung J-H, Choung Y-H, Kim E-S, Yang H-C, Choung P-H. 2007. Isolation and characterization of postnatal stem cells from human dental tissues. *Tissue Eng* 13(4), pp. 767–773.

Johnstone B, Hering TM, Caplan AI, Goldberg VM, Yoo JU. 1998. *In vitro* chondrogenesis of bone marrow-derived mesenchymal progenitor cells. *Exp Cell Res* 10;238(1), pp. 265-72.

Jolliffe I.T. 2002. Principal Component Analysis, Series: Springer Series in Statistics, 2nd ed. *Springer* 487, p. 28 illus.

Jones PH and Watt FM. 1993. separation of human epidermal stem cells from transit amplifying cells on the basis differences in integrin function and expression. *cell* 73, pp. 713-24.

Ju Z, Choudhury AR, Rudolph KL. 2007. A dual role of p21 in stem cell aging. *Ann N Y Acad Sci* 1100, pp. 333-44.

Justesen J, Stenderup K, Eriksen EF, Kassem M. 2002. Maintenance of osteoblastic and adipocytic differentiation potential with age and osteoporosis in human marrow stromal cell cultures. *Calcif Tissue Int* 71(1), pp. 36-44.

Kachynski AV, Kuzmin AN, Prasad PN, Smalyukh II. 2008. Realignment-enhanced coherent anti-Stokes Raman scattering and three-dimensional imaging in anisotropic fluids. *Opt Express* 7;16(14), pp. 10617-32.

Kähäri,VM and Saarialho-Kere,U.1997.Matrix metalloproteinases in skin. *Exp Dermatol* 6, pp. 199-213.

Kalcheim C and Burstyn-Cohen T. 2005. Early stages of neural crest ontogeny: formation and regulation of cell delamination. *Int J Dev Biol* 49(2-3), pp. 105-16.

Kamio K, Liu XD, Sugiura H, Togo S, Kawasaki S, Wang X, Ahn Y, Hogaboam C, Rennard SI. 2010. Statins inhibit matrix metalloproteinase release from human lung fibroblasts. *Eur Respir J* 35(3), pp. 637-46.

Kamp, DW. 2003. Idiopathic pulmonary fibrosis: The inflammation hypothesis revisited. *Chest* 124, pp. 1187-90.

Kanis JA, Melton LJ 3rd, Christiansen C, Johnston CC, Khaltaev N. 1994. The diagnosis of osteoporosis. *J Bone Miner Res* 9(8), pp. 1137-41.

Karamichos D, Brown RA, Mudera V. 2007. Collagen stiffness regulates cellular contraction and matrix remodeling gene expression. *J Biomed Mater Res A* 1;83(3), pp. 887-94.

Karaöz E, Doğan BN, Aksoy A, Gacar G, Akyüz S, Ayhan S, Genç ZS, Yürüker S, Duruksu G, Demircan PC, Sariboyaci AE. 2010. Isolation and *in vitro*

characterisation of dental pulp stem cells from natal teeth. *Histochem Cell Biol* 133(1), pp. 95-112.

Karbanová J, Soukup T, Suchánek J, Pytlík R, Corbeil D, Mokrý J. 2011. Characterization of dental pulp stem cells from impacted third molars cultured in low serum-containing medium. *Cells Tissues Organs* 193(6), pp. 344-65.

Karystinou A, Dell'Accio F, Kurth TB, Wackerhage H, Khan IM, Archer CW, Jones EA, Mitsiadis TA, De Bari C. 2009. Distinct mesenchymal progenitor cell subsets in the adult human synovium. *Rheumatology (Oxford)* 48(9), pp. 1057-64.

Kasper G, Glaeser JD, Geissler S, Ode A, Tuischer J, Matziolis G, Perka C, Duda GN. 2007. Matrix metalloprotease activity is an essential link between mechanical stimulus and mesenchymal stem cell behavior. *Stem Cells* 25(8), pp. 1985-94.

Kawanabe N, Murata S, Fukushima H, Ishihara Y, Yanagita T, Yanagita E, Ono M,Kurosaka H, Kamioka H, Itoh T, Kuboki T, Yamashiro T. 2012. Stage-specific embryonic antigen-4 identifies human dental pulp stem cells. Exp Cell Res 10;318(5), pp. 453-63.

Kelly DJ and Jacobs CR. 2010. The role of mechanical signals in regulating chondrogenesis and osteogenesis of mesenchymal stem cells. *Birth Defects Res C Embryo Today* 90(1), pp. 75-85.

Kerkis I, Kerkis A, Dozortsev D, Stukart-Parsons GC, Gomes Massironi SM, Pereira LV, Caplan AI, Cerruti HF. 2006. Isolation and characterization of a population of immature dental pulp stem cells expressing OCT-4 and other embryonic stem cell markers. *Cells Tissues Organs* 184(3-4), pp. 105-16.

Khademhosseini, A, Vacanti, J, Langer, R. 2009. Tissue Engineering: next generation tissue constructs and challenges to clinical practice. *Sci Am* 300 (5), pp. 64-71.

Khan KM, Falcone DJ, Kraemer R. 2002. Nerve growth factor activation of Erk-1 and Erk-2 induces matrix metalloproteinase-9 expression in vascular smooth muscle cells. *J Biol Chem*. 18;277(3), pp. 2353-9.

Khanna-Jain R, Mannerström B, Vuorinen A, Sándor GK, Suuronen R, Miettinen S. 2012. Osteogenic differentiation of human dental pulp stem cells on β-tricalcium phosphate/poly (l-lactic acid/caprolactone) three-dimensional scaffolds. *J Tissue Eng* 3(1):2041731412467998.

Kihara T, Hirose M, Oshima A, Ohgushi H. 2006. Exogenous type I collagen facilitates osteogenic differentiation and acts as a substrate for mineralization of rat marrow mesenchymal stem cells *in vitro. Biochem Biophys Res Commun* 24;341(4), pp. 1029-35.

Kim BS and Mooney DJ. 1998. Development of biocompatible synthetic extracellular matrices for tissue engineering. *Trends Biotechnol* 16(5), pp. 224-30.

Kim JW and Simmer JP. 2007. Hereditary Dentin Defects. *J Dent Res* 86(5), pp. 392-399.

Kim JC, Lee YH, Yu MK, Lee NH, Park JD, Bhattarai G, Yi HK. 2012. Anti-inflammatory mechanism of PPARγ on LPS-induced pulp cells: role of the ROS removal activity.*Arch Oral Biol* 57(4), pp. 392-400.

Kim BC, Bae H, Kwon IK, Lee EJ, Park JH, Khademhosseini A, Hwang YS. 2012a. Osteoblastic/cementoblastic and neural differentiation of dental stem cells and their applications to tissue engineering and regenerative medicine. Tissue Eng Part B Rev 18(3), pp. 235-44.

Kim M, Kim C, Choi YS, Kim M, Park C, Suh Y. 2012b. Age-related alterations in mesenchymal stem cells related to shift in differentiation from osteogenic to adipogenic potential: implication to age-associated bone diseases and defects. *Mech Ageing Dev* 133(5), pp. 215-25.

Kimura M, Stone RC, Hunt SC, Skurnick J, Lu X, Cao X, Harley CB, Aviv A. 2010. Measurement of telomere length by the Southern blot analysis of terminal restriction fragment lengths. *Nat Protoc* 5(9), pp. 1596-607.

King GN, King N, Cruchley AT, Wozney JM, Hughs FJ . 1997. Recombinant human bone morphogenic protein-2 promotes wound healing in rat periodontal fenestration defects. *Journal of Dental Research* 76, pp. 1460–70.

Kippin TE, Martens DJ, van der Kooy D. 2005. p21 loss compromises the relative quiescence of forebrain stem cell proliferation leading to exhaustion of their proliferation capacity. *Genes Dev* 15;19(6), pp. 756-67.

Koch TG, Heerkens T, Thomsen PD, Betts DH. 2007. Isolation of mesenchymal stem cells from equine umbilical cord blood. *BMC Biotechnol* 30, pp. 7-26.

Komada Y, Yamane T, Kadota D, Isono K, Takakura N, Hayashi S, Yamazaki H. 2012. Origins and properties of dental, thymic, and bone marrow mesenchymal cells and their stem cells. *PLoS One* 7(11):e46436.

Komori T, Yagi H, Nomura S, Yamaguchi A, Sasaki K, Deguchi K, Shimizu Y, Bronson RT, Gao YH, Inada M, Sato M, Okamoto R, Kitamura Y, Yoshiki S, Kishimoto T. 1997. Targeted disruption of Cbfa1 results in a complete lack of bone formation owing to maturational arrest of osteoblasts. *Cell* 30;89(5), pp. 755-64.

Komori T. 2010. Regulation of osteoblast differentiation by Runx2. *Adv Exp Med Biol* 658, pp. 43-9.

Kopen GC, Prockop DJ, Phinney DG. 1999. Marrow stromal cells migrate throughout forebrain and cerebellum, and they differentiate into astrocytes after injection into neonatal mouse brains. *Proc Natl Acad Sci USA* 96, pp. 10711-16.

Kowluru RA and Chan PS. 2007. Oxidative stress and diabetic retinopathy. *Exp Diabetes Res* 2007:43603.

Kuhn NZ and Tuan RS. 2009. Regulation of Stemness and Stem Cell Niche of Mesenchymal Stem Cells: Implications in Tumorigenesis and Metastasis. *Journal of cellular physiology* 222, pp. 268-277.

Koyama N, Okubo Y, Nakao K, Bessho K. 2009. Evaluation of pluripotency in human dental pulp cells. *J Oral Maxillofac Surg* 67(3), pp. 501-6.

Kratchmarova I, Blagoev B, Haack-Sorensen M, Kassem M, Mann M. 2005. Mechanism of divergent growth factor effects in mesenchymal stem cell differentiation. *Science* 3,308(5727), pp. 1472-7.

Kretlow JD, Jin YQ, Liu W, Zhang WJ, Hong TH, Zhou G, Baggett LS, Mikos AG, Cao Y. 2008. Donor age and cell passage affects differentiation potential of murine bone marrow-derived stem cells. *BMC Cell Biol* 28, pp. 9-60.

Kubo Y, Kaidzu S, Nakajima I, Takenouchi K, Nakamura F. 2000. Organization of extracellular matrix components during differentiation of adipocytes in long-term culture. *In Vitro Cell Dev Biol Anim* 36(1), pp. 38-44.

Kuçi S, Kuçi Z, Kreyenberg H, Deak E, Pütsch K, Huenecke S, Amara C, Koller S, Rettinger E, Grez M, Koehl U, Latifi-Pupovci H, Henschler R, Tonn T, von Laer D, Klingebiel T, Bader P. 2010. CD271 antigen defines a subset of multipotent stromal cells with immunosuppressive and lymphohematopoietic engraftment-promoting properties. *Haematologica* 95(4), pp. 651-9.

Langer R and Vacanti JP. 1993. Tissue engineering. *Science* 14;260(5110) pp. 920-6.

Lanza RP, Langer RS, Vacanti J. 2007. Principles of tissue engineering. Amsterdam; Boston: Elsevier / Academic Press. xxvii, 1307 p.p.

Lavrentieva A, Hatlapatka T, Neumann A, Weyand B, Kasper C. 2013. Potential for Osteogenic and Chondrogenic Differentiation of MSC. *Adv Biochem Eng Biotechnol* 129, pp. 73-88.

Lee MH and Murphy G. 2004. Matrix metalloproteinases at a glance. *J Cell Sci* 15;117(Pt 18), pp. 4015-6.

Lee G, Kim H, Elkabetz Y, Al Shamy G, Panagiotakos G, Barberi T, Tabar V, Studer L. 2007. Isolation and directed differentiation of neural crest stem cells derived from human embryonic stem cells. *Nat Biotechnol* 25(12), pp. 1468-75.

Lee S, Song JY, Kwon ES, Roe JH. 2008. Gpx1 is a stationary phase-specific thioredoxin peroxidase in fission yeast. *Biochem Biophys Res Comms* 367, pp. 67–71.

Lee JH, Yu HS, Lee GS, Ji A, Hyun JK, Kim HW. 2011. Collagen gel three-dimensional matrices combined with adhesive proteins stimulate neuronal differentiation of mesenchymal stem cells. *J R Soc Interface* 6;8(60), pp. 998-1010.

Lefebvre V, Huang W, Harley VR, Goodfellow PN, de Crombrugghe B. 1997. SOX9 is a potent activator of the chondrocyte-specific enhancer of the pro alpha1(II) collagen gene. *Mol Cell Biol* 17(4), pp. 2336-46.

Leite MF, Ganzerla E, Marques MM, Nicolau J. 2008. Diabetes induces metabolic alterations in dental pulp. *J Endod* 34(10), pp. 1211-4.

Lengner CJ, Welstead GG, Jaenisch R. 2008. The pluripotency regulator Oct4: a role in somatic stem cells? *Cell Cycle* 15;7(6), pp. 725-8.

Lesot H, Bègue-Kirn C, Kübler MD, Meyer JM, Smith AJ, Cassidy N, Ruch J.V. 1993. Experimental induction of odontoblast differentiation and stimulation during reparative processes. *Cell Mater* 3, pp. 201–17.

Li C, Vepari C, Jin HJ, Kim HJ, Kaplan DL. 2006. Electrospun silk-BMP-2 scaffolds for bone tissue engineering. *Biomaterials* 27, pp. 3115-24.

Li HX, Xiao L, Wang C, Gao JL, Zhai YG. 2010. Review: Epigenetic regulation of adipocyte differentiation and adipogenesis. *J Zhejiang Univ Sci B* 11(10), pp. 784-91.

Li JH, Liu DY, Zhang FM, Wang F, Zhang WK, Zhang ZT. 2011. Human dental pulp stem cell is a promising autologous seed cell for bone tissue engineering. *Chin Med J (Engl)* 124(23), pp. 4022-8.

Li M, Xu J, Romero-Gonzalez M, Banwart SA, Huang WE. 2012. Single cell Raman spectroscopy for cell sorting and imaging. *Curr Opin Biotechnol* 23(1), pp. 56-63.

Lian JB, Stein GS, Javed A, van Wijnen AJ, Stein JL, Montecino M, Hassan MQ, Gaur T, Lengner CJ, Young DW. 2006. Networks and hubs for the transcriptional control of osteoblastogenesis. *Rev Endocr Metab Disord* 7(1-2), pp. 1-16.

Liao SM. 2005. Rescuing human embryonic stem cell research: the Blastocyst Transfer Method. *Am J Bioeth* 5(6), pp. 8-16.
Liedtke S, Enczmann J, Waclawczyk S, Wernet P, Kögler G. 2007. Oct4 and its pseudogenes confuse stem cell research. *Cell Stem Cell* 11;1(4), pp. 364-6.

Lin HJ, Wang X, Shaffer KM, Sasaki CY, Ma W. 2004. Characterization of H_2O_2-induced acute apoptosis in cultured neural stem/progenitor cells. *FEBS Lett* 16;570(1-3), pp. 102-6.

Lin NH, Gronthos S, Bartold PM. 2008. Stem cells and periodontal regeneration. *Aust Dent J*. 53(2), pp. 108-21.

Linde A. 1985. The extracellular matrix of the dental pulp and dentin. *J Dent Res* 64, pp. 523-9.

Linde A. 1989. Dentin matrix proteins: composition and possible functions in Calcification. *Anat Rec*, pp. 224:154.

Lindroos B, Ma¨enpa¨a¨ K, Ylikomi T, Oja H, Suuronen R, Miettinen S. 2008. Characterisation of human dental stem cells and buccal mucosa fibroblasts. *Biochemical Biophysical Research Communications* 368, pp. 329–35.

Liu L, DiGirolamo CM, Navarro PA, Blasco MA, Keefe DL. 2004. Telomerase deficiency impairs differentiation of mesenchymal stem cells. *Exp Cell Res* 10;294(1), pp. 1-8.

Liu Y and Xiao A. 2011. Epigenetic regulation in neural crest development. *Birth Defects Res A Clin Mol Teratol* 91(8), pp. 788-96.

Lizier NF, Kerkis A, Gomes CM, Hebling J, Oliveira CF, Caplan AI, Kerkis I. 2012. Scaling-up of dental pulp stem cells isolated from multiple niches. *PLoS One* 7(6), e39885.

Lo Celso C, Wu JW, Lin CP. 2009. *In vivo* imaging of hematopoietic stem cells and their microenvironment. J Biophotonics 2(11), pp. 619-31.
Long LH, Lan AN, Hsuan FT, Halliwell B. 1999. Generation of hydrogen peroxide by
"antioxidant" beverages and the effect of milk addition. Is cocoa the best beverage? Free Radic Res 31(1), pp. 67-71.

Long MW. 2001. Osteogenesis and bone-marrow-derived cells. *Blood Cells Mol Dis* 27(3), pp. 677-90.

Lorenz M, Saretzki G, Sitte N, Metzkow S, von Zglinicki T. 2001. BJ fibroblasts display high antioxidant capacity and slow telomere shortening independent of hTERT transfection. *Free Radic Biol Med* 15;31(6), pp. 824-31.

Løvschall H, Tummers M, Thesleff I, Füchtbauer EM, Poulsen K. 2005. Activation of the Notch signaling pathway in response to pulp capping of rat molars. *Eur J Oral Sci* 113(4), pp. 312-7.

Lozito TP and Tuan RS. 2011. Mesenchymal stem cells inhibit both endogenous and exogenous MMPs via secreted TIMPs. *J Cell Physiol* 226(2), pp. 385-96.

Lu X, Alshemali S, de Wynter EA, Dickinson AM. 2009. Mesenchymal stem cells from CD34 human umbilical cord blood. *Transfus Med* 19, pp. 1-7.

Lu C, Li XY, Hu Y, Rowe RG, Weiss SJ. 2010. MT1-MMP controls human mesenchymal stem cell trafficking and differentiation. *Blood* 14;115(2), pp. 221-9.

Ma T, Li Y, Yang ST, Kniss DA. 1999. Tissue engineering human placenta trophoblast cells in 3-D fibrous matrix: spatial effects on cell proliferation and function. *Biotechnol Prog*15, pp. 715-24.

Ma K, Laco F, Ramakrishna S, Liao S, Chan CK. 2009. Differentiation of bone marrow-derived mesenchymal stem cells into multi-layered epidermis-like cells in 3D organotypic coculture. *Biomaterials* 30(19), pp. 3251-8.

MacDougall M, Dong J, Acevedo AC. 2006. Molecular basis of human dentin diseases. *AmJ Med Genet A* 1; 140(23), pp. 2536-46.

Maciejewska I, Spodnik JH, Wójcik S, Domaradzka-Pytel B, Bereznowski Z. 2006. The dentin sialoprotein (DSP) expression in rat tooth germs following fluoride treatment: an immunohistochemical study. *Arch Oral Biol* 51(3), pp. 252-61.

Matsuo K and Otaki N. 2012. Bone cell interactions through Eph/ephrin: bone modeling, remodeling and associated diseases. *Cell Adh Migr* 6(2), pp. 148-56.

Maes C, Kobayashi T, Selig MK, Torrekens S, Roth SI, Mackem S, Carmeliet G, Kronenberg HM. 2010. Osteoblast precursors, but not mature osteoblasts, move into

developing and fractured bones along with invading blood vessels. *Dev Cell* 17;19(2), pp. 329-44.

Mangano C, De Rosa A, Desiderio V, d'Aquino R, Piattelli A, De Francesco F, Tirino V, Mangano F, Papaccio G. 2010. The osteoblastic differentiation of dental pulp stem cells and bone formation on different titanium surface textures. *Biomaterials* 31(13), pp. 3543-51.

Maniatopoulos C, Sodek J, Melcher AH. 1988. Bone formation *in vitro* by stromal cells obtained from bone marrow of young adult rats. *Cell Tissue Res* 254(2), pp. 317-30.

Mantripragada KK, Caley M, Stephens P, Jones CJ, Kluwe L, Guha A, Mautner V,Upadhyaya M. 2008. Telomerase activity is a biomarker for high grade malignant peripheral nerve sheath tumors in neurofibromatosis type 1 individuals. *Genes Chromosomes Cancer* 47(3), pp. 238-46.

Mareddy S, Crawford R, Brooke G, Xiao Y. 2007. Clonal isolation and characterization of bone marrow stromal cells from patients with osteoarthritis. *Tissue Eng* 13(4), pp. 819-29.

Mareschi K, Biasin E, Piacibello W, Aglietta M, Madon E, Fagioli F. 2001. Isolation of human mesenchymal stem cells: Bone marrow versus umbilical cord blood. *Haematologica* 86, pp. 1099-1100.

Mareschi K, Ferrero I, Rustichelli D, Aschero S, Gammaitoni L, Aglietta M, Madon E, Fagioli F. 2006. Expansion of mesenchymal stem cells isolated from pediatric and adult donor bone marrow. *J Cell Biochem* 1;97(4), pp. 744-54.

Market CD, Atala A, Cann JK, Christ G, Furth M, Ambrosio F and Childers MK. 2009. Mesenchymal Stem Cells: Emerging Therapy for Duchenne Muscular Dystrophy. *American Academy of Physical Medicine and Rehabilitation*, Vol. 1, Iss. 6, pp. 547-559.

Martins EA and Meneghini R. 1994. Cellular DNA damage by hydrogen peroxide is attenuated by hypotonicity. *Biochem J* 1;299 (Pt 1), pp. 137-40.

Martin AA, Bitar Carter RA, De Oliveira Nunesa L, Loschiavo Arisawa EA, Landulfo SJ. 2004. Principal Components Analysis of FT-Raman Spectra of *ex vivo* Basal Cell Carcinoma. *Proc SPIE* 5321, pp. 198–204.

Massaia M, Perrin L, Bianchi A, Ruedi J, Attisano C, Al- tieri D, Rijkers G. T, Thompson L. 1990. Human T cell activation Synergy between CD73 (Ecto-5'- Nucleotidasaen) d Signals Delivered through CD3 and CD2 Molecules. *J. Immunol* 145, pp. 1664–74.

Massart DL, Vandeginste BGM, Buydens LMC, De Jong S, Lewi PJ, Smeyers-Verbeke J. 1998. Handbook of Chemometrics and Qualimetrics: Part A. Volume 20, Part A, Pages 1-867.

Matsumura T, Pfendt EA, Zerrudo Z, Hayflick L. 1980. Senescent human diploid cells (WI-38). Attempted induction of proliferation by infection with SV40 and by fusion with irradiated continuous cell lines. *Exp Cell Res* 125(2), pp. 453-7.

Matsuo K and Otaki N. 2012. Regulation of bone metabolism by Eph-ephrin family members. *Clin Calcium* 22(11), pp. 1669-75.

Mazzoni A, Mannello F, Tay FR, Tonti GA, Papa S, Mazzotti G, Di Lenarda R, Pashley DH, Breschi L. 2007. Zymographic analysis and characterization of MMP-2 and -9 forms in human sound dentin. *J Dent Res* 86(5), pp. 436-40.

McManus LL, Burke GA, McCafferty MM, O'Hare P, Modreanu M, Boyd AR, Meenan BJ. 2011. Raman spectroscopic monitoring of the osteogenic differentiation of human mesenchymal stem cells. *Analyst*. 2011 21;136(12), pp. 2471-81.

Mehrazarin S, Oh JE, Chung CL, Chen W, Kim RH, Shi S, Park NH, Kang MK. 2011. Impaired odontogenic differentiation of senescent dental mesenchymal stem cells is associated with loss of Bmi-1 expression. *J Endod* 37(5), pp. 662-6.

Mergui X, Puiffe ML, Valteau-Couanet D, Lipinski M, Bénard J, Amor-Guéret M.2010. p21Waf1 expression is regulated by nuclear intermediate filament vimentin in neuroblastoma. *BMC Cancer* 2;10:473.

Mets T and Verdonk G. 1981. *In vitro* aging of human bone marrow derived stromal cells; *Mech Ageing Dev* 16, pp. 81-89.

Messent AJ, Tuckwell DS, Knäuper V, Humphries MJ, Murphy G, Gavrilovic J. 1998. Effects of collagenase-cleavage of type I collagen on alpha2beta1 integrin-mediated cell adhesion. *J Cell Sci* 111(8), pp. 1127-35.

Mikami Y, Ishii Y, Watanabe N, Shirakawa T, Suzuki S, Irie S, Isokawa K, Honda MJ. 2011. CD271/p75(NTR) inhibits the differentiation of mesenchymal stem cells into osteogenic, adipogenic, chondrogenic, and myogenic lineages. *Stem Cells Dev* 20(5), pp. 901-13.

Miletich I and Sharpe PT. 2004. Neural crest contribution to mammalian tooth formation. *Birth Defects Res C Embryo Today* 72(2), pp. 200-12.

Min JH, Ko SY, Cho YB, Ryu CJ, Jang YJ. 2011. Dentinogenic potential of human adult dental pulp cells during the extended primary culture. *Hum Cell* 24(1), pp. 43-50.

Mina M, Kollar EJ. 1987. The induction of odontogenesis in non-dental mesenchyme combined with early murine mandibular arch epithelium. *Arch Oral Biol* 32, pp. 123–127.

Mitsiadis TA, Barrandon O, Rochat A, Barrandon Y, De Bari C. 2007. Stem cell niches in mammals. *Exp Cell Res* 1;313(16), pp. 3377-85.

Miura T and Thomas GJ Jr. 1995. Raman spectroscopy of proteins and their assemblies. *Subcell Biochem* 24, pp. 55-99.

Miura M, Gronthos S, Zhao M, Lu B, Fisher LW, Robey PG, Shi S. 2003. SHED: stem cells from human exfoliated deciduous teeth. *Proc Natl Acad Sci U S A* 13;100(10), pp. 5807-12.

Mizuno M and Kuboki Y. 2001. Osteoblast-related gene expression of bone marrow cells during the osteoblastic differentiation induced by type I collagen. *J Biochem* 129(1), pp. 133-8.

Mizuno M, Miyamoto T, Wada K, Watatani S, Zhang GX. 2003. Type I collagen regulated dentin matrix protein-1 (Dmp-1) and osteocalcin (OCN) gene expression of rat dental pulp cells. *J Cell Biochem* 15;88(6), pp. 1112-9.

Moerman EJ, Teng K, Lipschitz DA, Lecka-Czernik B. 2004. Aging activates adipogenic and suppresses osteogenic programs in mesenchymal marrow stroma/stem cells: the role of PPAR-gamma2 transcription factor and TGF-beta/BMP signaling pathways. *Aging Cell* 3(6), pp. 379-89.

Mokry J, Soukup T, Micuda S, Karbanova J, Visek B, Brcakova E, Suchanek J, Bouchal J, Vokurkova D, Ivancakova R. 2010. Telomere attrition occurs during *ex vivo* expansion of human dental pulp stem cells. *J Biomed Biotechnol* 2010:673513.

Molofsky AV, Pardal R, Iwashita T, Park IK, Clarke MF, Morrison SJ. 2003. Bmi-1 dependence distinguishes neural stem cell self-renewal from progenitor proliferation. *Nature* 30;425(6961), pp. 962-7.

Montgomery RK, Carlone DL, Richmond CA, Farilla L, Kranendonk ME, Henderson DE, Baffour-Awuah NY, Ambruzs DM, Fogli LK, Algra S, Breault DT. 2011. Mouse telomerase reverse transcriptase (mTert) expression marks slowly cycling intestinal stem cells. *Proc Natl Acad Sci U S A* 4;108(1), pp. 179-84.

Moody B, Haslauer CM, Kirk E, Kannan A, Loboa EG, McCarty GS. 2010. In situ monitoring of adipogenesis with human-adipose-derived stem cells using surface-enhanced Raman spectroscopy. *Appl Spectrosc* 64(11), pp. 1227-33.

Mori G, Brunetti G, Oranger A, Carbone C, Ballini A, Lo Muzio L, Colucci S, Mori C, Grassi FR, Grano M. 2011. Dental pulp stem cells: osteogenic differentiation and gene expression. *Ann N Y Acad Sci* 1237, pp. 47-52.

Morikawa S, Mabuchi Y, Kubota Y, Nagai Y, Niibe k, Hiratsu E, Suzuki S, Miyauchi-Hara C, Nagoshi N, Sunabori T, Shimmura S, Miyawaki A, Nakagawa T, Suda T, Okano H, and Matsuzaki Y. 2009. Prospective identification, isolation, and systemic transplantation of multipotent mesenchymal stem cells in murine bone marrow. *J. Exp. Med* Vol. 206 No. 11, pp. 2483-96.

Moussa SA. 2008. Oxidative stress in diabetes mellitus. *Rom J Biophys* 18, pp. 225-236.

Moyzis RK, Buckingham JM, Cram LS, Dani M, Deaven LL, Jones MD, Meyne J, Ratliff RL, Wu JR. 1988. A highly conserved repetitive DNA sequence, (TTAGGG)n, presentat the telomeres of human chromosomes. *Proc Natl Acad Sci U S A* 85(18), pp. 6622-6.

Mudera VC, Pleass R, Eastwood M, Tarnuzzer R, Schultz G, Khaw P, McGrouther DA, Brown RA. 2000. Molecular responses of human dermal fibroblasts to dual cues: contact guidance and mechanical load. *Cell Motil Cytoskeleton* 45(1):1-9.

Müller AM, Mehrkens A, Schäfer DJ, Jaquiery C, Güven S, Lehmicke M, Martinetti R, Farhadi I, Jakob M, Scherberich A, Martin I. 2010. Towards an intraoperative engineering of osteogenic and vasculogenic grafts from the stromal vascular fraction of human adipose tissue. *Eur Cell Mater* 3;19, pp. 127-35.

Müller HD, Cvikl B, Gruber R, Watzek G, Agis H. 2012. Prolyl hydroxylase inhibitors increase the production of vascular endothelial growth factor in dental pulp-derived cells. *J Endod* 38(11), pp. 1498-503.

Muraglia A, Cancedda R, Quarto R. 2000. Clonal mesenchymal progenitors from human bone marrow differentiate *in vitro* according to a hierarchical model. *J Cell Sci* 113 (Pt 7), pp. 1161-6.

Muruganandan S, Roman AA, Sinal CJ. 2009. Adipocyte differentiation of bone marrow-derived mesenchymal stem cells: cross talk with the osteoblastogenic program. *Cell Mol Life Sci*. 66(2), pp. 236-53.

Nagata T, Kai H, Shibata R, Koga M, Yoshimura A, Imaizumi T. 2003. Oncostatin M, an interleukin-6 family cytokine, upregulates matrix metalloproteinase-9 through the mitogen-activated protein kinase kinase-extracellular signal-regulated kinase pathway in cultured smooth muscle cells. *Arterioscler Thromb Vasc Biol* 1;23(4), pp. 588-93.

Nicoll BK and Peters RJ. 1998. Heat generation during ultrasonic instrumentation of dentin as affected by different irrigation methods. J Periodontol 69, pp. 884–8.

Notingher I. 2007. Raman Spectroscopy Cell-based Biosensors. *Sensors* 7, pp. 1343-1358.

Oberdoerster J, Guizzetti M, Costa LG. 2000. Effect of phenylalanine and its metabolites on the proliferation and viability of neuronal and astroglial cells: possible relevance in maternal phenylketonuria. *J Pharmacol Exp Ther* 295(1):295-301.

Oh SA, Lee HY, Lee JH, Kim TH, Jang JH, Kim HW, Wall I. 2012. Collagen three-dimensional hydrogel matrix carrying basic fibroblast growth factor for the cultivation of mesenchymal stem cells and osteogenic differentiation. *Tissue Eng Part A* 18(9-10), pp. 1087-100.

Okamoto T, Aoyama T, Nakayama T, Nakamata T, Hosaka T, Nishijo K, Nakamura T, Kiyono T, Toguchida J. 2002. Clonal heterogeneity in differentiation potential of immortalized human mesenchymal stem cells. *Biochem Biophys Res Commun* 12;295(2), pp. 354-61.

Olson, H.E., Rooney, G.E., Gross, L., Nesbitt, J.J., Galvin, K.E., Knight, A., Chen, B., Yaszemski, M.J., and Windebank, A.J. 2009. Neural stem cell- and Schwann cell-loaded biodegradable polymer scaffolds support axonal regeneration in the transected spinal cord. *Tissue Eng Part A* 15 (7), pp. 1797-805.

Ong YH, Lim M, Liu Q. 2012. Comparison of principal component analysis and biochemical component analysis in Raman spectroscopy for the discrimination of apoptosis and necrosis in K562 leukemia cells. Opt Express 24;20(20), pp. 22158-71.

Pagès G, Lenormand P, L'Allemain G, Chambard JC, Meloche S, Pouysségur J. 1993. Mitogen-activated protein kinases p42mapk and p44mapk are required for fibroblast proliferation. *Proc Natl Acad Sci U S A* 15;90(18), pp. 8319-23.

Palosaari H, Pennington CJ, Larmas M, Edwards DR, Tjäderhane L, Salo T. 2003. Expression profile of matrix metalloproteinases (MMPs) and tissue inhibitors of MMPs in mature human odontoblasts and pulp tissue. *Eur J Oral Sci* 111(2), pp. 117-27.

Pan G and Thomson JA. 2007. Nanog and transcriptional networks in embryonic stem cell pluripotency. *Cell Res* 17(1), pp. 42-9.

Parsch D, Fellenberg J, Brümmendorf TH, Eschlbeck AM, Richter W. 2004. Telomere length and telomerase activity during expansion and differentiation of human mesenchymal stem cells and chondrocytes. *J Mol Med (Berl)* 82(1), pp. 49-55.

Patel M, Smith AJ, Sloan AJ, Smith G, Cooper PR. 2009. Phenotype and behaviour of dental pulp cells during expansion culture. *Arch Oral Biol* 54(10), pp. 898-908.

Pearson M, Carbone R, Sebastiani C, Cioce M, Fagioli M, Saito S, Higashimoto Y, Appella E, Minucci S, Pandolfi PP, Pelicci PG. 2000. PML regulates p53 acetylation and premature senescence induced by oncogenic Ras. *Nature*. 2000 406(6792), pp. 207-10.

Pepper M. S. 1999. Transforming growth factor-b: vasculogenesis, angiogenesis, and vessel wall integrity. *Cytokine Growth Factor Rev* 8, pp. 21-43.

Perez-Iratxeta C, Palidwor G, Porter CJ, Sanche NA, Huska MR, Suomela BP, Muro EM, Krzyzanowski PM, Hughes E, Campbell PA, Rudnicki MA, Andrade MA. 2005. Study of stem cell function using microarray experiments. *FEBS Lett* 21;579(8), pp. 1795-801.

Petersen T and Niklason L. 2007. Cellular lifespan and regenerative medicine. *Biomaterials* 28(26) pp. 3751-6.

Philippe B, Luc S, Valerie PB, Jerome R, Alessandra BR, et al. 2010. Culture and use of mesenchymal stromal cells in phase I and II clinical trials. *Stem Cells Int* 503593.

Pierelli L, Bonanno G, Rutella S, Marone M, Scambia G, Leone G. 2001. CD105 (endoglin) expression on hematopoietic stem/progenitor cells. *Leuk Lymphoma* 42(6), pp. 1195-206.

Pijanka JK, Kumar D, Dale T, Yousef I, Parkes G, Untereiner V, Yang Y, Dumas P, Collins D, Manfait M, Sockalingum GD, Forsyth NR, Sulé-Suso J. 2010. Vibrational spectroscopy differentiates between multipotent and pluripotent stem cells. *Analyst* 135(12), pp. 3126-32.

Pittenger MF, Mackay AM, Beck SC, Jaiswal RK, Douglas R, Mosca JD, Moorman MA, Simonetti DW, Craig S, Marshak DR. 1999. Multilineage potential of adult human mesenchymal stem cells. *Science* 2;284(5411), pp. 143-7.

Pouryamout L, Dams J, Wasem J, Dodel R, Neumann A. 2012. Economic evaluation of treatment options in patients with Alzheimer's disease: a systematic review of cost-effectiveness analyses. *Drugs* 16;72(6), pp. 789-802.

Pöschl E, Schlötzer-Schrehardt U, Brachvogel B, Saito K, Ninomiya Y, Mayer U. 2004. Collagen IV is essential for basement membrane stability but dispensable for initiation of its assembly during early development. *Development* 131(7), pp. 1619-28.

Prescott RS, Alsanea R, Fayad MI, Johnson BR, Wenckus CS, Hao J, John AS, George A. 2008. *In vivo* generation of dental pulp-like tissue by using dental pulp stem cells, a collagen scaffold, and dentin matrix protein 1 after subcutaneous transplantation in mice. *J Endod* 34(4):421-6.

Qin C, D'Souza R, Feng JQ. 2007. Dentin matrix protein 1 (DMP1): new and important roles for biomineralization and phosphate homeostasis. *J Dent Res* 86(12), pp. 1134-41.

Quarto R, Mastrogiacomo M, Cancedda R, Kutepov SM, Mukhachev V, Lavroukov A, Kon E, Marcacci M. 2001. Repair of large bone defects with the use of autologous bone marrow stromal cells. *N Engl J Med* 1;344(5), pp. 385-6.

Quirici N, Soligo D, Bossolasco P, Servida F, Lumini Cand Deliliers GL. 2002.Isolation of bone marrow mesenchymal stem cells bt anti- nerve growth fctor receptor antibodies. *Exp Hamatol* 20(7), pp. 783-91.

Rallapalli S, Bishi DK, Verma RS, Cherian KM, Guhathakurta S. 2009. A multiplex PCR technique to characterize human bone marrow derived mesenchymal stem cells. *Biotechnol Lett* 31(12), pp. 1843-50.

Reddel RR. 1998. A reassessment of the telomere hypothesis of senescence. *Bioessay* 20(12), pp. 977-84.

Rege TA and Hagood JS. 2006. Thy-1 as a regulator of cell-cell and cell-matrix interactions in axon regeneration, apoptosis, adhesion, migration, cancer, and fibrosis. *FASEB J* 20(8), pp. 1045-54.

Reyes M, Dudek A, Jahagirdar B, Koodie L, Marker PH, Verfaillie CM. 2002. Origin of endothelial progenitors in human postnatal bone marrow. *J Clin Invest* 109(3), pp. 337-46.

Rhee SG. 2006. Cell signaling. H_2O_2, a necessary evil for cell signalling. *Science* 30;312(5782), pp. 1882-3.

Rhee S and Grinnell F. 2007. Fibroblast mechanics in 3D collagen matrices. *Adv Drug Deliv Rev* 10;59(13), pp. 1299-305.

Rickard DJ, Kassem M, Hefferan TE, Sarkar G, Spelsberg TC, Riggs L. 1996. Isolation and characterization of osteoblasts precursor cells from human bone marrow. *J Bone Miner Res* 11, pp. 312–324.

Riddle RC, Taylor AF, Genetos DC, Donahue HJ. 2006. MAP kinase and calcium signalling mediate fluid flow-induced human mesenchymal stem cell proliferation. *Am J Physiol Cell Physiol* 290(3), pp.776-84.

Ries C, Egea V, Karow M, Kolb H, Jochum M, Neth P. 2007. MMP-2, MT1-MMP, and TIMP-2 are essential for the invasive capacity of human mesenchymal stem cells: differential regulation by inflammatory cytokines. *Blood* 1;109(9), pp. 4055-63.

Rodda DJ, Chew JL, Lim LH, Loh YH, Wang B, Ng HH, Robson P. 2005. Transcriptional regulation of nanog by OCT4 and SOX2. *J Biol Chem* 1;280(26), pp. 24731-7.

Rodríguez-Lozano FJ, Bueno C, Insausti CL, Meseguer L, Ramírez MC, Blanquer M, Marín N, Martínez S, Moraleda JM. 2011. Mesenchymal stem cells derived from dental tissues. *Int Endod J* 44(9), pp. 800-6.

Roy NS, Cleren C, Singh SK, Yang L, Beal MF, Goldman SA. 2006. Functional engraftment of human ES cell-derived dopaminergic neurons enriched by coculture with telomerase-immortalized midbrain astrocytes. *Nat Med* 12(11), pp. 1259-68.

Rosenbaum AJ, Grande DA, Dines JS. 2008. The use of mesenchymal stem cells in tissue engineering: A global assessment. *Organogenesis* 4(1), pp. 23-7.

Rosenfeldt H and Grinnell F. 2000. Fibroblast quiescence and the disruption of ERK signaling in mechanically unloaded collagen matrices. *J Biol Chem* 4;275(5), pp. 3088-92.

Rossi DJ, Jamieson CH, Weissman IL. 2008. Stems cells and the pathways to aging and cancer. *Cell* 22;132(4), pp. 681-96.

Rubio MA, Davalos AR, Campisi J. 2004. Telomere length mediates the effects of telomerase on the cellular response to genotoxic stress. *Exp Cell Res* 1;298(1), pp. 17-27.

Ruch JV, Lesot H, Bègue-Kirn C. 1995. Odontoblast differentiation. *Int J Dev Biol*. 39(1), pp. 51-68.

Rufer N, Brümmendorf TH, Chapuis B, Helg C, Lansdorp PM, Roosnek E. 2001. Accelerated telomere shortening in hematological lineages is limited to the first year following stem cell transplantation. *Blood* 15;97(2), pp. 575-7.

Rupp PA, Visconti RP, Czirók A, Cheresh DA, Little CD. 2008. Matrix metalloproteinase 2-integrin alpha(v)beta3 binding is required for mesenchymal cell invasive activity but not epithelial locomotion: a computational time-lapse study. *Mol Biol Cell* 19(12), pp. 5529-40.

Russell KC, Phinney DG, Lacey MR, Barrilleaux BL, Meyertholen KE, O'Connor KC. 2010. *In vitro* high-capacity assay to quantify the clonal heterogeneity in trilineage potential of mesenchymal stem cells reveals a complex hierarchy of lineage commitment. *Stem Cells* 28(4):788-98.

Rutherford RB and Gu K. 2000. Treatment of inflamed ferret dental pulps with recombinant bone morphogenic protein-7. *European Journal of Oral Sciences* 108, pp. 202–6.

Ruwhof C and van der Laarse A. 2000. Mechanical stress-induced cardiac hypertrophy: mechanisms and signal transduction pathways. *Cardiovasc Res* 47(1), pp. 23-37.

Sabeh F, Li XY, Saunders TL, Rowe RG, Weiss SJ. 2009. Secreted versus membrane-anchored collagenases: relative roles in fibroblast-dependent collagenolysis and invasion. *J Biol Chem* 21;284(34), pp. 23001-11.

Sadi G and Güray T. 2009. Gene expressions of Mn-SOD and GPx-1 in streptozotocin-induced diabetes: effect of antioxidants. *Mol Cell Biochem* 327(1-2), pp. 127-34.

Saito T, Ogawa M, Hata Y, Bessho K. 2004. Acceleration effect of human recombinant bone morphogenic protein-2 on differentiation of human pulp cells into odontoblasts. *Journal of Endodontics* 30, pp. 205–8.

Saito R, Nakauchi H, Watanabe S. 2012. Serine/threonine kinase, Melk, regulates proliferation and glial differentiation of retinal progenitor cells. *Cancer Sci* 103(1), pp. 42-9.

Sakai K, Yamamoto A, Matsubara K, Nakamura S, Naruse M, Yamagata M, Sakamoto K, Tauchi R, Wakao N, Imagama S, Hibi H, Kadomatsu K, Ishiguro N, Ueda M. 2012. Human dental pulp-derived stem cells promote locomotor recovery after complete transection of the rat spinal cord by multiple neuro-regenerative mechanisms. *J Clin Invest* 3;122(1), pp. 80-90.

Samassekou O, Gadji M, Drouin R, Yan J. 2010. Sizing the ends: normal length of human telomeres. *Ann Anat* 20;192(5), pp. 284-91.

Sanchez-Ramos J, Song S, Cardozo-Pelaez F, Hazzi C, Stedeford T, Willing A, Freeman TB, Saporta S, Janssen W, Patel N, Cooper DR, Sanberg PR. 2000. Adult bone marrow stromal cells differentiate into neural cells *in vitro. Exp Neurol* 164(2), pp. 247-56.

Sanka K, Maddala R, Epstein DL, Rao PV. 2007. Influence of actin cytoskeletal integrity on matrix metalloproteinase-2 activation in cultured human trabecular meshwork cells. *Invest Ophthalmol Vis Sci* 48(5), pp. 2105-14.

Saretzki G, Walter T, Atkinson S, Passos JF, Bareth B, Keith WN, Stewart R, Hoare S, Stojkovic M, Armstrong L, von Zglinicki T, Lako M. 2008. Downregulation of multiple stress defense mechanisms during differentiation of human embryonic stem cells. *Stem Cells* 26(2), pp. 455-64.

Saretzki G. 2009. Telomerase, mitochondria and oxidative stress. *Exprimental Gerontology* 44, pp. 485-492.

Sasaki M, Abe R, Fujita Y, Ando S, Inokuma D, Shimizu H. 2008. Mesenchymal stem cells are recruited into wounded skin and contribute to wound repair by transdifferentiation into multiple skin cell type. *J Immunol* 180, pp. 2581-2587.

Scadden DT. 2006. The stem cell niche as an entity of action. *Nature* 44, pp. 1075-79.

Scharstuhl A, Schewe B, Benz K, Gaissmaier C, Bühring HJ, Stoop R. 2007. Chondrogenic potential of human adult mesenchymal stem cells is independent of age or osteoarthritis etiology. *Stem Cells* 25(12), pp. 3244-51.

Schofield, R. 1978. The relationship between the spleen colony-forming cell and the haemopoietic stem cell. *Blood Cells* 4, pp. 7–25.

Schmitz N, Laverty S, Kraus VB, Aigner T. 2010. Basic methods in histopathology of joint tissues. *Osteoarthritis Cartilage* 18 Suppl 3, pp.113-6.

Schwab KE and GargeTT. 2007. Co-expression of two perivascular cell markers isolates mesenchymal stem-like cells from human endometrium. *Hum Reprod* 22(11), pp. 2903-11.

Sen S, McDonald SP, Coates PT, Bonder CS. 2011. Endothelial progenitor cells: novel biomarker and promising cell therapy for cardiovascular disease. *Clin Sci (Lond)* 120(7), pp. 263-83.

Sensebé L, Krampera M, Schrezenmeier H, Bourin P, Giordano R. 2010. Mesenchymal stem cells for clinical application. *Vox Sang* 98(2), pp. 93-107.

Seo YJ, Lee JW, Lee EH, Lee HK, Kim HW, Kim YH. 2004. Role of glutathione in the adaptive tolerance to H_2O_2. *Free Radic Biol Med* 15;37(8), pp. 1272-81.

Seon B. K and Kumar S. 2001. CD105 antibody for targeting of tumour vascular endothelial cells. *In The New Angiotherapy*, pp. 499-515.

Serakinci N, Graakjaer J, Kolvraa S. 2008. Telomere stability and telomerase in mesenchymal stem cells. *Biochimie* 90, pp. 33-40.

Serra V, von Zglinicki T, Lorenz M, Saretzki G. 2003. Extracellular superoxide dismutase is a major antioxidant in human fibroblasts and slows telomere shortening. *J Biol Chem* 28;278(9), pp. 6824-30.

Sethe S, Scutt A, Stolzing A. 2006. Aging of mesenchymal stem cells. *Ageing Res Rev* 5(1), pp. 91-116.

Severino J, Allen RG, Balin S, Balin A, Cristofalo VJ. . 2000. Is beta-galactosidase staining a marker of senescence *in vitro* and *in vivo*? *Exp Cell Res* 25;257(1), pp. 162-71.

Shakibaei M, Shayan P, Busch F, Aldinger C, Buhrmann C, Lueders C, Mobasheri A. 2012. Resveratrol mediated modulation of Sirt-1/Runx2 promotes osteogenic differentiation of mesenchymal stem cells: potential role of Runx2 deacetylation. *PLoS One* 7(4), e35712.

Sharpless and DePinho RA. 1999. The INK4A/ARF locus and its two gene products. *Curr Opin Genet Dev* 9(1), pp. 22-30.

Sharpless and DePinho RA. 2007. How stem cells age and why this makes us grow old. *Nat Rev Mol Cell Biol* 8, pp. 703–713.

Shi S and Gronthos S. 2003. Perivascular niche of postnatal mesenchymal stem cells in human bone marrow and dental pulp. *J Bone Miner Res* 18(4), pp. 696-704.

Shiomi T, Lemaître V, D'Armiento J, Okada Y. 2010. Matrix metalloproteinases, a disintegrin and metalloproteinases, and a disintegrin and metalloproteinases with thrombospondin motifs in non-neoplastic diseases. *Pathol Int* 60(7), pp. 477-96.

Shirasawa S, Sekiya I, Sakaguchi Y, Yagishita K, Ichinose S, Muneta T. 2006. *In vitro* chondrogenesis of human synovium-derived mesenchymal stem cells: optimal condition and comparison with bone marrow-derived cells. *J Cell Biochem* 1;97(1), pp. 84-97.

Shovlin C. L and Letarte M. 1999. Hereditary hemorrhagic telangiectasia and pulmonary arteriovenous malformations: issues in clinical management and review of pathogenic mechanisms; *Thorax,* 54, pp. 714-729.

Shugart EC and Umek RM. 1997. Dexamethasone signaling is required to establish the postmitotic state of adipocyte development. *Cell Growth Differ* 8(10), pp. 1091-8.

Shui C, Spelsberg TC, Riggs BL, Khosla S. 2003. Changes in Runx2/Cbfa1 expression and activity during osteoblastic differentiation of human bone marrow stromal cells. *J Bone Miner Res* 18(2), pp. 213-21.

Sies H. 1997. Oxidative stress: Oxidants and antioxidants. *Exp Physiol* 82, pp. 291-295.

Siddappa R, Licht R, van Blitterswijk C, de Boer J. 2007. Donor variation and loss of multipotency during *in vitro* expansion of human mesenchymal stem cells for bone tissue engineering. *J Orthop Res* 25(8):1029-41.

Silva TA, Rosa AL, Lara VS. 2004. Dentin matrix proteins and soluble factors: intrinsic regulatory signals for healing and resorption of dental and periodontal tissues? *Oral Dis* 10(2), pp. 63-74.

Silver FH and Pins G. 1992. Cell growth on collagen: a review of tissue engineering using scaffolds containing extracellular matrix. *J Long Term Eff Med Implants* 2(1), pp. 67-80.

Silvera, M. R and Phipps R. P.1995. Synthesis of interleukin-1 receptor antagonist by Thy-1_ and Thy-1- murine lung fibroblast subsets. *J. Interferon Cytokine Res* 15, pp. 63–70.

Sinanan AC, Hunt NP, Lewis MP. 2004. Human adult craniofacial muscle-derived cells: neural-cell adhesion-molecule (NCAM; CD56)-expressing cells appear to contain multipotential stem cells. *Biotechnol Appl Biochem* 40, pp. 25–34.

Sittinger M, Bujia J, Rotter N, Reitzel D, Minuth WW, Burmester GR. 1996. Tissue engineering and autologous transplant formation: practical approaches with resorbable biomaterials and new cell culture techniques. *Biomaterials* 17(3), pp. 237-42.

Sloan A.J and Smith A.J. 1999. Stimulation of the dentine-pulp complex of rat incisor teeth by TGF-b isoforms 1±3 *in vitro*; *Archives of Oral Biol* 44, pp. 149-156.

Sloan AJ, Rutherford RB, Smith AJ. 2000. Stimulation of rat dentine–pulp complex by bone morphogenic protein-7 *in vitro; Archives of Oral Biology* 45, pp. 173–7.

Sloan AJ and Smith AJ. 2007. Stem cells and the dental pulp: potential roles in dentine regeneration and repair. *Oral Dis* 13(2), pp. 151-7.

Sloan AJ and Waddington RJ. 2009. Dental pulp stem cells: what, where, how? *Int J Paediatr Dent* 19(1), pp. 61-70.

Smith AJ, Cassidy N, Perry H, Bègue-Kirn C, Ruch JV and Lesot H. 1995. Reactionary dentinogenesis. *Int J Dev Biol* 39(1), pp. 273-80.

Smith JR, Pochampally R, Perry A, Hsu SC, Prockop DJ. 2004. Isolation of a highly clonogenic and multipotential subfraction of adult stem cells from bone marrow stroma. *Stem Cells* 22(5), pp. 823-31.

Smith K and Rennie MJ. 2007. New approaches and recent results concerning human-tissue collagen synthesis. *Curr Opin Clin Nutr Metab Care* 10(5), pp. 582-90.

Sperka T, Wang J, Rudolph KL. 2012. DNA damage checkpoints in stem cells, ageing and cancer. *Nat Rev Mol Cell Biol* 13(9), pp. 579-90.

Stains JP and Civitelli R. 2003. Genomic approaches to identifying transcriptional regulators of osteoblast differentiation. *Genome Biol* 4(7), pp.222.

Stenderup K, Justesen J, Clausen C, Kassem M. 2003. Aging is associated with decreased maximal life span and accelerated senescence of bone marrow stromal cells. *Bone* 33(6), pp. 919-26.

Stephens P, Davies KJ, al-Khateeb T, Shepherd JP, Thomas DW. 1996. A comparison of the ability of intra-oral and extra-oral fibroblasts to stimulate extracellular matrix reorganization in a model of wound contraction. *J Dent Res* 75(6), pp. 1358-64.

Stephens P, Cook H, Hilton J, Jones CJ, Haughton MF, Wyllie FS, Skinner JW, Harding KG, Kipling D, Thomas DW. 2003. An analysis of replicative senescence in dermal fibroblasts derived from chronic leg wounds predicts that telomerase therapy would fail to reverse their disease-specific cellular and proteolytic phenotype. *Exp Cell Res* 1;283(1), pp. 22-35.

Stephens P, Grenard P, Aeschlimann P, Langley M, Blain E, Errington R, Kipling D, Thomas D, Aeschlimann D. 2004. Crosslinking and G-protein functions of transglutaminase 2 contribute differentially to fibroblast wound healing responses. *J Cell Sci* 1;117(Pt 15), pp. 3389-403.

Sternlicht MD and Werb Z. 2001. How matrix metalloproteinases regulate cell behavior.*Annu Rev Cell Dev Biol* 17, pp. 463-516.

Steward AJ, Wagner DR, Kelly DJ. 2013. The pericellular environment regulates cytoskeletal development and the differentiation of mesenchymal stem cells and determines their response to hydrostatic pressure. *Eur Cell Mater* 7;25, pp. 167-78.

Stocum DL. 2001. Stem cells in regenerative biology and medicine. *Wond Rep Reg* 9, pp. 429-442.

Stokowski A, Shi S, Sun T, Bartold PM, Koblar SA, Gronthos S. 2007. EphB/ephrin-B interaction mediates adult stem cell attachment, spreading, and migration: implications for dental tissue repair; migration: implications for dental tissue repair. *Stem Cells* 25(1), pp. 156-64.

Stolzing A, Jones E, McGonagle D, Scutt A. 2008. Age-related changes in human bone marrow-derived mesenchymal stem cells: consequences for cell therapies. *Mech Ageing Dev* 129(3), pp. 163-73.

Stops AJ, Heraty KB, Browne M, O'Brien FJ, McHugh PE. 2010. A prediction of cell differentiation and proliferation within a collagen-glycosaminoglycan scaffold subjected to mechanical strain and perfusive fluid flow. *J Biomech* 3;43(4), pp. 618-26.

Stringer B, Waddington R, Houghton A, Stone M, Russell G, Foster G. 2007. Serum from postmenopausal women directs differentiation of human clonal osteoprogenitor cells from an osteoblastic toward an adipocytic phenotype. *Calcif Tissue Int* 80(4), pp. 233-43.

Suchánek J, Soukup T, Ivancaková R, Karbanová J, Hubková V, Pytlík R, Kucerová L. 2007. Human dental pulp stem cells--isolation and long term cultivation. *Acta Medica (Hradec Kralove)* 50(3), pp. 195-201.

Suon S, Jin H, Donaldson AE, Caterson EJ, Tuan RS, Deschennes G, Marshall C, Iacovitti L. 2004. Transient differentiation of adult human bone marrow cells into neuron-like cells in culture: Development of morphological and biochemical traits is mediated by different molecular mechanisms. *Stem Cells, Dev* 13, pp. 625-635.

Swain RJ and Stevens MM. 2007. Raman microspectroscopy for non-invasive biochemical analysis of single cells. *Biochem Soc Trans* 35(Pt 3), pp. 544-9.

Takahashi N, Kawanishi-Tabata R, Haba A, Tabata M, Haruta Y, Tsai H, and Seon B. K. 2001. Association of serum endoglin with metastasis in patients with

colorectal, breast, and other solid tumors, and suppressive effect of chemotherapy on the serum endoglin. *Clin. Cancer Res* 7, pp. 524-532.

Tai BC, Wan AC, Ying JY. 2010. Modified polyelectrolyte complex fibrous scaffold as a matrix for 3D cell culture. *Biomaterials* 31(23), pp. 5927-35.

Takubo K, Izumiyama-Shimomura N, Honma N, Sawabe M, Arai T, Kato M, Oshimura M, Nakamura K. 2002. Telomere lengths are characteristic in each human individual. *Exp Gerontol* 37(4), pp. 523-31.

Tamaki Y, Nakahara T, Ishikawa H, Sato S. . 2012. *In vitro* analysis of mesenchymal stem cells derived from human teeth and bone marrow. *Odontology* ahead of print

Tan BS, Lonic A, Morris MB, Rathjen PD, Rathjen J. 2011. The amino acid transporter SNAT2 mediates L-proline-induced differentiation of ES cells. *Am J Physiol Cell Physiol* 300(6), pp. 1270-9.

Téclès O, Laurent P, Zygouritsas S, Burger AS, Camps J, Dejou J, About I. 2005. Activation of human dental pulp progenitor/stem cells in response to odontoblast injury. *Arch Oral Biol* 50(2), pp. 103-8.

Theise, N.D, Nimmakayalu, M, Gardner, R, Illei, P.B, Morgan, G, Teperman, L, Henegariu, O, Krause, D.S. 2000. Liver from bone marrow in humans. *Hepatology* 32, pp. 11–16.

Théret N, Lehti K, Musso O, Clément B. 1999. MMP2 activation by collagen I and concanavalin A in cultured human hepatic stellate cells. *Hepatology* 30(2), pp. 462-8.

Thirumala S, Goebel WS, Woods EJ. 2013. Manufacturing and banking of mesenchymal stem cells. *Expert Opin Biol Ther* 13(5), pp. 673-91.

Thomas GJ Jr. 1999. Raman spectroscopy of protein and nucleic acid assemblies. *Annu Rev Biophys Biomol Struct* 28, pp. 1-27.

Thum T, Fraccarollo D, Galuppo P, Tsikas D, Frantz S, Ertl G, Bauersachs J. 2006. Bone marrow molecular alterations after myocardial infarction: Impact on endothelial progenitor cells. *Cardiovasc Res* 1;70(1), pp. 50-60.

Titushkin IA and Cho MR. 2009. Controlling cellular biomechanics of human mesenchymal stem cells. *Conf Proc IEEE Eng Med Biol Soc* 2009, pp. 2090-3.

Tormin A, Li O, Brune JC, Walsh S, Schütz B, Ehinger M, Ditzel N, Kassem M, Scheding S. 2011. CD146 expression on primary nonhematopoietic bone marrow stem cells is correlated with in situ localization. *Blood* 12;117(19), pp. 5067-77.

Toth M, Sohail A, Fridman R. 2012. Assessment of gelatinases (MMP-2 and MMP-9) by gelatin zymography. *Methods Mol Biol* 878, pp. 121-35.

Trent JF and Kirsner RS. 1998. Tissue engineered skin: Apligraf, a bi-layered living skin equivalent. *Int J Clin Pract* 52(6), pp. 408-13.

Trowbridge H. 2002. Histology of pulpal inflammation In: Hargreaves KM, Goodis HE, editors. Seltzer and Bender's Dental Pulp. Quintessence Publishing Co., Inc; Carol Stream, pp. 227–245.

Trowbridge HO. 2003. Pulp biology: progress during the past 25 years. *Australian Endodontic Journal* 29, pp. 5–12.

Tziafas D, Smith AJ, Lesot H. 2000. Designing new treatment strategies in vital pulp therapy. *J Dent* 28, pp. 77–92.

Ubaldini AL, Baesso ML, Medina Neto A, Sato F, Bento AC, Pascotto RC. 2013. Hydrogen Peroxide Diffusion Dynamics in Dental Tissues. *J Dent Res* 92(7) pp. 661-5.

Ueda J, Saito N, Shimazu Y, Ozawa T. 1996. A comparison of scavenging abilities of antioxidants against hydroxyl radicals. *Arch Biochem Biophys* 15;333(2), pp. 377-84.

Ulloa-Montoya F, Kidder BL, Pauwelyn KA, Chase LG, Luttun A, Crabbe A, Geraerts M, Sharov AA, Piao Y, Ko MS, Hu WS, Verfaillie CM. 2007. Comparative transcriptome analysis of embryonic and adult stem cells with extended and limited differentiation capacity. *Genome Biol* 8(8):R163.

Urish KL, Vella JB, Okada M, Deasy BM, Tobita K, Keller BB, Cao B, Piganelli JD, Huard J. 2009. Antioxidant levels represent a major determinant in the regenerative capacity of muscle stem cells. Mol *Biol Cell* 20(1), pp. 509-20.

Valko M, Leibfritz D, Moncol J, Cronin MT, Mazur M, Telser J. 2007. Free radicals and antioxidants in normal physiological functions and human disease. *Int J Biochem Cell Biol* 39(1), pp. 44-84.

Vargas CR, Wajner M, Sitta A. 2011. Oxidative stress in phenylketonuric patients. *Mol Genet Metab* 104 Suppl, pp. 97-9.

Vargová V, Pytliak M, Mechírová V. 2012. Matrix metalloproteinases. *EXS* 103, pp. 1-33.

Vater C, Kasten P, Stiehler M. 2011. Culture media for the differentiation of mesenchymal stromal cells. *Acta Biomater* 7(2), pp. 463-77.

Vavilova T, Ostrovskaya I, Axenova L, Buneeva O, Medvedev A. 2009. Monoamine oxidase and semicarbazide sensitive amine oxidase activities in normal and inflamed human dental pulp. *Med Sci Monit*,15(10), pp. 289-292.

Vazin T and Schaffer DV. 2010. Engineering strategies to emulate the stem cell niche. *trends Biotechnol* 28(3), pp. 117-24.

Vaziri H, Dragowska W, Allsopp RC, Thomas TE, Harley CB, Lansdorp PM. 1994. Evidence for a mitotic clock in human hematopoietic stem cells: loss of telomeric DNA with age. *Proc Natl Acad Sci U S A* 11;91(21), pp. 9857-60.

Vaziri H, West MD, Allsopp RC, Davison TS, Wu YS, Arrowsmith CH, Poirier GG, Benchimol S. 1997. ATM-dependent telomere loss in aging human diploid fibroblasts and DNA damage lead to the post-translational activation of p53 protein involving poly(ADP-ribose) polymerase. *EMBO J* 1;16(19), pp. 6018-33.

Veal EA, Day AM, Morgan BA. 2007. Hydrogen peroxide sensing and signaling. *Mol Cell* 13;26(1), pp. 1-14.

Veronesi F, Giavaresi G, Tschon M, Borsari V, Nicoli Aldini N, Fini M. 2013. Clinical use of bone marrow, bone marrow concentrate, and expanded bone marrow mesenchymal stem cells in cartilage disease. *Stem Cells Dev* 15;22(2), pp. 181-92.

Verstappen J, Katsaros C, Torensma R, Von den Hoff JW. 2009. A functional model for adult stem cells in epithelial tissues. *Wound Repair Regen* 17(3), pp. 296-305.

Visse R and Nagase H. 203. Matrix metalloproteinases and tissue inhibitors of metalloproteinases: structure, function, and biochemistry. *Circ Res* 2;92(8), pp. 827-39.

Volponi AA, Pang Y, Sharpe PT. 2010. Stem cell-based biological tooth repair and regeneration. *Trends Cell Biol* 20(12), pp. 715-22.

Von Marschall Z and Fisher LW. 2008. Dentin matrix protein-1 isoforms promote differential cell attachment and migration. *J Biol Chem*, 21;283(47), pp. 32730-40.

von Zglinicki T, Saretzki G, Döcke W, Lotze C. 1995. Mild hyperoxia shortens telomeres and inhibits proliferation of fibroblasts: a model for senescence? *Exp Cell Res* 220(1), pp. 186-93.
von Zglinicki T, Pilger R, Sitte N. 2000. Accumulation of single-strand breaks is the major cause of telomere shortening in human fibroblasts. *Free Radic Biol Med* 1;28(1), pp. 64-74.

von Zglinicki T. 2002. Oxidative stress shortens telomeres. *Trends Biochem Sci* 27(7), pp. 339-44.

von Zglinicki T, Petrie J, Kirkwood TB. 2003. Telomere-driven replicative senescence is a stress response. *Nat Biotechnol* 21(3), pp. 229-30.

Voog J and Jones DL. 2010. Stem Cells and the Niche: A Dynamic Duo. *Cell Stem Cell* 5;6(2), pp. 103-115.

Wachsmann-Hogiu S, Weeks T, Huser T. 2009. Chemical analysis *in vivo* and *in vitro* by Raman spectroscopy--from single cells to humans. *Curr Opin Biotechnol* 20(1), pp. 63-73.

Waddington RJ, Moseley R, Embery G. 2000. Reactive oxygen species: a potential role in the pathogenesis of periodontal diseases. *Oral Dis* 6(3), pp. 138-51.

Waddington, R.J, Youde, S.J, Chi, P.L, and Sloan, A.J. 2009. Isolation of distinct progenitor stem cell populations from dental pulp. *Cells Tissues Organs* 189, pp. 268–274.

Wagner, W and HO, A.D. 2007. Mesenchymal stem cell preparations- comparing apples and oranges. *Stem Cell Rev* 3, pp. 239-248.

Wagner W, Ho AD, Zenke M. 2010. Different facets of aging in human mesenchymal stem cells. *Tissue Eng Part B Rev* 16(4), pp. 445-53.

Wagner W, Horn P, Bork S, Ho AD. 2008. Aging of hematopoietic stem cells is regulated by the stem cell niche. *Experimental Gerontology* 43, pp. 974–980.

Wakitani S, Saito T, Caplan AI. 1995. Myogenic cells derived from rat bone marrow mesenchymal stem cells exposed to 5-azacytidine. *Muscle Nerve* 18, pp. 1417-26.

Wall ME, Bernacki SH, Loboa EG. 2007. Effects of serial passaging on the adipogenic and osteogenic differentiation potential of adipose-derived human mesenchymal stem cells. *Tissue Eng* 13(6), pp. 1291-8.

Wang E and Gundersen D. 1984. Increased organization of cytoskeleton accompanying the aging of human *fibroblasts in vitro. Exp Cell Res* 154(1), pp. 191-202.

Wang JH and Thampatty BP.2008. Mechanobiology of adult and stem cells. *Int Rev Cell Mol Biol* 271, pp. 301-46.

Wang J, Liu X, Jin X, Ma H, Hu J, Ni L, Ma PX. 2010. The odontogenic differentiation of human dental pulp stem cells on nanofibrous poly(l-lactic acid) scaffolds *in vitro* and *in vivo. Acta Biomater* 6(10), pp. 3856-63.

Wang Y, Zang X, Wang Y, Chen P. 2010. High expression of p16^{INK4a} and low expression of Bmi1 are associated with endothelial cellular senescence in the human cornea. *Mol Vis* 18, pp. 803-15.

Watson JT, Foo T, Wu J, Moed BR, Thorpe M, Schon L, Zhang Z. 2013. CD271 as a Marker for Mesenchymal Stem Cells in Bone Marrow versus Umbilical Cord Blood. *Cells Tissues Organs* 197(6), pp. 496-504.

Wei S, Wei S, Sedivy JM. 199. Expression of catalytically active telomerase does not prevent premature senescence caused by overexpression of oncogenic Ha-Ras in normal human fibroblasts. *Cancer Res* 1;59(7), pp. 1539-43.

Weng NP, Granger L, Hodes RJ. 1997. Telomere lengthening and telomerase activation during human B cell differentiation. Proc *Natl Acad Sci U S A* 30;94(20), pp. 10827-32.

Whatling C, McPheat W, Hurt-Camejo E. 2004. Matrix management: assigning different roles for MMP-2 and MMP-9 in vascular remodeling. *Arterioscler Thromb Vasc Biol* 24(1), pp. 10-1.

Wikstrom P, Lissbrant I, Stattin P, Egevad L, and Bergh A. 2002. Endoglin (CD105) is expressed on immature blood vessels and is a marker for survival in prostate cancer. *Prostate* 51, pp. 268-275.

Williams DF. 2006. To engineer is to create: the link between engineering and regeneration. *Trends Biotechnol* 24(1), pp. 4-8.

Woodbury D, Schwarz EJ, Prockop DJ, Black IB. 2000. Adult rat and human bone marrow stromal cells differentiate into neurons. *J Neurosci Res* 15;61(4), pp. 364-70.

Xu J, Wang W, Kapila Y, Lotz J, Kapila S.2009. Multiple differentiation capacity of STRO-1+/CD146+ PDL mesenchymal progenitor cells. *Stem Cells Dev* 18(3), pp. 487-96.

Xue M and Jackson CJ. 2008. Autocrine actions of matrix metalloproteinase (MMP)-2 counter the effects of MMP-9 to promote survival and prevent terminal differentiation of cultured human keratinocytes. *J Invest Dermatol* 128(11), pp. 2676-85.

Yagyuu T, Ikeda E, Ohgushi H et al. 2010. Hard tissue-forming potential of stem/progenitor cells in human dental follicle and dental papilla. *Archives of Oral Biology* 55, pp. 68–76.

Yamakoshi Y, Hu JC, Fukae M, Iwata T, Kim JW, Zhang H, Simmer JP. 2005. Porcine dentin sialoprotein is a proteoglycan with glycosaminoglycan chains containing chondroitin 6-sulfate. *J Biol Chem* 14;280(2), pp. 1552-60.

Yamamoto K, Sokabe T, Watabe T, Miyazono K, Yamashita JK, Obi S, Ohura N, Matsushita A, Kamiya A, Ando J. 2005. Fluid shear stress induces differentiation of

Flk-1-positive embryonic stem cells into vascular endothelial cells *in vitro. Am J Physiol Heart Circ Physiol* 288(4), pp. 1915-24.

Yang NC and Hu ML. 2005. The limitations and validities of senescence associated-beta-galactosidase activity as an aging marker for human foreskin fibroblast Hs68 cells. *Exp Gerontol* 40(10), pp. 813-9.

Yao H, Tao Z, Ai M, Peng L, Wang G, He B, Li Y. 2009. Raman spectroscopic analysis of apoptosis of single human gastric cancer cells. *Vib Spectrosc* 50(2), pp. 193-197.

Yates A and Chambers I. 2005. The homeodomain protein Nanog and pluripotency in mouse embryonic stem cells. *Biochem Soc Trans* 33 (6), pp. 1518-21.

Ying QL, Nichols J, Chambers I, Smith A. 2003. BMP induction of Id proteins suppresses differentiation and sustains embryonic stem cell self-renewal in collaboration with STAT3. *Cell* 31;115(3), pp. 281-92.

Yoke Yin C, So Ha T, Abdul Kadir K. 2010. Effects of Glycyrrhizic Acid on Peroxisome Proliferator-Activated Receptor Gamma (PPARgamma), Lipoprotein Lipase (LPL), Serum Lipid and HOMA-IR in Rats. *PPAR Res* 2010, pp. 530265.

Yong VW, Krekoski CA, Forsyth PA, Bell R, Edwards DR. 1998. Matrix metalloproteinases and diseases of the CNS. *Trends Neurosci* 21(2), pp. 75-80.

Yu GL, Bradley JD, Attardi LD, Blackburn EH. 1990. *In vivo* alteration of telomere sequences and senescence caused by mutated Tetrahymena telomerase RNAs. *Nature* 8;344(6262), pp. 126-32.

Zelko IN, Mariani TJ, Folz RJ. 2002. Superoxide dismutase multigene family: A comparison of the CuZn-SOD (SOD1), Mn-SOD (SOD2), and EC-SOD (SOD3) gene structures, evolution and expression. *Free Rad Biol Med* 33, pp. 337-349.

Zeng W, Yuan W, Li L, Mi J, Xu S, Wen C, Zhou Z, Xiong J, Sun J, Ying D, Yang M, Li X, Zhu C. 2010. The promotion of endothelial progenitor cells recruitment by nerve growth factors in tissue-engineered blood vessels. *Biomaterials* 31(7), pp. 1636-45.

Zhang J, Niu C, Ye L, Huang H, He X, Tong WG, Ross J, Haug J, Johnson T, Feng JQ, Harris S, Wiedemann LM, Mishina Y, Li L. 2003. Identification of the haematopoietic stem cell niche and control of the niche size. *Nature* 425(6960), pp. 836-41.

Zhang W, Walboomers XF, Shi S, Fan M, Jansen JA. 2006. Multilineage differentiation potential of stem cells derived from human dental pulp after cryopreservation. *Tissue Eng* 12(10), pp. 2813-23.

Zhang W, Walboomers XF, Van Kuppevelt TH, Daamen WF, Van Damme PA, Bian Z, Jansen JA. 2008. *In vivo* evaluation of human dental pulp stem cells differentiated towards multiple lineages. *J Tissue Eng Regen Med* 2(2-3), pp. 117-25.

Zhao LR, Duan WM, Reyes M, Keene CD, Verfaillie CM, Low WC. 2002. Human bone marrow stem cells exhibit neural phenotypes and ameliorate neurological deficits after grafting into the ischemic brain of rats. *Exp Neurol* 174, pp. 11–20.

Zhao Y, Wang C, Li S, Song H, Wei F, Pan K, Zhu K, Yang P, Tu Q, Chen J. 2008. Expression of Osterix in mechanical stress-induced osteogenic differentiation of periodontal ligament cells *in vitro. Eur J Oral Sci* 116(3), pp. 199-206.

Zimmermann S, Voss M, Kaiser S, Kapp U, Waller CF, Martens UM. 2003. Lack of telomerase activity in human mesenchymal stem cells. *Leukemia* 17(6), pp. 1146-9.

Zippel N, Schulze M, Tobiasch E. 2010. Biomaterials and mesenchymal stem cells for regenerative medicine. *Recent Pat Biotechnol* 4(1), pp. 1-22.

Appendix

CARDIFF UNIVERSITY

PRIFYSGOL CAERDYDD

Version1
06/03/2007

PARTICIPANT CONSENT FORM

Title of Project:

Effects of Dental Materials on Dentine and tooth pulp

Name of Researcher:

Leili Sadaghiani, Alan Gilmour, Alastair Sloan, Rachel Waddington

Please initial box

1. I confirm that I have read and understand the information sheet Version1 dated 06/03/2007
for the above study and have had the opportunity to ask questions. ☑

2. I understand that my participation is voluntary and that I am free to withdraw at any time,
without giving any reason. ☑

3. I agree to take part in the above study. ☑

_____   28/05/10   _____
Name of Participant   Date   Signature

PRASANNA KUMAR
_____   28/05/2010   _____
Name of Person taking consent   Date   Signature
(if different from researcher)

281

Version1
06/03/2007

PARTICIPANT CONSENT FORM

Title of Project:

Effects of Dental Materials on Dentine and tooth pulp

Name of Researcher:

Leili Sadaghiani, Alan Gilmour, Alastair Sloan, Rachel Waddington

Please initial box

1. I confirm that I have read and understand the information sheet Version1 dated 06/03/2007

   for the above study and have had the opportunity to ask questions.

2. I understand that my participation is voluntary and that I am free to withdraw at any time,

   without giving any reason.
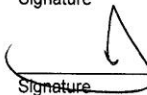
3. I agree to take part in the above study.

_____ 23/09/11 _____
Name of Participant   Date   Signature

L. Sadaghiani 23·9·11 _____
Name of Person taking consent   Date   Signature
(if different from researcher)

coleg meddygaeth
wales   cymru
college of medicine

School of Dentistry
Division of Adult Dental Health
Head of Division Professor Jeremy S Rees BDS MScD PhD FDSRCS(Ed) ILTM

Ysgol Am Deintyddiaeth
Adran Iechyd Deintyddol i Oedolion
Pennaeth Adran Yr Athro Jeremy S Rees BDS MScD PhD FDSRCS(Ed) ILTM

Version1
06/03/2007

PARTICIPANT CONSENT FORM

Title of Project:

Effects of Dental Materials on Dentine and tooth pulp

Name of Researcher:

Leili Sadaghiani, Alan Gilmour, Alastair Sloan, Rachel Waddington

Please initial box

1. I confirm that I have read and understand the information sheet Version1 dated 06/03/2007

   for the above study and have had the opportunity to ask questions.

2. I understand that my participation is voluntary and that I am free to withdraw at any time,

   without giving any reason.

3. I agree to take part in the above study.

~~Name of Participant~~

Date 23/09/11

Signature

L. Sadaghiani
Name of Person taking consent
(if different from researcher)

Date 23.9.11

Signature